An investigation into the regulation of transcription of the splice factor kinase gene SRPK1 in prostate and leukaemia cancer cell lines

Tareg Belali

A thesis submitted in partial fulfilment of the requirements of the University of the West of England, Bristol for the degree of Doctor of Philosophy

Faculty of Health and Applied Sciences, University of the West of England, Frenchay Campus, Coldharbour Lane, Frenchay, Bristol, BS16 1QY

September 2019

I. Author's Declaration

This thesis is submitted in fulfilment of the requirements of a Ph.D., and except where duly acknowledged or referenced, it is entirely my work. It has not been submitted, either in whole or part, for any other award at the University of the West of England or elsewhere.

Signed..... 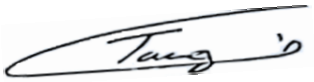 ..... Date 01/07/2019

II. Project Supervisors' Declarations

I confirm that I have read this PhD thesis and that the work it describes was undertaken under my supervision.

Prof. Michael R. Ladomery
Associate Professor in Biomedical Science & Senior Fellow HEA
Faculty of Health and Applied Sciences
University of the West of England, Bristol
T: +44-117-3283531
www.ladomerylab.org
Michael.Ladomery@uwe.ac.uk

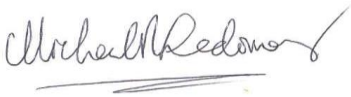

Signed Date 01/07/2019

III. Abstract

The *SRPK1* gene encodes a protein kinase that phosphorylates a class of splice factors called serine/arginine-rich proteins (SR proteins) modifying their ability to regulate alternative pre-mRNA splicing. Studies have linked high SRPK1 levels to tumour proliferation, growth and metastatic ability but little is known about how its expression is regulated. Different transcription factors including WT1 and ERG are thought to have some level of involvement in the regulation of SRPK1 transcription. The aim of this project was to study the transcriptional regulation of the splice factor kinase gene SRPK1. In this study, the regulation of SRPK1 expression was investigated in cancer cells and the results suggest that both the transcription factor WT1 and the co-repressor BASP1 are present on the *SRPK1* promoter region. SRPK1 transcription is activated by WT1, but not when the WT1 binding site is mutated. Consistent with these findings, the knock-down of WT1 with siRNAs also resulted in decreased expression of endogenous SRPK1. The activity of the *SRPK1* promoter in BASP1-expressing K562 cells or in PC3 cells transfected with a BASP1-expressing vector was repressed, consistent with BASP1 turning WT1 into a transcriptional repressor rather an activator. The effect of SRPK1 chemical inhibition via SPHINX and the overexpression of BASP1 on the alternative splicing of the vascular endothelial growth factor (VEGF) was also examined in this study; both SRPK1 inhibition and BASP1 expression promoted the expression of anti-angiogenic VEGF. The transcription factor ERG, on the other hand, was also shown to bind to the *SRPK1* promoter but it repressed its transcription. The overexpression of ERG isoforms reduced endogenous SRPK1 expression, whereas ERG knockdown increased SRPK1 expression. Finally, following manipulation of the expression of SRPK1, WT1, BASP1 and ERG in K562, PC3 and MG63 cell lines, changes in apoptosis, cell

proliferation and migration were observed, suggesting that this regulatory axis could present a valid cancer therapy target

IV. Acknowledgements

Firstly, I would like to thank my supervisor, Prof. Michael Ladomery, for his valuable support during the project and the production of this thesis. Despite an extremely busy eventful few years, he was able to provide a perfect balance of input, project guidance and support, while still allowing me the freedom to work and progress the project independently. This has been optimum for my development as a researcher and I am very grateful for everything he has done.

I'm very much thankful to my other supervisors Dr Gabrielle Wheway and Dr Tim Craig for their sustained support and valuable guidance throughout my research programme.

I also want to thank my research team members Dr Sean Porazinski and Dr Samantha Jumbe for teaching me most of the experimental procedures used in this project and providing valuable advice, throughout the majority of the project, particularly when navigating any experimental difficulties that arose. My thanks are also extended to Chigeru Wodi who, in the absence of Sam, helped me towards the end of the project, particularly with SPHINX treatments.

I would like to thank my family, primarily my parents and my loving wife and kids for their unconditional love, support and believe in my ability to accomplish my full potential. Without their constant support, I would have been distressed and lost track of my goals, they reminded me constantly of my responsibilities and guided my compass toward my target.

V.Table of Contents

Contents

VI. List of Figures

VII. List of Tables

VIII. Abbreviations

µ

µg	Microgram
µm	Micrometer
µM	Micromolar

A

aa	Amino acid
Ab	Antibody
ABL1	Abelson murine leukaemia viral oncogene homology
AD	Accessory domain
AKT/PKB	Phosphatidylinositol 3-kinase /Protein kinase B
AML	Acute Myelogenous Leukaemia
AP	Ammonium Per sulphate
AS	Alternative splicing

B

BASP1	Brain abundant membrane attached signal protein 1
Bcl-xL	B-cell lymphoma extra large
BCR	Breakpoint cluster region
BLAST	Basic Local Alignment Search Tool
bp	Base pair
BRG1	Brahma Related Gene 1
BSA	Bovine Serum Albumin

C

°C	Celsius
CBP	CREB Binding Protein
cDNA	Complimentary Deoxyribonucleic acid
CRC	colorectal cancer
CLKS	CDC-like kinases

D

DDS	Denys-Drash Syndrome
DLR	Dual-Luciferase Reporter Assay
DMEM	Dulbeco Modified Eagle Media
DNA	Deoxyribonucleic acid

E

EC	Endothelial cells
E. coli	*Escherichia coli*
EDTA	Ethylenediaminetetraacetic acid
EGF	Epidermal growth factor

ERG ETS-related gene
EMT Epithelial to mesenchymal mransition
et al. *et al*ia
EtBr Ethidium Bromide

F

FBS Foetal Bovine Serum
FLI1 Flightless 1

H

H_2O_2 Hydrogen peroxide
HDAC Histone Deacetylase
HEK Human Embryonic Kidney
HRP Horseradish peroxidase

I

IGF-1 Insulin-like growth factor - 1
IgG Immunoglobulin g

K

kb Kilobase

L

L Litre
LB Luria-Bertani
LHX9 LIM Homeobox 9

M

M Molar
MAPK Mitogen-activated protein kinase
mg Milligram
min Minute(s)
ml Millilitre
mM MilliMolar
mTOR Mammalian target of rapamycin
MYO1C Myosin -1C

N

NaCl Sodium chloride
NCAM Neural Cell Adhesion Molecule
NCBI National Centre for Biotechnology Information
NSCLC Non-small-cell lung carcinoma
NFW Nuclease-free water were
ng Nanogram,
NLS Nuclear Localisation Sequence
nm Nanometer

P

PBS	Phosphate buffered Saline
PC-3	Prostate cancer cell line
PCR	Polymerase Chain Reaction
PEST	Proline, Glutamic acid, Serine, Threonine
PH	Pleckstrin homology
PI	Protease Inhibitor
PI3K/Akt	Phosphatidylinositol-4, 5-bisphosphate 3 Kinase
PIP2	Phosphatidylinositol-4, 5-bisphosphate
PKC	Protein Kinase C
PRP8	pre-mRNA processing 8
PRPF31	pre-mRNA processing factor 31 homolog
PVDF	Polyvinyidene Fluoride, ii

R

RBP	RNA-binding Proteins
RLU	Relative Luciferase Units
RPMI	Roswell Park Memorial Institute
RRM	RNA recognition motif
rpm	round per minute
RS	Arginine/serine-rich domain
Runx1	Runt-related transcription factor 1
RUNX1-ETO	Runt-related transcription factor 1- eight twenty-one

S

SDS	Sodium Dodecyl Sulfate
SE	Standard Error
SF1	Splice factor 1
SF1	steroidogenic factor 1
siRNA	Small interfering RNA
snRNP	Small nuclear ribonucleoprotein
SOC	Super Optimal broth with Catabolite repression
SPHINX	SR protein Inhibitor X
SR	Serine/argenine rich proteins
SR proteins	Serine/arginine-rich proteins
SRPIN340	Specific serine/threonine protein kinase inhibitor 340
SRPIN340	N-[2-(1-piperidinyl)-5-(trifluoromethyl) phenyl] isonicotinamide
SRPK1	Serine rich protein kinase-1
SRSF-1	Serine rich splice factor-1
SSO	Splice switching oligonucleotides

T

TAE	Tris base, acetic acid and EDTA
Taq	DNA polymerase from Thermus aquaticus
TBST	Tris-buffered saline and Tween-20
TE	Tris, EDTA

TEMED	Tetramethylethylenediamine
Temp	Temperature
TGF	Transforming Growth Factor
TPM	Transcripts per million

U

U	Unit(s) of enzyme activity
UV	Ultraviolet

V

V	Volts
VEGF	Vascular endothelial growth factor

W

WT	Wild type
WT-1	Wilms' tumour-1

1 Chapter One: Introduction

1.1 Alternative splicing and disease

1.1.1 Discovery of pre-mRNA splicing

In eukaryotic cells, the initial pre-mRNA transcript must be processed into mature messenger RNA (mRNA) required for protein synthesis. Pre-mRNA splicing, which is essential for gene expression, is the removal of introns and formation of a final mRNA consisting of the remaining sequences, called exons.

Pre-mRNA splicing was first characterised in the 1970s in adenoviruses (Chow *et al*., 1977). Six years later, researchers discovered that more than one mRNA could be generated from a single immunoglobulin μ gene by a process called alternative splicing (Early *et al*., 1980). There are several modes of alternative splicing (AS). At least 94% of human multi-exon genes undergo alternative splicing (Zhou *et al* 2012). Alternative pre-mRNA splicing is a prevalent phenomenon in developed eukaryotic genomes that provides a mechanism that increases the complexity of proteins expressed by a genome. Alternative splicing plays a significant role in the control of cellular function. Minor changes in AS regulation can significantly alter an important cellular process that can lead to disease. For example, autosomal dominant forms of retinitis pigmentosa are caused by a mutation in the splicing factors PRPF31/U4-61k and PRP8 (Tazi, Bakkour, and Stamm, 2009). Altered activity, expression, or subcellular localization of splicing factor kinases may be one of the causes of the irregular splicing events linked to cancer and other diseases. Through AS, several splice variants can arise from a single gene with

different isoforms performing different biological functions. For instance, Troponin I (TnI), is a protein that plays an important role in muscular contraction. TnI expressed three isoforms in different types of muscle tissue that perform different functions, (ssTnI isoform in the slow skeletal muscle, fsTnI isoform in the fast skeletal muscle and cTnI isoform in the cardiac muscle) (Feng *et al*., 2012 & Yin, Ren, and Guo, 2015). In different cell types, alternative splicing gives additional layers for regulating cell-specific gene expression.

1.1.2 Pre-mRNA splicing catalysed by the spliceosome

A large macromolecular complex, known as the spliceosome, catalyses pre-mRNA splicing. This complex consists of five small nuclear ribonucleoprotein particles (U1, U2, U4, U5, and U6 snRNPs) and more than 200 auxiliary proteins. It is the relative expression and activity of these auxiliary proteins that have a big impact on alternative splicing. The activity of the spliceosome is regulated by cis-acting RNA sequence elements and trans-acting RNA-binding Proteins (RBP). Regulated reversible phosphorylation is vital for modulating the activity of both core spliceosomal components and accessory splicing factors. For instance, phosphorylation of the SR protein splicing factor SRSF1 modulates its interaction with U1snRNP, consequently modulating the assembly of the spliceosome. The function of SR proteins is regulated by their phosphorylation or dephosphorylation and splicing can be inhibited by both hypo- and hyperphosphorylation (Zhong *et al*., 2009). For example, dephosphorylation of SRSF1 is essential for the catalysis of the first transesterification reaction, while its phosphorylation promotes spliceosome assembly. Several important families of splicing kinases are involved in pre-mRNA splicing regulation, including the SR protein kinases

(SRPKs), the CDC2-like kinases (CLKs) and pre-mRNA splicing 4 kinases (PRP4K/PRPF4B).

1.1.3 Alternative splicing events: types and extent

75% of all human genes undergo cassette exon (exon skipping) events where it greatly increases in biodiversity. Therefore, exon skipping is the most common form of alternative splicing in eukaryotes (Weatheritt, Sterne-Weiler and Blencowe, 2016). The other types include alternative 3′ splice site selection (3′ SS selection), alternative 5′ splice site selection (5′ SS selection) and intron retention and mutually exclusive exons (Keren, Lev-Maor and Ast, 2010).

Figure 1.1 shows the different AS mechanisms. Exon skipping or cassette exon occurs when exons are spliced out from the transcript with flanking introns. Alternative 3′ splice site and 5′ splice site selection happen when two or more splice sites are recognised by splice factors at the beginning or end of an exon, respectively. Intron retention occurs when an intron remains in the mRNA transcript while one of two exon remains in the mRNA after splicing, but not both this is known as mutually exclusive exons (Cartegni, Chew and Krainer, 2002).

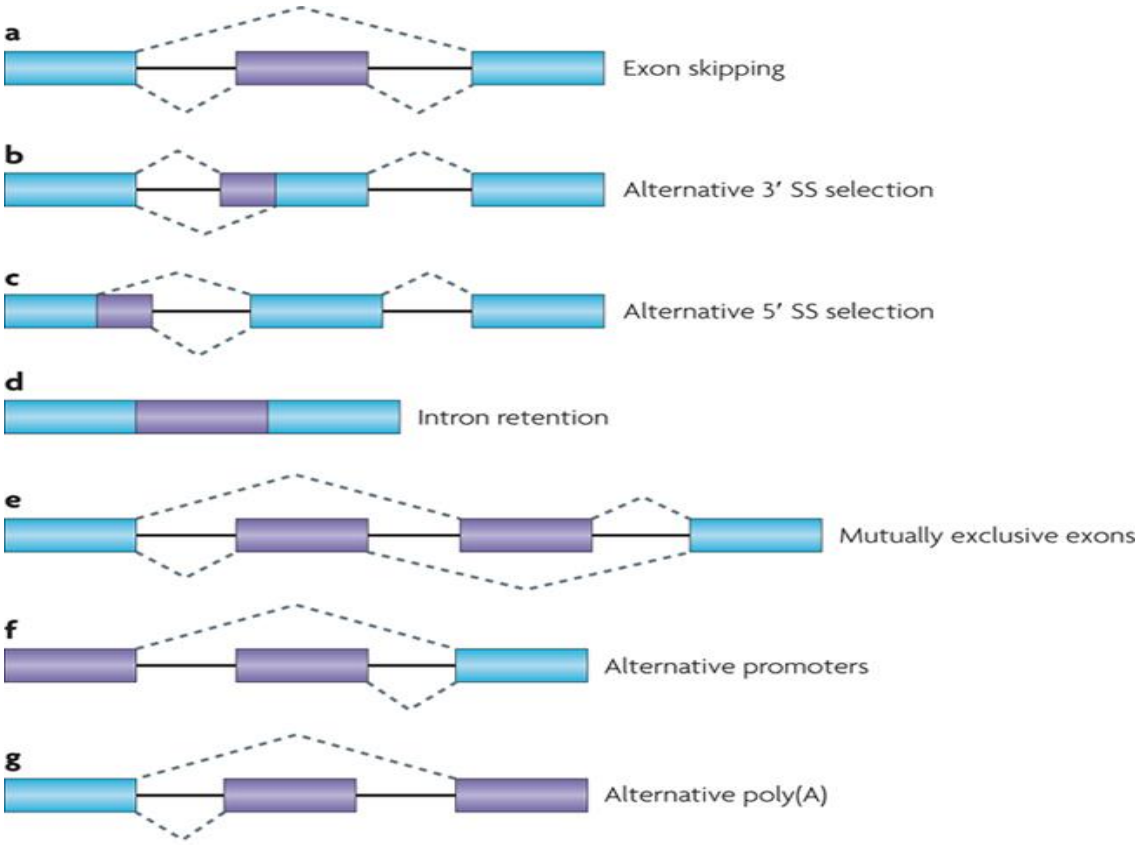

Figure 1. 1: Different types of alternative splicing (AS) events.

Shows different modes of alternative splicing (exon skipping (a), alternative 3′ splice-site selection (b), alternative 5′ splice-site selection (c), intron retention (d), mutually exclusive exons (e), alternative promoters (f) and alternative polyadenylation (g). by alternative splicing, the same initial transcript could be spliced in many ways giving deferent isoforms of the final transcript (figure adapted from Keren, Lev-Maor, and Ast, 2010)

1.1.4 Regulation of alternative splicing and splice factor kinases

Regulated reversible phosphorylation is vital for modulating the activity of both central spliceosomal components and accessory splicing factors. For instance, phosphorylation of the splicing factor SRSF1 modulates its interaction with U1snRNP, consequently modulating the assembly of the spliceosome. The function of SR proteins is regulated by

their phosphorylation or dephosphorylation and splicing can be inhibited by both hypo- and hyperphosphorylation.

Another study demonstrated the importance of AS in regulating histone methylation and demethylation in neurons (Fiszbein and Kornblihtt, 2016). It has also been reported that suppressing or activating some protein kinases, such as Serine/Arginine splicing factor kinase (SRPK1) affects splicing during angiogenesis (Amin *et al*., 2011 and Wagner *et al*., 2019). Therefore, controlling gene expression through protein kinase activity has allowed us to hypothesise that inhibiting SRPK1 and Clk1 could significantly change the splicing of different key genes such as VEGF.

Several important families of splicing kinases are involved in pre-mRNA splicing regulation, including the SR-Protein Kinases (SRPKs), the CDC2-like kinases (CLKs) and pre-mRNA splicing 4 kinases (PRP4K/PRPF4B). It has been observed that SR proteins interact with other proteins, the SR-related proteins, to regulate splicing. SR-related proteins carry RS domains and RNA binding motifs (PWI), or zinc finger motifs (Zn) (Zhou and Fu, 2013). The interaction between SR proteins and SR-related proteins occurs through the SR domains of both proteins, thereby initiating splicing (Shepard and Hertel, 2009). Some examples of SR-related proteins include both subunits of the U2AF heterodimer (U2AF-35 and U2AF-65), U1-70K, and the splicing co-activators SRm 160/300 (Long and Caceres, 2009).

PRP4 binds pre-mRNA splicing factors SRSF1 (SRp30a or ASF/SF2), PRP6 and pinin. It is an essential kinase that associates with both the U5 snRNP and the N-CoR deacetylase complexes. PRP4 manage pre-mRNA splicing with chromatin remodelling and transcriptional regulation.

1.1.5 Atypical alternative splicing in cancer

Errors in splicing regulation have been shown to contribute to disease states. Figure1.2 summarize the different types of mutation that can affect splicing. The 5′ and 3′ splice site, as well as the branchpoint A, are important for the excision of introns and the joining of the exon. Thus any mutation in the splice site can result in mis-splicing. There are regulatory sites that contribute to the regulation of AS, exonic and intronic splice enhancers and silencers are known as ESE, ESS, ISS and ISE. They play a very important role in alternative splicing regulation and mutations in them may lead the trans factors such as the SR protein to bind incorrectly or be unable to bind the sequences, thus resulting in mis- splicing. Here a few examples are given to illustrate the importance of alternative splicing in different tumours.

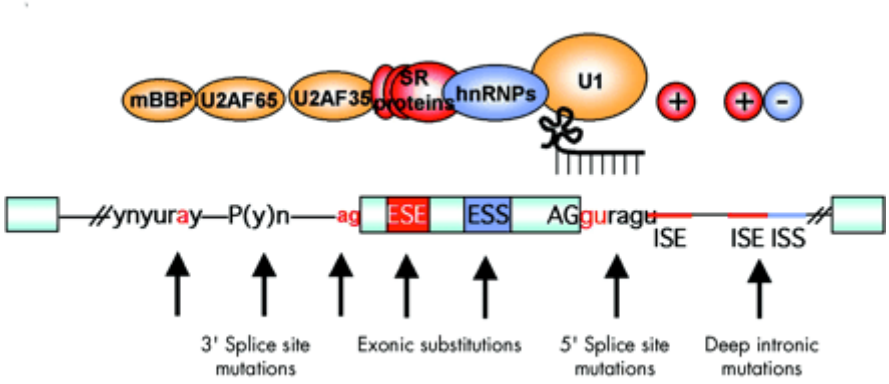

Figure 1. 2: possible mutations that can occur that affect splicing.

The regulatory sequences on the pre-mRNA such as the splicing sites, pyrimidine tract, exonic splicing enhancer (ESE), Exonic splicing silencer (ESS), intronic splicing enhancer (ISE), and intronic splicing silencer (ISS) are important as any mutation will result in the improper binding of the Trans factors involved in splicing. This will then lead to mis-splicing. Figure adapted from Baralle, 2005.

The Runt-related transcription factor 1 gene (*RUNX1*), also known as acute myeloid leukaemia 1 (AML1) is located on chromosome 21q22. It encodes a crucial haematopoietic transcription factor and regulates gene expression by binding to specific DNA sequences (Komeno *et al*., 2014). RUNX1 is essential for haematopoietic development (Zhao *et al*., 2012). The RUNX1 expresses two isoforms through alternative splicing of exon 6: Runx1 (with exon 6) and ΔRunx1 (without exon 6). The ΔRunx1 isoform blocks blood cell differentiation resulting in the massive accumulation of immature cells. It has been shown that ΔRunx1 is overexpressed in malignancies (Komeno *et al*., 2014). Acute myeloid leukaemia originates from different chromosomal abnormalities, such as t(8;21)(q22;q22) resulting in the fusion of RUNX1-ETO (Runt-related transcription factor 1- eight twenty-one) genes, the second is t(12;21)(p12;q22) resulting in the fusion of TEL-RUNX1 genes, the third is t(3;21)(q26;q22) resulting in the fusion of RUNX1/MDS1/EVI1 genes (Zhao *et al*., 2012). However, it has been reported that rare cases of patients with Philadelphia chromosome-positive (Ph+) are detected in AML. However, common cases of Ph+ are found in chronic myeloid leukaemia (CML) and they are considered as blast phases due to a rapid expansion of immature blood cells (blasts) (Bacher *et al*., 2011). Therefore, co-expression of RUNX1 with BCR–ABL1 (fusion gene necessary for the pathogenesis of CML) induces the acute myeloid leukaemia (AML) transformation in CML patients (Zhao *et al*., 2012), suggesting the importance of evaluating the effect of combinations of ΔRunx1 expression in CML cells.

Alternative splicing patterns are altered in cancer (Venable 2006). The expression of alternative splicing or tumour specific splice variants affects many cellular events that are critical in tumorigenesis (Skotheim 2007). For example, KLF6, a member of the

kruppel like transcription factor (KLF) family is a known transcription factor and a tumour suppressor in colorectal (Reeves *et al* 2004), lung (Ito *et al*.,2004) and gastric cancer (Cho *et al*., 2005). The expression of KLF6 is also able to reverse tumorigenic phenotypes (Kimmelman *et al*., 2004). KLF6 can be alternatively spliced to KLF6 SV1 (Narla *et al*., 2005). KLF6 SV1 is formed due to the use of an alternatively cryptic splice site in exon 2; the resultant protein doesn't contain the activation and DNA binding domain (Narla *et al*., 2005). KLF6 SV1 is able to compete with wild type KLF6 and thereby affect KLF6 function. KLF6 SV1 overexpression leads to tumour aggressiveness and poor prognosis for the patient. Also, there is twice as much KLF6 SV1 mRNA compared to KLF6 in prostate cancer samples compared to wild type prostate samples (Narla *et al*., 2005). This also has been observed in ovarian cancer. (DiFeo *et al*., 2006).

1.2 Splice factor kinase-1 (SRPK1)

1.2.1 SRPK kinases: structure and function

The SRPK family of kinases is highly specific for the SR family of splicing factors. The human genome encodes the SRPK family of kinases which through alternative splicing generate SRPK1, SRPK2 & SRPK3. SRPK1 is expressed predominantly (Zhou and Fu, 2013) and functions as a tumour suppressor or an oncogene in different cell types (Wang *et al.*, 2014). SRPK2 and SRPK3 are expressed in the nervous system and muscle cells, respectively (Zhou and Fu, 2013). Unless the cell is stimulated by a signal, most of the SRPKs are contained in the cytoplasm, However, SRPKs can mobilise to the nucleus during the M phase of the cell cycle and stimulate the aggregation of splice factors. For example, a number of studies suggest that SRSF1 phosphorylation mediated by SRPK1 is essential for its nuclear localization and the resulting splicing activity triggered by

stimulation of specific signalling pathways (e.g., IGF-1 and EGF growth factor treatments). There are other conditions that may contribute to increasing SRPK1 nuclear localisation such as cellular stress or osmotic stress. The human *SRPK1* gene is located on chromosome 6p21.2-p21.3. The SRPK1 protein has two kinase domains separated by a spacer sequence. The accessory domain is known to regulate SRPK1 localization as its deletion results in limited nuclear localization (Wang *et al*., 1998; Zhong *et al*., 2008). The accessory domain is essential for protein substrate phosphorylation as well (Plocinik *et al*., 2011). SRPKs phosphorylate specific serine amino acids of proteins rich in serine/arginine repeats (RS-domain). The N-terminus and C-terminus of SRPK1 play an auxiliary role as their deletion does not inactivate the catalytic activity kinase (Gosh and Adam, 2011).

1.2.2 Regulation of SRPK1 activity

An added layer of complexity comes from the finding that SRPK1 activity is regulated by the Akt cell signalling pathway. Akt (v-Akt Murine Thymoma Viral Oncogene)/ PKB (Protein Kinase-B) is a serine/threonine kinase that is involved in mediating different biological responses, such as inhibition of apoptosis and stimulation of cell proliferation. Zhou *et al* 2012 found that Akt activation plays a major role in EGF-induced splicing in HEK 293T cells through modulation of SRPK1 activity. In most cell signalling transduction cascades, Akt directly phosphorylates its targets, but in EGF treated cells, activated Akt binds and induces SRPK1 autophosphorylation. Using mass spectrometry (Zhou *et al* 2012) determined four in vitro phosphorylation sites in SRPK1. Two autophosphorylation sites (S33 and S309) and two other additional sites (T326 and S587) (figure1.3), which are phosphorylated only in the presence of active Akt. Consequently, they mutated both sites to alanine either in combination (K1-326A587A) or individually

(K1-587A, for S587) and (K1-326A for T326) and the result showed only the double mutation eliminated Akt-induced SRPK1 autophosphorylation in vitro. The kinase activity of SRPK1 on SR protein substrates such as SRSF1 was not affected by the mutation. (figure1.4).

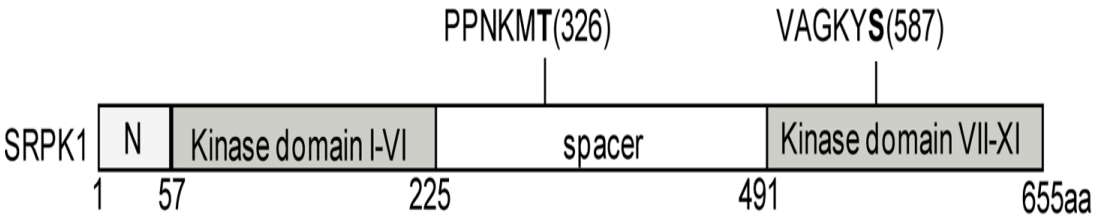

Figure 1. 3: Schematic presentation of SRPK1 domains.

Two candidate phosphorylation sites are highlighted in bold (T326 and S587) separated by a spacer sequence; an accessory domain (Zhou *et al*., 2012).

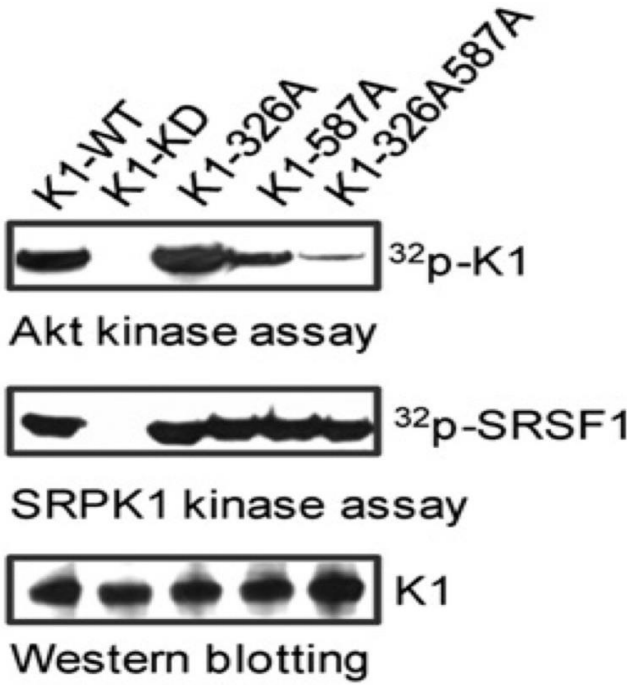

Figure 1. 4: Akt-mediated phosphorylation of SRPK1 at T326 and S587.

Double Alanine mutations (K1-326A587A) on two phosphorylation sites abolished Akt-mediated phosphorylation but had no effect on the kinase activity of SRPK1 on the SR protein SRSF1. There was

no major effect on Akt-induced SRPK1 autophosphorylation by individual phosphorylation site mutation (K1-587A, for S587) and (K1-326A for T326) (taken from Zhou *et al*., 2012).

How then does Akt signalling cause changes in the alternative splicing of genes? Following Akt signalling, SRPK1 autophosphorylation causes SRPK1 to concentrate in the nucleus where it can then phosphorylate nuclear splice factors, thus affecting alternative splicing outcomes (Zhou *et al* 2012). Might this apply in other cancer cells? Data suggests that alteration in Akt cell signalling in cancer cells leads to abnormal SRPK1 activity through autophosphorylation followed by nuclear accumulation, resulting in altered Hsp splicing from Hsp70- to Hsp90-containing complexes. This leads to enhanced SRPK nuclear translocation and SR protein phosphorylation in these cells. Thus one mechanism through which SRPK1 activity can be regulated is through its autophosphorylation. Chaperones which have been identified are the heat shock family and co-chaperones Hsp40/Hsp70 and Hsp90/Aha1. While Hsp40 targets region outside the accessory domain, Hsp90 targets the accessory domain (Zhong *et al*., 2008). Chaperone complex assembly is initiated by the binding of Hsp40/Hsp70 SRPK1 followed by the binding of Hsp90 and Aha1 a co-chaperone. Formation of SRPK1-chaperone-cochaperone complex also ensures the folding of SRPK1 into its active conformation as well as protects it from proteasome degradation. This model has been validated as inhibition of the chaperone Hsp90 ATPase activity has resulted in dissociation of the chaperone complex and SRPK1 nuclear localization (Pratt and Toft, 2003; Zhong *et al*., 2008).

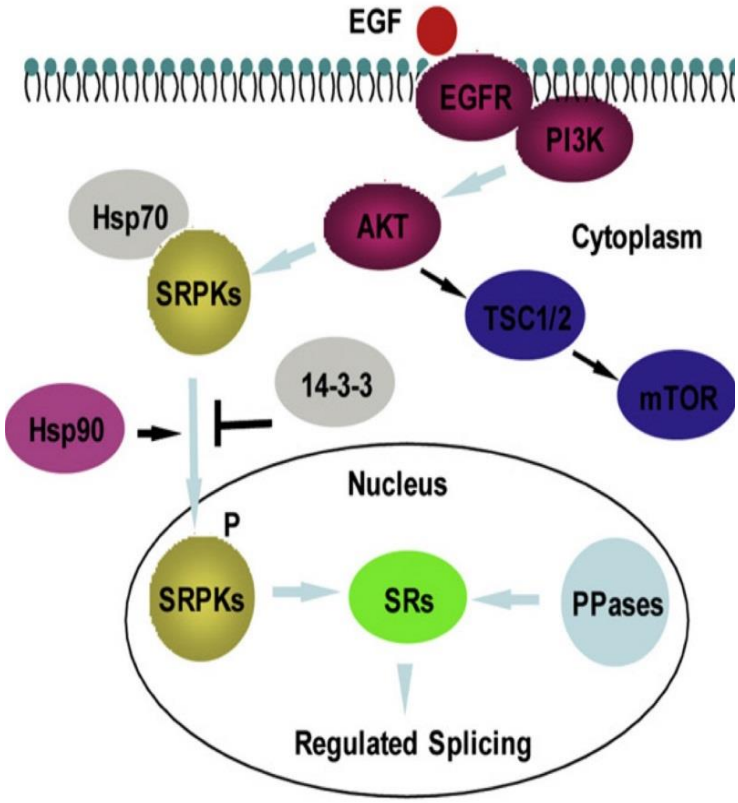

Figure 1. 5: Summary of EGF signalling through the Akt-SRPK-SR axis to regulate alternative splicing in the nucleus.

Hsp70 is responsible for inhibiting nuclear import of the splicing kinases, Hsp90 knocks off Hsp70 to facilitate nuclear import, and 14-3-3 functions to prevent excessive accumulation of the splicing kinases in the nucleus while PPases enzyme regulates the SRs phosphorylation (Adapted from Zhou *et al* 2012).

1.2.3 Molecular interactions of SRPK1

Like other protein kinases, SRPK1 interacts with several molecules which serve as a substrate or control its association with substrates. Such interactions result in the propagation of cellular function by the substrate or regulation of their activity either directly or indirectly. The SR-protein family of splice factors are its best-known substrate, especially SRSF1 (previously known as ASF/SF2). SR-proteins are a family of splice

factor which is characterised by the presence of at least one amino-terminal RNA recognition motif (RRM) and a C-terminal rich in RS peptides. SR proteins play an important role in the regulation of pre-mRNA splicing, mRNA nuclear export, translation and non-sense mediated RNA decay (Long and Caceres, 2009; Plocinik *et al*., 2011; Corkery *et al*., 2015). Phosphorylation of SR proteins by SRPK1 results in nuclear import of SR proteins and their localization into nuclear speckles (thought to be sites of splice factor storage). SRSF1 is a member of the SR protein family which has been extensively studied and to be strongly phosphorylated by SRPK1. SRSF1 has two RNA recognition motifs (RRM) and an RS domain of about 50 amino acids in length. It is known that SRPK1 interacts with about 10-12 amino-acid of the RS domain; an interaction which produces high-affinity binding and considered critical for the regulation of the extent to which SRSF1 is phosphorylated (Ngo *et al*., 2007; Plocinik *et al*., 2011). Phosphorylation of SRSF1 by SRPK1 has been shown to be in C- to N-terminal direction irrespective of the presence (SRPK1-FL) or absence of N-terminal (SRPK1ΔN) and spacer domain (SRPK1ΔS).

Furthermore, SRPK1 has been shown to regulate epidermal growth factor (EGF) activation of multiple signal transduction pathways such as JAK/STAT pathway. EGF is a proto-oncogene known to be up-regulated in tumour cells and also able to activate several oncogenic pathways in several cancers. This study suggests that EGF can be activated by SRPK1 via the phosphatidylinositol-3-kinase/protein kinase-B (PI3/Akt) pathway other than the well-known downstream mammalian target of rapamycin (mTOR) pathway to induce an alternative splicing events that result in series of re-arrangements with molecular chaperones and other regulatory factors to regulate the cellular distribution of the splicing kinases. in the nucleus (Zhou *et al*., 2012). Supporting

this finding is a mass spectrometry analysis of SRPK1phosphopeptides showing multiple phosphorylation sites which could be induced by EGF or Akt (Zhou *et al.*, 2012). Since SRPK1 has been shown to have both cytoplasmic and nuclear localization, it is thought that SRPK1 may have other substrates which underpin its cellular functions.

1.2.4 SRPK1 expression in malignancies

Abnormal SRPK1 expression is observed in epithelial malignancies, such as pancreatic carcinoma in which SRPK1 levels are increased (Bullock and Oltean, 2017). Hayes *et al* 2007 showed that SRPK1 levels are similarly upregulated in breast and colon tumours, with SRPK1 expression increases with tumour grade. Thus, SRPK1 could be used as a marker for tumour progression. Increased apoptosis in breast and colon tumour cells is associated with lower expression of SRPK1. In breast cancer cells, Xing-hua Li *et al* 2014 described that SRPK1 is up-regulated at both mRNA and protein level. The same up-regulation of SRPK1 at the mRNA and protein level was shown in non-small cell lung cancer (Liu H *et al* 2016), prostate cancer (Mavrou *et al*., 2014), glioma (Wu *et al*., 2013) and hepatocellular carcinoma (Zhou *et al*., 2013). Down-regulation of SRPK1 has been reported with tumours of germinal origin (ovarian cancer) where elevated expression of UCA1 RNA was identified which is linked to cisplatin resistance (Wang *et al*., 2014). SRPK1is also expressed in normal human retinal tissue where it might play an important role in the regulation of proliferation, migration, differentiation, and maturation of neurons and neuronal synapses of retinal tissue. Reduction in cells positive for SRPK1 protein was noticed in advanced and large retinoblastoma tumours as well as recurrences or metastases. Low levels of SRPK1 protein could be relevant to drug resistance mechanism in RB (Krishnakumaret *et al*., 2008; Wang *et al*., 2014). Thus both the upregulation and downregulation of SRPK1 might be oncogenic, in different contexts.

SRPK2 has also been reported to be upregulated in multiple types of cancers. In clinical colon cancer samples, SRPK2 was found to be up-regulated although its contribution to colon cancer is not yet clear. SRPK2 overexpression enhanced growth and migration of colon cancer cells (HCT-15 and HT-29) while SRPK2 knockdown resulted in inhibition of growth, migration and tumorigenicity of colon cancer cells (Wang *et al*., 2016).

1.2.5 SRPK1 as a therapeutic target

Therapeutic intervention targeting SRPK1 represents a promising approach to treating cancers in which SRPK1 is involved. In pancreatic cancer cell lines Capan-1, Capan-2, MiaPaCa2, Panc1, BxPC3, and Su86.86, siRNA-mediated down-regulation of SRPK1 resulted in a dose-dependent decrease in proliferation and an increase in apoptosis and an improved sensitivity of tumour cells to gemcitabine and/or cisplatin, suggesting that SRPK1 is a new potential target for ductular pancreatic cancer treatment (Hayes GM *et al* 2006). In metastatic melanoma, the existing treatment doesn't target angiogenesis, which is a vital part of any tumour progression. The current therapies for melanoma target either cancer mutations driving growth or immune-based therapies. Gammons *et al* 2014 suggested inhibiting splice-site selection with SRPK1 inhibitors (e.g. SRPIN340) to alter VEGF splicing, reducing expression of the pro-angiogenic VEGF165 isoform, thereby repressing angiogenesis in the context of melanoma. Accordingly, SRPK1 inhibitors may be used as therapeutic agents. In prostate cancer (PCa) Mavrou *et al* 2014 showed that in PC-3 cells with SRPK1 knockdown, or using SRPK1 inhibitors that were administrated intraperitoneally in an orthotopic mouse model of PCa, VEGF splicing switched toward anti-angiogenic splice isoform, VEGF165b. This resulted in tumours that developed more slowly in xenografts with reduced vascular density. In PC-3 cells in which SRPK1

was knocked-down by RNA interference, no effects were observed on growth, migration, proliferation and invasion abilities of PC-3 cells in vitro. These results could provide the basis for anti-angiogenic therapeutic strategies that target SRPK1 inhibition in prostate cancer.

1.3 The Wilms tumour suppressor (WT1)

1.3.1 WT1; background

The tumour suppressor gene *WT1* was cloned in 1990 due to its association with WAGR syndrome (Wilms tumour, aniridia, genital anomalies and intellectual disability; Rose *et al*., 1990). WT1 is a zinc finger protein that is essential for the development of multiple different mammalian tissues including the mesothelium, gonads, heart, blood vessels, blood, spleen, nervous system, eyes, lungs, liver and kidneys. Knockout of the *WT1* gene in mice is embryonically lethal and the mice fail to develop kidney and gonads thus indicating that WT1 is important in urogenital development (Kreidberg *et al*., 1993). In adult humans, WT1 is highly expressed in the spleen, smooth muscle and kidney as well as both male and female reproductive systems. Mutations in *WT1* are associated with Wilms' tumour, in Denys Drash Syndrome, and Frasier Syndrome (Barbaux *et al*., 1997; Klampt *et al*., 1998). DDS is characterised by childhood nephrotic syndrome, glomerular sclerosis**,** end-stage renal failure and Wilms tumours. Frasier Syndrome is very similar to DDS and is characterized by focal glomerular sclerosis, male to female sex reversal and gonadal dysgenesis (Moorty *et al*., 1987).

1.3.2 WT1 in cancer

Leukaemias, melanomas and breast cancers are all examples of adult cancers which, in some cases, can be WT1-dependent. In adult cancers in which WT1 is implicated, WT1 often exhibits oncogenic activity. WT1 can even be found to be expressed in adult cancers of tissues in which WT1 would not normally be expressed. Adult cancers which have been found to be WT1-dependent in some cases include leukaemias, melanomas, renal cancers and breast cancers. WT1 is overexpressed in as many as 80% of cases of some subsets of leukaemia which indicates that WT1 can also have oncogenic activity (Inoue *et al*., 1997). In addition, WT1 mutations can also be associated with poor prognosis such as in both adult and childhood cases of acute myelogenous leukaemia (AML) (Paschka *et al*., 2008 and Hollink *et al*., 2009). WT1, therefore, is a highly complex, context-specific transcription factor with multiple different functions and mutations in different cancer types. WT1 has even been found to be overexpressed in some leukaemia cases whereas there is loss of function mutations in others (Artibani *et al*., 2017 and Lee *et al*., 2017).

1.3.3 WT1 structure and function

WT1 can exhibit a range of different activities and functions, in part due to the alternative splicing of the *WT1* gene. The *WT1* gene spans 50kb on chromosome 11p13 and it encodes a transcription factor that contains four zinc fingers domain used for DNA binding; it is structurally homologous to the early growth response (EGR) family of transcription factors (Rauscher *et al*., 1993). In addition, the N-terminus of WT1 contains a putative RNA recognition motif and also a proline/glutamine-rich region involved in transcriptional transactivation or repression domain. There is a self-dimerization domain; however, the significance of the ability of WT1 to dimerise remains unclear (reviewed in

Scholz and Kirschener 2005). WT1 is also alternatively spliced as there are several different isoforms of WT1 following post-transcriptional modifications (including alternative splicing and alternative upstream CUG translation start site). The four main splice variants of WT1 arise from either including or excluding exon 5 from the mature mRNA, and this results in proteins that contain or lack a 17 amino acid sequence (between the N-terminus and the zinc finger domains) and a three amino acid insertion of lysine, threonine and serine (KTS) due to an alternative 5′ splice site in exon 9 (between the third and fourth zinc fingers domain). The –KTS isoforms have strong DNA binding capacities and act as a transcriptional regulator while the +KTS isoforms have been found to be active post-transcriptionally and are able to bind to RNA. The +KTS isoform is also able to bind to the splice factor U2AF65 (Davies *et al*., 1998) and localise to nuclear speckles (Larsson *et al*., 1995). +/-KTS ratios are conserved in evolution and disruption of the ratio from 2:1 to 1:2 results in Frasier Syndrome (Klamt *et al*., 1998). (figure1.6).

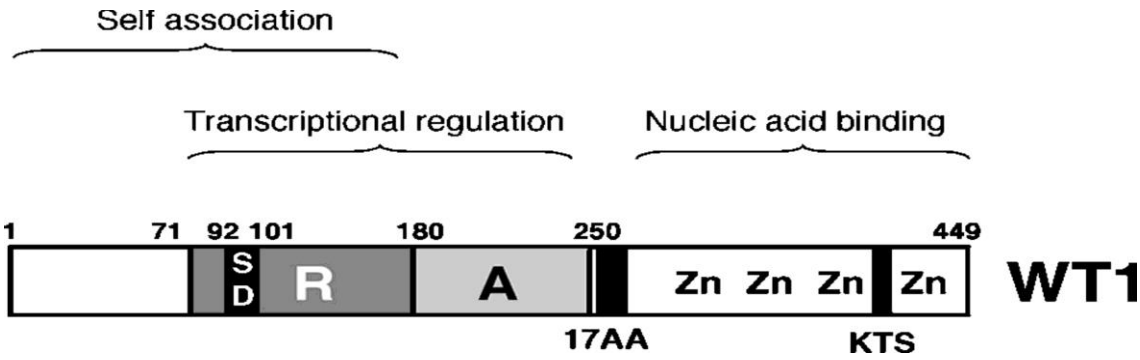

Figure 1. 6: structure of the WT1 protein.

WT encodes four zinc fingers, annotated as ZF in the figure, and is alternatively spliced into four major isoforms. The four major isoforms are formed due to the inclusion or exclusion of 17 amino-acids encoded by cassette exon five and the amino acids KTS that arise from an alternative 5′ splice site in exon nine. (Adapted from Roberts, 2005).

1.3.4 The BASP1-WT1 interaction

Brain acid-soluble protein (BASP1) is a transcription co-repressor that interacts directly with WT1. In human embryonic kidney (HEK) cells, BASP1 was shown to translocate to the nucleus where it regulates WT1 to exert its effect on WT1 target genes. The mechanism of transcriptional regulation by BASP1 involves the recruitment of a large, repressive protein complex containing histone deacetylase. BASP1's nuclear localisation sequence (NLS) allows it to translocate to the nucleus where it binds to WT1 at the promoters of WT1 target genes (Carpenter *et al*., 2004).

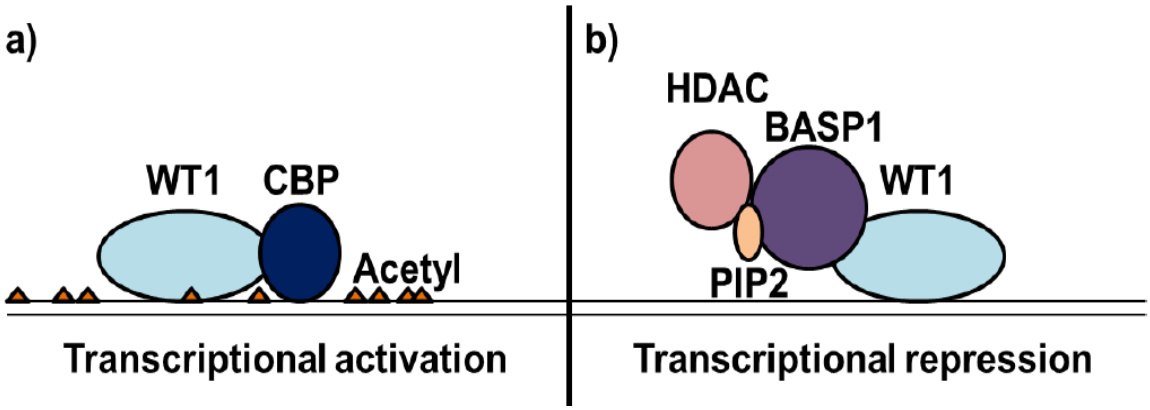

Figure 1. 7: BASP1 acting as a transcriptional co-suppressor for WT1.

a) WT1 (Wilms tumour 1) binds to target genes and recruits CBP (CREB binding protein), resulting in histone acetylation and activation of transcription. b) BASP1 binding to WT1 results in the dissociation of CBP and the recruitment of HDAC1 (Histone Deacetylase) resulting in deacetylation of histones and repression of transcription. BASP1 binding of PIP2 (phosphatidylinositol 4, 5 bisphosphate) allows the recruitment of HDAC (Adapted from Toska *et al*., 2012).

The N-terminal myristoyl group of myristoylated BASP1 allows the recruitment of phosphatidylinositol 4, 5 bisphosphate (PIP2) to the BASP1-WT1 complex located at the WT1 target gene promoter (figure1.7a). BASP1 binding of PIP2, in turn, allows the recruitment of histone deacetylase 1 (HDAC1) (12). HDAC1 is a histone remodelling factor that removes the acetyl side chain from a histone lysine residue (H3K9) resulting in chromatin condensation. The recruitment of HDAC1 to a WT1 target gene results in local condensation of chromatin and thus transcriptional repression of the target (figure1.7b). BASP1 is also able to recruit prohibitin, another transcriptional co-repressor. Prohibitin, in turn, recruits ATP dependent chromatin remodelling factors such as Brahma related gene 1 (BRG1) which results in the dissociation of CREB binding protein (CBP) from the promoter (Toska *et al*., 2012). CBP has histone acetyltransferase activity (results in relaxation of chromatin structure) and is a scaffold protein for the transcriptional complex (Ogryzko *et al*., 1996). The dissociation of CBP, therefore, results in further transcriptional repression of WT1 target genes. BASP1 is, therefore, able to convert WT1 activity from a transcriptional activator to a transcriptional repressor of WT1 target genes.

1.3.5 Regulation of SRPK1 transcription by Wilms' tumour gene-1 (WT1)

Several studies have linked WT1 to the regulation of *SRPK1* transcription. Up-regulation in SRPK1 expression has been observed in a wide variety of tumours such as hepatocellular carcinoma (Zhou *et al*., 2013), lung adenocarcinoma, squamous cell lung carcinoma (Gout *et al*., 2012), pancreatic, colon and breast cancer. Moreover, expression of SRPK1 was noticed to be increased in Denys Drash Syndrome (DDS) podocytes, epithelial cells of the visceral layer of a renal glomerulus. DDS is a rare disorder consisting of the triad of congenital nephropathy, Wilms tumours, and intersex disorders.

DDS podocytes harbour a mutated *WT1* gene. WT1 was found to bind and represses *SRPK1* promoter and downregulate its expression in normal podocytes, but is unable to repress SRPK1 in DDS podocytes (Amin *et al*., 2011). Upregulation of SRPK1 has been linked to hyperphosphorylation of SRSF1, leading to increases in the nuclear import of SRSF1 and hence a splice shift in VEGF to favour the proangiogenic isoform in DDS.

The cellular interactions of SRPK1 with SRSF1 have become a major pathway through which SRPK1 affects angiogenesis. Recent research has shown that SRPK1 and its best -studied substrate, SRSF1 form an essential pathway responsible for the regulation of the alternative splicing of vascular endothelial growth factor (VEGF) pro/antiangiogenic isoform in renal epithelial cells (podocytes) (Amin *et al*., 2011) and in colon carcinoma cells (Oltean *et al*., 2012). The latter study further demonstrated that a knockdown of SRPK1 increased levels of VEGF anti-angiogenic isoform as well as prevents tumour growth in xenograft by a reduction in microvessel density. Similar findings have been observed in a study using the prostate cancer cell line PC3 (Mavrou *et al*., 2014).

A recent study has observed the transcriptional regulation of SRPK1 by WT1 in a different context, making use of *SRPK1* promoter: luciferase reporters designed in the Ladomery laboratory, (Amin *et al*., 2011). Wagner *et al*., 2019 has revealed that WT1, SRPK1, SRSF1, and the angiogenic VEGF isoform were highly expressed in tumour endothelium compared to normal lung endothelium. An inducible conditional vessel-specific knockout of WT1 reduced WT1, SRPK1, and SRSF1 expression in endothelial cells and induced a shift towards the antiangiogenic VEGF isoform. WT1 (-KTS) isoform directly binds and activates both the promoters of SRPK1 and SRSF1 better than WT1 (+KTS) isoform in endothelial cells. This suggests that WT1, potentially, has the ability not only to repress SRPK1 but also to activate its transcription.

1.4 Brain abundant membrane attached signal protein 1 (BASP1)

1.4.1 BASP1; background

Brain acid-soluble protein 1 (BASP1) is a multifunctional protein found in many different tissues and cell types throughout the human body. The RNA and protein expression levels of BASP1 are particularly high in the brain and are found across a vast array of cell types within multiple areas of the brain including neuronal cells and glial cells of the cerebral cortex, hippocampus and caudate, endothelial cells and neuropils of the cerebral cortex and cells of both the granular layer and the molecular layer of the cerebellum (The Human Protein Atlas. 2018). BASP1 was first characterised in the axonal termini of neuronal cells as a member of the GAP-43 family, a group of proteins which were known to be involved in axon growth and memory formation (Mosevitsky *et al*., 1994). However, BASP1 has since been identified in a vast array of different organs, tissues and cell types throughout the body including but not limited to those of the endocrine tissues, bone marrow, lungs, stomach, kidneys and skin, as well as both male and female reproductive tissues (H. P. Atlas. 2018). Depending on the cell type and location, BASP1 has been proposed to perform a range of different context-specific activities and functions (Mosevitskiĭ *et al*., 1996).

1.4.2 BASP1 in cancer

BASP1 has been shown to exhibit various tumour suppressive activities in acute myelogenous leukaemia cell lines including proliferation inhibition and increased apoptosis. In addition, the BASP1 promoter is methylated and silenced by the AML1-ETO fusion protein in AML cells (Zhou *et al*., 2018). As WT1 is overexpressed in many

cases of AML it is possible that BASP1 exerts its tumour suppressor activity by co-repression of WT1 target genes. Similarly, BASP1 has been shown to be downregulated by DNA methylation in some hepatocellular carcinoma cases (Moribe *et al*., 2008). BASP1 has also been shown to have reduced expression in thyroid cancer cells compared with normal tissue, and restoration of BASP1 resulted in inhibition of cell growth and migration (Guo *et al*., 2016). These reports show that BASP1 can act as a tumour suppressor in multiple cancer types and is often a target of repression in cancer cells. However, one exception has been demonstrated in cervical cancer cells. In the latter context, BASP1 expression was shown to promote cancer cell proliferation, colony formation efficiency and tumourigenicity as well as being associated with increased stage progression and poor prognosis (Tang *et al*., 2017).

However, in breast cancer, BASP1 acts as a tumour suppressor (Marsh *et al*., 2017). In addition to exhibiting tumour suppressor activity, BASP1 expression has been associated with increased breast cancer patient survival. Interestingly, BASP1 was also found to colocalise with several components of the nuclear actin network including β-actin, gelsolin, myosin-1C (MYO1C) and flightless 1 (FLI1). These nuclear actin network proteins are known to interact with ERα, the hyperproliferative hormone receptor protein target of the breast cancer drug tamoxifen (Ambrosino *et al*., 2010). In the same study, BASP1-ERα colocalisation was then observed and it was shown that BASP1 colocalises with ERα in the nucleus, suggesting BASP1 as an ERα cofactor. Subsequent investigation of the effect of BASP1 expression on tamoxifen action was conducted and it was shown that 40% of the genes regulated by tamoxifen in MCF7 cells were BASP1-dependent. BASP1 expression was also found to enhance the inhibitory effects of tamoxifen on cell proliferation and colony formation (Marsh *et al*., 2017).

In summary, in most contexts, BASP1 appears to act as a tumour suppressor. In terms of its interaction with WT1, the implication is that where BASP1 is active, WT1 acquires tumour suppressor functions; whereas when BASP1 is absent, WT1 is more oncogenic.

1.4.3 BASP1 structure

The primary structure of BASP1 is highly conserved between species and in most cases, BASP1 knockdown is lethal in animal models (Carpenter *et al*., 2004). Notable structural motifs of BASP1 are its PEST (Proline, Glutamic acid, Serine, Threonine) sequences, phosphorylation sites, nuclear localisation sequence and N-terminal myristoylation motif (Mosevitsky *et al*., 1997 and Khan *et al*., 2003) (figure 1.8).

Figure 1. 8: Structure of human BASP1

Notable regions are denoted by MM (Myristoylation motif), NLS (Nuclear Localisation Sequence), P-site (phosphorylation sites) and PEST (PEST motifs). Residue number is indicated by a scale above the diagram. Many more phosphorylation sites have now been proposed but only the four most referenced sites were included. (Adapted from Roberts, 2005).

PEST motifs are regions of protein rich in proline, glutamic acid, serine and threonine that are strongly associated with a fast protein turnover rate (Mosevitskiĭ *et al*., 1996). The multiple phosphorylation sites can be targeted by protein kinases such as protein kinase C (PKC) which can affect BASP1 activity and membrane binding capability (Maekawa, H Murofushi and Nakamura, 1994). The N-terminal myristoylation motif allows BASP1 to anchor to lipid membranes with some specificity for certain lipids such as neutral phosphatidylcholine (Khan *et al*., 2003). Once bound to the membrane, BASP1 is able to modify the lipid makeup of the membrane in close proximity by accumulating cholesterol at the site, in some cases to such an extent that cholesterol crystals can form (Epand, Epand and Maekawa, 2003). The N-terminal myristoyl motif provides BASP1 with some hydrophobic character, despite it being a mostly hydrophilic protein (Mosevitskiĭ *et al*., 1996). N-terminal myristoylation of this motif is required for many of BASP1s functions (Korshunova *et al*., 2008 and Toska *et al*., 2012).

1.4.4 BASP1 functions

BASP1 can have many different functions depending on the tissue environment, cell type and presence of other cofactors and transcription factors. Within neurons, BASP1 has been proposed to have a range of functions that include involvement with synaptic signal transmission, neuronal signal transduction, neurite growth, regeneration and memory formation. BASP1 has been shown to be upregulated following multiple forms of nerve injury in several neurone subtypes and this upregulation is associated with neuron regeneration (Mason *et al*., 2002). Increased expression of BASP1 has also been shown to promote both NCAM (neural cell adhesion molecule) independent neurite outgrowth and nerve sprouting. This is an essential process in the development of proper brain

structure, particularly in the later stages of development. It is now known that BASP1 likely has additional functions in other cell types. BASP1 has been shown, in the presence of WT1 to be capable of altering K562 myelogenous leukaemia cell's properties to differentiate into cells with neuron-like morphology (Goodfellow *et al*., 2011). BASP1 also likely has roles in the development of other tissues, such as the kidneys. BASP1 is expressed during kidney nephrogenesis and continues to be expressed into adulthood, with expression being limited to the podocyte cells (Carpenter *et al*., 2004). This expression pattern seen in kidney development is shared by the transcription factor WT1 that is essential for proper kidney development (Kreidberg *et al*., 1993). The co-expression of WT1 and the co-repressor BASP1 is consistent with the ability of WT1 to repress SRPK1 in podocytes (Amin *et al*., 2011).

1.5 *ERG* (ETS-related gene)

1.5.1 *ERG* (ETS-related gene)

The oncogene ETS-related gene (*ERG*) was first described in 1987 in the context of colorectal cancer (Reddy, Rao and Papas, 1987). ERG is a member of the E-26-transformation-specific (ETS) family of transcription factors. This family play an important biological role in the human body such as bone development, angiogenesis and haematopoiesis. ERG has been proposed to perform a range of different context-specific activities and functions. Recently ERG was found to be highly associated with several malignancies as it plays transcriptional regulatory roles. In several cancers, ERG has been used as a marker to evaluate the tumorigenicity and prognosis. Thus it has become a target for multiple therapeutic approaches (Adamo and Ladomery, 2016).

1.5.2 ERG in cancer

Acute T-lymphoblastic leukaemias and prostate carcinomas are all examples of adult cancers in which *ERG* is overexpressed. For instance, ERG overexpression is a sign of poor prognosis as the relapse rate of acute T-lymphoblastic leukaemias cases with ERG-positive T lymphoblast is four times higher (Baldus *et al*., 2006). In prostate carcinoma, overexpression of *ERG* result from a gene fusion with the androgen-driven promoter of the *TMPRSS2* gene (Tomlins *et al*., 2005) ERG is not normally expressed in prostate epithelia (Deramaudt, Remy and Stiegler, 2001) but in the malignant prostate cancer, *ERG* is one of the most overexpressed oncogenes, in as many as 50% of cases (Vanaja *et al*., 2003 and Tomlins *et al*., 2008). Poor prognosis in prostate cancer is associated with ERG overexpression as the tumour stage, metastasis and high Gleason score shorter

survival times is the characters of prostate cancer with up-regulated ERG (Tomlins *et al*., 2005).

ERG is considered to be a prognostic marker for prostate cancer and AML. In prostate cancer patients, a higher rate of TMPRSS2: ERG fusion protein is associated with an increase in the possibility of recurrence compared to patients without the fusion protein (Nam *et al*., 2007). In AML, for instance, ERG expression was proven to be a useful negative prognostic factor and provided more information about the stage of the AML with the additional established molecular markers (Metzeler *et al*., 2009).

1.5.3 ERG structure and regulation

Full-length ERG protein is a 486 amino-acid 54kDa and the *ERG* gene is located on chromosome 21q22.3 cancer (Reddy, Rao and Papas, 1987). The ETS DNA-binding domain (EBD) is the main identifiable structural character of the ETS family of transcription factors. EBD is important in defining ERG activities and functions. The EBD is a domain of 85 amino-acids with DNA recognition and binding activity. ERG is alternatively spliced as there are several different isoforms following is post-transcriptional modifications. Exon skipping is a common splicing event that alters the splicing of the cassette exon 7b. There are several documented alternative splicing events involving *ERG* pre-mRNA that generate at least 15 protein variants.

The regulation of ERG transcription and expression is not fully understood. However, hypermethylation in cancer regulates the activity of the *ERG* promoter (Schwartzman *et al*., 2011). The hypermethylation of *ERG* promoter leads to transcriptional repression of ERG expression in T-lymphoblastic leukaemia. Downstream of ERG's promoter, the ERG +85 enhancer region is highly active in T-cell acute lymphoblastic leukaemia (T-ALL) in mice. In contrast in human T-ALL cell lines, the binding of ERG +85 enhancer

region to ETS transcription factors results in ERG overexpression and increased leukaemic cell proliferation (Thoms *et al*., 2011). In prostate cancer, ERG was described to transactivate its transcription as a result of feedback in which ERG binds to ETS motifs present in its own promoter. This is usually associated with highly invasive prostate cancer cells (Mani *et al*., 2009 and Mani *et al*., 2011).

1.5.4 ERG function

ERG perform several biologically important roles throughout the human body. ERG knockout in mice leads to embryonic lethality associated with vascular defects (Birdsey *et al*., 2015). ERG protein expression and RNA levels are particularly high in the embryonic neural crest and embryonic mesoderm and endothelium where it is important for the synthesis of urogenital and vascular systems (Birdsey *et al*., 2008 and Vijayaraj *et al*., 2012). During vascular development, ERG levels decrease but still play a vital role in regulating angiogenesis, the pluripotency of hematopoietic stem cells and the homeostasis of endothelial cells (McLaughlin *et al*., 2001). ERG is expressed in bone and soft tissue neoplasms where it regulates cartilaginous differentiation and bone development (Shon, Folpe and Fritchie, 2014). Moreover, ERG was described by (Thoms *et al*., 2011) to be essential for the maintenance of normal blood platelet numbers, haematopoiesis, and normal hematopoietic stem cell function. Since B and T cell lymphocytes both arise from hematopoietic stem cells, ERG was found to be expressed in both pre and mature lymphocytes while ERG expression in T lymphocytes was only detected transiently during T-lineage specification but not in mature T-lymphocytes (Anderson *et al*., 1999). In the case of acute lymphoblastic leukaemia, abnormal ERG expression in T-cells promotes the accumulation of immature lymphoblasts (Thoms *et al*., 2011).

Our laboratory has had an active interest in the ERG transcription factor since 2008. Inspection of the SRPK1 promoter (figure 1.9), from sequence -499 to +100, looking for the core ETS binding site, GGA(A/T) (so, therefore (A/T)TCC on the complementary strand), suggests the presence of at least nine potential binding sites. This core sequence could be recognised by different ETS transcription factors (ERG's precise target sequences are not yet clear; Adamo and Ladomery 2016); but it is tempting to speculate that ERG, alongside WT1, might transcriptionally regulate SRPK1.

GGGTCACAGGTTCT**TTCCTTCC**AGTCTTTTTGTGTTGCTCCCACTCCCTTTTCTTTCT

CACATGTAATTTTT**TTCC**ATTTTCTTTAAATAGTATCTCAACTGGGCTCACAATAGCT

CAGGGAAGGAGAAACTGGGACATGCCTGATTAATCCATTTTACAGGCCA**GGAA**ACTGA

GGCAGATCCCAGTTGCCTCCGAAGCTCTGACTCAGCAGCATGCAGAGAGCCCTGCCGC

TCTCTGCGCCTTTTCTAAACAAATAGAACAAAACTAACCTTGCCAGGT**TTCC**AAGCTT

GGATCTCTAACACTCCTTCAACGTTCACCCCGGCG**TTCC**TCCCCGCTGCGCCCCCTCC

CTCTCCTTGCCGCCCCCTCCTCGGGAGCAGGTGGTAGGCTCCGCGCCCAACGCGCAAG

CGCGCGGCATCGTGGGGCGGGGGTGGGGCGGGACTGAGGGCGGAGTGTGAGCGGGCTC

GGTTTTGGGCCGCGGCGGGAGCGGGAGTCGCCGCCACTCGAGTGCGCAGGCGCCTGGC

GATTACCGGTCTCACCATGGAGC**GGAA**AGGTGAGCGGTGGAGCGGCCTCCGCCACGAG

GGGCAATGGTCGCCGGGGCG

Figure 1. 9: Human SRPK1 promoter sequence

Putative core ETS binding sites are indicated in bold (GGAA or TTCC)

1.6 Hypothesis and aims

1.6.1 Hypothesis

In summary, based on the published work showing the involvement of SRPK1 in cancer pathology, it is important to understand in further details how SRPK1 expression and activity is regulated in cancer cells. Could SRPK1 expression be regulated by the WT1 transcription factor in cancer cells? Are other WT1 transcriptional cofactors such as BASP1 involved in the regulation of SRPK1? Do other transcription factors such as ERG contribute?

1.6.2 Aim and objectives of the project

The overall aim of this project was to investigate the potential regulation of SRPK1 transcription in cancer cells by WT1, BASP1 and ERG with a view to gaining a better understanding of how SRPK1, and the alternative splicing events downstream of it, might be regulated. Prostate cancer cells (PC3), osteosarcoma (MG63) and leukaemia (K562) cell lines were used as a model system to address this aim. The specific objectives were as follows:

- Objective 1) Confirm the effect of SRPK1 inhibition on cancer cell biology properties.
- Objective 2) Determine whether or not the transcription factor WT1 contributes to the regulation of SRPK1 transcription in cancer cell lines.
- Objective 3) Investigate whether or not WT1's effect on SRPK1 transcription in cancer cell lines can be modified by the co-repressor BASP1.
- Objective 4) Determine whether or not the transcription factor ERG contributes to the regulation of SRPK1 transcription in cancer cell lines.

2 Chapter Two: Material and Methods

2.1 Tissue culture

2.1.1 K562 and B-K562 cells

The K562 cell line (ATCC® CRL-3344) which grows in suspension was cultured using RPMI-1640 culture medium with L-glutamine both purchased from Sigma Aldrich (product code: R8758). Culture medium was further supplemented with 10% foetal bovine serum (FBS) and 5ml of 10mg/ml of a penicillin/streptomycin mixture which was used to prevent cell infection. Both foetal bovine serum (FBS) (F9665/lot: 045M3318) and antibiotics were purchased from Sigma Aldrich (Lot: P4333/025M4818V). Cells used were between passage six to nineteen. Sub-culturing of K562 cells involves the collection of the cell suspension into a tube then centrifugation at 1000rpm for 5mins (Allegra™ X-22R Benchtop Centrifuge), remove the media and resuspended the pellet in a fresh media. Cells were seeded at the density of 0.3-0.5x10^5 in a T_{75} flask and sub-cultured every 48-72hours. B-K562 cells (obtained from a collaborator at the University of Bristol) were grown in similar conditions except for 2 mg/ml G418 (Sigma) was added to the media to maintain selection for BASP1-expressing K652 cells.

2.1.2 PC3, DU145 and MG63 cells

PC3, DU145 human prostate cancer cells and MG63 osteosarcoma cells between passage 7 and 10 were used for this study. Cells were purchased from ATCC (PC-3, ATCC® CRL-1435™, DU 145, ATCC® HTB-81™ and ATCC® CRL-1427). These cells lines are adherent and were cultured in DMEM (Sigma Aldrich) supplemented with 10% foetal bovine serum (BSA) (Sigma Aldrich) and a final concentration of 10mg/ml of a penicillin-streptomycin mix (PS) (Sigma Aldrich). Using this media, cells were seeded

at densities of 0.3-0.5x10^5 in a T_{75} flasks and were sub-cultured every 48-72hours, detached from flasks using trypsin EDTA.

2.1.3 Cell line thawing and freezing

To defrost cells, cryovials were removed from liquid nitrogen and thawed at 37°C for 1 minute; they were centrifuged at ≥13,000 × g for 3 minutes and cultured in 3 mL of appropriate media in a T_{25} flask.

To freeze the cells, cells re-suspended in freeze medium (75% RPMI-1640, 20% FBS and 5% dimethyl sulfoxide (DMSO) at > 1 × 10^6 cells/mL, and transferred to cryogenic vials. They were then stored at -80°C in a Mr Frosty (Nalgene® Mr Frosty, Sigma-Aldrich, UK), a slow freezing chamber with isopropanol, for 24 hours before being transferred to liquid nitrogen for long term storage. Adherent cells densities of > 2 × 10^6 cells/mL were re-suspended in 85% FBS and 15% DMSO and treated as above.

2.1.4 Plasmid transfections

PC3, DU145, K562 and MG63 cells were seeded in 24 well plates at 5 x 10^4 per well and left for 24 hours before transfection. 24 hours after plating, cells were transfected with a ratio of transfection reagent (Lipofectamine™ 2000) to plasmid DNA of 4:1 (2µg/100µl). Transfection was performed according to the standard manufacturer's protocol. According to Lipofectamine™ 2000 (life technologies) protocol 7.5µl of the transfection reagent was mixed with 2500 ng of plasmid DNA and Opti-MEM® Medium (Gibco) then incubated for 20 minutes prior addition to the cells. Following that Opti-MEM® Medium and culture media were added to the cells then the cells were incubated for the desired amount of time (48-72 hrs) at 37°C. (See appendix for plasmid maps)

2.1.5 Overexpression of WT1, ERG and BASP1

Plasmid transfections were carried out as detailed in section 2.1.4. To detect the effect of the overexpression of WT1 on SRPK1 at the transcriptional level, (+/- KTS) WT1 isoforms were transfected at a range of different concentrations (e.g. titrating 0µg, 1µg, 1.2µg, 1.5µg, 2.0µg and 2.5µg) into K562, PC3 and DU145 cells with constant concentrations of Renilla expressing plasmid and SRPK1 promoter: luciferase constructs, wild-type and mutant (table2.3), then the promoter's activity was monitored through DLR assay (for details see section 2.3). To observe the effect of WT1 overexpression on SRPK1 at the protein levels, K562, PC3, and DU145 were transfected with either with WT1 (-KTS) or (+KTS) separately, and the cells were lysed after 48 hours and prepared for western blotting (section 2.12). For experiments involving BASP1, two different concentrations (0.5-1.5µg) of BASP1-expressing plasmid (table 2.3) was transfected and the effect was monitored through DLR and western blotting. To detect the effect of ERG overexpression on SRPK1, plasmid constructs that contain +/- 7b ERG or different concentration (0µg-2.5µg) of full-length ERG (Table 2.3) were transfected into cells and the effect was monitored through the DLR assay and western blotting. ERG plasmids express DDK as epitope tag which was used for validation by western blot using ANTI-FLAG® M2 antibody against DDK (see appendix; fig 9.10). All plasmids containing expression or reporter constructs were transfected to the cells following the same protocol in section (2.1.4).

2.1.6 siRNA mediated knockdown of SRPK1, WT1 and ERG

Fluorescein-labelled siRNAs targeting WT1, GL2 luciferase control siRNA and ERG were described at (Jamie *et al.*, 2003) and (Urbinati *et al.*, 2016) respectively. siRNAs were produced by Eurofins Genomics (Table 2.1). siRNA against SRPK1 was used as

well to evaluate the effect of SRPK1 on cell biology. siRNA targeting SRPK1 was as described by (Zhao *et al*., 2018). Lipofectamine RNAiMAX was used as a transfection reagent (Life Technologies). All the surfaces where the experiment was conducted were cleaned using RNaseZAP (Sigma) to get rid of RNase. The cells were seeded at least for 24 hours before transfection to achieve around 80% confluence. After 24 hours, cells were transfected with 10nM or 50nM or 100nM final concentrations siRNA with Lipofectamine RNAiMAX following manufacturer's instructions.

siRNA	Target sequence	Fluorescent label
WT1- 1180	AATGCATGACCTGGAATCAGA	FAM
ERG	GCAGGAACUCUCCUGAUGAAU	CY5
SRPK1	UUAAUGACUUCAAUCACUCCAUUGC	FAM
GL2 control	CGTACGCGGAATACTTCGATT	CY5

Table 2. 1: Individual siRNA components including their target sequences and fluorescent labels.

2.1.7 Small molecule inhibitor (SPHINX)

K562 or PC3 cell lines were treated with either SRPK1 specific small molecule inhibitors 5-methyl-N-[2-(morpholin-4-yl)-5-(tri-fluoromethyl) phenyl] furan-2-carboxamide (SPHINX), a chemical inhibitor of SRPK1 purchased from Enamine (Kiev, Ukraine). SPHINX was dissolved in 100% sterile dimethyl sulfoxide (DMSO) (Sigma; code: 101546280/ lot: SHBF7360V). A further 10µM dilution was prepared in 1%DMSO. In a typical experiment, $4.0x10^6$ cells were in a sterile T_{25} flask. To each well, aliquot of 2mls of the appropriate concentration of SPHINX was made up in an individual culture media (RPMI or DMEM) containing $2.0x10^6$ cells and then incubated for the desired amount of time at 37°C.

2.1.8 Splice-switching oligonucleotides (Vivo-Morpholinos)

Splice-switching oligonucleotides were used as a different approach to verify the findings. MG63 and PC3 cells were exposed to Vivo-Morpholinos that induce skipping of Exon4 and 7b in the *ERG* gene as well as blocking the splicing of exon 3 of the *WT1* gene. In this study, SSOs were designed against 3′ splice sites by Gene Tools, LLC (Philomath, OR, USA. Table 2.2). Stocks of each vivo-morpholino were prepared in WFI (Gibco™ water for injection for cell culture) at a concentration of 0.5mM. $7x10^5$ cells were seeded into compartments of a 6-well plate and cultured at 37°C overnight. The media was replaced with 1ml fresh media where the required SSO concentration was added directly. Vivo-morpholinos are fused with octaguanidine dendrimer moiety that enhances cellular uptake. After 48-72 hours of vivo-, morpholino treatment, cells were harvested for the subsequent analysis.

Description	Sequence	Concentration
Vivo-Morpholino EWING-7b-3'SS	CTGCACCCCCTGCAGACAAAAGGAA	400 nmol
Vivo-Morpholino EWING-4-3'SS	GCTTCCTGAATGCCCAAAGAAACAC	400 nmol
Vivo-Morpholino WT1 103 SS	GCGTCCTCAGCAGCAAAGCCTG	400 nmol
Scrambled control	GACAATATAGGACGCCACCGCAACC	400 nmol

Table 2. 2: sequence and concentration of Splice-switching oligonucleotides.

2.2 Plasmid constructs to study SRPK1 transcriptional regulation

The *SRPK1* promoter was cloned into a pGL3 luciferase vector (Promega) allowing *in vitro* transcription assays to be performed (Amin *et al*., 2011). These assays were performed in PC3 and DU145 human prostate cancer and K562 chronic myeloid leukaemia cell lines models. Using the *SRPK1* promoter-luciferase reporter construct we tested the effect of WT1 binding to the *SRPK1* promoter on SRPK1 expression. The presumed WT1 binding site (GGGGCGGGGG) located -119 bp to -110 bp upstream of the *SRPK1* transcription start site in the *SRPK1* promoter was also mutated. The effect on *SRPK1* transcription was measured using the Dual- Luciferase Renilla (DLR) assay.

2.2.1 Plasmid preparations

The following plasmids were cloned into *E. coli* strain TOP10 and maintained in LB media with 100 mg/L ampicillin (Table 2.3).

pMKC130	*pGL3 basic vector with firefly luciferase gene under the control of 511 bp (-391 relative to WT1* binding site*) wild-type human SRPK1 promoter)*
pMKC132	*pGL3 basic vector with firefly luciferase gene under the control of511 bp (-391 relative to WT1) mutant human SRPK1 promoter*
pRL-TK	*Plasmid containing Renilla luciferase gene under the control of a constitutive HSV TK promoter.*
pGL3	*Basic vector (negative control).*
P118	*CMV -WT1 (+/-) - Ampicillin - 100µg/ml*
P77	*1 to 449 (full-length WT1+KTS) - Vector backbone - pCDNA3 - Ampicillin - 100µg/ml*
pCDNA3-BASP1-FH	*BASP1 expressing plasmid*
ERG 227	*ERG+72bp (exon 7b included) pCMV6*
ERG 218	*ERGΔ72bp (exon 7b skipped) pCMV6*
ERG	*pCMV-SPORT6 containing full length ERG 'variant 1'*

Table 2. 3: Plasmids used to perform the DLR assay and overexpression experiments.

To help differentiate between pMKC130 from pMKC132 an additional *Eco*RI restriction enzyme site has been created within the mutagenized WT1 binding site in pMKC132. At the time of cloning, there were 2 different versions of *SRPK1* promoter. Longer (1668bp) and shorter (511 bp) version of the human *SRPK1* promoter. For the experiments described in this thesis, we used the shorter promoter construct. See appendix for detailed plasmid maps.

2.2.2 Growth of *E.coli* in Luria Broth

E.coli transformed with various plasmids described above were inoculated into Luria broth (LB) agar and incubated at 37°C incubator overnight, then single identifiable colonies were picked by a sterilized lube and inculcated into a freshly prepared LB and then incubated in a shaking incubator (to allow air exchange) at 37° overnight. LB broth recipe: 5g NaCl, 5g tryptone, 2.5g yeast extract, 7.5g agar, add dH_2O to 500mL then after it dissolved completely, autoclave. One the agar cooled down, ampicillin was added to a final concentration of 100 mg/ml to select for transformants.

2.2.3 Plasmid miniprep

A plasmid DNA Miniprep kit (New England Biolabs) was used to extract the plasmids. 5 ml overnight cultured samples were processed using a spin anion exchange minicolumn according to standard manufacturer's instructions. At the end of the procedure, 40ul of plasmid DNA was eluted with elution buffer. Yield and quality of plasmid DNA concentration were measured using a Nanodrop spectrophotometer (Life Technologies). Plasmids were restricted with appropriate restriction enzymes (see section 2.2.5) and run on agarose gels (1% agarose run in standard Tris-Acetate-EDTA (TAE) buffer). HyperLadder™ 1kb DNA marker (Bioline) was used to estimate the sizes of bands.

2.2.4 Plasmid Midiprep

Plasmid DNA Midiprep kit (Qiagen) was also used to purify the plasmids when larger amounts were needed for transfection into mammalian cell lines. 50 ml overnight cultured (bacteria in the logarithmic growth phase) samples were processed according to the standard manufacturer's instructions. At the end of the procedure, 200µl containing plasmid DNA was eluted with elution buffer. Yield and quality of plasmid DNA were checked by Nanodrop spectrophotometer (LifeTechnologies) and agarose gel electrophoresis.

2.2.5 Plasmid restriction digestion

The identity of the plasmids was confirmed through restriction digestion. Restriction enzymes cleaved each DNA molecule at a specific sequence of bases (Table2.4). Different combinations of *Kpn*I, *Xba*I, *Hind* III, *Nco* I, *Bam* HI and *EcoR*I (New England Biolabs) using the appropriate restriction enzyme buffers were used. HyperLadder™ were used to estimate the fragment size. (See appendix fig 9.1, 2&7)

Enzyme	sequence digestion
KpnI	7G-GTACC
XbaI	2173-TCTAG-A
HindIII	265-AAGCT-T
Nco I	517-CCATG-G
BamHI	2435-GGT-C-
EcoRI	400-GAATT-C
XhoI	5000-CTCGAG
SalI	2000-GTCGAC

Table 2. 4: Restriction enzymes and their digested sequence of bases.

Plasmids were digested by corresponding restriction enzymes (KpnI, XbaI, HindIII, Nco I, BamHI, EcoRI, XhoI and SalI). Numbers and sequences corresponds to the digestion sites used in the cloning. Restriction digest reaction was optimized according to the manufacturer's instructions (Fermentas). 1-5µg DNA was

cut at restriction sites using restriction enzymes in 76.5µl reaction incubated at 37 °C for 40minutes. Suitable pH and salt concentration were used using the buffer solution provided by the manufacturer.

2.2.6 Bacterial transformation

Since DH5 alpha *E.coli* is the competent strain for both P77& P118 plasmids, Competent DH5 alpha *E.coli* cells were prepared as per manufacturer instruction (Invitrogen™Lot#18258012). To prevent low transformation efficiency plasmids DNA were diluted to the concentrations of 50ng/µl before adding 5µl to 50µl of DH5 *E.coli*. The transformation vials were chilled on ice for 30 minutes before heat shocking them in a water bath at 42°c for 30sec. the mix was briefly incubated on ice before adding 250µl of pre-warmed S.O.C rich medium to it, then the mix was incubated at a 37° shaking incubator for 1 hour at 225rpm to allow the cells to express the ampicillin resistance gene. 20-200µl of these samples were spread onto LB agar plates containing ampicillin as a selective medium (described in section 2.2.2) then incubated overnight at 37°c. The next morning, single identifiable colonies of the transformed cells were inoculated into LB broth to obtain an overnight culture in preparation for plasmid midiprep (section 2.2.4).

2.2.7 Plasmid DNA and cell strains storage

For short-term storage, the plasmid DNA was stored in sealed 1.5 ml Eppendorf tubes at -20°c and at -80 °c for longer-term storage. Top10 and DH5 alpha *E.coli* bacterial strains were kept at 4°c as colonies on LB agar plates that contain 100 mg/ml ampicillin. Stocks of plasmids containing bacterial strains were stored at -80 for long-term storage.

2.3 Dual luciferase reporter assay

The dual luciferase reporter (DLR) assay was used to evaluate regulated specific gene expression, in this case, of the *SRPK1* gene. The system depends on two different reporters, firefly (*Photinus pyralis*) and renilla (*Renilla reniformis*) luciferases to make this evaluation. As a control for normalizing the assay, the sequence encoding firefly luciferase reporter gene (luc+) is fused to a promoter and integrated into the pGL3 plasmid. Renilla luciferase works as an internal control for normalizing the activity of the experimental reporter. The DLR assay was performed by consecutively measuring the firefly and renilla luciferase activities of the same sample using GloMax® 20/20 Luminometer. The results are expressed as the ratio of firefly to renilla luciferase activity (relative luciferase units, RLU). The results reflect the promoter's activity.

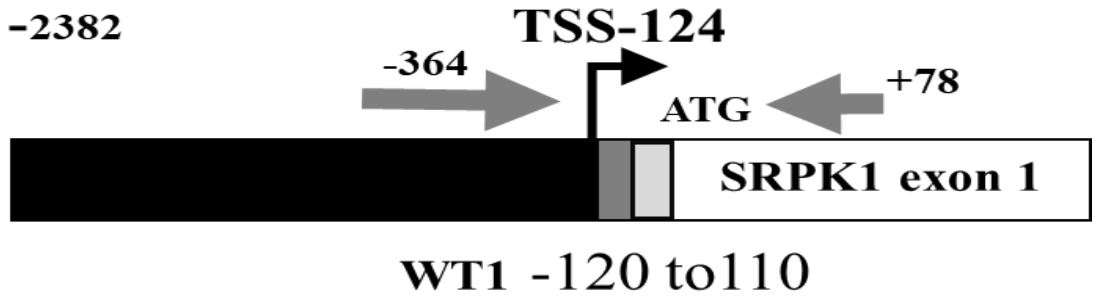

Figure 2. 1: SRPK1 promoter structure.

Black= promoter region. Grey=WT1 binding site (GCG GGG GCG) silver=5′UTR, white=coding sequence of exon 1. Arrows=primer locations. Numbers are bp relative to the transcription start site (TSS).

siRNA GL2	Nonspecific Control siRNA
siRNA *WT1*	WT1 targeting siRNA
WT1(+KTS)	Plasmid encodes +*KTS WT1* isoform
WT1(- KTS)	Plasmid encodes -*KTS WT1* isoform
SPHINX	SRPK1 chemical inhibitor

WT1 SSOs	Splice switching oligos that induce exon 3 skipping in WT1 gene
siRNA *SRPK1*	*SRPK1* targeting siRNA
pCDNA-*BASP1*	Plasmid encodes *BASP1*
pCMV6-ER227	Plasmid encodes *ERG* (+7b) isoform
pCMV6-ER218	Plasmid encodes *ERG* (-7b) isoform
ERG pSPORT	Plasmid encodes full length *ERG*
siRNA ERG	ERG targeting siRNA
Control SSOs	Nonspecific Splice switching oligos
E4 3′ SSOs	Splice switching oligos that induces exon 4 skipping in *ERG* gene
E7b 3′ SSOs	Splice switching oligos that induces exon 7b skipping in *ERG* gene

Table 2. 5: Transcriptional regulators cotransfected with SRPK1 promoter.

2.4 RNA extraction from cell lines

Cell pellets were collected after treatments from human prostate cancer cell lines; (PC-3, ATCC® CRL-1435™), (MG63 ATCC® CRL-1427™) cells human osteosarcoma cell line and K562 (ATCC® CCL-243™)-a human erythroleukemic cell line. RNA extraction was performed using the Agilent absolute RNA miniprep kit following the standard manufacturer's protocol for isolation of total RNA. Cell pellets were collected in a 1.5ml micro-centrifuge tube followed by lysing in a solution made up by 1:100 dilutions of Lysing buffer and 7µL β-mercaptoethanol. Purified RNA was eluted in an appropriate amount of elution buffer. The RNA yields were quantified using the Nanodrop and the samples then stored at -20 °C for short term storage and at -80 °C for long term storage.

2.5 cDNA synthesis

A New England Biolabs kit was used for cDNA synthesis. Up to 2µg of RNA was added to 1ml micro-centrifuge tube where 2µl of 40,000U/ml random primers (Promega) and 2µl of 2.5mM deoxynucleotide triphosphate (dNTP) (Sigma Aldrich) were added and brought to a final volume of 16µl with nuclease-free water (Qiagen; Lot: 129115/151034210). On each tube, 2µl of 40,000U/ml random primers (Promega; cat; A5000) were added and incubated at 70°C for 5mins. The RNA with primers was spun down and placed immediately on ice. While on ice, 2µl of 10x M-MLV reverse transcriptase buffer (NEB; Lot: B0253S/0101505), 1µl of 2x reverse transcriptase (NEB: Lot: M0253S/0271503) and RNA inhibitor (NEB: Lot: M0307S/ 0321410) respectively was added to the tubes followed by incubation at 42 °C for one hour, followed by enzyme inactivation at 90 °C for 10mins. The final products were quantified using the Nanodrop and stored at -20 °C.

2.6 Assessment of RNA and cDNA yield

RNA and cDNA purity and concentration was assessed using a Nanodrop 1000A UV spectrophotometer (Thermo Fisher Scientific, USA). 1µL of each sample was used and the degree of purity assayed by calculating the ratio of the sample absorbance at 260/280 nm (A260 /A280), where a ratio of 2.0 denotes pure RNA.

2.7 Polymerase chain reaction (PCR)

Following treatment and transfections, PCR was carried out to evaluate the effect of SRPK1 transcriptional manipulations and chemical inhibition on the alternative splicing of genes of interest which included *caspase-9,* and *BCL2L1*. The alternative splicing of

ERG after subjecting the cells to SSOs that induce exon 4 and 7b skipping was also evaluated through PCR. Screening the cancer cell lines for the possibility of the presence of the SRPK1 splice variant (SRPK1a) was also performed via PCR. Beta actin (β-actin) was amplified and used to determine the quality of the cDNA as well as a loading control. Table 2.6 describes all primer sequences used for standard PCR. The master mix for PCR was prepared following the New England Biolabs protocol (Hot Start Taq 2X Master Mix lot: M0496S). In a sterile, thin-walled PCR tube, 1µl of 10µM Forward Primer, 1µl 10 µM Reverse Primer, 2µl of Template DNA, 25µl of Hot Start Taq 2X Master Mix and 21µl Nuclease-free water were mixed then placed in MJ Research MiniCycler PTC-150 Thermal Cycler for amplification.

Gene name	**Primer sequence/ length** **5′ – 3′**	**Alignment**	**Amplicon length (bp)**
SR protein kinase 1 (*SRPK1*) NM_003137	**F**: CGCGCAAGCGCGCGGCATCGT (21) **R**: CTGCGCACTCGAGTGGCGGCG (21)	**F** :1329 – 1353 **R** :1430 – 1403	102
SRPK1a NM_003137	**F**:GGTCTCACCATGGAGCGGAAA (21) **R**: CTTCCTGCTCTGGTAGATCAC (21)	**F** :1326 – 1349 **R** :1426 – 1399	120
Beta – actin (*β-actin*) NM_001101	**F**: TTAAGGAGAAGCTGTGCTACG (21) **R**: GTTGAAGGTAGTTTCGTGGAT (21)	**F**: 719 – 739 **R**: 924 – 904	206
BCL2 like 1 (BCL2L1)xl NM_138578	**F**: CATGCCAGCAGTGAAGCAAG (20) **R**: GCATTGTTCCCGTAGAGATCC (21)	**F**: 627 – 646 **R**: 977 – 957	351
Caspase-9 NM_001229	**F**: GCTCTTCCTTTGTTCATCTCC (21) **R**: CATCTGGCTCGGGGTTACTGC (21)	**F**: 1248 – 1251 **R**: 1436 – 1458	742

GAPDH NM_002046	**F**: CAATTCCCCATCTCAGTCGT (21) **R**: TAGTAGGCCGGGCCCTACTTT (21)	**F** :1239 – 1349 **R** :1230 – 1303	100
ERG (Exon 4 skipping) NM_182918	**F**: TTTGGAGACCCGAGGAAAGC (20) **R**: AGAGAAGGATGTCGGCGTTG (20)	**F**: 637 – 656 **R**: 937 – 959	300 200
ERG (Exon 7b skipping) NM_182918	**F**:GAATATGGCCTTCCAGACGTCAAC (24) **R**:GGTGGCCGTGACCGGTCCAGGCTG (24)	**F**: 640 – 659 **R**: 940 – 962	300 200

Table 2. 6: Primers used for PCR.

2.8 Agarose gel electrophoresis

For sonication optimisation and PCR amplicons, DNA fragment size was measured using agarose gel electrophoresis. Following sonication and PCR, 20µL of each sample was added to 5µL 5X DNA loading dye (NEB, UK) and resolved on an agarose gel alongside gene ruler low range DNA ladder (NEB, UK). The agarose gel was made up of 1% (w/v) agarose (Fisher). Gels were electrophoresed in 1X Tris-Acetate-EDTA (TAE) buffer at 100V for approximately 45minutes in a BIO-RAD Mini-sub Cell GT. Gels were stained with 0.01% of 10µg/ml ethidium bromide (Sigma Ltd, UK). Gels were imaged using the LI-COR Odyssey FC imaging system (USA) at 600nm.

2.9 Chromatin immunoprecipitation assay

Chromatin immunoprecipitation was performed on PC3, K562, B-K562 and MG63 cells using the Imprint Chromatin Immunoprecipitation Kit (Sigma; lot# CHP1-24RXN). Briefly, according to the manufacturer protocols, 1x 10^6 cells were incubated for 10

minutes with 1% (w/v) formaldehyde at RT to allow DNA to be cross-linked to the protein. The cells were then lysed and DNA sheared to about 1000bp using a sonicator for 6x at 15seconds at 50% for PC3 and MG63, 30% for a minute for K562 and B-K562 power output followed by incubation on ice for 60 seconds after each pulse. The DNA-protein mixture was incubated with 3µg of WT1, ERG and BASP1 antibodies or with 1µg RNA Polymerase II antibody (positive control) or 1µg nonspecific IgG (negative control) coated on a well at room temperature for 3 hours, then washed 6 times with the IP wash buffer. The cross-linked DNA-transcription factor complexes were released using Proteinase K at 65°C for 15mins. The DNA was cleaned up and eluted using GeneElute Binding Colum (Sigma). The eluted DNA was subsequently used in a PCR to detect the genomic regions of SRPK1 and GAPDH promoter regions that were being pulled down by the antibodies. Using the primers on (table 2.6), PCR was performed at 95°C initially for 2mins followed by 95°C for 1 minute, 55°C for 1 min and 72°C for 1 minute for 35 cycles followed by a final elongation at 72°C for 5 minutes for GAPDH, but for WT1 PCR was performed at 95°C for 2mins followed by 95°C for 1 minute, 68°C for 1 min and 72°C for 1 mins for 15 cycles followed by 95°C for 1 mins, 60°C for 1 min and 72°C for 1 mins for 20 cycles followed by a final elongation at 72°C for 5 minutes.

2.10 Gel extraction and purification of PCR products

To sequence the chIP assay products (from section 2.9) a gel extraction kit (Monarch DNA gel extraction kit Lot#T1020) was used to purify and collect the products. Bands were cut out of the gel above a UV light keeping the amount of gel around the bands as little as possible. As per the manufacturer's instructions, 4 volumes of the gel dissolving buffer were added to each gel slice before incubating the samples at 40 °C. Samples were

vortexed periodically during the incubation period until the gel slices were dissolved completely. Then the samples were passed through columns to get rid of the agarose. The columns were placed into collection tubes then the DNA was washed with the provided buffer twice. After that, DNA was eluted out of the columns In 1.5 ml Eppendorf tubes with nuclease-free water (Ph7-8.5). The concentration of the yield was measured using the Nanodrop (described in section 2.6). The collected DNA was concentrated up to 10 ng/µl (for purified PCR product 1-10 ng/µl) at the volume of 15µl. 1ng/µl of each sample was mixed with 10 pmol/µl of forward and reverse primers then the samples were sent to Eurofins MWG Operon (Germany) to be sequenced.

2.11 Protein extraction and quantification

After treatments and transfections, 5 x 10^4 cells at 80% confluence from each well were lysed using ice-cold RIPA buffer containing 10 mM Tris-Cl pH 7, 140 mM NaCl, 0.1% (w/v) SDS and protease inhibitor tablets (Roche). Lysates were passed through a 21mm needles, then centrifuged at 1000rpm/4°C for 15 minutes. The supernatant was collected into a fresh microcentrifuge tube and the pellet discarded. The protein concentration in the supernatant was measured using the Bradford reagent (Sigma). Briefly, 1µl of protein extract was added to 200µl of Bradford reagent and measured at OD_{595}nm for its absorbance using a fluorstar machine (BMG labtech). The protein concentration was calculated using a slandered curve of known amounts of BSA.

2.12 Western Blotting

Western blots were performed with the whole cell samples mixed with Laemmli buffer (Sigma; code: 1001521749/lot: SLBG2398V). Cells were lysed with RIPA buffer on ice then the appropriate volume of Laemmli buffer was added and the samples were then heated to 95°c for 5 minutes.

SDS-PAGE gels consisted of a resolving gel and a stacking gel. For 10% acrylamide resolving gel, gels were poured in an aired lamina flow hood due to the toxicity of acrylamide, AP and TEMED, 3mls of 30% acrylamide (Sigma; SLBM3534) was added to 2.5ml of 1.5M resolving buffer (18.17g Tris and 100ml dH_2O; pH 8.8), 4.1ml of nuclease-free water, 100µl of ammonium persulphate (AP) (Sigma; 20 MKBN6480V) solution and tetramethylethylenediamine (TEMED) (Sigma; 101360618/BCBL1646V) then dispensed immediately to a pre-assembled gel casts using a pasture pipette. The resolving gel was allowed to polymerise for approximately 25 minutes. After that, a stacking gel was prepared by adding 670µl of 30% acrylamide to 500µl of 1M stacking buffer (6.17g tris 100ml dH_2O; pH 6.6), 2.4ml of nuclease-free water, and 100µl of AP and 40µl of TEMED then added immediately and was allowed to polymerise, with a gel comb inserted, for approximately 20 minutes. The gels were then placed in a BIO-RAD Mini-tank (BIORAD) which was filled with 10X SDS PAGE running buffer (25mM Tris, 190mM glycine and 0.1% (w/v) SDS with adjusted pH of 8.3). To each well, 10-15µL of cell samples were added and resolved against 8µL of prestained protein marker (Cell Signaling Technology). Gels were electrophoresed at 70V for 20 minutes and then at 100V for approximately a further 50 minutes.

Proteins were transferred from the gel to a (PVDF) membrane (Thermo) using a BIO-RAD tank. In a transfer cassette, gels were placed on a membrane soaked in methanol, in between three pieces of filter papers (Thermo) and sponges soaked in transfer buffer (25mM Tris, 190mM glycine and 20% methanol). After that, the cassette was placed in the transfer tank containing cold transfer buffer. A magnetic stirrer and an ice pack are placed in the tank to maintain the cold temperature. Transfers were done for 3hrs at 70V. Post-transfer, membranes were blocked in 10mL blocking buffer (3% non-fat dry milk and 1xTBST; 1x Tris-buffered saline 20mM Tris pH 7.5, 150mmNaCl, 0.1% (v/v) Tween20) on a rocking platform for an hour. The membranes were then incubated with antibodies of choice (Table 2.7) on a rocking platform at 4°C overnight. Antibody buffer was removed and the membranes were washed in (3x) in 10ml of TBST for about 15 mins. Membranes were then incubated with 20mL blocking buffer containing 1/5000 HRP-linked secondary antibody on a rocking platform for 1 hour. Membranes were then washed a further 3 times in TBST to remove unbound secondary antibodies. Membranes were placed in HPR-substrate (Millipore; cat: WBLUF0100/lot: 151223) for 2 mins prior to visualization using LI-COR Odyssey FC imaging system (USA) at 600nm and chemiluminescent channels.

Antibody/ Specie	**Concentration**	**Dilution used**	**Source**	**Secondary antibody used**
Anti-β-actin (Mouse)	1mg/ml	1:5000	Abcam	Horse anti-mouse IgG) HRP-linked antibody (Cell Signalling) (1:1000)
Anti-SRPK1 (Mouse)	200µg/ml	1:500	Santa Cruz Biotechnology	
Anti-$VEGF_{165b}$ (Mouse)	100µg/ml	1:200	R&D system	
Anti-DDK flag (Mouse)	200µg/ml	1:50	Sigma	

Anti-$VEGF_{165}$ (Goat)	100µg/ml	1:25	R&D system	Donkey Anti-Goat IgG HRP-linked antibody (Abcam) (1:1000)
Anti-WT1 (Rabbit)	100µg/ml	1:1000	Abcam	Horse anti-Rabbit IgG) HRP-linked antibody (Cell Signalling) (1:1000)
Anti-BASP1 (Rabbit)	100µg/ml	1:1000	Abcam	
Anti-ERG (Rabbit)	100µg/ml	1:1000	Abcam	

Table 2. 7: Antibodies used for western blotting.

2.13 Cell biology assays

2.13.1 MTT Assay; cell proliferation and viability

Cell proliferation and viability were assessed by monitoring the transformation of MTT to formazan. The conversion of water-soluble MTT (3-(4, 5-dimethylthiazol-2-yl)-2, 5-diphenyltetrazolium bromide) compound to an insoluble formazan product is catalysed by mitochondrial dehydrogenase enzymes. Briefly, cells (200µl/well) were seeded at seeding densities of $1x10^5$ into 96 well plates and allowed to adhere for overnight except for cells grow in suspension. Following subjecting the cells to the proper treatments and transfections, the media was removed, then 50µL of serum-free media and 50µL of MTT solution (ab211091, Abcam, Cambridge, MA) were added to each well. After incubation at 37 °C for 3 h, 150µL of MTT solvent was added to each well. The absorbance at OD=590 nm was measured and used for cellular proliferation and cell viability was calculated using the following formula: Cell viability = control- absorbance of treatment wells/absorbance of control well ×100%.

2.13.2 Transwell cell migration and invasion assay

Assays were performed in an insert for 24 well plates (Greiner Bio-One; 8 µm pore size 662638) according to the manufacturer's protocol. For cell migration, cells ($2.5–5 \times 10^5$) were re-suspended in 100µL serum-free medium were plated in the top of each chamber insert transwell insert then incubate for 10 minutes at 37 °C and 5% CO_2 to allow the cells to settle down. For invasion assay, inserts were coated with 50µL of a 1:4 Matrigel/ Tris; Sodium Chloride (Corning® Matrigel® matrix 54230) and allowed to solidify at overnight in a sterile environment then the same steps were applied. Cells were subjected to the proper treatments inside the inserts. The bottom chambers were filled with 500µL complete medium containing 10% FBS. Cells were allowed to migrate for 24 h. cells that have not migrated on the top surface of the inserts were removed with an ethanol coated cotton swab, and the cells that migrated to the bottom side of the inserts were fixed in 4% (w/v) paraformaldehyde, washed, and stained with 0.2% (w/v) crystal violet in 2% methanol. For each insert, representative images in 3 evenly distributed x20 fields of view were captured using a light microscope (Zeiss AX10) and coloured using ImageJ software. To quantify the migration of cells, 0.1% SDS in PBS was added to the lower chambers and absorbance intensity measured on a plate reader at an excitation of 590 nm. Each experiment was repeated in triplicate.

2.13.3 Analysis of apoptosis signals; caspase-3/7 activity assay

After subjecting the cells to the proper treatments and transfections, cells were labelled with 5µM CellEvent™ caspase-3/7 green detection reagent (Life Technologies, Carlsbad, CA, USA) in PBS for 30 min at 37 °C in the dark. DAPI (4', 6-diamidino-2-phenylindole dihydrochloride) (Thermo Fischer: D1306) was added to the cells for 1 minute as a counterstain. The apoptotic cells labelled with green fluorescence were visualized using

20x Nikon Plan Fluor Objective Ph1 with FITC Filter Set to visualize FAM Fluorescein label.

2.14 Fluorescence microscopy

A Nikon Eclipse TE300 Inverted Phase Contrast Microscope was used to verify that the fluorescein-labelled siRNAs are inside the cells after the incubation period. The fluorescent microscopy was also used to examine caspase activity in apoptotic cells. Each plate was visualized using 20x Nikon Plan Fluor Objective Ph1 with FITC Filter Set to visualize FAM Fluorescein label, DAPI was used for DAPI staining and TxRed Filter Set to visualize CY5 Fluorescein label.

2.15 Normalisation of western blots and PCR

To ensure that the changes in the protein and gene expressions have resulted from different treatments and transfections, PCR gels and WB membranes were analysed using image studio lite software (LiCOR Odyssey) that measures the densities of bands and the generated data were exported to Excel sheets and GraphPad software. The graphs depicted the relative expression of splice variants of different genes or proteins from different cells lines, such as VEGF165a/b ratios. Data were presented as mean ± SE. Statistical differences between treatments groups were compared using one-way ANOVA calculate the P values that show the Statistical significance of a given treatment.

3 Chapter Three: Effect of SRPK1 inhibition and knockdown on SRPK1 expression and cell biology

3.1 Background

SRPK1 has been shown to phosphorylate SR proteins that contain serine-arginine-rich domains. SR proteins act like substrates to the kinase and act as key regulators of mRNA AS (alternative splicing). SRPK1 interacts with several molecules which serve as a substrate or control its association with substrates. Such interactions result in the propagation of cellular function by the substrate or regulation of their activity either directly or indirectly. SRSF1 is one of the best-studied SR proteins and is phosphorylated by SRPK1. SRSF1 has two RNA recognition motifs (RRM) and an RS domain consisting of about 50 amino-acids (rich in serine and arginine). It is known that SRPK1 interacts with about 10-12 amino-acid of the RS domain; an interaction which produces high-affinity binding and is considered critical for the regulation of the extent to which SRSF1 is phosphorylated (Ngo *et al.,* 2007; Plocinik *et al.,* 2011). Amin *et al.,* 2011 and Mavrou *et al.,* 2015 have shown that the SRPK1 and its main substrate, SRSF1 forms an essential pathway responsible for the regulation of the alternative splicing of vascular endothelial growth factor (VEGF) mRNA to produce pro/antiangiogenic isoforms in renal epithelial cells (podocytes), colon and prostate carcinoma cells. SRPK1 knockdown increases the levels of VEGF anti-angiogenic isoform and thereby prevents tumour growth in xenografts through the reduction in microvessel density. A similar finding has been observed in a study using a prostate cancer cell line (Mavrou *et al.,* 2015).

Since SRPKs are overexpressed in several tumours, there has been an increased interest in targeting SRPKs for the management of several cancers. Batson *et al.,* 2017 described

a selective SRPK1 inhibitor with moderate potency known as SPHINX, 5-methyl-N-[2-(morpholin-4-yl)-5-(tri-fluoromethyl) phenyl] furan-2-carboxamide, that induce an alteration in the splicing of VEGF isoforms through SRPK1 inhibition. This alteration involves a splicing switch from pro to antiangiogenic VEGF isoform which could cause a significant change in the extent of angiogenesis supporting the growth of several tumours.

A novel isoform of SRPK1, SRPK1a, has been described as being expressed in testes and leukemic cells; it has not been widely studied. The properties of the SRPK1a isoform are similar in terms of subcellular localization, substrate specificity and in their ability to induce alternative splicing of target genes (Sanidas *et al.,* 2010). They are structurally different since SRPK1a results from the retention of 513bp interionic segment and contains an additional 171 amino acids in its N-terminal domain. SRPK1 is the most highly expressed isoform in chronic myeloid leukaemia K562 cells; the global patterns of SRPK1a expression are yet to be studied. Sanidas *et al.,* 2010 studied the impact of SRPK1/SRPK1a ratio on erythroid differentiation. They found that the ratio of SRPK1 to SRPK1a is critical in determining K562 cell fate, with SRPK1 favouring proliferation and SRPK1a favouring differentiation. However, since the latter report, there have not been any further publications on SRPK1a and therefore its significance remains controversial.

3.2 Aims and objectives

- Aim 1: To obtain evidence of SRPK1a isoform expression in cancer cell lines.
- Aim 2: To investigate the possibility of SRPK1 auto-regulation through
    a. siRNA mediated SRPK1 knockdown.
    b. chemical inhibitor (SPHINX) treatment
- Aim 3: To investigate the effect of SRPK1 knockdown or of chemical inhibition on:
    - The alternative splicing of VEGF-A.
    - The alternative splicing of apoptotic factor; *BCL2L1* and *caspase* 9
    - Cell migration, invasion, viability, and proliferation.

3.3 Results

3.3.1 Expression of the SRPK1a splice isoform

Multiple cancer cell lines were tested to look for *SRPK1a* isoform expression by PCR Specific primers were used to detect *SRPK1a* based on the primers used by previous publications studying the expression of this isoform in K562 cell lines (Sanidas *et al.*, 2010); actin was also amplified as a cDNA control. Whereas overall *SRPK1* expression was confirmed in all cell lines tested (PC3, DU145 and VCaP prostate cancer cell lines and TK6 and K562 leukemic cell lines), *SRPK1a* was not detected by PCR in any of the cell lines (Figure.3.1a &b).

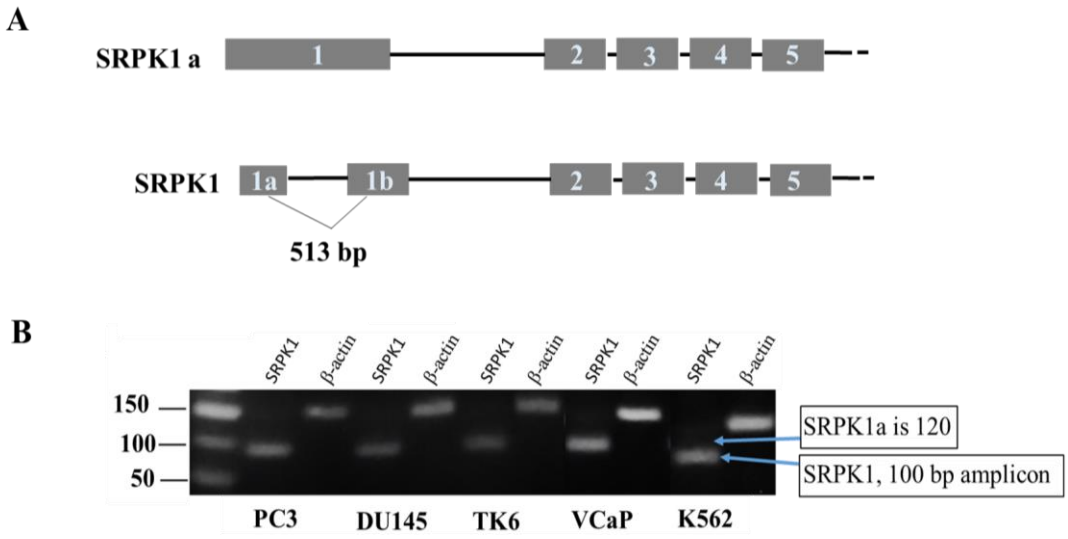

Figure 3. 1 a: Schematic representation of human SRPK1a and SRPK1.

Splicing in of the 513-bp segment yields SRPK1a isoform, whereas splicing out of a 513-bp segment, which is located between the first two exons of the SRPK1 locus, results in the production of SRPK1. (Sanidas *et al.*, 2010).

Figure 3. 1 b: PCR products electrophoresis.

SRPK1 isoforms amplified from cDNA from five different cell lines**.** For SRPK1a (120 bp amplicon), S1; sense primer: 5'-CTCCACATTCGCCCTTCATC-3', A1; antisense primers: 5'-CCTCGGTGCTGAGTTTCAGAT-3', probe: ATCCCTCTCTCCTGCAGTG. For SRPK1 (100 bp

amplicon), S2; sense primer: 5'-CACCATGGAGCGGAAAGTG-3', A2; antisense: 5'-GCCTCGGTGCTGAGTT TCAG-3', probe: CCCGAAAGAAAAGGACCA. Arrows point to the *SRPK1* band (100bp) and the expected location of *SRPK1a* band (120bp). Quick-load Purple 50bp DNA Ladder was used to estimate the band sizes.

3.3.2 Effect of siRNA mediated SRPK1 knockdown on SRPK1 expression

The splice factor kinase CLK1 is involved in an autoregulatory loop. When it is inhibited its expression increases (Duncan *et al*., 1997). More recently, its inhibition in PC3 and DU145 prostate cancer cells has been shown to alter CLK1's own alternative splicing, favouring the production of more full length CLK1 (Uzor *et al*. 2018). It is conceivable that SRPK1 is also involved in an autoregulatory loop. This was examined in PC3 and K562 cell lines. Cells were transfected with siRNA that target SRPK1 (Table 2.1) previously described in (Zhao *et al.,* 2018), alone at first to verify that the knockdown occurred, then the siRNA were co-transfected with *SRPK1* promoter constructs fused to luciferase reporter (Amin *et al.,* 2011) to see whether or not the knockdown would have an effect on the promoter's activity. A western blot was performed on protein lysates prepared from the cell lines following the siRNA knockdown (Figure.3.2.A &B).

Significant reduction on SRPK1 levels was observed at higher concentrations of the siRNA (50&100nM) confirming that the siRNA is effective. The next step was to examine the impact of the higher siRNA concentration on *SRPK1* transcription through co-transfecting the siRNA with wild type/mutant *SRPK1*promoters (Figure.3.2.C). The activity of the promoter showed no significant change after SRPK1 knockdown which suggests that SRPK1 might not be involved in an autoregulatory loop.

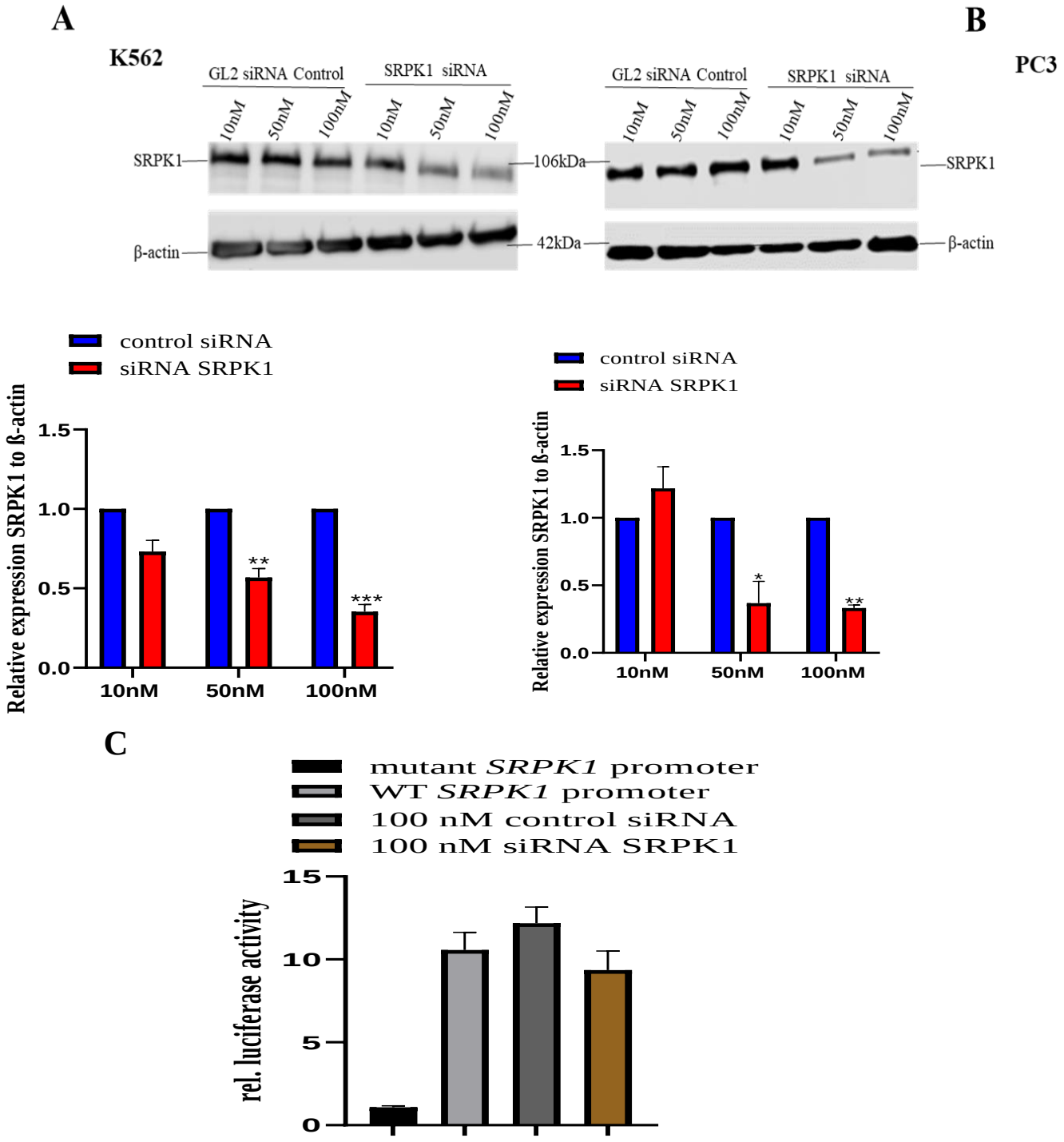

Figure 3. 2 Effect of SRPK1 knockdown on SRPK1 expression.

K562 (A) and PC3 (B) cells were transfected with increasing concentration of SRPK1 siRNA (10nM, 50nM, and 100nM) or control GL2 siRNA for 48 hours. A&B. Western blots of protein lysates collected after SRPK1 siRNA knockdown. Membranes were blotted with anti-SRPK1 or anti-beta actin antibodies as a loading control. Graphs represent relative expression determined by densitometric measurement of the

bands and are expressed relative to actin. Bar-graph shown is the average of three independent experiments. **= p<0.0016 and *** p= 0.0001 significant change compared to control using a one way ANOVA test. (C) DLR assay of *SRPK1* promoter activity in PC3 cells transfected with siRNA SRPK1. Measurement of *SRPK1* promoter activity using a dual luciferase reporter (DLR) assay. WT/mutant *SRPK1* promoters were co-transfected with 100nM SRPK1 siRNA or control siRNA into PC3 cells. Data expressed as relative luciferase units (RLU). Data presented as mean ± S.E. for independent experiments n=3. The figure shows no significant reduction using a one way ANOVA test in the activity of the promoter where SRPK1 has been knocked down.

3.3.3 Effect of the SRPK1 inhibitor SPHINX on SRPK1 protein levels and transcription

As discussed, CLK1, another splice factor kinase that phosphorylates SR protein in the nucleus, is involved in its auto-regulation; inhibition of CLK1 results in increased CLK1 expression (Duncan *et al*., 1997; Uzor *et al*., 2018). Thus it was of interest to determine whether or not this is applicable following SRPK1 inhibition. The expression of SRPK1 after subjecting the cells to SPHINX treatment, a specific SRPK1 chemical inhibitor, treatment was assessed by western blotting. Western blot was performed on cell lysates harvested from K562 and PC3 cells after 72 hrs of SPHINX treatment. The blot shows that SRPK1 inhibition using 10μM SPHINX resulted in decreased levels of SRPK1 protein (Figure 3.3 A&B). That suggests the possibility of SRPK1 inhibition might also result in decreased SRPK1 protein expression through a feedback loop. Cells were also transfected with wild type/mutant *SRPK1* promoters while treated with 10μM SPHINX to test the inhibitor's treatment on SRPK1 transcription. The wild-type promoter's activity was reduced suggesting that SPHINX does cause a reduction in SRPK1 transcription in K562 and PC3 cell lines (Figure 3.3C&D).

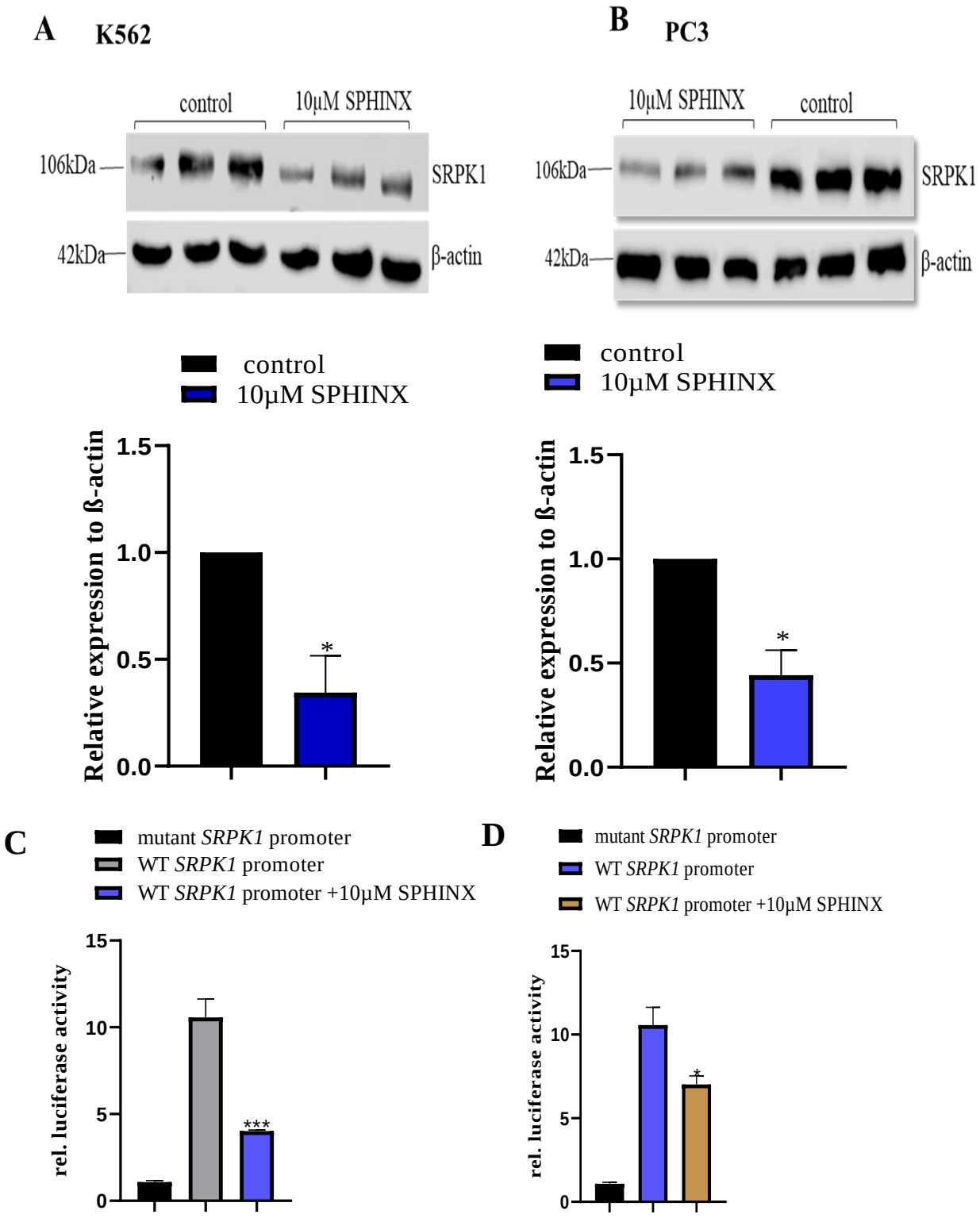

Figure 3. 3 Effect of SPHINX on SRPK1 protein levels and transcription

A&B Protein levels of SRPK1 in SPHINX treated K562 (A) and PC3 (B) cells. Western blot of protein lysate collected from K562 and PC3 cells Subjected to 10µM SPHINX for 72 hours. Membranes were

blotted with anti SRPK1 or anti-beta actin antibodies as a loading control. Graphs represent relative expression determined by densitometric measurement of the bands and are expressed relative to actin. Bar-graph shown is the average of three independent experiments. Although there is a slight reduction in SRPK1 levels, this reduction is not statically significant using unpaired t test. Three independent repeats are shown in each case.

C&D DLR assay of *SRPK1* promoter activity in K562 and PC3 cells treated with SPHINX. Measurement of *SRPK1* promoter activity using a dual luciferase reporter (DLR) assay. WT/mutant *SRPK1* promoters were transfected into cells treated with 10μM SPHINX. Data are expressed as relative luciferase units (RLU). Data presented as mean ± S.E. for independent experiments n=3. *** $p<0.0005$ and * $p<0.0178$, are statistically significant using a one way ANOVA test. Figures show a reduction of the promoter's activity in cells treated with SPHINX.

3.3.4 Effect of SPHINX treatment on VEGF-A alternative splicing

Numerous studies showed that different SRPK1 inhibitors (SRPIN340, SPHINX) induce vascular endothelial growth factor VEGF-A (VEGF) splice switching from pro to anti-angiogenic isoforms in vitro causing anti-angiogenic effects in vivo. Mavrou *et al*., 2014 has demonstrated that SRPK1 inhibition with SPHINX in PC3 cells causes a similar splice switch in VEGF. Therefore, it was of interest to observe changes in VEGF splicing following SPHINX treatment. To determine whether or not SPHINX treatment induced a splicing change in VEGF, PC3 cells were treated with 10μM SPHINX followed by protein extraction. The whole cell protein extracts were immunoblotted. The protein band shown in Figure 3.4 at 22kDa corresponds to the isoforms VEGF165b and total VEGF165. The western blot showed regular VEGF165 expression and an increase in the anti-angiogenic isoform VEGF165b following SPHINX treatment which suggests that, as expected, the inhibition of SRPK1 by SPHINX results in a splicing switch from pro- to anti-angiogenic VEGF isoforms in PC3 cells.

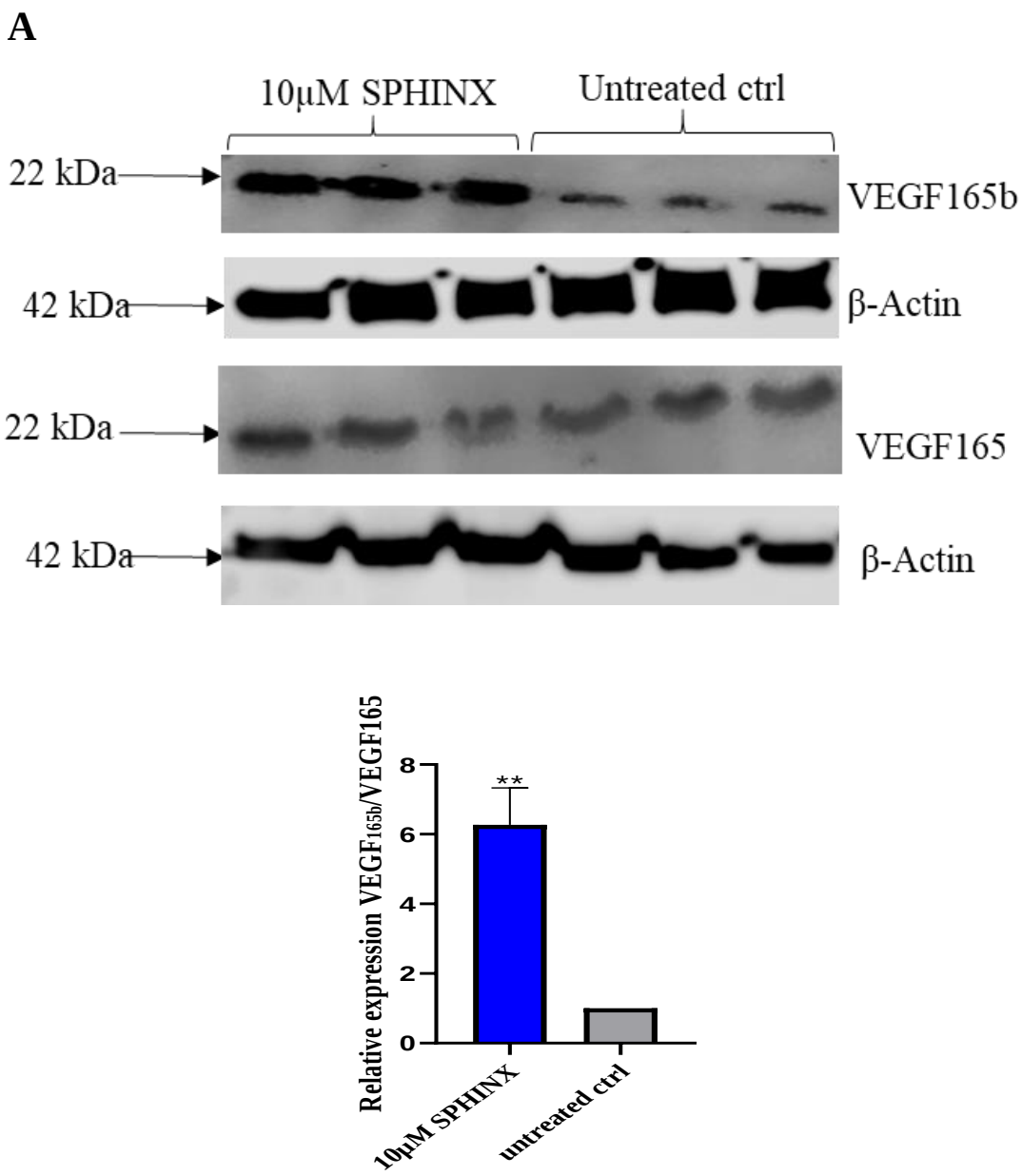

Figure 3. 4: Inhibition of SRPK1 by SPHINX results in a splicing switch from pro- to anti-angiogenic VEGF isoforms in PC3 cells.

Western blot analysis of VEGF165 and VEGF165b isoforms in PC3 cells after exposure to 10μM SPHINX. The blots were re-probed with actin which was used as a loading control. Three independent repeats are shown in each case. The graph represents relative expression determined by densitometric measurement of the bands and is expressed relative to VEGF 165. The bar graph shown is the average of three independent

experiments. (**P= 0.0076) a significant change of VEGF Splicing compared to untreated using unpaired t test.

3.3.5 Effect of SPHINX treatment on the alternative splicing of apoptotic genes *BCL2L1* and *CASPASE-9*

Wang *et al.,* 2017 demonstrated that knocking down SRPK1 with siRNA result in increased splicing of the cleaved *caspase-3* and other pro-apoptotic splice isoforms of PARP and p53. Specifically, the study suggests that knocking down SRPK1 by siRNA allows the activation of the PARP- caspase3 pathway and helps to limit the proliferation rate in K562 cells.

To investigate whether SRPK1 inhibition using a chemical inhibitor would result in any change in the splicing of other caspase family members such as caspase-9 and another apoptotic factor such as BCL2L1, mRNA was extracted from the K562 and PC3 cells following 10μM SPHINX treatment. Then a PCR was performed using the primers listed in Table 2.6. PCR bands show that the splicing ratio (PSI-Ψ) of *caspase-9a/caspase-9b* (Figure 3.5) and *Bcl-xl/Bcl-xs* (Figure 3.6) was significantly higher in the SPHINX treated group than in the control group in K562 cells. The splice ratio of *caspase-9a/9b* isoform in the control was 0.67 while in SPHINX treated cells 0.87 (**P= 0.0025 using unpaired t-test) in PC3 cells, *caspase-9a/9b* splicing ratio of the control was 0.48 while 0.83 in (*P= 0.0351 using unpaired t-test). The expression ratio *Bcl-xl/xs* isoform in the control was 0.83 while in SPHINX treated cells 0.94 (**P= 0.0012 using unpaired t-test). On the other hand, in PC3 cells there was no significant change in the ratio of *Bcl-xl/Bcl-xs* isoforms following SPHINX treatment (figure 3.7 and 3.8). Taken together, these experiments do clearly show that SPHINX causes changes in the alternative splicing of apoptosis-associated genes.

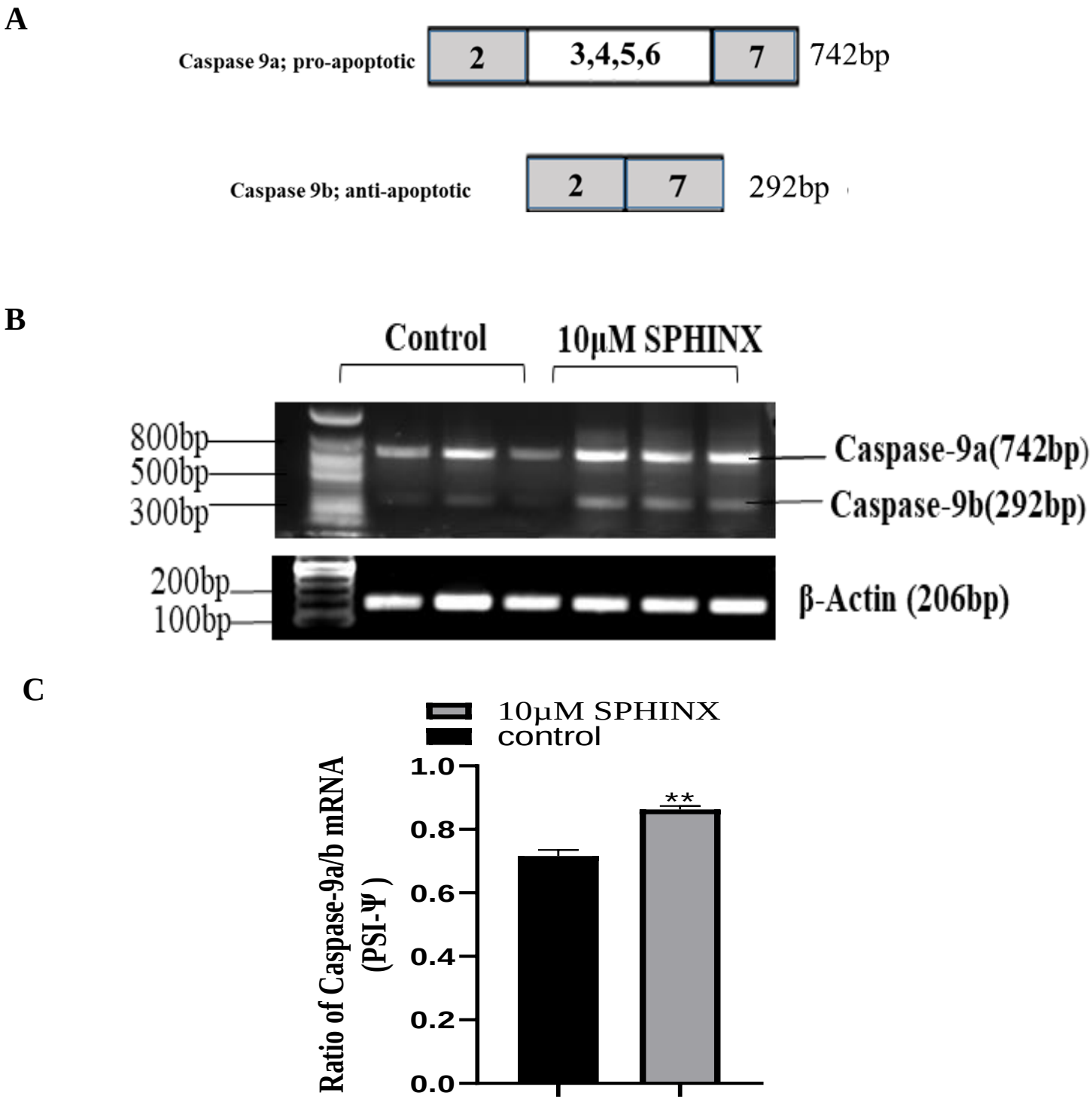

Figure 3. 5: Caspase-9 mRNA levels in SPHINX treated K562 cells.

K562 cells treated with 10µM of SPHINX for 72hrs followed by RNA extraction and cDNA synthesis. PCR was performed using *Caspase-9* specific primers. (A). Representation of *Caspase-9* PCR amplicon sizes and (B) Showing band intensity and size and corresponding loading control, *β-actin*. (C). Densitometry showing *caspase-9a/9b* PSI-Ψ values for 72hrs. The result shows significance in splice ratio of *caspase-9* (PSI-Ψ, **P= 0.0025) using unpaired t test. *n*=3. Three independent repeats are shown in each case.

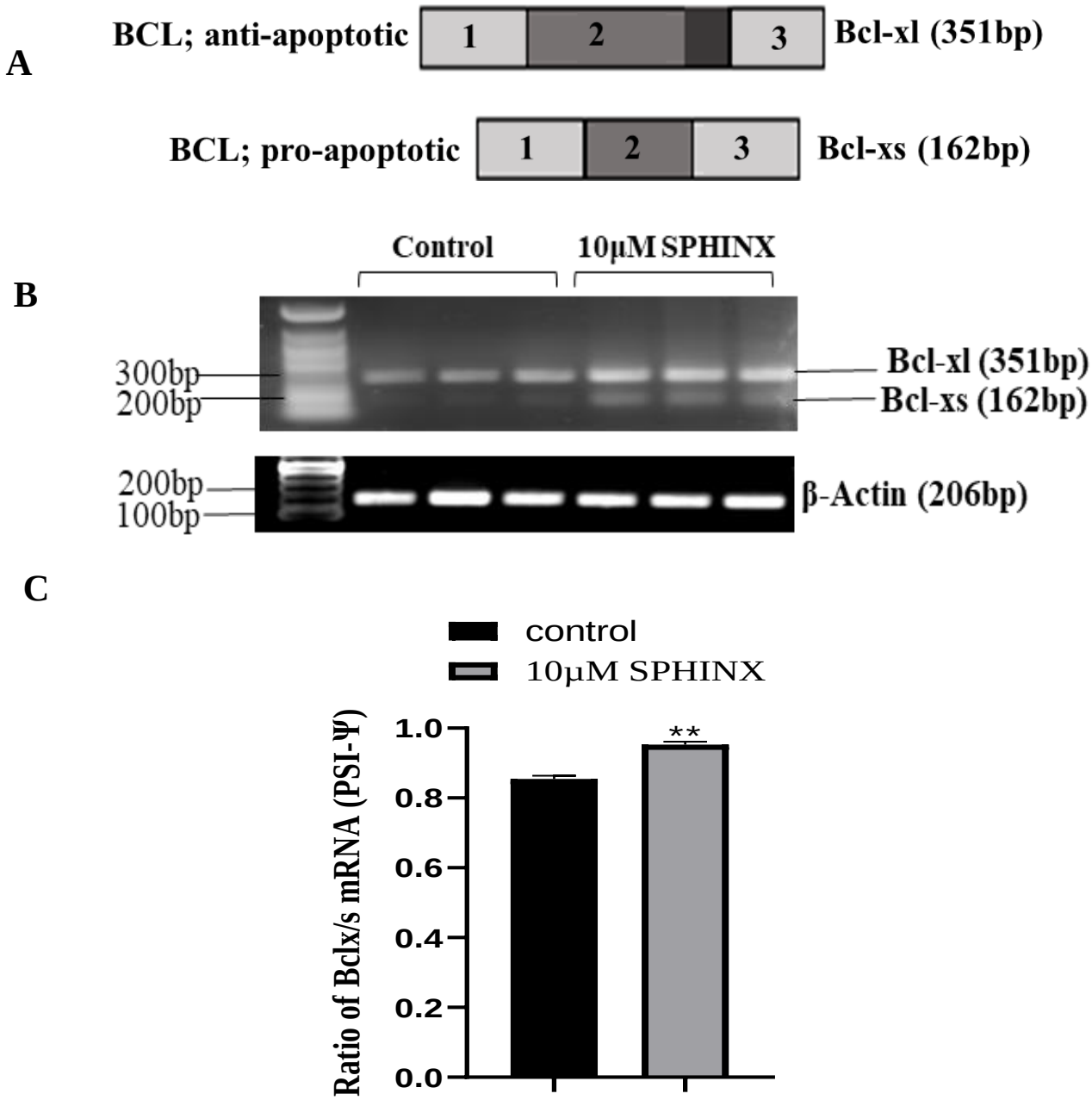

Figure 3. 6: BCL2L1 mRNA levels in SPHINX treated K562 cells.

K562 cells treated with 10µM of SPHINX for 72hrs followed by RNA extraction and cDNA synthesis. PCR was performed using *Bclx*-specific primers. A. Representation of *Bclx* PCR amplicon (B) PCR gel at 72hrs showing band intensity and size and corresponding loading control, *β-actin*. **(C)**. Graph showing relative densitometry of *Bcl-xl/s* PCR bands 72hrs after SPHINX treatment. There was a significant change in splice ratio of *caspase-9* (PSI-Ψ, **P= 0.0012) using unpaired t test. *n*=3. Three independent repeats are shown in each case.

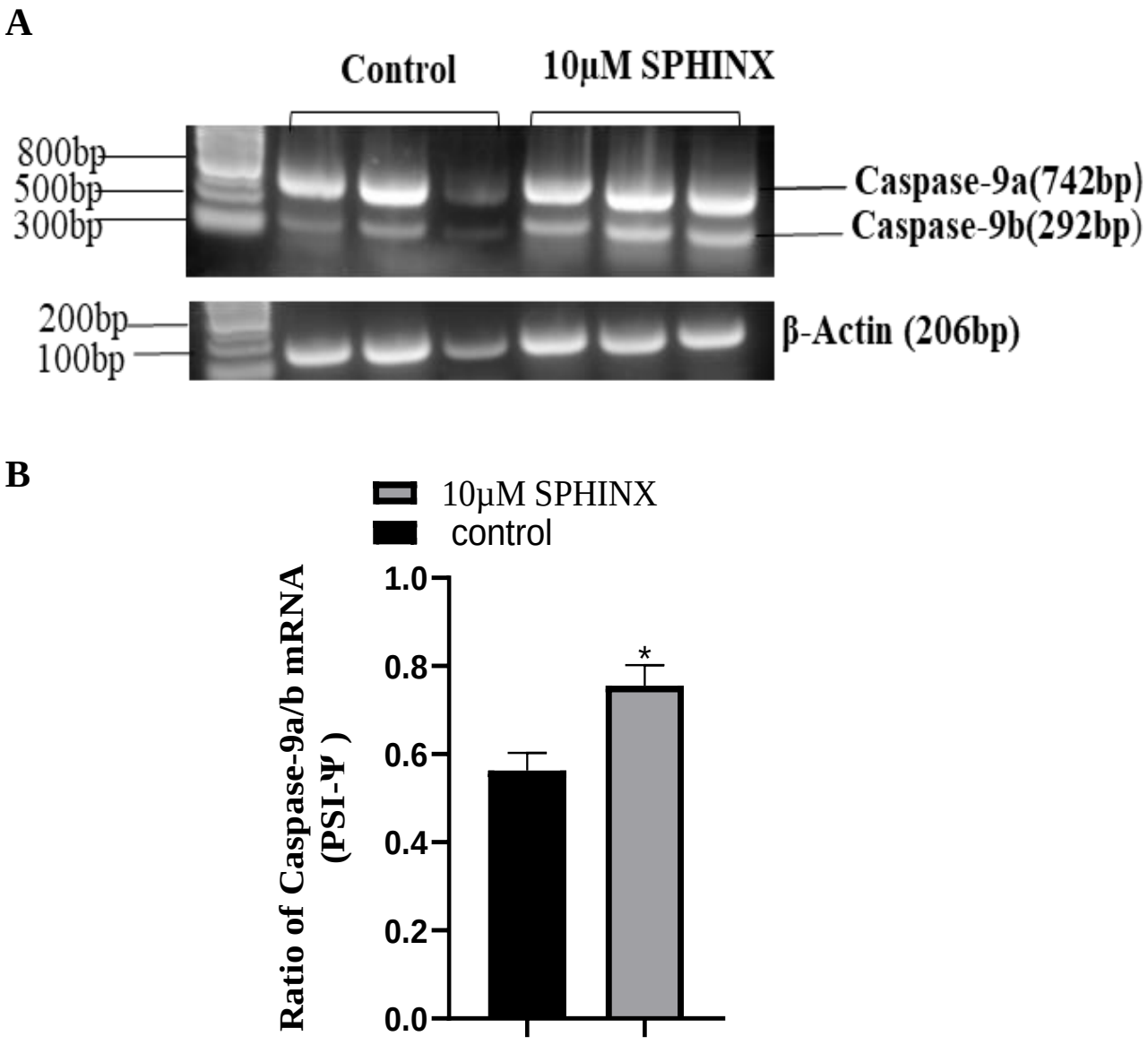

Figure 3. 7: Caspase-9 mRNA levels in SPHINX treated PC3 cells.

PC3 cells treated with 10µM of SPHINX for 72hrs followed by RNA extraction and cDNA synthesis. PCR was performed using *Caspase-9* specific primers. (**A**) Showing *caspase-9a* and b band intensity and size and corresponding loading control, *β-actin.* **(B)**. Graph of relative densitometry showing *caspase-9a/9b* PSI-Ψ values for 72hrs. The result shows significance in splice ratio of *caspase-9* (PSI-Ψ, *P= 0.0351) using unpaired t test. *n*=3. Three independent repeats are shown in each case.

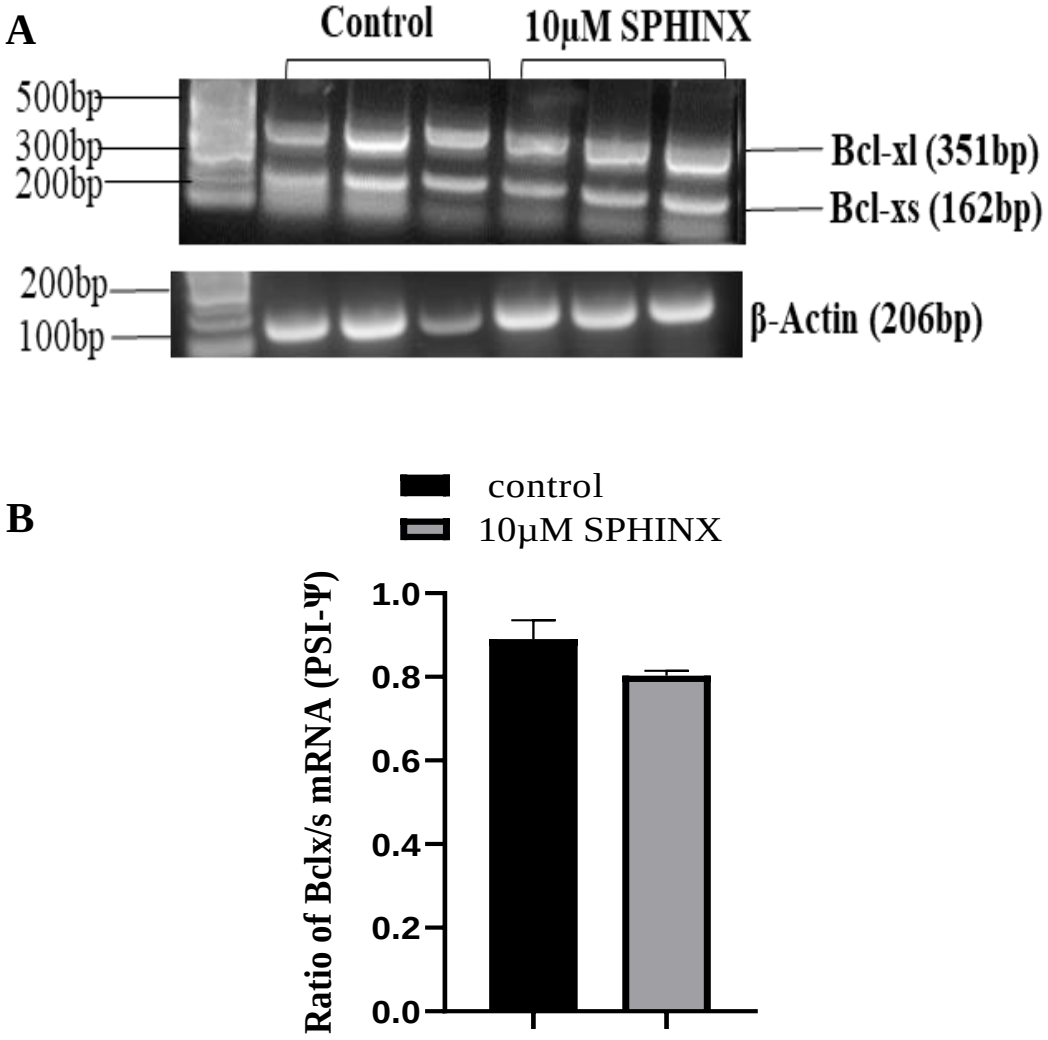

Figure 3. 8: BCL2L1 mRNA levels in SPHINX treated PC3 cells.

PC3 cells treated with 10µM of SPHINX for 72hrs followed by RNA extraction and cDNA synthesis. PCR was performed using *Bcl* specific primers. (**A**) PCR gel at 72hrs showing band intensity and size and corresponding loading control, *β-actin*. **(B)**. Densitometry showing *Bcl-xl/s* PSI-Ψ values for 72hrs. The

result shows no significance in the splicing ratio of *caspase-9* using unpaired t test. *n*=3. Three independent repeats are shown in each case.

3.3.6 The Effect of SRPK1 chemical inhibition and siRNA knockdown on cellular viability and proliferation

Slower cellular growth was observed in K562 and PC3 cells when SRPK1 was inhibited with SPHINX and siRNA SRPK1. An MTT assay was performed to evaluate the proliferation and viability of K562 and PC3 (figure 3.9 C&D) cells following siRNA transfections and SPHINX treatments (Ren *et al.*, 2010). Cells were subjected to 100nM siRNA and 10μM of SPHINX for 48hrs and 72hrs respectively. The results suggest that SRPK1 inhibition suppresses cellular proliferation and viability compared to the group where SRPK1 was not subjected to any inhibition. A similar effect of SRPK1 inhibition was described by (Wang *et al.*, 2017) for K562 and (Mavrou *et al.*, 2014) for PC3 cells. In K562 (figure 3.9 A&B) cellular proliferation rate was similar after SRPK1 inhibition using siRNA and SPHINX (*p = 0.0125 and 0.0176, two-way ANOVA). Cell viability was the lowest in cells treated with SPHINX (***p = 0.0003 two-way ANOVA). For PC3 cells (figure 3.9 C&D), the cellular proliferation rate was similar after SRPK1 inhibition using siRNA and SPHINX (**p = 0.0032 and 0.0019, two-way ANOVA). PC3 cellular viability was reduced in a similar way following SRPK1 inhibition using siRNA and SPHINX (****p < 0.0001 two-way ANOVA).

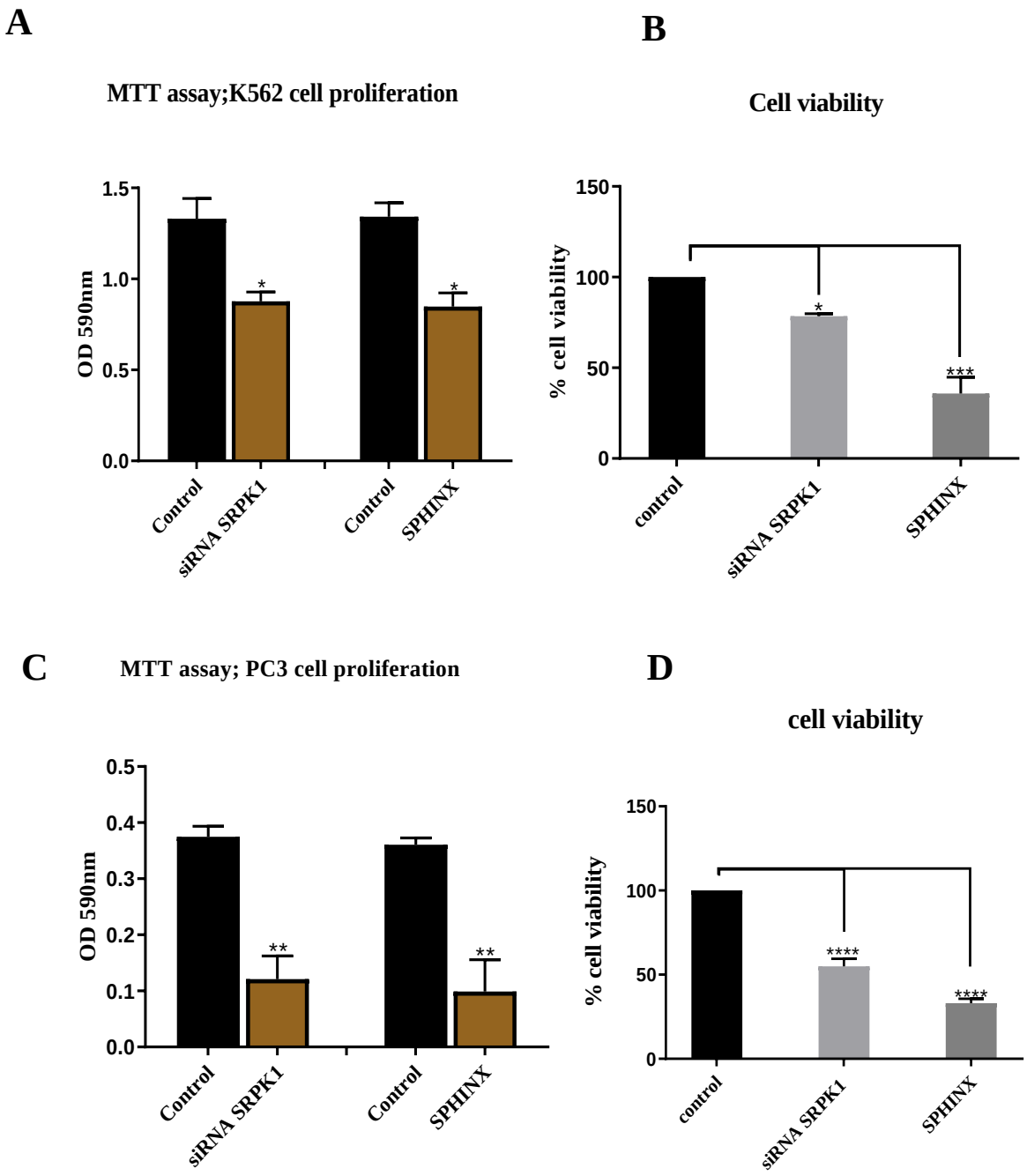

Figure 3. 9: Cellular proliferation and viability in K562 and PC3 cells after SRPK1 inhibition by siRNA and SPHINX treatment.

MTT assay was used to analyse the effect of siRNA induced SRPK1 knockdown for 48 hrs and SPHINX treatment for 72hrs on cellular proliferation and viability in K562 (A&B) and PC3 (C&D) cells. The absorbance of each well was measured at 590 nm using a plate reader. Results represent the mean ± SEM of three experiments and are presented as graphs after normalizing to the respective controls. Cell viability

was calculated using the following formal: viability= control- absorbance of treatment wells/absorbance of control well ×100%. (*p = 0.0125 and 0.0176, ****p < 0.0001 using two-way ANOVA)

3.3.7 The effect of SRPK1 chemical inhibition and siRNA knockdown on cellular migration and invasion

SRPK1 inhibition modifies VEGF splicing causing antiangiogenic effects (Mavrou *et al*., 2014). However, genes involved in other hallmarks of cancer, such as those involved in migration and invasion (metastatic phenotypes) could be affected. So it was of interest to evaluate how the cellular invasion and migration ability are affected by SPHINX treatment and siRNA SRPK1 knockdown. At first, cellular migration and invasion were assayed using Transwell migration and invasion assay (Mavrou *et al*., 2014). (Figure 3.10 & 3.11) shows an observed difference in the number of migrating and invasive cells between SPHINX treated PC3 and the untreated control groups (*p=0.0211 and **p=0.0089 unpaired t-test) respectively. In another experiment, SRPK1 was knocked down in the cells and the potential of the cells to migrate and invade was determined using the same assay. (Figure 3.12 &13) shows an observed difference in the number of migrating and invasive cells between PC3 SRPK1-KD PC3 and the control siRNA and the un-transfected cells groups (**** p<0.000, unpaired t-test). These data considered together suggest that SRPK1 inhibition using a chemical compound or siRNA knockdown significantly suppress PC3 capacity to migrate and invade.

A

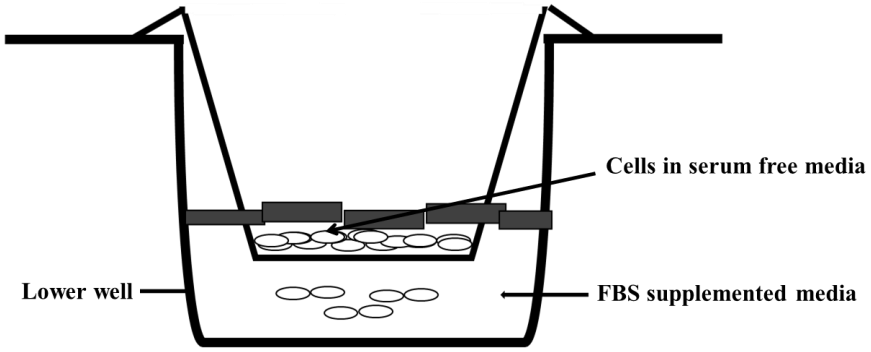
Cells in serum free media
Lower well
FBS supplemented media

B

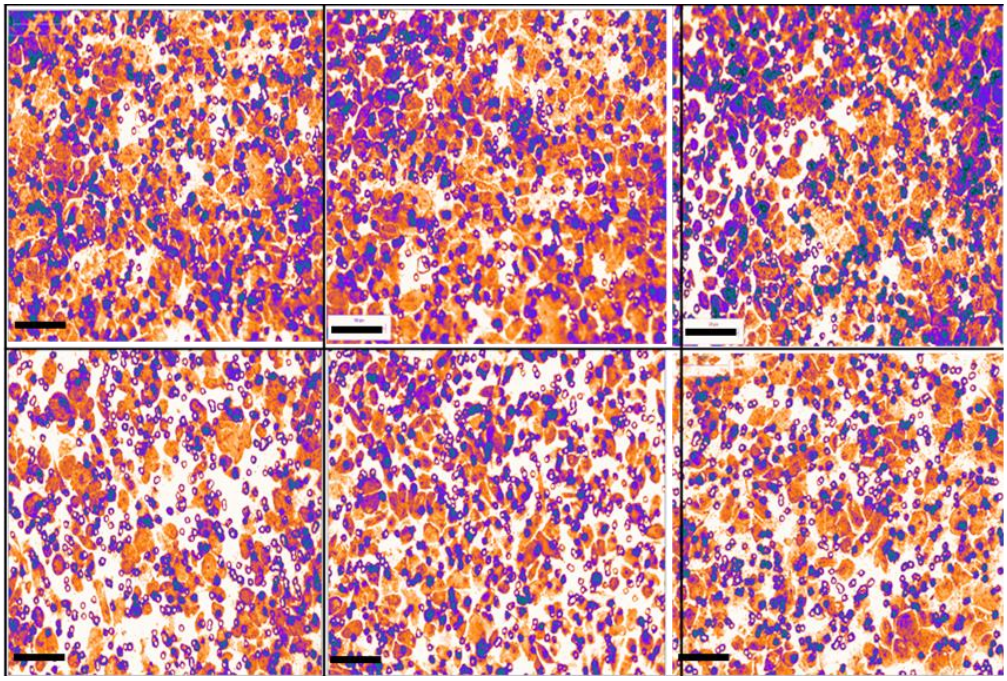
DMSO
10μM SPHINX

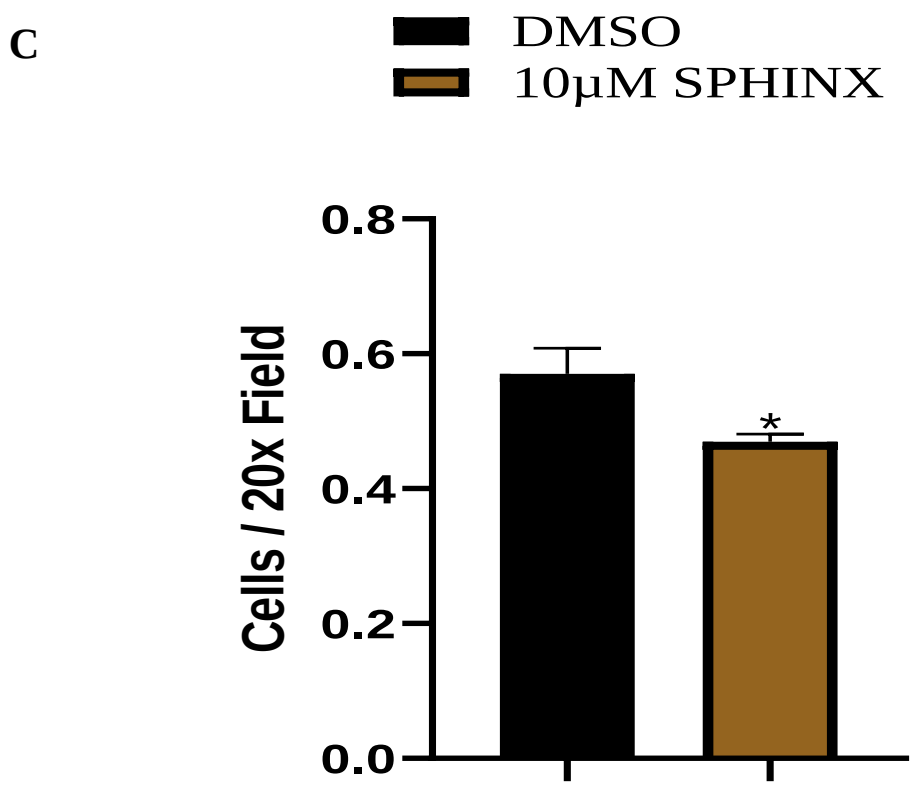

Figure 3. 10: Transwell migration assay of PC3 cells.

PC3 cells treated with 10µM of SPHINX for 72hrs (A). Representation of the transwell insert used to measure cell migration and invasion. (B). Representative Pictures of PC3 cell transwell migration. Serum-free medium was added to the lower chamber as the negative control. After cell migration and staining with crystal violet, pictures of the migrated cells were captured by Nikon Eclipse TE300 Inverted Phase Contrast Microscope using a 20x objective (scale bare = 50µM). (C) Quantification of cells migrating toward the FBS sublimated medium (Average of 5 picture fields at 100x total magnification). *P=0.0211 using unpaired t test. Three independent repeats are shown in each case.

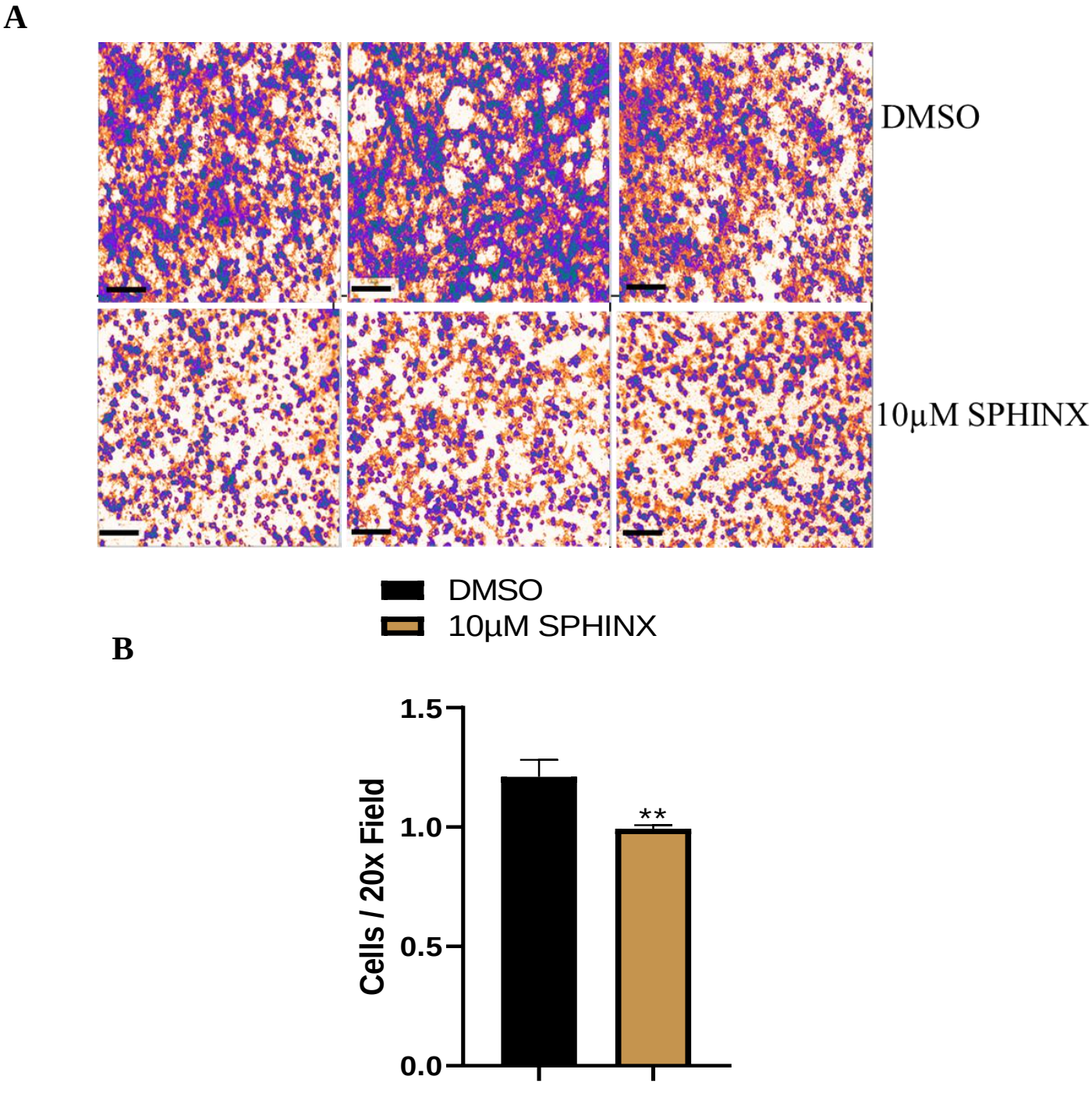

Figure 3. 11: Transwell cell invasion assay of PC3 cells.

PC3 cells treated with 10µM of SPHINX for 72hrs. (A). Representative Pictures of PC3 cell transwell invasion. The transwell membrane was coated with Matrigel and then the cell- Serum-free medium was added on top of the Matrigel. After cell invasion and staining with crystal violet, pictures of the migrated cells were captured by Nikon Eclipse TE300 Inverted Phase Contrast Microscope using a 20x objective

(scale bare = 50μM). (B) Quantification of invasive cells moving to the FBS supplemented medium (Average of 5 picture fields at 100x total magnification). **P=0.0089 using unpaired t test. Three independent repeats are shown in each case.

A

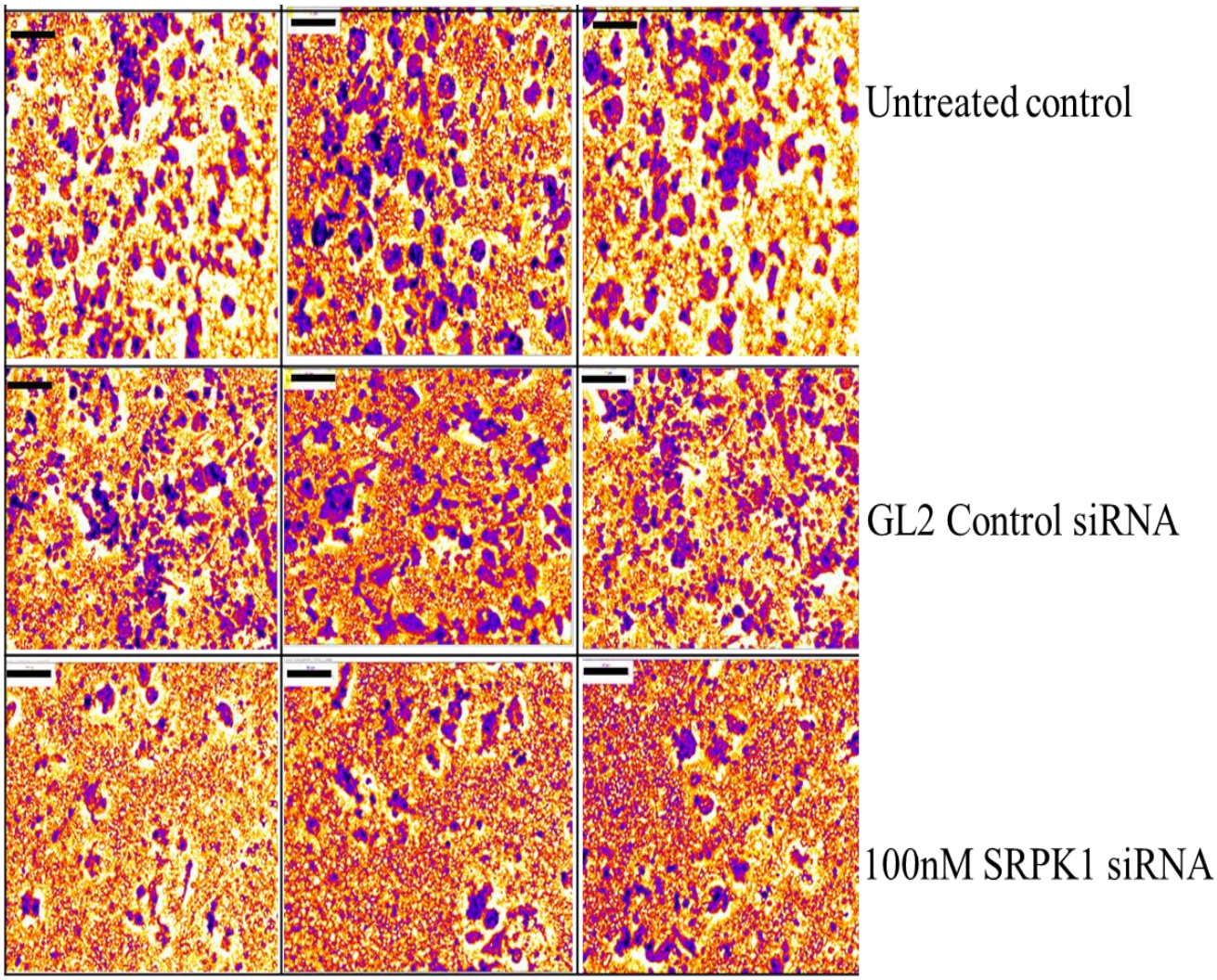

B

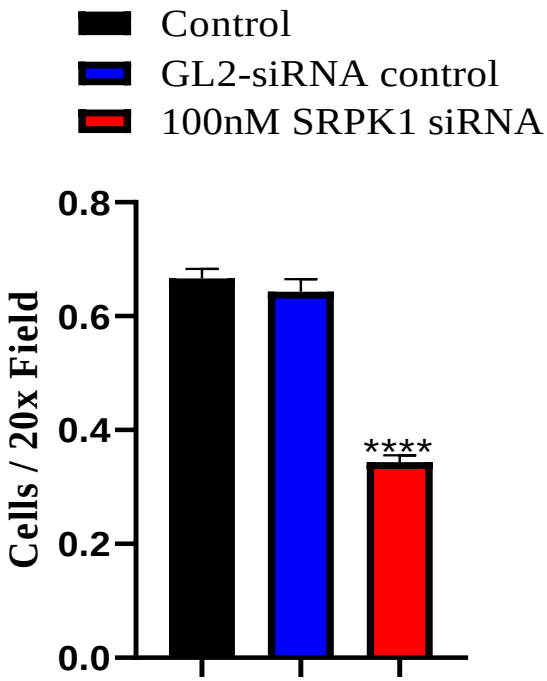

Figure 3. 12: Transwell migration assay of PC3 cells.

PC3 cells transfected with 100nM SRPK1 siRNA or GL2 control siRNA for 48hrs. (A). Representative Pictures of PC3 cell transwell migration. After cell migration and staining with crystal violet, pictures of the migrated cells were captured by Nikon Eclipse TE300 Inverted Phase Contrast Microscope using a 20x objective (scale bare = 50µM). (B) Quantification of cells migrating toward the FBS sublimated medium (Average of 5 picture fields at 20x total magnification). ****P<0.0001 using unpaired t test. Three independent repeats are shown in each case.

A

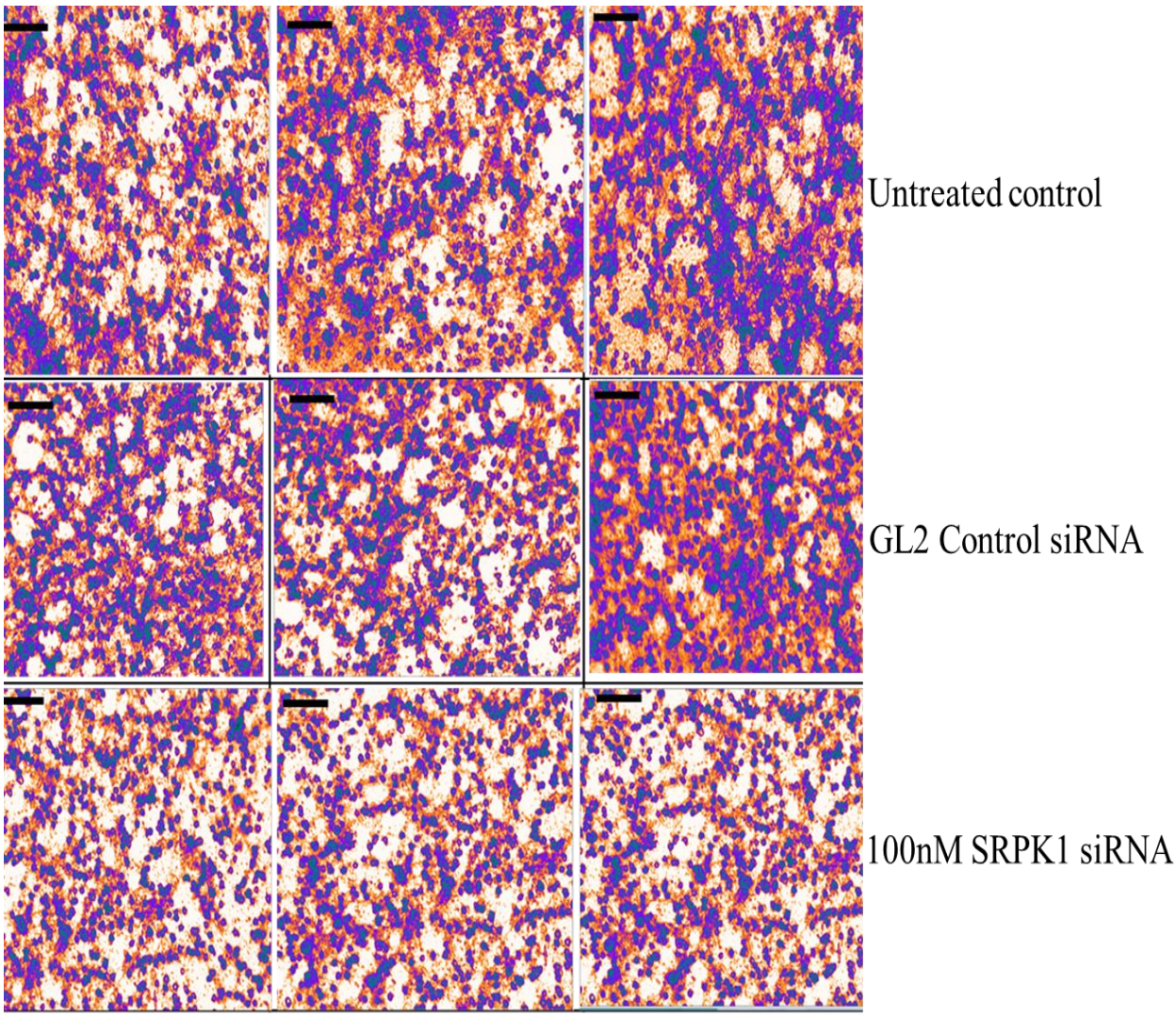

B

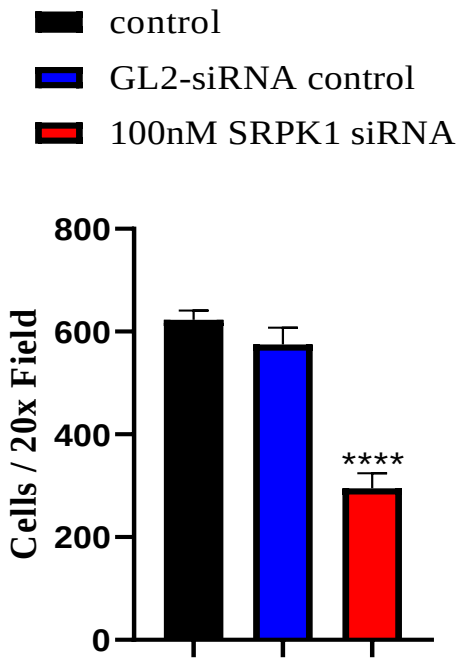

Figure 3. 13: Transwell cell invasion assay of PC3 cells.

PC3 cells transfected with 100nM SRPK1 siRNA or GL2 control siRNA for 48hrs. (A) Representative Pictures of PC3 cell transwell invasion. The transwell membrane was coated with Matrigel and then the cell- Serum-free medium was added on top of the Matrigel. After cell invasion and staining with crystal violet, pictures of the migrated cells were captured by Nikon Eclipse TE300 Inverted Phase Contrast Microscope using a 20x objective (scale bare = 50μM). (B) Quantification of invasive cells moving to the FBS sublimated medium (Average of five picture fields at 20x total magnification). ****P<0.0001 using a one way ANOVA test. Three independent repeats are shown in each case.

3.4 Summary

The results in this section have confirmed the expression of SRPK1 in a range of cancer cell lines. The presumed SRPK1a isoform was not detectable in the cell lines, at least not by standard PCR (fig.3.1). The SRPK1a isoform has only been described in a single publication where SRPK1/SRPK1a ratio on erythroid differentiation was studied. The existence of this isoform needs to be corroborated by other studies. It was not detected in this study. It is conceivable that SRPK1a is expressed at very low, barely detectable levels in these specific cell lines.

Evidence for an autoregulatory loop involving SRPK1 was examined. The siRNA knockdown of SRPK1 apparently did not affect the transcription of SRPK1. The chemical inhibition of the kinase activity did, however, appear to affect levels of SRPK1. In summary, in K562 and PC3 cells, inhibition of SRPK1 using siRNA knockdown reduced SRPK1 protein levels as expected. The SRPK1 inhibitor (SPHINX) did, however, appear to reduce protein levels of SRPK1, and the transcription of the SRPK1 gene (fig.3.2&3), suggesting that an autoregulatory loop may exist. Conceivably, SRPK1 might be involved in regulating the activity of factors that regulate SRPK1 transcription. The chemical inhibition of SRPK1 in K562 and PC3 cells resulted in the alteration of the splicing of a panel of key apoptotic genes. Specifically, SRPK1 inhibition resulted in a change in the splicing of the apoptotic factors such as *BCL2L1* and *CASPASE-9* splicing toward the pro-apoptotic isoforms in the same cell lines (fig.3.5, 6&7). A shift in the splicing of VEGF165 was clearly observed in this study as SRPK1 inhibition using SPHINX induced a splicing switch toward the anti-angiogenic isoform VEGF165b (fig.3.4).

Cellular proliferation, viability, migration and invasion were also affected by SRPK1 inhibition. Following SRPK1 inhibition using siRNA and SPHINX, the proliferation and viability of K562 and PC3 cells were significantly reduced (fig.3.9). A similar reduction was observed in the migration and invasive ability of both cell lines in response to SRPK1 inhibition (fig.3.10, 11, 12 &13). Together these results are consistent with SRPK1 exerting pro-oncogenic effects. It is, therefore, necessary to examine how SRPK1 expression might be activated in cancer cells. The next chapter considers whether or not the transcription factor WT1 (Wilms' tumour) is involved in the regulation of SRPK1 transcription.

4 Chapter Four: SR protein kinase 1 (SRPK1) regulation by WT1

4.1 Background

As highlighted in the previous chapter, SRPK1 is a protein kinase that phosphorylates serine/arginine-rich proteins (SR-proteins) which are responsible for regulating constitutive and alternative mRNA splicing. Studies have linked high SRPK1 levels to tumour proliferation, growth, and metastatic ability (Zhou *et al.,* 2013). The overexpression of SRPK1 has been associated with pancreatic, breast and colorectal cancer (Hayes *et al.,* 2007). However, the regulation of SRPK1 expression is not well understood. This suggests that its inhibition might result in limiting tumour growth, increasing therapy responsiveness by modulating alternative splicing of key cancer genes. One of these key genes is vascular endothelial growth factor (VEGF) which regulates angiogenesis and other vital cellular pathways.

VEGF is highly expressed in the podocytes of the kidney glomerulus (Ermina and Quaggin 2004). The development and function of the podocytes might be linked to this high expression. In the development of the kidney, the interaction of the epithelial ureteric bud with metanephric mesenchyme, a histologically distinct patch of cells in the urogenital ridge, leads to condensation of the mesenchymal cells around the branching ureteric bud. This results in the subsequent induction of a mesenchymal-to-epithelial transformation of the condensed mesenchyme into a tubular structure known as a nephron (Saxen, 1987). Gao *et al.,* 2005 have shown that this developmental process is mediated by WT1 and VEGF.

The Wilms tumour suppressor WT1 was previously shown to repress the transcription of SRPK1 in normal podocytes and indirectly serine/arginine-rich splicing factor 1 (SRSF1) activity, thus altering VEGF splicing because of SRSF1 drives the expression of pro-angiogenic VEGF. SRPK1 expression was significantly elevated in Denys Drash Syndrome podocytes harbouring a WT1-activating mutation in the zinc finger domain (Amin *et al.* 2011). A recent study Wagner *et al.*, 2019; (see appendix) has demonstrated that WT1, SRPK1, SRSF1, and the angiogenic VEGF isoform are highly expressed in tumour endothelium compared to normal lung endothelium. Inducible conditional vessel-specific knockout of WT1 reduced WT1, SRPK1, and SRSF1 expression in endothelial cells and induced a shift towards the antiangiogenic VEGF isoform. WT1 (-KTS) isoform directly binds and activates both the promoters of SRPK1 and SRSF1 better than WT1 (+KTS) isoform in endothelial cells.

This suggests that WT1 activates SRPK1 and SRSF1 and induces expression of antiangiogenic VEGF isoforms in tumour endothelium. The ability of WT1 to either activate or repress its target genes in different contexts is well known. Whether or not WT1 contributes to the transcriptional regulation of SRPK1 in other cancer cells, has not yet been determined.

4.2 Aims and objective

1. To investigate the transcriptional regulation of the splice factor kinase gene SRPK1 by WT1 in K562, DU145 and PC3 cancer cell lines by assaying binding of WT1 to *SRPK1* promoter.
2. To evaluate the impact of WT1 knockdown or overexpression on the following:

- Transcription and protein levels of SRPK1 in K562, PC3, and DU145 cells.
- The alternative splicing of apoptotic factors; *BCL2L1* and *caspase 9*
- On cellular migration, invasion, viability, and proliferation.

4.3 Results

4.3.1 WT1 binds the *SRPK1* promoter

Since WT1 is a well-established transcription factor and given the fact that WT1's (-KTS) isoforms are efficient at DNA-binding (Laity *et al.*, 2000), the ability of WT1 to bind the *SRPK1* promoter was investigated. (Amin *et al.*, 2011) analysed the open reading frame of *SRPK1* and indicated that the putative core promoter sequence is located between -178 and + 40 relative to the ATG start codon in the open reading frame (the actual transcriptional start site is unclear; figure 4.1.A) WT1 is known to bind to the 9 base pair early growth response 1 (EGR-1) consensus sequence (GCG GGG GCG) (Rauscher *et al.*, 1990; Bickmore *et al.*, 1992); a similar sequence is apparently close to the presumed SRPK1 transcription start site. WT1 has already been shown to bind to the putative *SRPK1* promoter region of the gene in glomerular podocytes (Amin *et al.*, 2011). In this study, chromatin immunoprecipitation (ChIP) was performed on sheared cross-linked chromatin collected from K562 and PC3 cells (figure 4.2). Primers specific to the *SRPK1* promoter (table 2.6) were used based on Amin *et al.* 2011 and PCR was performed to detect the genomic regions around 100bp being pulled down by the antibodies. Figure 4.2. Shows that WT1 is binding to the *SRPK1* promoter in these cell lines. Rabbit monoclonal antibody against WT1 was used in the chip or anti- polymerase II antibody as a positive control. Normal Mouse IgG served as a negative control. Input DNA was used as an additional positive control for subsequent PCRs on the *SRPK1* promoter and the respective sequence. For additional confirmation, the amplicon was extracted from the gel and verified by sequencing (see Appendix)

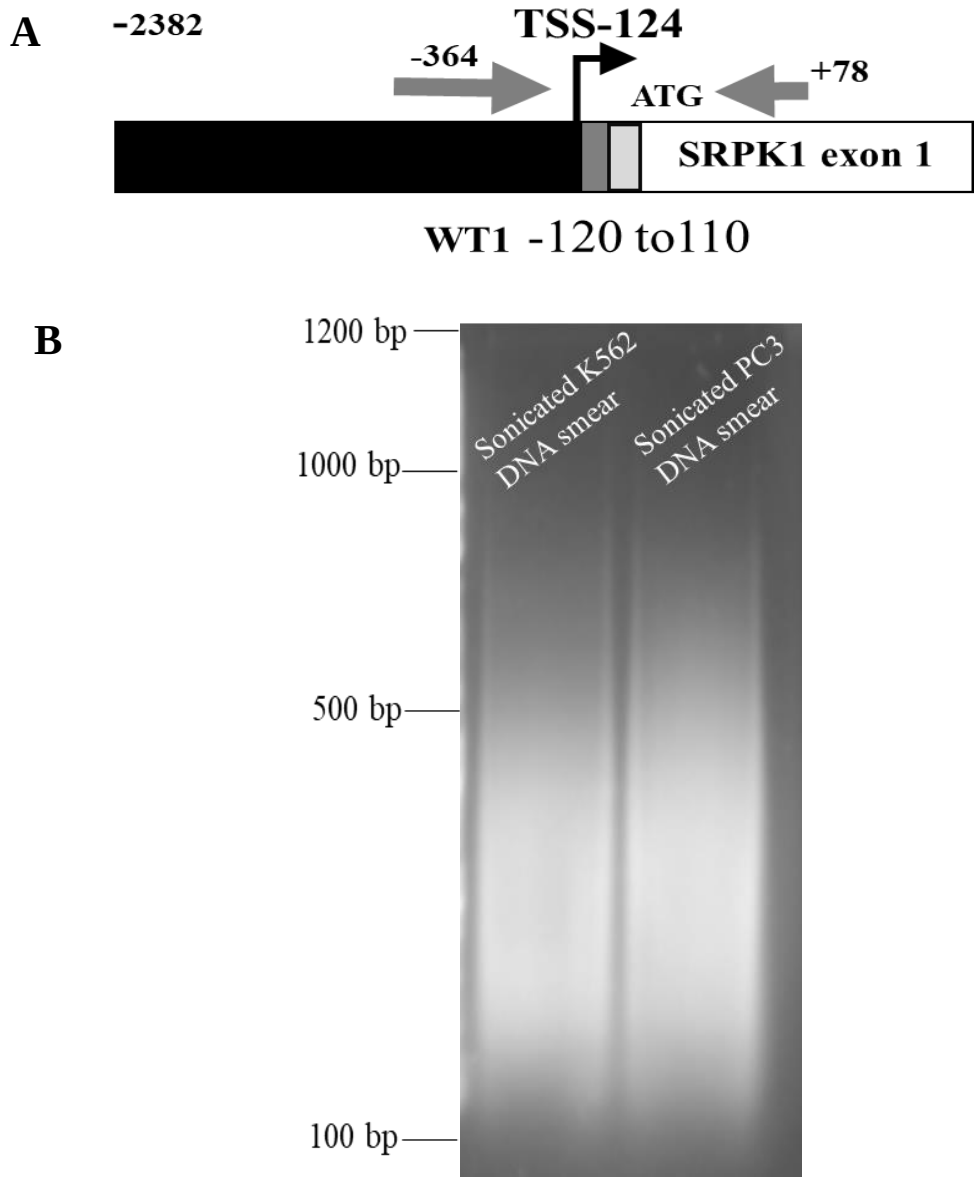

Figure 4. 1: Sonicated DNA smear for PC3 and K562 cells in preparation for Chromatin Immunoprecipitation assay.

A. Position of the WT1 binding site in the *SRPK1* core promoter. Black, promoter region; grey, WT1 binding site (B) Chromatin fragments resolved by agarose gel following sonication with varying sonication times, the cells were lysed and DNA sheared using a sonicator A**.** K562 cells were sheared at 30% power output for a minute for K562 followed by incubation on ice for 60 seconds after each pulse. B**.** 50% power output for 15seconds for PC3 followed by incubation on ice

A

K562

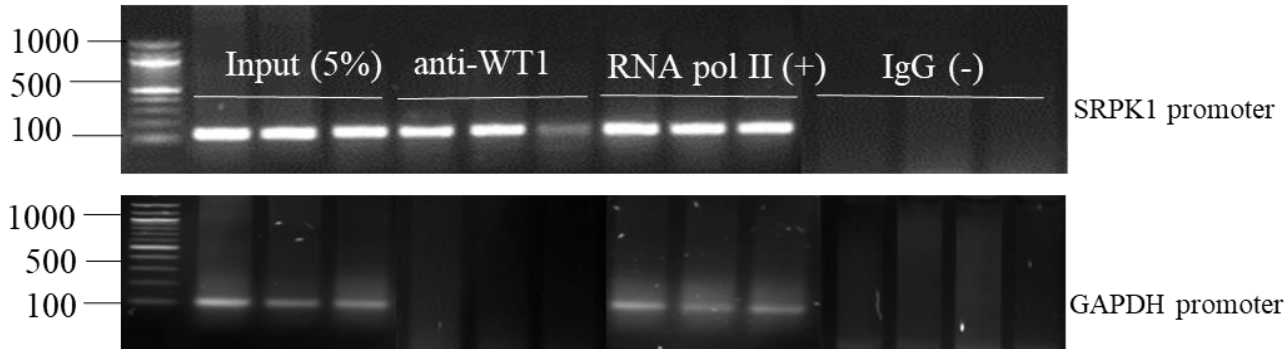
1000
500
100
Input (5%)
anti-WT1
RNA pol II (+)
IgG (-)
SRPK1 promoter
1000
500
100
GAPDH promoter

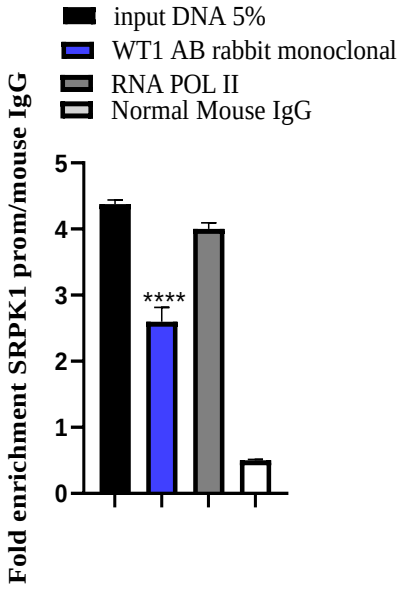
input DNA 5%
WT1 AB rabbit monoclonal
RNA POL II
Normal Mouse IgG
Fold enrichment SRPK1 prom/mouse IgG
5
4
3
2
1
0
****

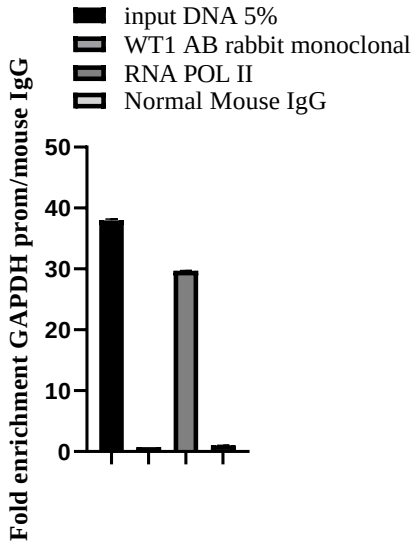
input DNA 5%
WT1 AB rabbit monoclonal
RNA POL II
Normal Mouse IgG
Fold enrichment GAPDH prom/mouse IgG
50
40
30
20
10
0

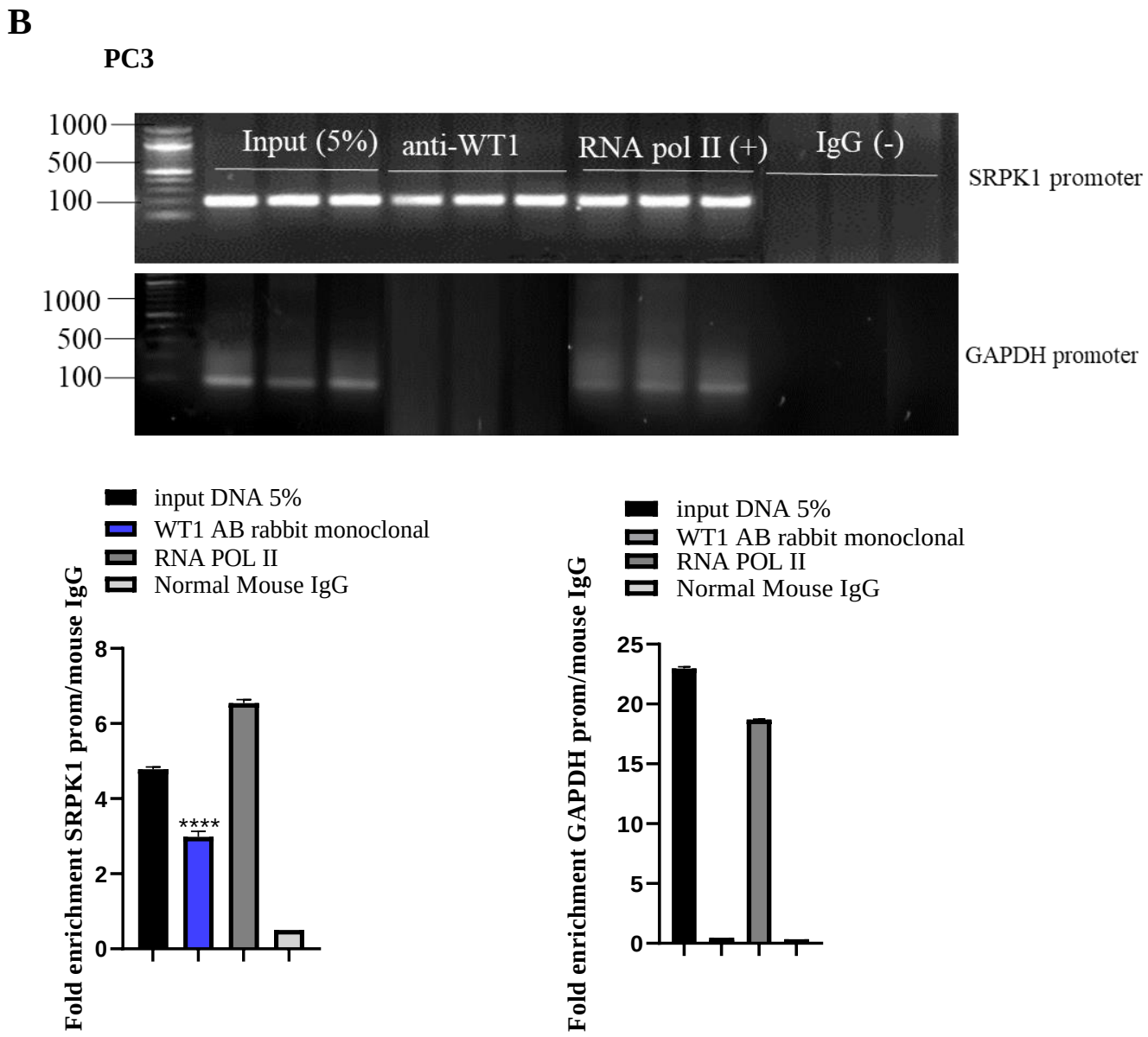

Figure 4. 2: WT1 binds the SRPK1 promoter.

Chromatin immunoprecipitation (ChIP), A. PCR assay for ChIP product for K562 cells using primers to detect the region around the *SRPK1* transcriptional start site (TSS) and *GAPDH* promoters. Representative agarose gel photographs of semi-quantitative ChIP PCR experiments for the *SRPK1* and *GAPDH* promoters. Data are expressed as means ± S.E.M. **** indicates $p < 0.0001$ which is statically significance ($n = 3$) using a one way ANOVA test. B. PCR assay for ChIP product for PC3 cells using primers to detect the region around the *SRPK1* transcriptional start site (TSS) and *GAPDH* promoters. Representative Agarose gel photographs of semi-quantitative ChIP PCR experiments for the *SRPK1* and *GAPDH*.

4.3.2 WT1 activates SRPK1 transcription in PC3, DU145 and K562

The previous experiment suggests that WT1 binds to *SRPK1* promoter. In a previous study (Amin *et al*., 2011), the binding of WT1 to the *SRPK1* promoter results in the repression of transcription of *SRPK1* by WT1 in glomerular podocytes. The aim here was to determine whether or not WT1 might contribute to *SRPK1* transcriptional regulation in cancer cells. As a model system, the leukemic cell line (K562) and prostate cancer cell lines (PC3 and DU145) were used. These cancer cell lines are known to express both WT1 and SRPK1. The results show that the ratio of Luciferase to Renilla was almost four times greater in K562, PC3 and DU145 cells (Figures 4.3) when cell lines were transfected with wild type promoter while when transfected with the mutated promoter the ratio was greatly reduced. In all of the three transfection repeats in all of the cell lines mutation of the GC-rich WT1 binding site disrupted *SRPK1* promoter activity. Therefore, findings support the hypothesis that WT1 is binding to the *SRPK1* promoter in these cell lines activating its transcription.

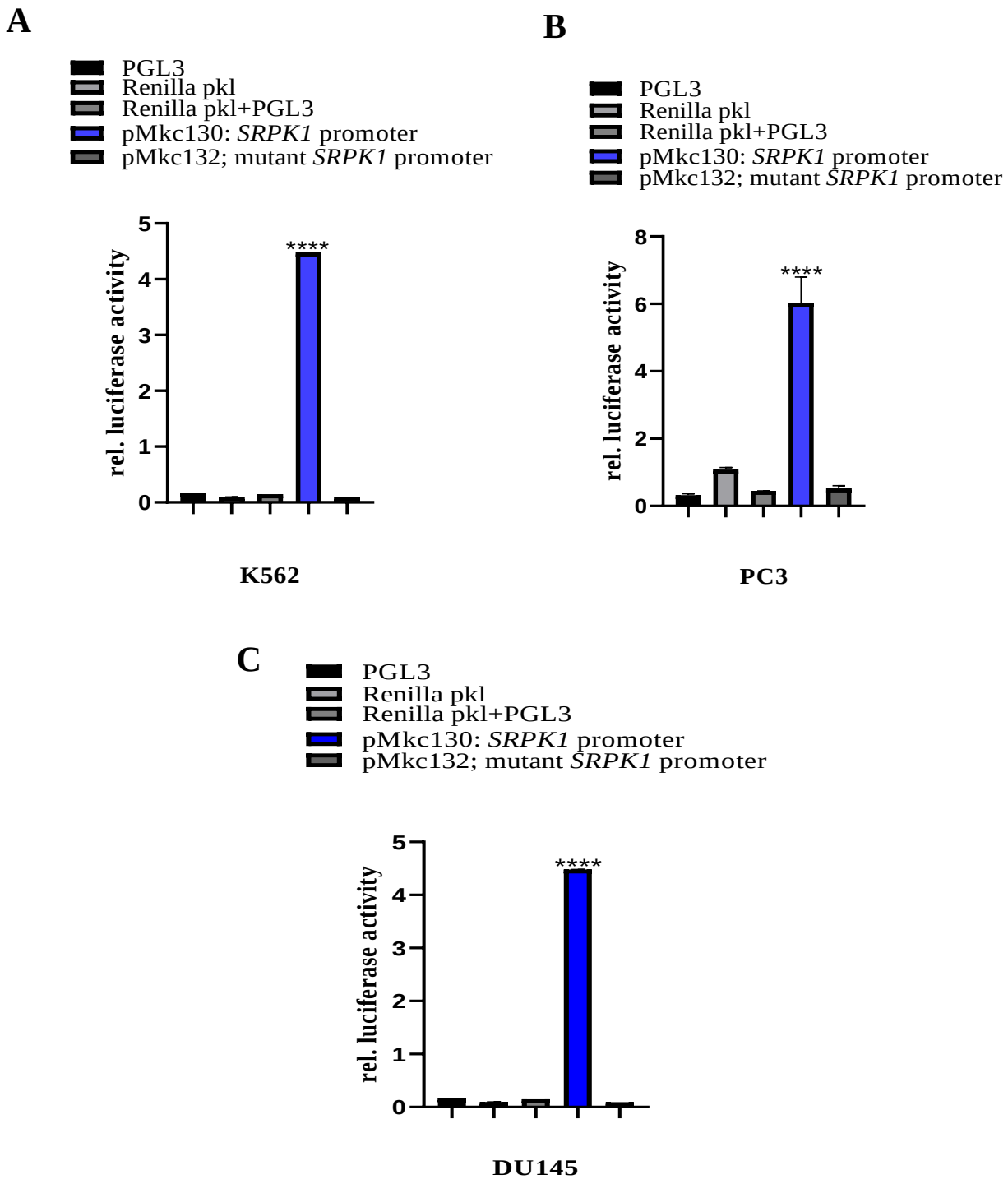

Figure 4. 3: DLR assay of SRPK1 promoter activity in K562 (A), PC3 (B) and DU145(C) cells.

Measurement of *SRPK1* promoter activity using a dual luciferase reporter (DLR) assay. An *SRPK1*: Luciferase construct (cloned into a pGL3 vector), with or without a mutation in the WT1 binding site in the *SRPK1* promoter (GGGGCGGGGG to GAATTCAAAA) was transfected into the cell lines with a Renilla expressing vector as a transfection control. Data are expressed as relative luciferase units (RLU). Data presented as mean ± S.E. for n=3.

**** indicates $p<0.0001$ which is statistically significant using a one way ANOVA test. Figures show a reduction of promoter's activity in cells when transfected with the mutant promoter and high activity when transfected with wild type promoter.

4.3.3 Effect of WT1-siRNA knockdown on SRPK1 transcription and protein level

So far, the experimental outcomes in this study suggest that WT1 binds to the *SRPK1* promoter and activates its expression. In order to investigate further the involvement of WT1 in SRPK1 transcriptional regulation, it was necessary to establish siRNA-mediated knock-down of WT1 in K562 and PC3 cell lines. The same WT1 siRNA (human specific) and the GL2 control sequences (table 2.1) previously described in (Davies *et al.*, 2003) were used in this study. To verify the transfection efficacy, siRNA were tagged with different fluorescent labels such as FAM & CY5 (Figure.4.4.A). At first, to verify that the knockdown occurred siRNA were transfected alone to the cells and western blot was performed on protein lysates prepared from the cell lines following the siRNA knockdown (Figure.4.4.B &C). Significant reduction on both WT1 and SRPK1 levels was observed at higher concentrations of the siRNA (50 and 100nM) which suggests that knocking down WT1 resulted in a reduction in SRPK1 expression in K562 and PC3 cell lines.

The next step was to evaluate the effect of WT1 knockdown on SRPK1 transcription by co-transfecting the highest concentration of siRNA WT1 with *SRPK1* wild-type and mutant promoters. Figure.4.6.D&E shows that the activity of the wild type promoter significantly decreased in K562 cells ($*p= 0.0014$) (Figure.4.6.D) and PC3 cells ($*p< 0.0001$) when co-transfected with WT1 siRNA (Figure.4.7.E). The mutant promoter showed no change in the activity in response to WT1 siRNA transfection.

A

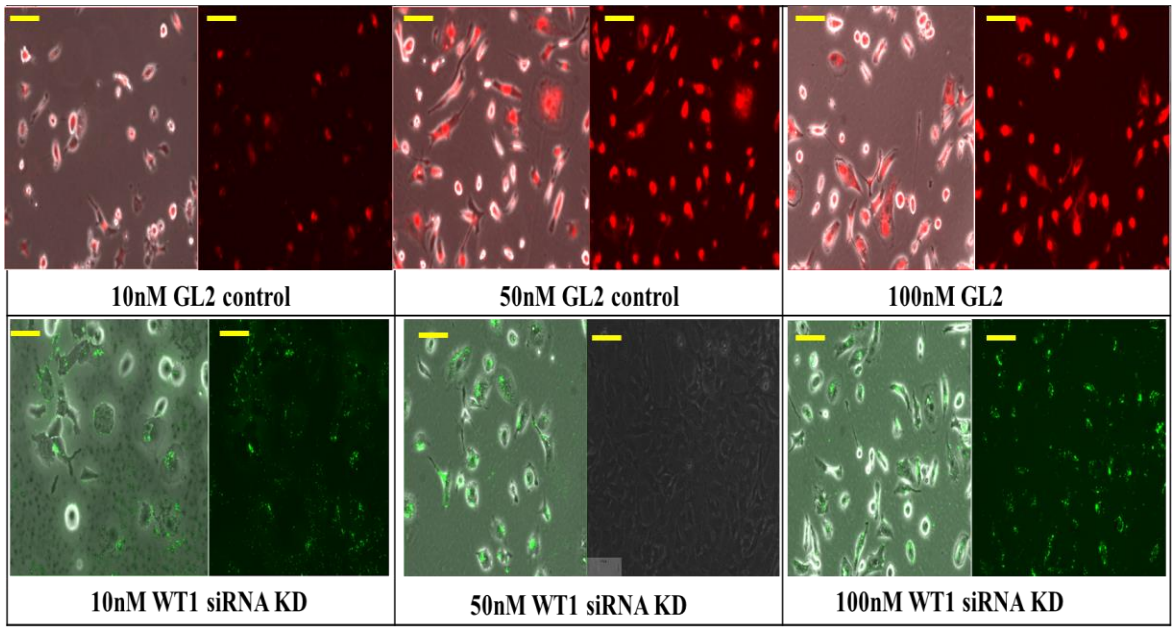
10nM GL2 control
50nM GL2 control
100nM GL2
10nM WT1 siRNA KD
50nM WT1 siRNA KD
100nM WT1 siRNA KD

B

K562

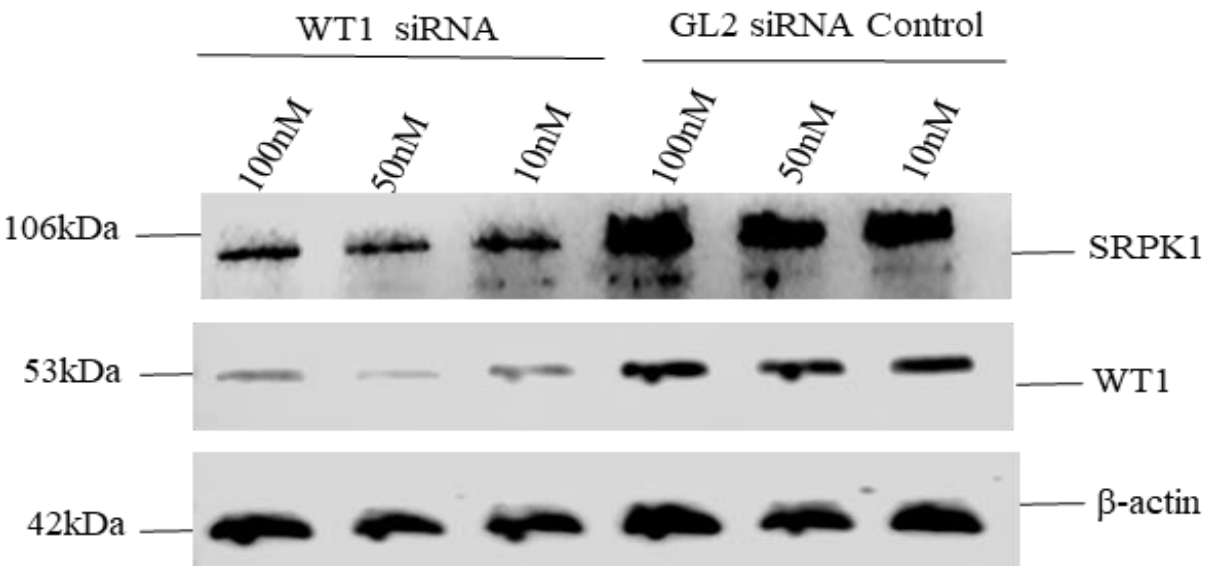
WT1 siRNA
GL2 siRNA Control
100nM
50nM
10nM
100nM
50nM
10nM
106kDa
SRPK1
53kDa
WT1
42kDa
β-actin

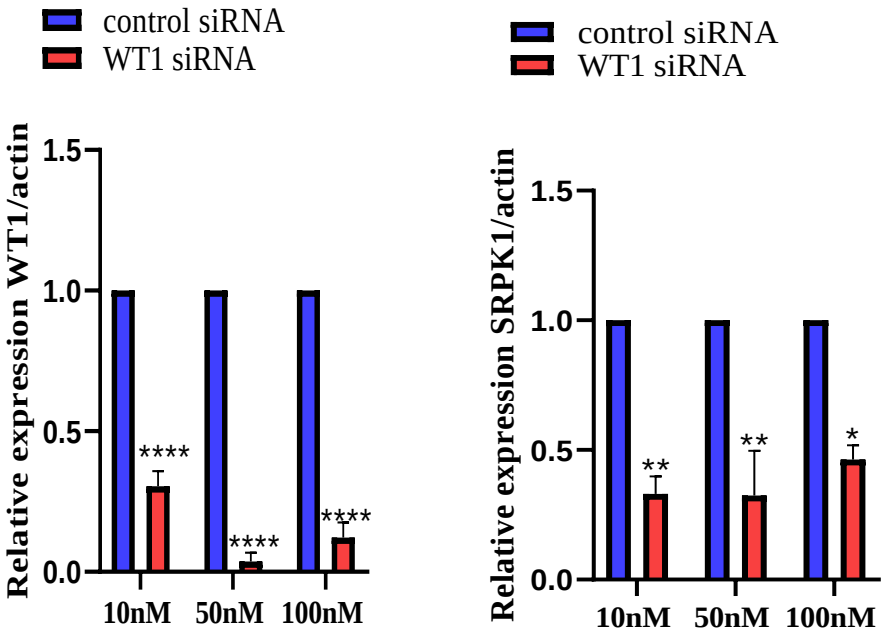
control siRNA
WT1 siRNA
Relative expression WT1/actin
1.5
1.0
0.5
0.0
****
****
****
10nM
50nM
100nM
control siRNA
WT1 siRNA
Relative expression SRPK1/actin
1.5
1.0
0.5
0.0
**
**
*
10nM
50nM
100nM

C

PC3

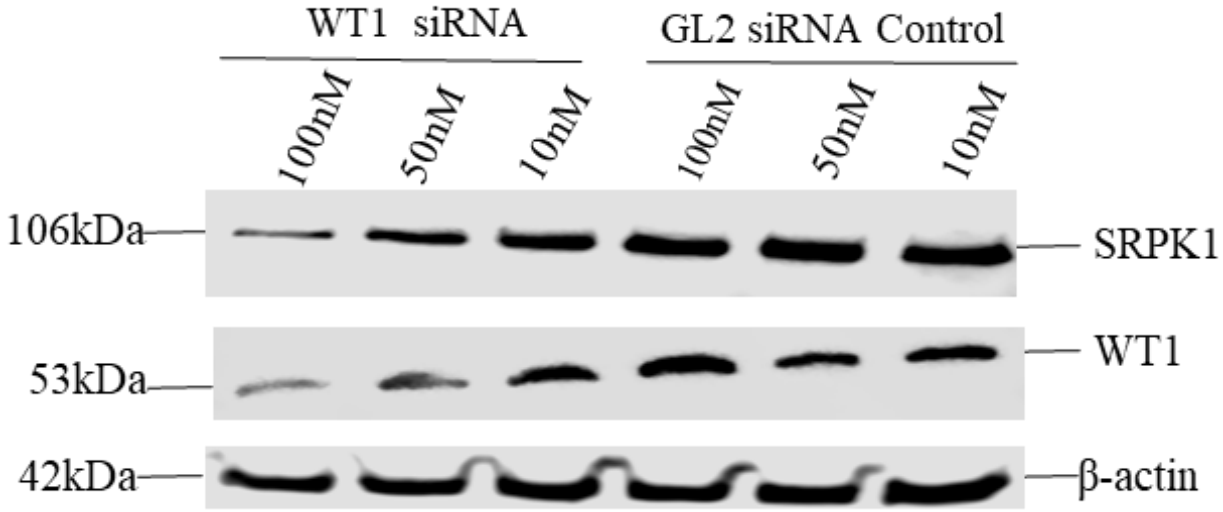
WT1 siRNA
GL2 siRNA Control
100nM
50nM
10nM
100nM
50nM
10nM
106kDa
SRPK1
53kDa
WT1
42kDa
β-actin

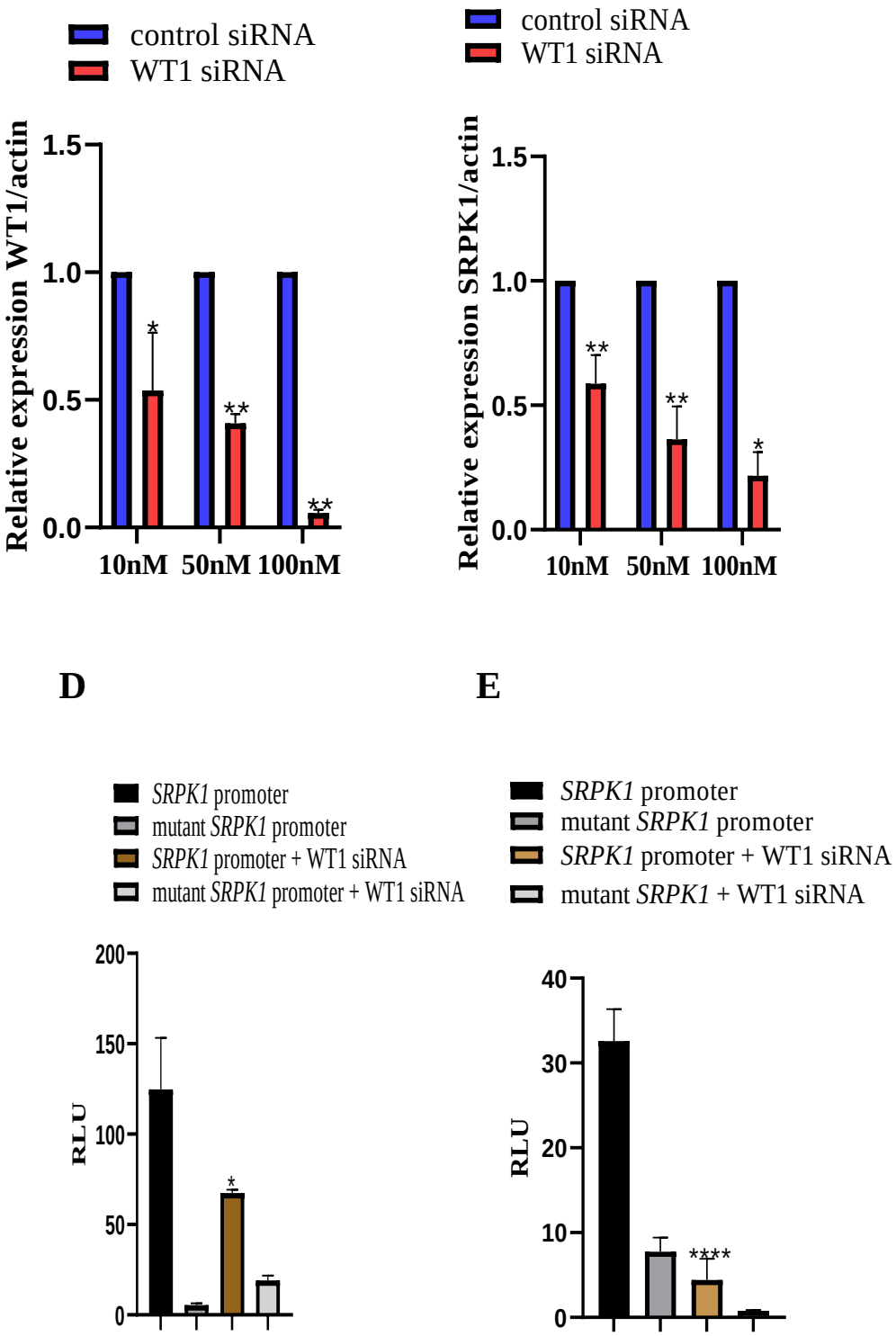

Figure 4. 4: Effect of WT1 knockdown on SRPK1 levels in K562 and PC3 cells.

(A). representative fluorescence microscopy images of siRNA transfected PC3 cells where the GL2 control siRNA was tagged with CY5 and the WT1 targeting siRNA was tagged with FAM fluorescent tags. Pictures were captured by Inverted phase contrast microscope using a 20x objective (scale bare = 50µM).

Western blot of protein lysate from K562 (B) and PC3 (C) cell lines subjected to increasing concentration (10nM, 50nM, and 100nM) of WT1 siRNA knockdown control GL2 siRNA for 48 hours.

Membranes were blotted with anti-WT1 or anti SRPK1 anti-beta Actin antibodies as a loading control. Graphs represent relative expression determined by densitometric measurement of the bands and are expressed relative to actin. Bar-graph shown is the average of 3 independent experiments. **** = $p<0.0001$ significant change compared to control using 2-way ANOVA test. DLR assay of *SRPK1* promoter activity after a knockdown of WT1, using siRNA in K562 (D) and PC3 (E) cells**.** Measurement of *SRPK1* promoter activity using a dual luciferase reporter (DLR) assay. WT or mutant *SRPK1*: Luciferase construct, was co-transfected with 100nM WT1 siRNA into the cell lines. Data is expressed as relative luciferase units (RLU). Data presented as mean ± S.E. for n=3. * indicates $p=0.0014$, **** $p<0.0001$, which is statistically significant using one way ANOVA test. Figures show reduction in the promoter's activity in cells where WT1 has been knocked down.

4.3.4 Effect of splice switching oligonucleotide-mediated WT1 knockdown on *SRPK1* promoter activity

Splice-switching oligonucleotides (SSOs) new emerging molecular tool that has been recently used to change the way that exon segments of RNA are spliced (joined) together and result in inclusion or exclusion of a given exon. In chapter 6 SSOs, based on morpholino chemistry, are used to modify ERG splicing thereby diminishing ERG expression. Since the previous section shows that knowing down WT1 impacted the transcription and expression of SRPK1, we tested a WT1-specific SSO to see if we could confirm the results obtained with a siRNA.

Gene tools (SSOs' manufacturer) were approached with the idea to synthesis a morpholino that targets the human *WT1* oncogene. The idea was to target the 3' and 5′ splice site of a constitutive, early exon on the WT1 gene. They proposed a sequence (table 2.2). That is complementary to WT1 exonic splice junction as a target as shown in figure 4.5.A.

The self-transfecting SSOs were added to PC3 cells followed by western blotting and DLR assay to evaluate the possible effect. (Figure 4.5.C) Shows no impact on *SRPK1* transcription (figure.4.5.B) or the protein levels of SRPK1 and WT1, suggesting that the SSO was not effective.

A

```
                        Self-complementarity report:
.......................CCTGCAGAGAGAACCGAAGACAGCT.........................
........TCGACAGAAGCCAAGAGAGACGTCC.........................................16
```

B

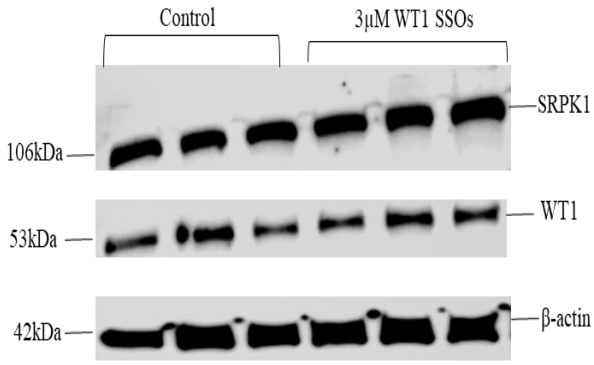

C

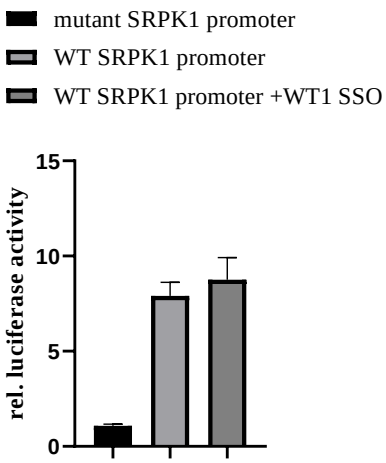

Figure 4. 5: Effect of splice switching oligonucleotides mediated WT1 knockdown on SRPK1 expression.

(A) Representation of the target sequence for the SSOs on the WT1 gene. (B) Western blot of protein lysate from PC3 cell line subjected to 3μM WT1 SSOs for 48 hours. Membranes were blotted with anti-WT1 or anti SRPK1 Anti-beta Actin antibodies as a loading control. There wasn't any noticeable difference in the bands between the controls and WT1 SSOs transfections. Three independent repeats are shown in each case. DLR assay of *SRPK1* Promoter's activity (C) Measurement of *SRPK1* promoter activity using a dual luciferase reporter (DLR) assay. Where WT or mutant *SRPK1*: Luciferase construct, were co-transfected

with 3µM WT1 SSOs into PC3 cell line for 48 hrs. Data are expressed as relative luciferase units (RLU). Data presented as mean ± S.E. for independent experiments n=3 and shows no significant change in the activity of the promoters using one way ANOVA test.

4.3.5 WT1 overexpression and the effect of co-transfection of +/- KTS WT1 expressing plasmids on *SRPK1* promoter activity

WT1, like other oncogenes, express several splice isoforms. Through alternative splicing, the *WT1* gene generates several isoforms. This study focused on studying the effect of -/+KTS isoforms of WT1. These two WT1 variants differ by the presence or absence of three amino acids (KTS) in the zinc finger domain of the molecule at the very end of zinc-finger three (Haber *et al.*, 1991; Gessler *et al.*, 1992). The results in the previous sections of this chapter suggest that WT1 is activating SRPK1 transcription in K562 and PC3 cells lines. To determine how (-/+KTS) WT1 isoforms influence the activation of SRPK1, WT1 (-KTS) or WT1 (+KTS) expressing plasmids constructs were used for this purpose in transient transfections. At first, to examine the degree of WT1 overexpression induced by the different isoforms, the constructs were transfected into the K562 and PC3 cell lines. Western blot was performed on protein lysates prepared from the cell lines following the overexpression. (Figure.4.6.A&B) shows a significant increase (***p=0.0003) in WT1 bands was noticed with –KTS isoform transfection in K562 cells (A) and (**p=0.0052) in PC3 cells (B). +KTS isoform didn't induce the same significant overexpression. No significant change was observed in SRPK1 protein levels in both cell lines after overexpression of WT1 isoforms. With the caveat that these are transient transfections, it appeared that whereas the –KTS expressing plasmid did increase WT1 levels, the +KTS expressing plasmid did not, suggesting that the plasmid did not work.

A

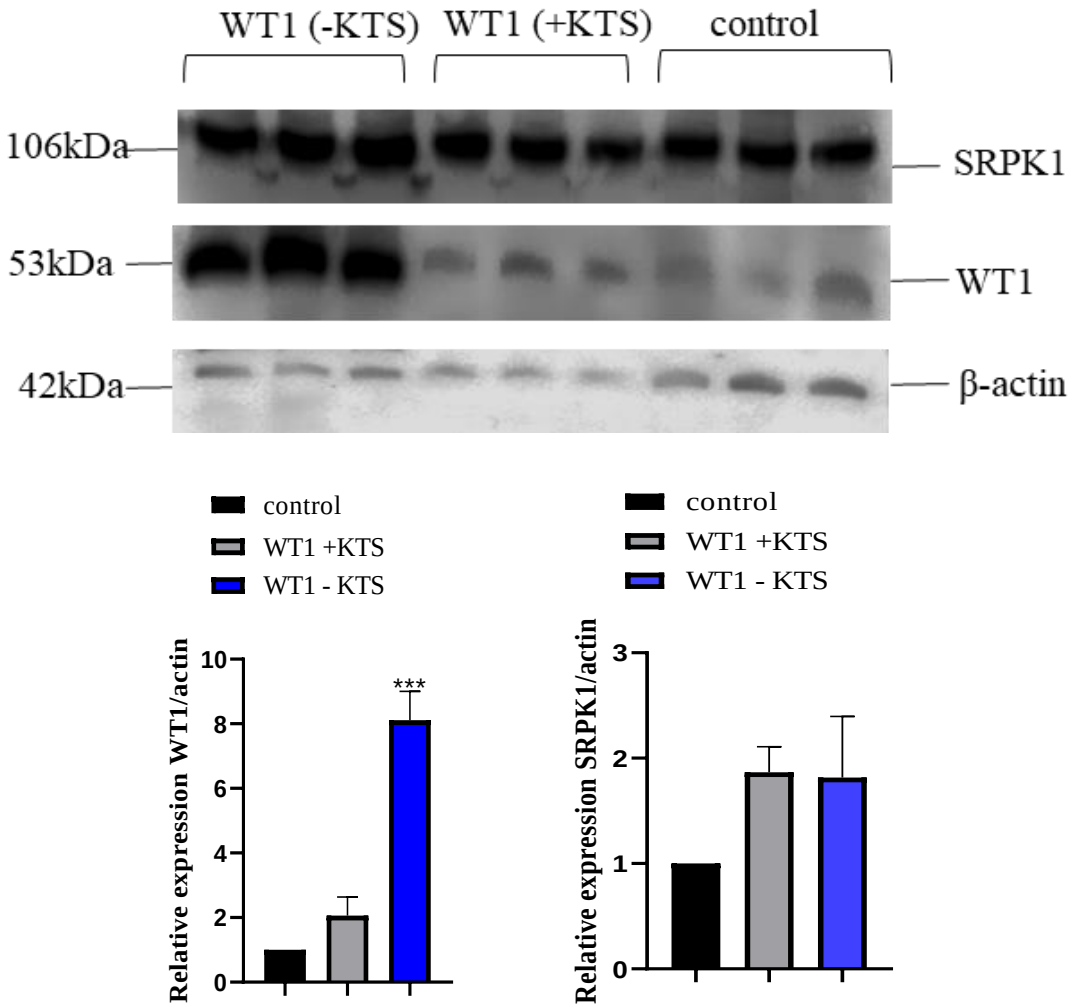
WT1 (-KTS)
WT1 (+KTS)
control
106kDa
SRPK1
53kDa
WT1
42kDa
β-actin
control
WT1 +KTS
WT1 - KTS
Relative expression WT1/actin
***
control
WT1 +KTS
WT1 - KTS
Relative expression SRPK1/actin

B

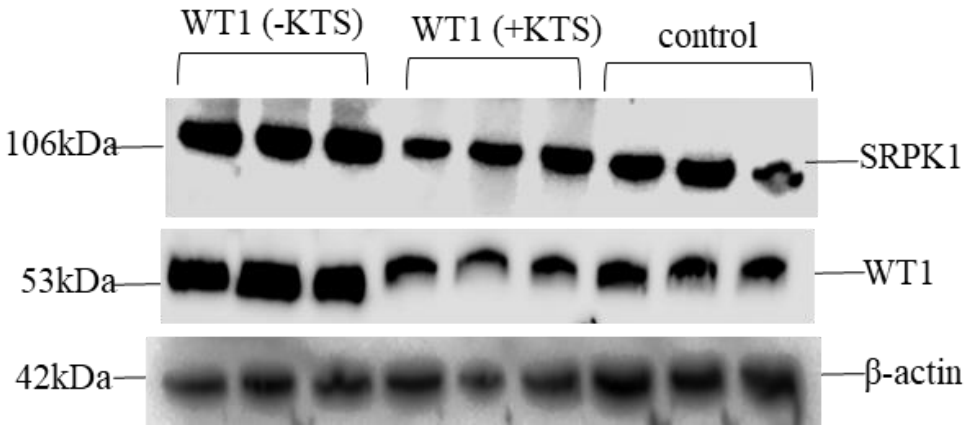
WT1 (-KTS)
WT1 (+KTS)
control
106kDa
SRPK1
53kDa
WT1
42kDa
β-actin

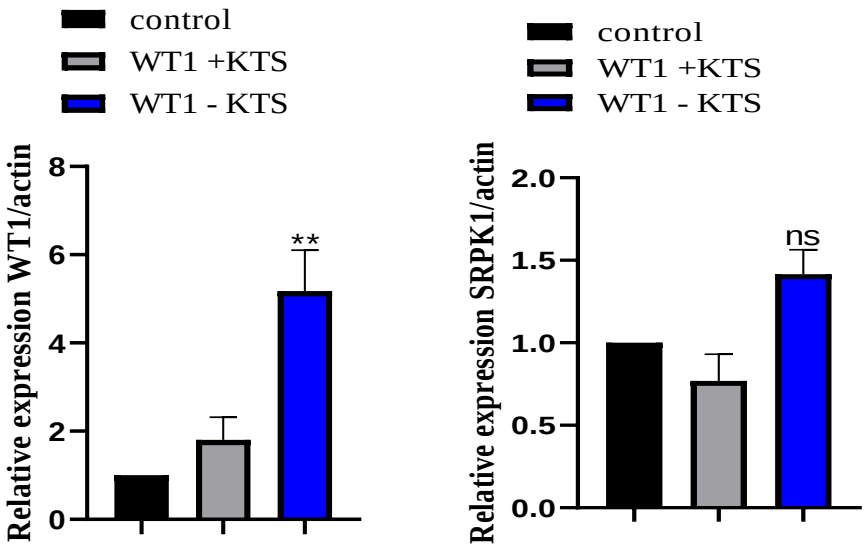

Figure 4. 6: Overexpression of WT1.

Western blot of protein lysates from K562 (A) and PC3 (B) cell lines where WT1 (+/- KTS isoform) expressing plasmids were transiently transfected for 48 hours. Membranes were blotted with anti-WT1 or anti SRPK1 or Anti-beta Actin antibodies as a loading control. Graphs represent relative expression determined by densitometric measurement of the bands and are expressed relative to actin. Bar-graph shown is the average of 3 independent experiments. ** = $p<0.0052$ and ***$p=0.0003$ significant change compared to the control determined by 2-way ANOVA test. Three independent repeats are shown in each case.

The next step was to test the effect of the overexpression of WT1 (-KTS) isoform on SRPK1 transcription. For that purpose, (-KTS) isoform was transiently co-transfected with WT *SRPK1* promoter at increasing concentrations into K562 and PC3 cells lines. (Figure 4.7) Shows that –KTS isoform significantly stimulated *SRPK1* promoter. +KTS isoform was excluded from this experiment due to the +KTS plasmid not working.

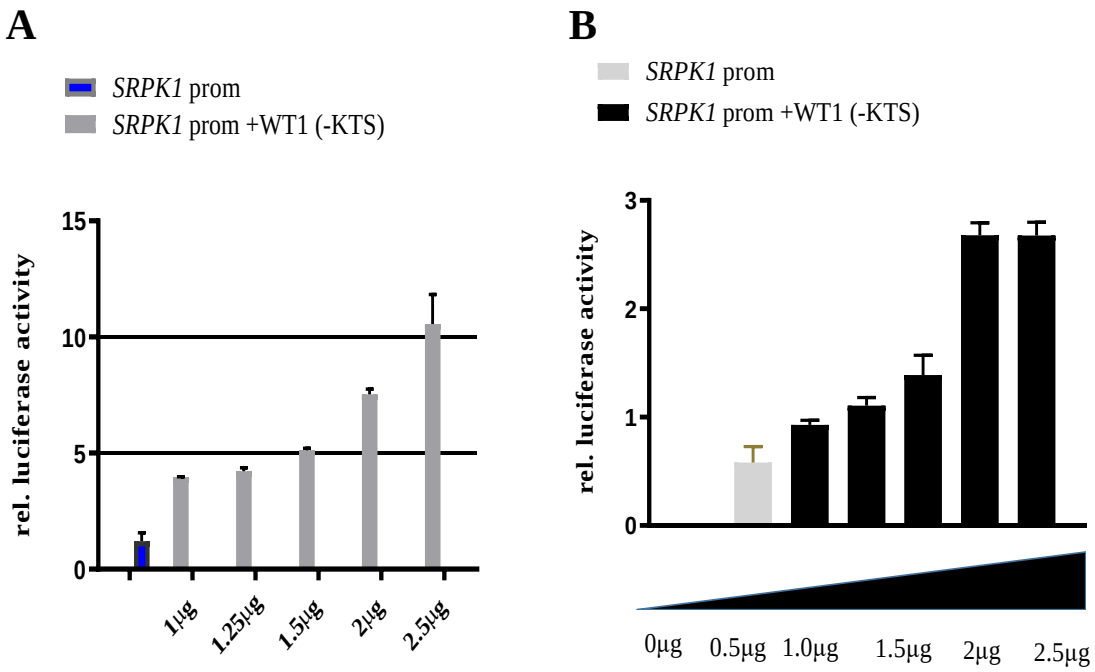

Figure 4. 7: Overexpression of WT1 (-KTS) isoform significantly enhances SRPK1 promoter's activity.

Plasmid encoding wild-type WT1 (- KTS isoform) were co-transfected with the WT *SRPK1* promoter: Luciferase and Renilla expressing vectors at increasing concentrations, 0-2.5 µg into K562 (A) and PC3 (B) cells. RLU = relative luciferase units.

4.3.6 Effect of WT1 siRNA knockdown on the alternative splicing of apoptotic factors *BCL2L1* and *CASPASE-9*

K Ito, *et al.*, 2017 demonstrated that WT1-specific siRNA induces apoptosis in a caspase-dependent manner in several leukemic cell lines; the knockdown activated caspase-3 and -9 in the intrinsic apoptosis pathway. In this study, caspases 3/ 7 staining was used to determine if knocking down WT1 resulted in a change in the apoptotic activity in K562 and PC3 cell lines. Figure 4.8 A shows that the signal of caspase 3/7 was significantly higher (****P<0.0001) in the cells where WT1 has been knocked down compared to the

untransfected cells. This indicates that reducing WT1 expression induces apoptosis in K562 and PC3 cell lines (figure 4.8.A&B).

To further investigate the possibility of knocking down WT1 would result in any change in the alternative splicing of other caspase family members such as *caspase-9* and another apoptotic factor such as *BCL2L1*, mRNA was extracted from the K562 and PC3 cells following WT1 knockdown. Then a PCR was performed using the primers listed in table 2.6. PCR shows that the splicing ratio (PSI-Ψ) of *caspase-9a/caspase-9b* mRNA was significantly higher in the siRNA WT1 transfected group compared to the control group while no significant change was observed on the splicing ratio *Bcl-xl/Bcl-xs* in both cell lines (figure 4.10 & 4.12). In K562 cells, (figure 4.9), the expression ratio of *caspase-9a/9b* isoform in the control was 0.71 siRNA WT1 transfected cells 0.95 (*P= 0.0276 using unpaired t-test). The expression ratio *caspase-9a/9b* isoform in the control was 0.69 while in siRNA WT1 transfected cells 0.80 (*P= 0.0148 using unpaired t-test) in PC3 cells (figure 4.11)

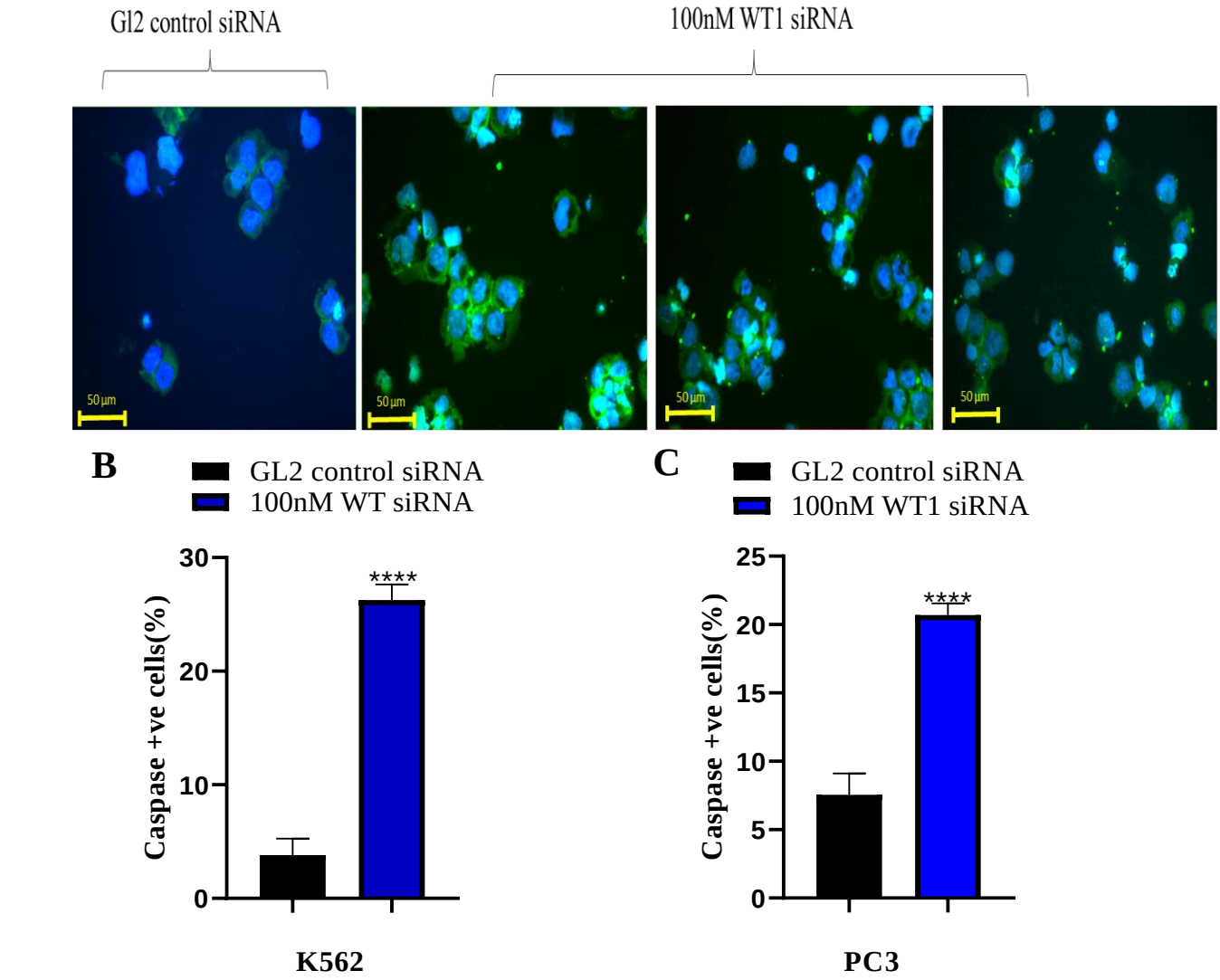

Figure 4. 8: Caspases 3 and 7 staining in K562 and PC3 cells where WT1 has been knocked down.

K562 and PC3 cells were transfected with 100nM WT1 siRNA or GL2 control siRNA for 48hrs followed by detection of active caspases 3 and 7 were performed using Caspase 3/7 Green Detection Reagent. A. Representative images of the stained PC3 cells taken under a fluorescent microscope. the graph represents the number of caspases positive in K562 (B) and PC3 (C) cells which shows significance in the ratio of caspase activity in the cells after WT1 KD, ****P<0.0001 using unpaired t-test. n=9.

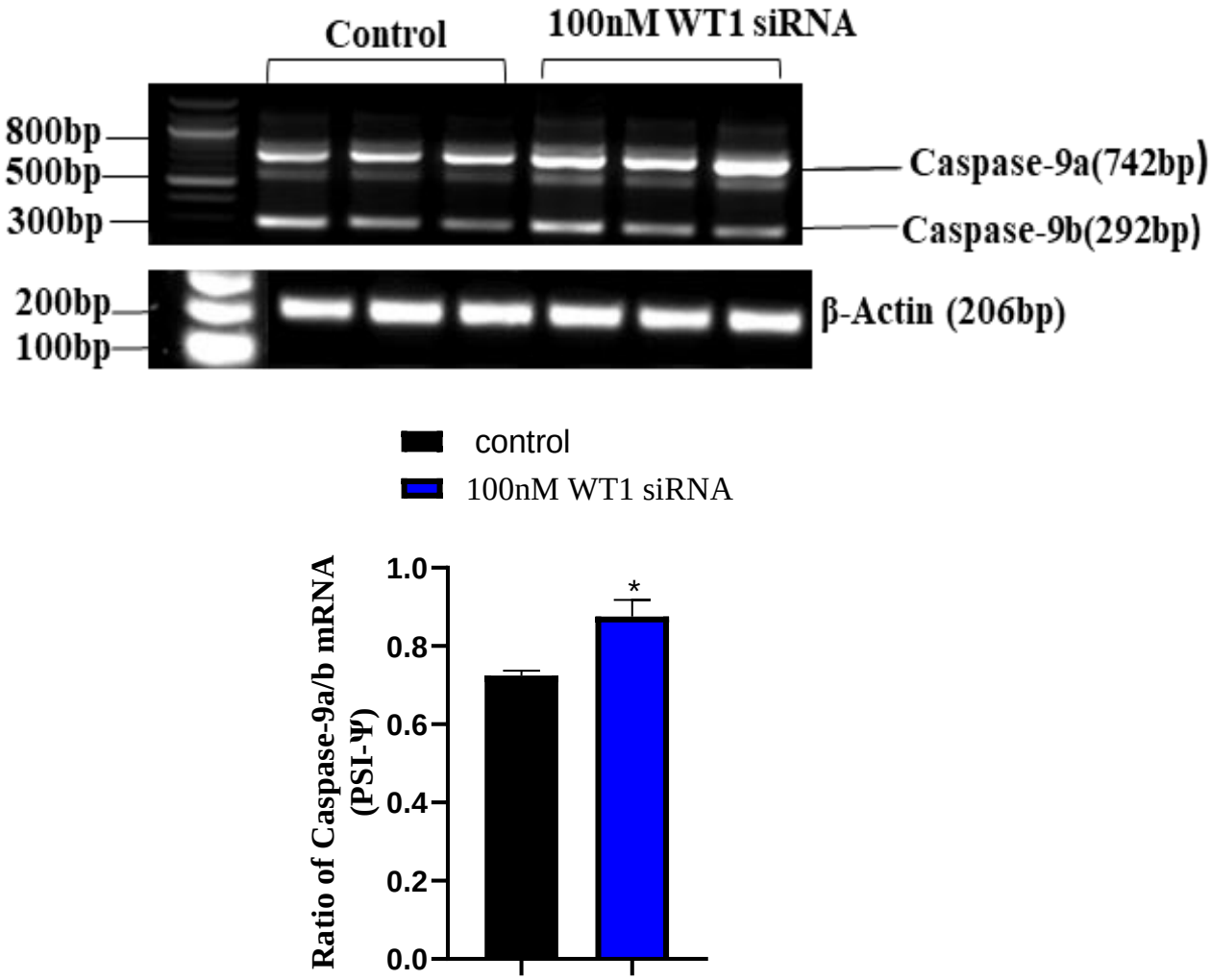

Figure 4. 9: Caspase-9 mRNA levels in K562 cells where WT1 has been knocked down.

K562 cells transfected with 100nM WT1 siRNA for 48hrs followed by RNA extraction and cDNA synthesis. PCR was performed using *caspase-9* specific primers. PCR shows band intensity and size and corresponding loading control, *β-actin*. Densitometry showing *caspase-9a/9b* PSI-Ψ values for 48hrs. The result shows a small but significant change in splice ratio of *caspase-9* (PSI-Ψ, *P= 0.0276) using unpaired t-test. *n*=3. Three independent repeats are shown in each case.

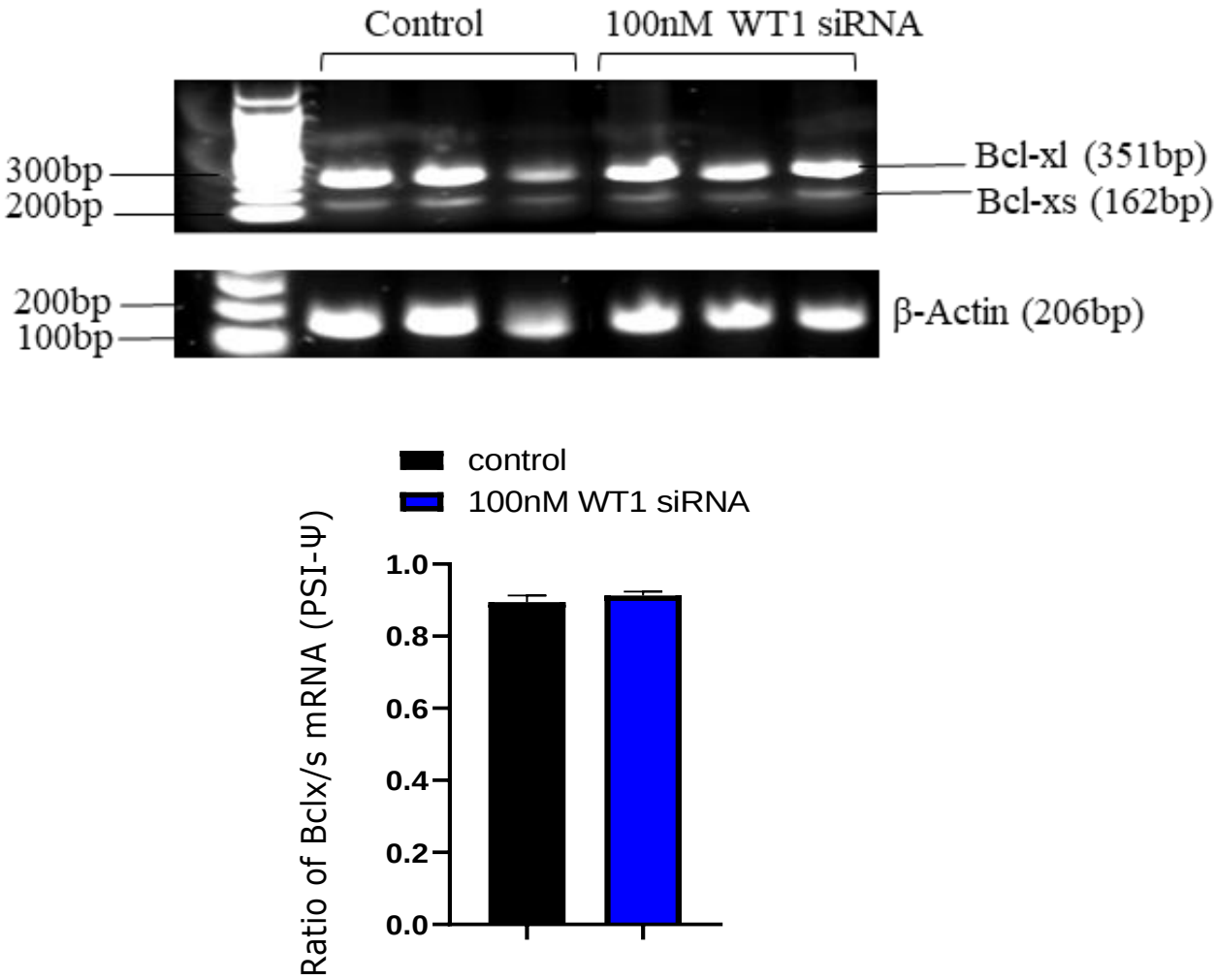

Figure 4. 10: BCL2L1 mRNA levels in K562 cells where WT1 has been knocked down.

K562 cells transfected with 100nM WT1 siRNA for 48hrs followed by RNA extraction and cDNA synthesis. PCR was performed using *Bcl* specific primers. PCR gel at 48hrs showing band intensity and size and corresponding loading control, *β-actin*. Densitometry showing *Bcl-xl/s* PSI-Ψ values for 48hrs. There was no significant change in splice ratio (PSI-Ψ) of Bcl using unpaired t-test. *n*=3. Three independent repeats are shown in each case.

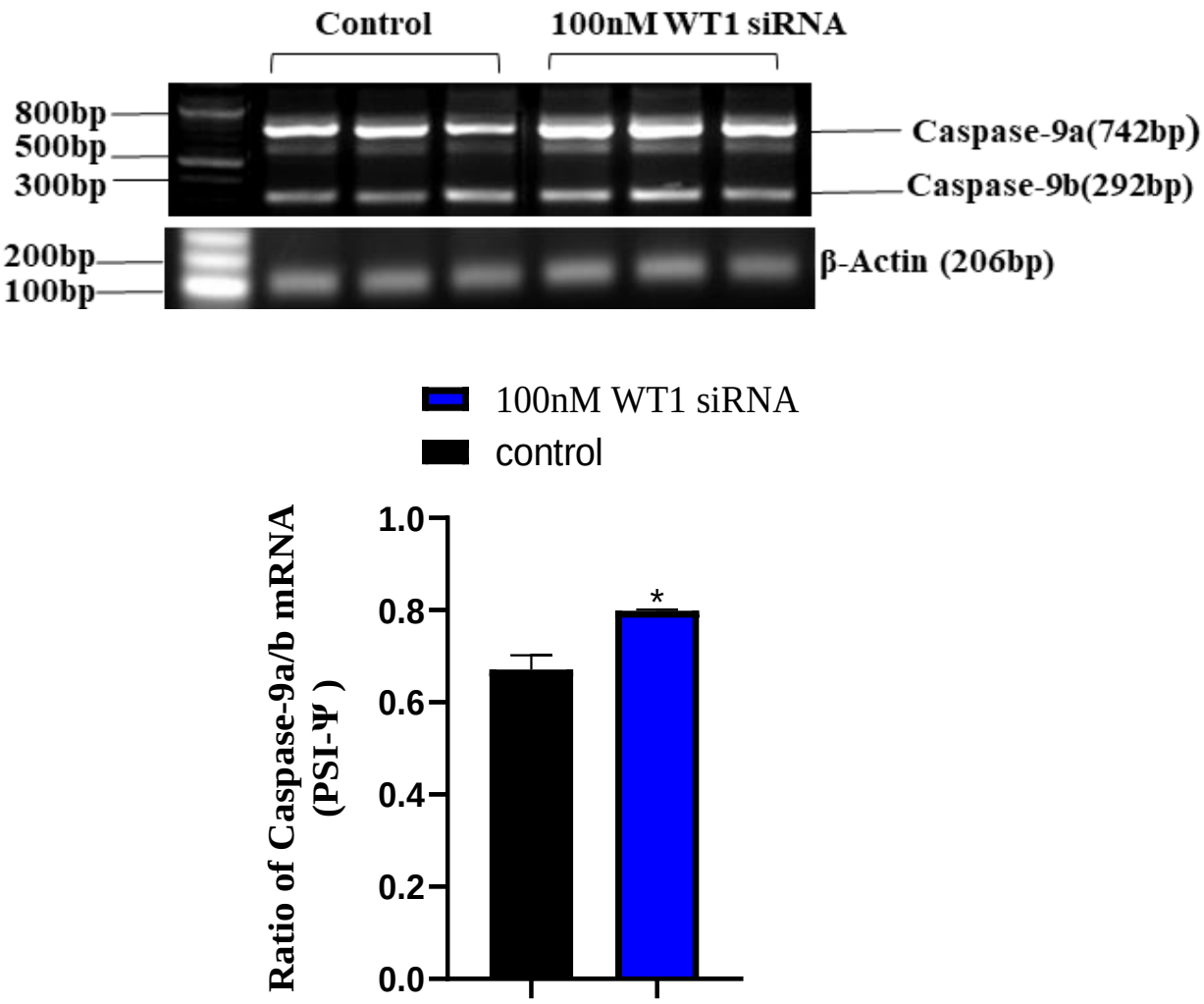

Figure 4. 11: Caspase-9 mRNA levels in PC3 cells where WT1 has been knocked down.

PC3 cells transfected with 100nM WT1 siRNA for 48hrs followed by RNA extraction and cDNA synthesis. PCR was performed using *Caspase-9* specific primers. PCR shows band intensity and size and corresponding loading control, *β-actin*. Densitometry showing *caspase-9a/9b* PSI-Ψ values for 48hrs. The result shows a small but significant chance splice ratio (PSI-Ψ, *P=. 0.0148) of *caspase-9a/9b* using unpaired t-test. *n*=3. Three independent repeats are shown in each case.

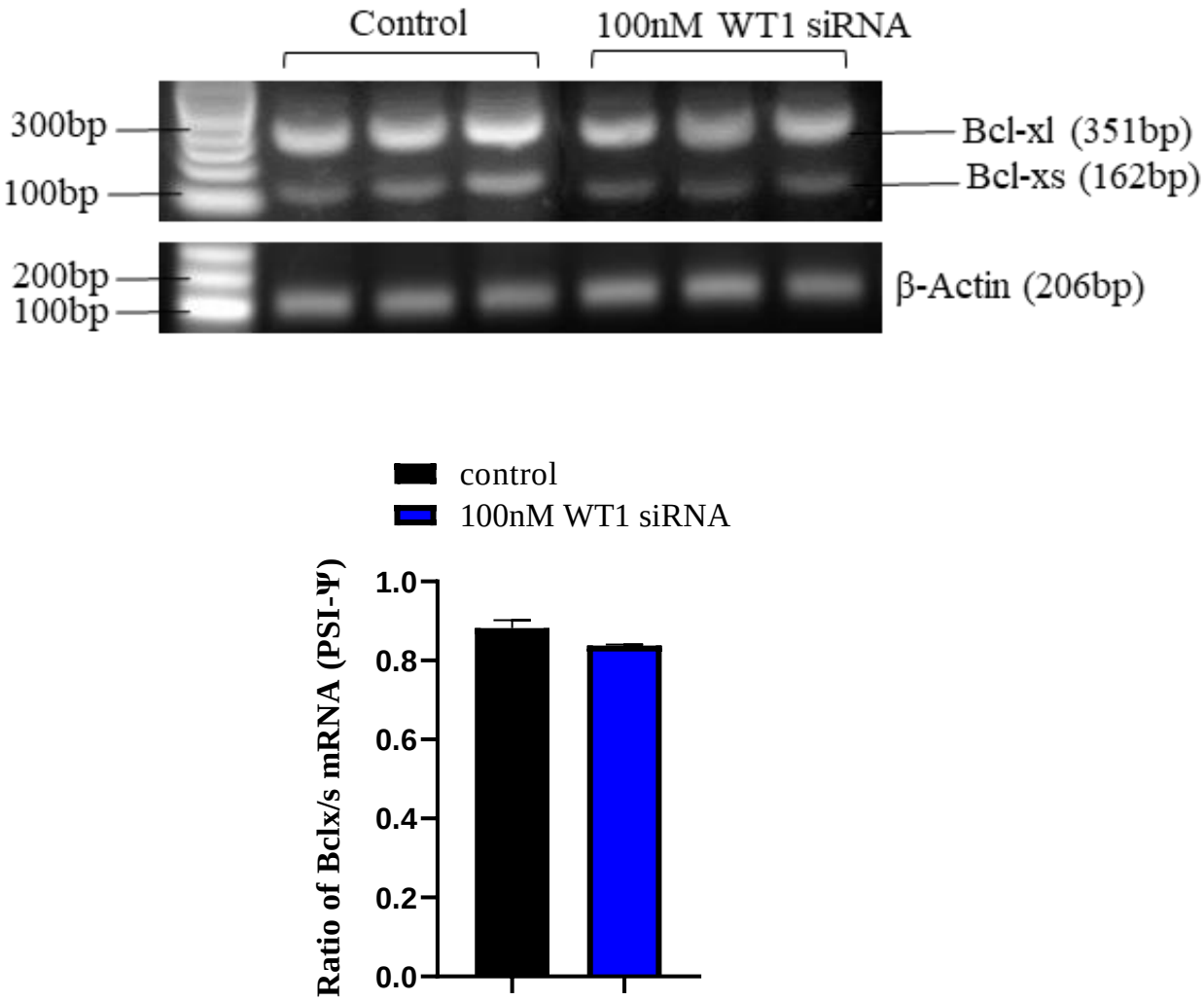

Figure 4. 12: BCL2L1 mRNA levels in PC3 cells where WT has been knocked down.

PC3 cells transfected with 100nM WT1 siRNA for 48hrs followed by RNA extraction and cDNA synthesis. PCR was performed using *Bcl* specific primers. PCR gel at 48hrs showing band intensity and size and corresponding loading control, *β-actin*. Densitometry showing *Bcl-xl/s* PSI-Ψ values for 48hrs. The result shows no significant change in the splicing ratio of *Bcl* using unpaired t-test. *n*=3. Three independent repeats are shown in each case.

4.3.7 The Effect siRNA WT1 knockdown and overexpression on cell proliferation and viability

Parenti, *et al.*, 2014 has demonstrated that silencing WT1 resulted in limiting cellular proliferation in nerve sheath tumour sNF96.2 cell line. This effect was likely a result of the interference with the cell cycle progression in which WT1 plays a major role. Hong *et al.*, 2017 report that WT1 overexpression in rhabdoid tumour G401 cell Line decreased cell proliferation rate. Thus, in this study, the effect of WT1 knockdown and overexpression on cellular proliferation and viability of K562 and PC3 cells was investigated. siRNA was used to reduce WT1 expression levels while (-KTS) WT1 isoform expressing plasmid was used to upregulate WT1. The effect of that on the protein levels was shown in the previous sections. Transfections were performed, followed by an MTT assay. Significant reduction in proliferation and viability occurred 48 h after transfections with siRNA and –KTS isoform compared with the control group. Additionally, the statistical analysis in (figure 4.13 A&B) indicated that with siRNA and –KTS expressing plasmid reduced K562 proliferation and cell viability (***P=0.0010 and *0.0447, respectively). A significant reduction in PC3 (figure 4.13 C&D) cellular proliferation and cell viability. These findings suggest that WT1 affects cell proliferation and viability in K562 and PC3 cells.

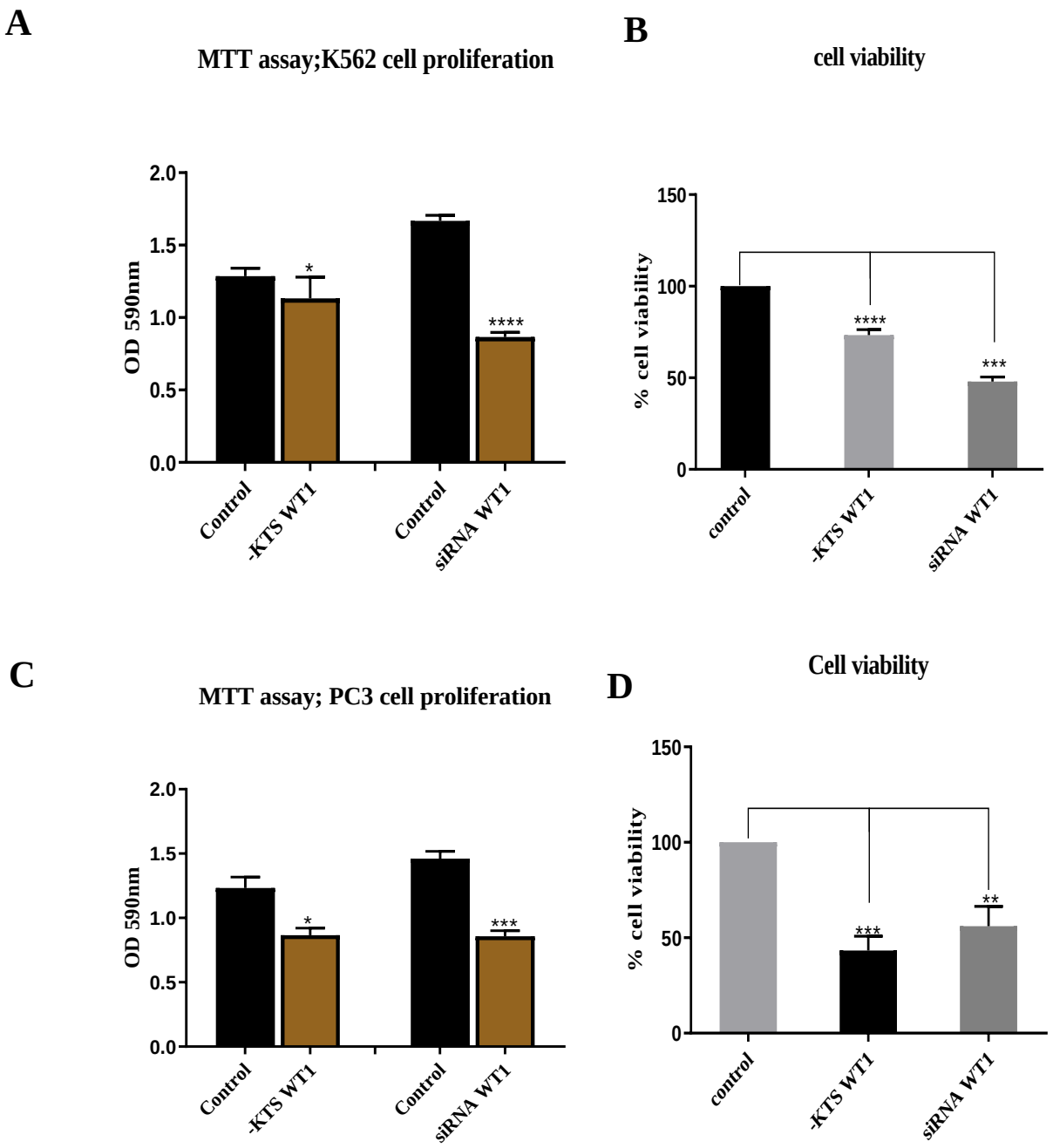

Figure 4. 13. Cellular proliferation and viability in K562 and PC3 cells after overexpression of WT1 isoform and WT1 knockdown.

MTT assays were used to analyse the effect of WT1 (- KTS isoform) or 100nM WT1 siRNA transfections for 48hrs on the cellular viability and proliferation in K562 (A&B) and PC3 (C&D) cells. The absorbance of each well was measured at 590 nm using a plate reader. Results represent the mean ± SEM of three independent experiments and are presented as a bar graph after normalizing to the respective controls. Cell

viability was calculated using the following formula: control- absorbance of treatment wells/absorbance of control well ×100%. (***P=0.0010, *0.0447 using one way ANOVA test).

4.3.8 Effect of WT1 knockdown on cellular migration and invasion

Yang, *et al.,* 2016 described how WT1 knockdown suppressed migration and invasion of two different human NSCLC cell lines. Therefore, in this experiment, the effect of siRNA WT1 knock down on the migration and invasion of PC3 cells was determined. WT1 knockdown was performed on PC3 cells and transwell migration and invasion assay was carried out. (Figure 4.14 &15) shows an observed difference in the number of migrating (*** p =0.0003) and (**** p<0.0001) invasive cells between PC3 WT1-KD and the control siRNA and the un-transfected cells groups. These data considered together suggest that WT1 knockdown significantly suppress PC3 capability to migrate and invade.

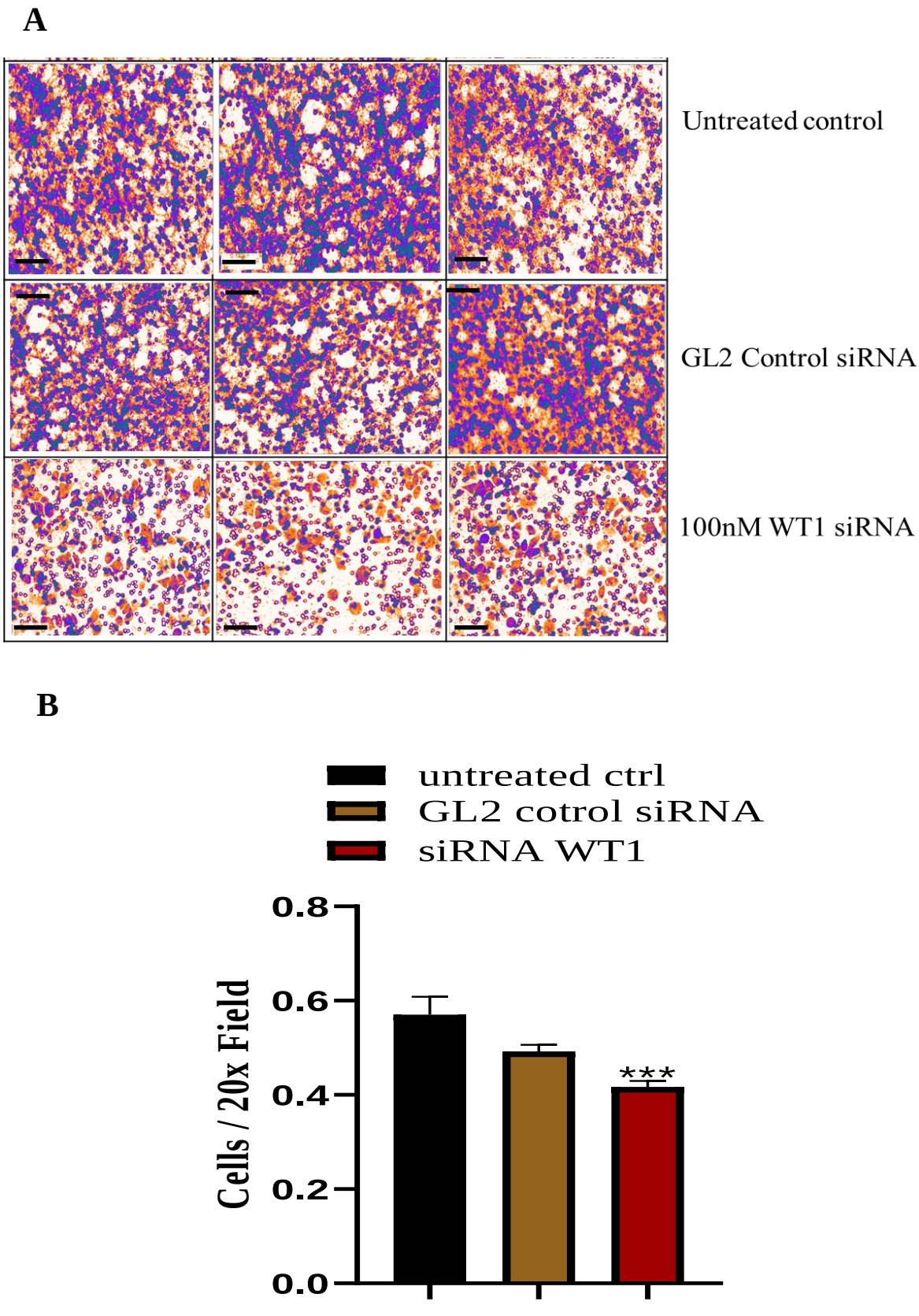

Figure 4. 14: Transwell migration assay of PC3 cells following WT1 knockdown

PC3 cells transfected with 100nM WT1 siRNA or GL2 control siRNA for 48hrs. (A) Representative Pictures of PC3 cell transwell migration. After cell migration and staining with crystal violet, pictures of the migrated cells were captured by Nikon Eclipse TE300 Inverted Phase Contrast Microscope using a 20x objective (scale bare = 50μM). (B) Quantification of cells migrating toward the FBS sublimated medium (average of 5 picture fields at 20x total magnification). ****P*=0.0003 using one way ANOVA test. Three independent repeats are shown in each case.

A

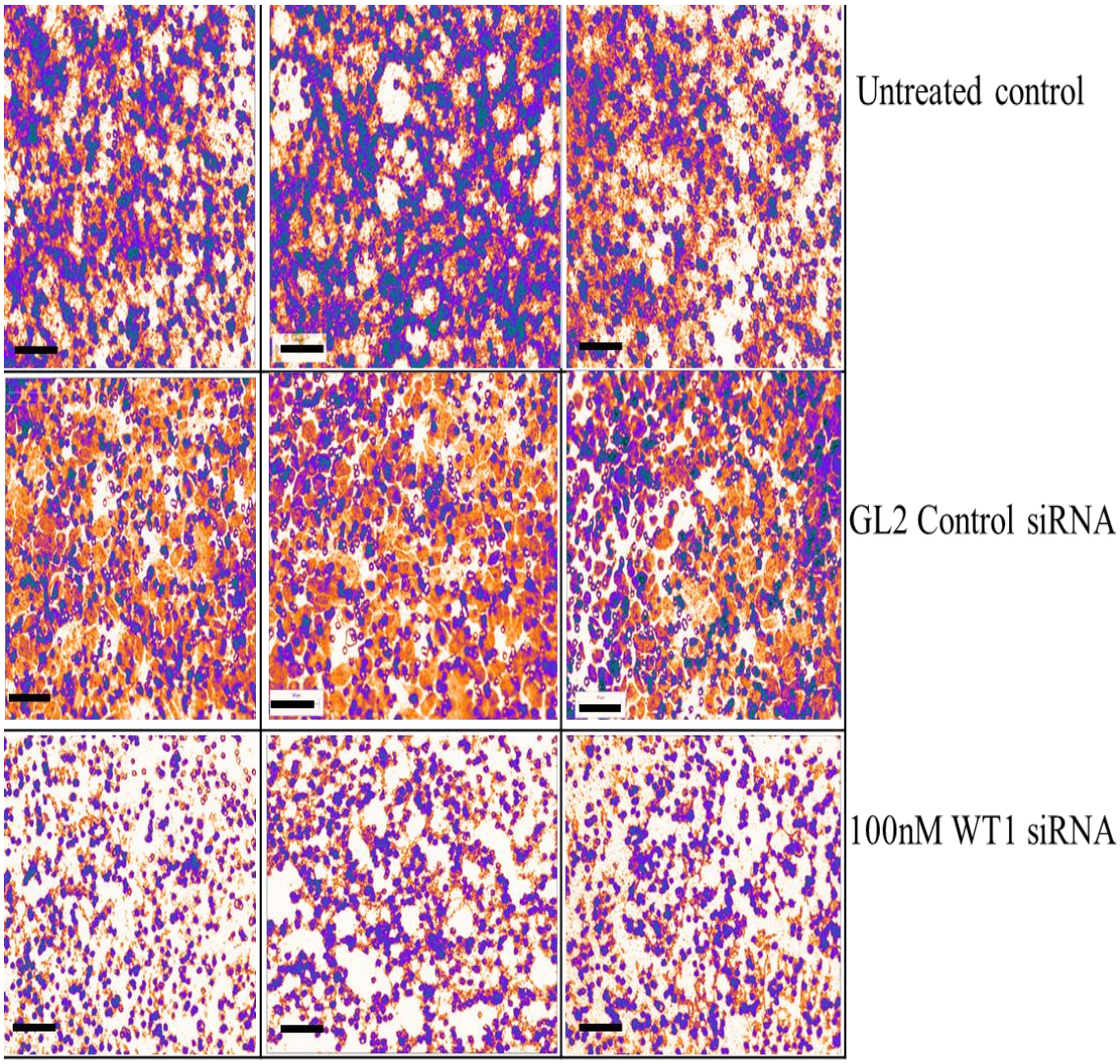

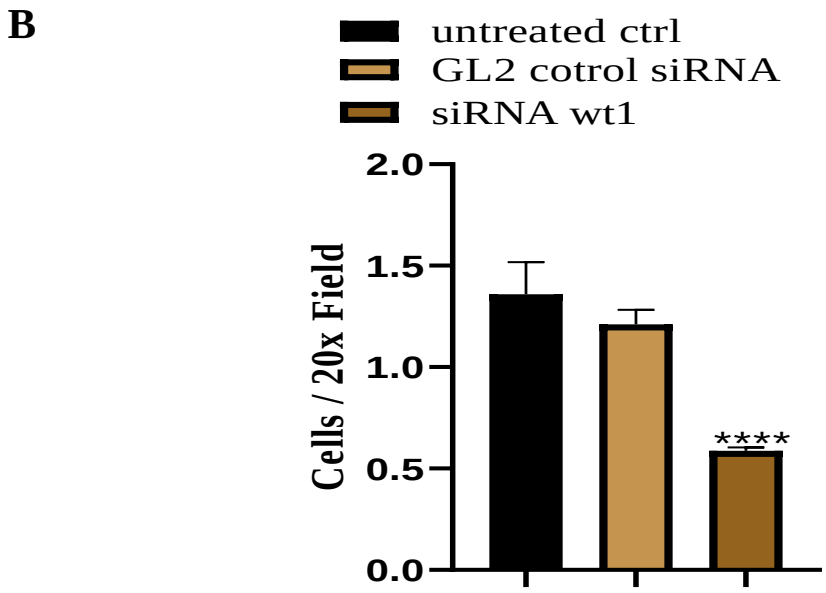

Figure 4. 15: Transwell cell invasion assay of PC3 cells following WT1 knockdown.

PC3 cells transfected with 100nM WT1 siRNA or GL2 control siRNA for 48hrs. (A). Representative Pictures of PC3 cell transwell invasion. The transwell membrane was coated with Matrigel and then the cell- Serum-free medium was added on top of the Matrigel. After cell invasion and staining with crystal violet, pictures of the migrated cells were captured by Nikon Eclipse TE300 Inverted Phase Contrast Microscope using a 20x objective (scale bare = 50μM). **(B)** Quantification of invasive cells moving to the FBS sublimated medium (Average of 5 picture fields at 20x total magnification). ****P<0.0001 using one way ANOVA test. Three independent repeats are shown in each case.

4.4 Summary

The data presented in this chapter has confirmed the previously described binding of WT1 to the *SRPK1* promoter. It was the effect of this binding what was different in this study. WT1 has been shown to repress SRPK1 in DDS podocytes. In contrast, SRPK1 transcription appeared to be activated by WT1 in K562, PC3 and DU145 cells (fig.4.2 &3). The activation of SRPK1 transcription by the –KTS isoform of WT1 is significantly higher compared to the activation by +KTS (fig.4.7) which is expected since –KTS isoform has been described to be better at binding to its DNA targets (Laity *et al.*, 2000). Additionally, –KTS WT1 isoform stimulated WT1 expression at a higher rate compared to the +KTS isoform following overexpression of both WT1 isoforms using plasmid constructs in K562 and PC3 cell lines (fig.4.6). Thus, it is possible that the observed effect of WT1 on SRPK1 is mediated by –KTS, and not +KTS isoforms. However, it is quite possible that the +KTS expressing plasmid was not working optimally; further experiments are needed therefore to compare the activity of + and –KTS isoforms in relation to regulating SRPK1 transcription.

The results in this chapter have confirmed that knocking down WT1 impacted the transcriptional activity of *SRPK1* as its promoter activity was diminished when siRNA WT1 was cotransfected with the wild type *SRPK1* promoter into K562 and PC3 cell lines. Moreover, WT1 inhibition mediated by siRNA resulted in not only in the reduction of WT1 protein levels but also of SRPK1 protein levels in both cell lines (fig.4.4).

WT1 is a major transcriptional regulator; therefore, its inhibition is likely to affect the transcription of other genes that play important roles in different cellular pathways including the regulation of apoptosis (K Ito *et al.*, 2017). In this study, WT1 knockdown was shown to induce an increase in the levels of active caspases 3 and 7 which suggests

a higher apoptotic activity in the cells (fig.4.8). This was accompanied by a change in alternative splicing of *caspase-9* mRNA. Following WT1 knockdown in K562 and PC3 cells, a splicing switch toward the pro-apoptotic *caspase-9a* isoform was observed (fig.4.9&11).

Cellular proliferation, viability, migration and invasion seemed to be influenced by WT1 knockdown. Following WT1 knockdown, the proliferation and viability of K562 and PC3 cells were significantly reduced (fig.4.13). A similar reduction was observed on the migration and invasive ability of both cell lines in response to SRPK1 inhibition (fig.4.14&15). It is therefore tempting to speculate that the consequences of knocking down WT1 on cell biology are at least in part due to a reduction in the expression of SRPK1.

5 Chapter Five: Effect of the co-suppressor BASP1 on the transcriptional regulation of *SRPK1* by WT1

5.1 Background

Genes that are involved in growth, differentiation and the regulation of cell division have been described to be transcriptionally regulated by WT1. The last chapter discussed how WT1 binds the putative *SRPK1* promoter and activates its transcription in K562 cells and PC3. This is the opposite of what happens in glomerular podocytes where SRPK1 is transcriptionally repressed by WT1. As discussed before, the ability of WT1 to activate or repress its target genes is fully dependent on the presence or absence of other transcriptional cofactors (Toska & Roberts, 2014). Numerous proteins have been described to be interaction partners for WT1. They add more specificity to WT1 function and determine whether it acts as a transcriptional activator or repressor (Roberts, 2005). Brain-abundant signal protein (BASP1) has been shown to influence transcriptional control and tumourigenicity in breast cancer cells, acute myelogenous leukaemia cells, hepatocellular carcinoma cells and thyroid cancer cells (Zhou *et al.*, 2018, Guo *et al.*, 2016 and Marsh *et al.*, 2017). It also has been described to interact with numerous major transcription factors including WT1, c-myc and ERα in a variety of cell types (Carpenter *et al.*, 2004 and Marsh *et al.*, 2017).

Carpenter *et al.*, 2004 revealed that BASP1 translocates into the nucleus of HEK cells where it influences WT1 activity and consequently its target genes. BASP1 modulates the transcriptional regulation of WT1 through direct binding to WT1 at the promoters of its target genes. BASP1 was also found to form a transcriptional complex with WT1 to regulate the transcription of WT1 target genes. For instance, Goodfellow *et al.*, 2011 has

shown that BASP1 binds to WT1 and converts it from a transcriptional activator to a transcriptional repressor of WT1 target genes. BASP1 does this by inducing the dissociation of CBP and the recruitment of HDAC1 to the WT1 transcriptional complex. Depending on the cell type and location, BASP1 has been proposed to perform a range of different context-specific activities and functions. WT1 induces tumour suppressor activity in the presence of BASP1. This indicates that in cell lines that express both proteins, BASP1 can promote WT1 tumour suppressive activity while the downregulation of endogenous BASP1 expression enhances the activation of transcription of cancer-associated by WT1.

5.2 Aims and objectives

1. To investigate the effect of the transcriptional co-suppression of WT1 by BASP1 on SRPK1 expression.
2. To evaluate the impact of the WT1 / BASP1 interaction on the following:
    - Expression of SRPK1 in K562, B-K562 (BASP1-overexpressing), PC3, and DU145 cells.
    - VEGF alternative splicing in PC3 cells.
    - The effect of BASP1 overexpression on cellular viability, and proliferation.

5.3 Results

5.3.1 BASP1 binds to the *SRPK1* promoter (ChIP)

The previous chapter examined the involvement of WT1 in the transcriptional regulation of *SRPK1*. The manner in which WT1 is involved in the transcriptional regulation of *SRPK1* appeared to be cell line dependent. WT1 activates SRPK1 in several cell lines while repressing its transcription in DDS podocytes. Several studies have suggested that this difference in regulating the transcriptional activity of the same target gene depends not only on the type of the cell line but also on the presence or absence of other transcriptional regulators. However, in both cases, there was a physical binding of WT1 to *SRPK1* promoter which confirmed by chromatin immunoprecipitation.

Since BASP1 had been identified as WT1 transcriptional co-suppressor (Carpenter *et al*., 2004), another study considered investigating the possible presence of a WT1/BASP1 transcriptional complex that represses WT1 target genes. Green *et al.*, 2008 revealed that WT1 and BASP1 bind the promoter of the *podocalyxin, Bak* and *c-Myc* genes in podocyte precursor, MPC5 cells. Through performing chromatin immunoprecipitation, they used an anti-WT1 and two different anti-BASP1 antibodies to pull down WT1/BASP1 complexes then amplified the regions of the promoters that contain the proposed WT1-binding sites. Results show that both WT1 and BASP1 are present at the *Bak* and *c-myc* promoters.

In this study, chromatin immunoprecipitation (ChIP) was performed on sheared cross-linked chromatin was collected from B-K562, a modified K562 cell generated to provide a stable K562 cell-line derivative that expresses BASP1 (Goodfellow *et al.*, 2011). Primers specific to the *SRPK1* promoter were designed and PCR was performed to detect

the genomic regions being pulled down by the antibodies. Figure 5.1. Shows that BASP1 binds to the *SRPK1* promoter. A rabbit polyclonal antibody against BASP1 was used with an anti- polymerase II antibody as a positive control. Total mouse IgG served as a negative control. Input DNA was used as an additional positive control for PCR. For additional confirmation, the BASP1-SRPK1 pull-down amplicon was extracted from the gel and sent for sequencing (see Appendix).

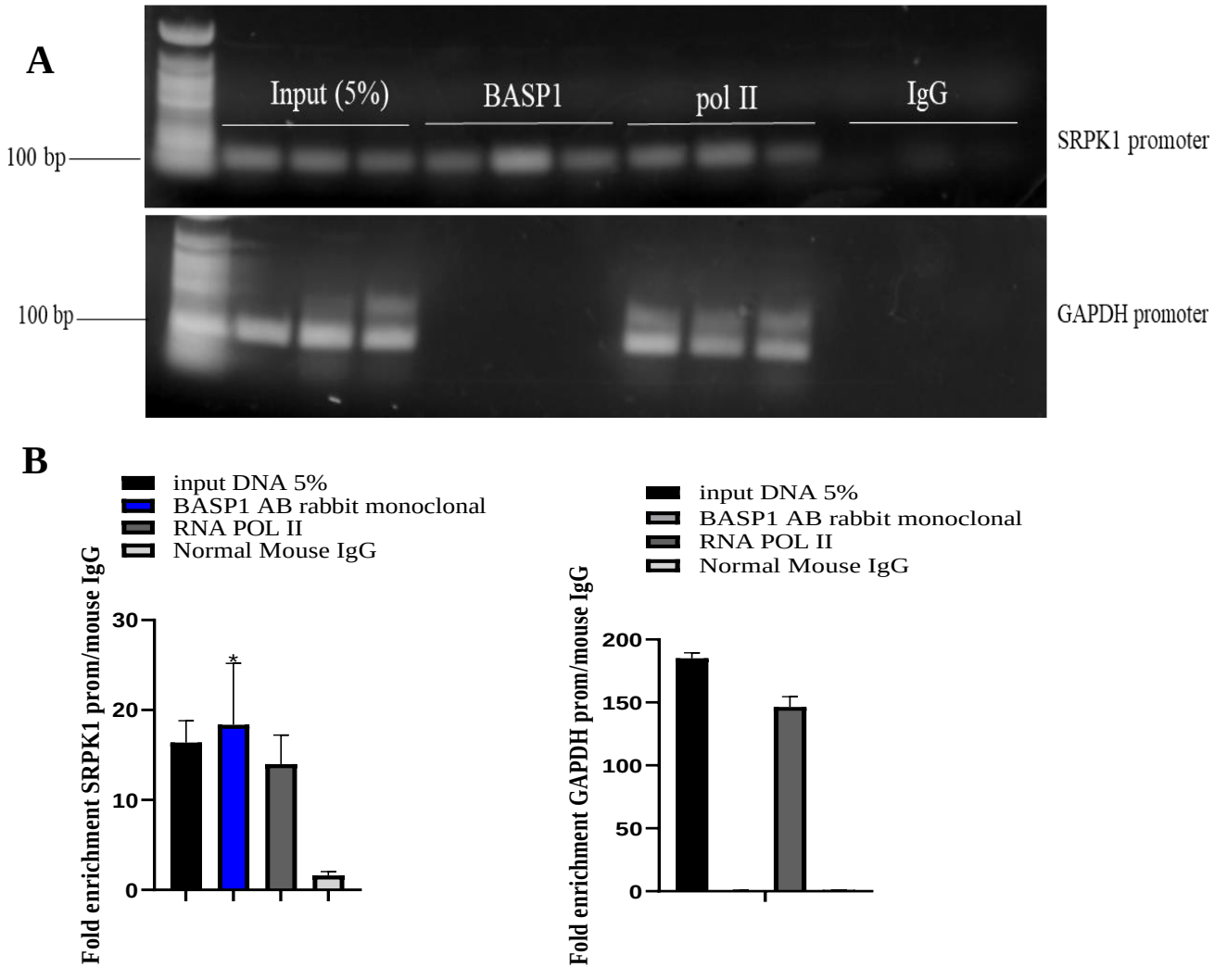

Figure 5. 1: BASP1 binds the SRPK1 promoter.

Chromatin immunoprecipitation (ChIP, n = 3 independent repeats) was performed using a rabbit monoclonal antibody against BASP1 or anti- polymerase II antibody as a positive control. Total Mouse

IgG served as a negative control. Input DNA was used as an additional positive control for subsequent PCRs on the *SRPK1* promoter and the respective sequence. PCR assay for ChIP product for B-K562 cells using primers to detect the region around the *SRPK1* transcriptional start site (TSS) and *GAPDH* promoters. (A) Representative agarose gel photographs of ChIP PCR experiments for the *SRPK1* and *GAPDH* promoters. (B) Quantified data are expressed as means ± S.E.M. * indicates $p < 0.0426$ which is statically significant using one way ANOVA test, based on three independent repeats are shown in each case.

5.3.2 Overexpression of the transcriptional co-repressor BASP1 prevents WT1 from activating *SRPK1* transcription

The previous experiment suggests that BASP1 binds to the *SRPK1*promoter where WT1 also was previously described to be present (chapter 4).

Given the fact that for WT1 to act as a transcriptional activator or suppressor depends on the presence or absence of other transcriptional regulator, and that Carpenter *et al.*, 2004 has described that BASP1 can promote WT1 tumour suppressive activity, in this study, the overexpression of BASP1 was used to determine whether or not WT1/BASP1 cosuppression mechanism is applicable in PC3 and K562 cell lines.

A full-length BASP1 cDNA construct (Carpenter *et al.*, 2004) and B-K562, a genetically modified K562 cell line that overexpresses BASP1, (Goodfellow *et al.*, 2011) were used for this purpose. At first, the stable expression of BASP1 in B-K562 cells was compared to the endogenous BASP1 in regular K562 by western blot. (Figure.5.2. A) shows significant expression of BASP1 (****$p < 0.0001$) in B-K562 cells compared to K562 cells. To examine the degree of BASP1 expression introduced by the vector, the construct was transfected into a PC3 cell line. Western blot was performed on protein lysates prepared from the cell line following BASP1 overexpression. (Figure.5.2.B) shows a significant increase (**$p=0.0064$) in BASP1 bands was noticed where BASP1 was

overexpressed in PC3 cells (B). While the untransfected group showed lower levels of BASP1.

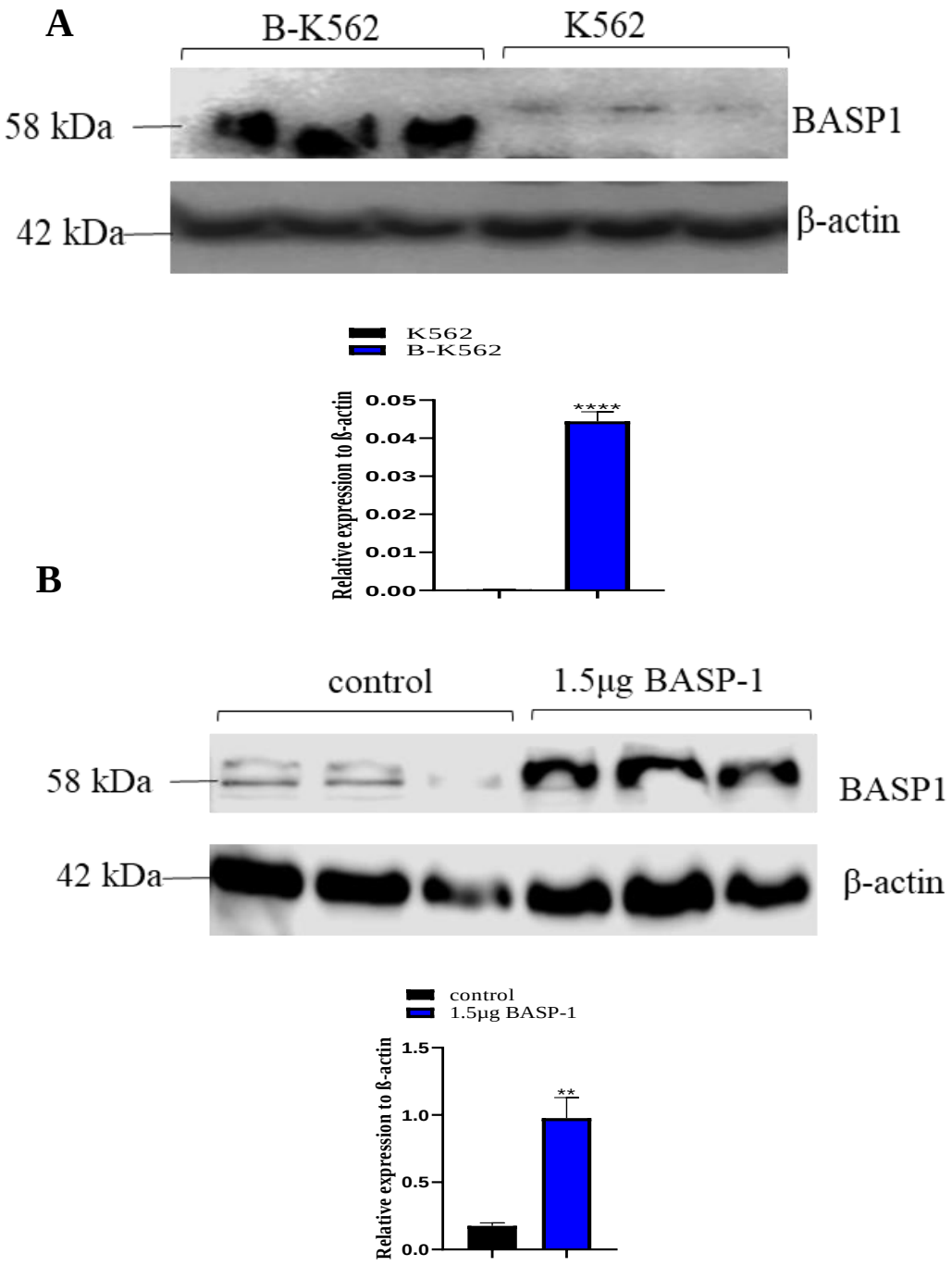

Figure 5. 2: Overexpression of BASP1 in B-K562 (A).

Western blot of protein lysate from B-K562 and K562 cell lines. Membranes were blotted with anti-BASP1 or anti-beta actin antibodies as a loading control. The graph represents relative expression determined by

densitometric measurement of the bands and is expressed relative to actin. Bar-graph quantifies the result of three independent experiments. **** = p<0.0001 significant change compared to the control determined by the T-test. (B) Overexpression of BASP1 in PC3 cells. Western blot of protein lysate from PC3 cells transfected with plasmids encoding wild-type BASP1. Membranes were blotted with anti-BASP1 or anti-beta actin antibodies as a loading control. The graph represents relative expression determined by densitometric measurement of the bands and is expressed relative to actin. Bar-graph shown is the average of three independent experiments. ** = p<0.0064 significant change compared to the control determined by T-test.

The next step was to test the effect of the BASP1 overexpression on *SRPK1* transcription. For that purpose, the BASP1 expressing construct was transiently co-transfected with wild-type and mutant *SRPK1* promoters. Figure 5.3 shows that BASP1 significantly diminished *SRPK1* promoter activity (****$p < 0.0001$) in both cell lines.

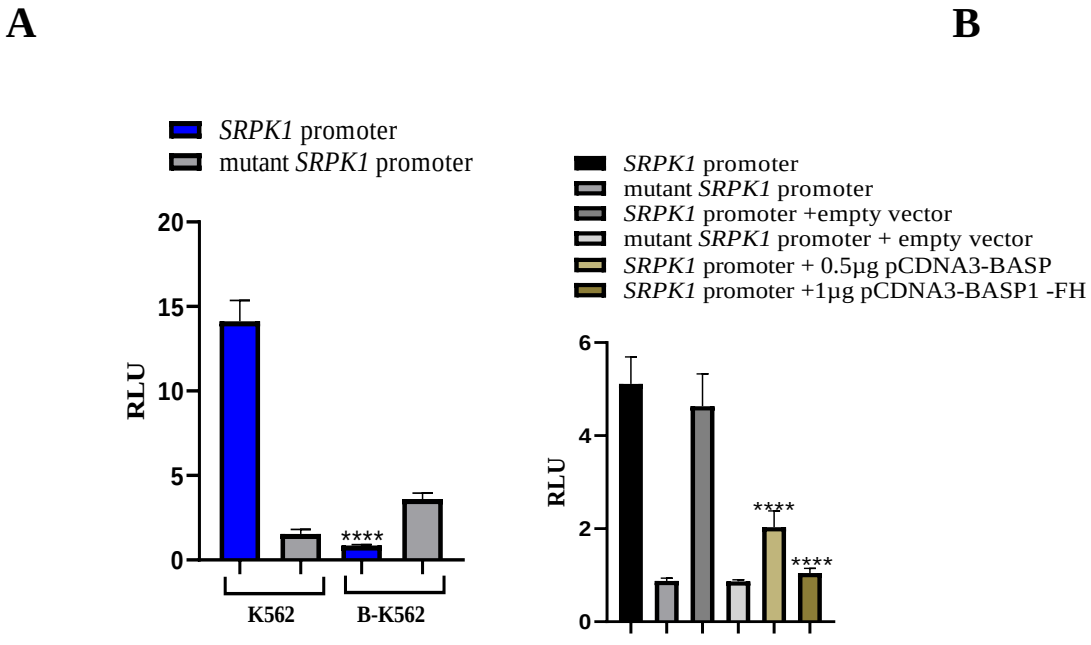

Figure 5. 3: Effect of BASP1 on SRPK1 transcription

(A) The transcriptional co-repressor BASP1 prevents WT1 from activating *SRPK1* transcription when expressed in K562**.** Relative luciferase activity of the WT and the mutant *SRPK1* promoters in B-K562 and K562. In B-K562 cells SRPK1 promoter's activity levels are significantly reduced (**** = p<0.0001) one

way ANOVA test. (B) Overexpression of BASP1 reduces *SRPK1* transcription in PC3. Plasmids encoding wild-type BASP1 at two concentrations, 0.5-1µg or empty vector were co-transfected with the WT or mutant *SRPK1* promoters into PC3 cells. RLU = relative luciferase units. (**** = p<0.0001) determined by 2-way ANOVA test. Three independent repeats are shown in each case.

5.3.3 BASP1 expression limits the endogenous protein levels of WT1 and SRPK1

The results in this chapter so far suggest that BASP1 binds to the *SRPK1* promoter and helps to repress its transcription. BASP1 is known to work as a WT1 co-suppressor; WT1 expression in K562 cells is high and there is no detectable amount of BASP1. In the developing podocytes, BASP1 expression overlaps with WT1 as its expression levels decrease while BASP1 levels become more prominent in the latter stages of kidney development. (Carpenter *et al.*, 2004). Here in this study, the transcriptional regulation of SRPK1 was repressed when BASP1 was overexpressed in PC3 and B-K562 cells while it remained unchanged in untransfected K562 cells. To determine if this repression could result in the down regulation of the endogenous protein levels of SRPK1 and WT1, protein lysates from PC3, DU145, K563 and B-K562 were prepared and western blot was carried out. (Figure.5.4.) shows the levels of SRPK1 and WT1 in different cell lines. A significant reduction in SRPK1 and WT1 levels combined with elevated BASP1 expression in B-K562 cells was observed. SRPK1 level was significantly lower in B-K562 compared to other cell lines (pc3 cells; *p= 0.0362. DU145; **p=0.0032. K562; ****p<0.0001). WT1 expression was lower in B-K562 as well compared to other cell lines (****p<0.0001) while BASP1 was elevated in B-K562 cells compared to other cell lines (*p=0.0362).

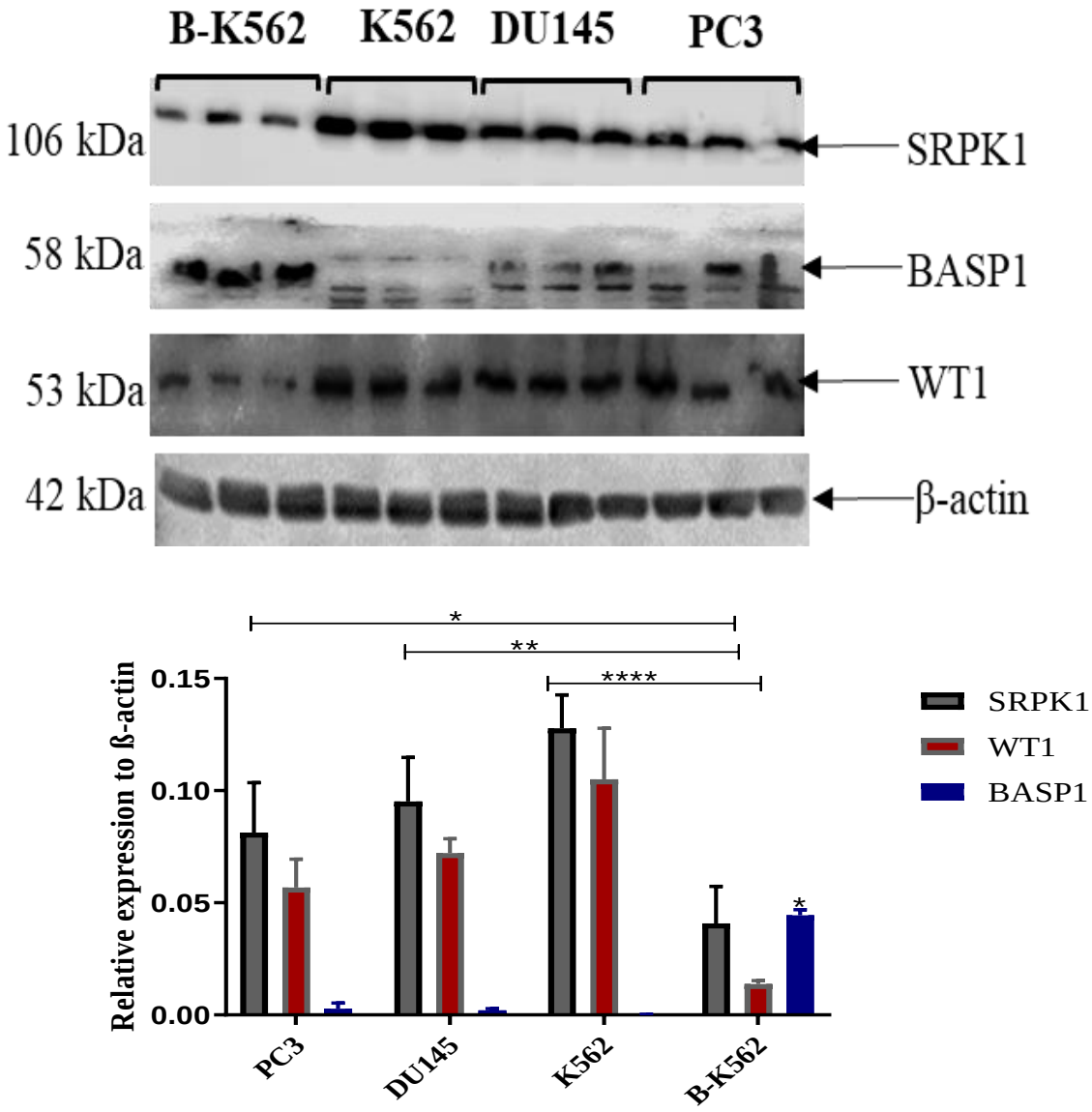

Figure 5. 4 BASP1 expression limits the expression of endogenous WT1 and SRPK1 protein.

Western blot of protein lysate from PC3, DU145, K562 and B-K562. Membranes were blotted with anti-BASP1 or anti SRPK1 or anti WT1 or anti-beta actin antibodies as a loading control. The graph represents relative expression determined by densitometric measurement of the bands and is expressed relative to actin. Bar-graph shown is the average of 3 independent experiments. **** = $p<0.0001$ represent a significant change compared to the control using 2-way ANOVA test.

5.3.4 Overexpression of WT1 co-suppressor BASP1 affects VEGF-A alternative splicing in PC3 cells

SRPK1 has been described to be a downstream target for WT1 regulation where WT1 can either activate (Wagner *et al.,* 2019) or repress *SRPK1* transcription (Amin *et al*., 2011) in different contexts. Data shown in chapter 3 of this study confirmed that the alternative splicing of VEGF has changed in response to the inhibition of SRPK1 by the chemical inhibitor SPHINX. Recently SRPK1 activation by WT1 in endothelial cells was found to enhance the expression of angiogenic VEGF isoforms (Wagner *et al.,* 2019). Thus, in this study, it was of interest to investigate whether or not the overexpression of WT1 co-suppressor BASP1 caused an alteration in VEGF alternative splicing.

For this purpose, a western blot was performed on protein lysates prepared from the PC3 cell lines transiently transfected with full-length BASP1-expressing construct (Carpenter *et al.*, 2004). The protein bands shown in (figure 5.5) at 22kda correspond to anti-angiogenic VEGF165b and total VEGF165 in different membranes. The western blot showed baseline VEGF165 expressions and an increase in the anti-angiogenic isoform VEGF165b following the overexpression of BASP1. This suggests that the WT1/BASP1 complex suppresses SRPK1 and therefore, results in a splicing switch from pro- to anti-angiogenic VEGF isoforms in PC3 cells.

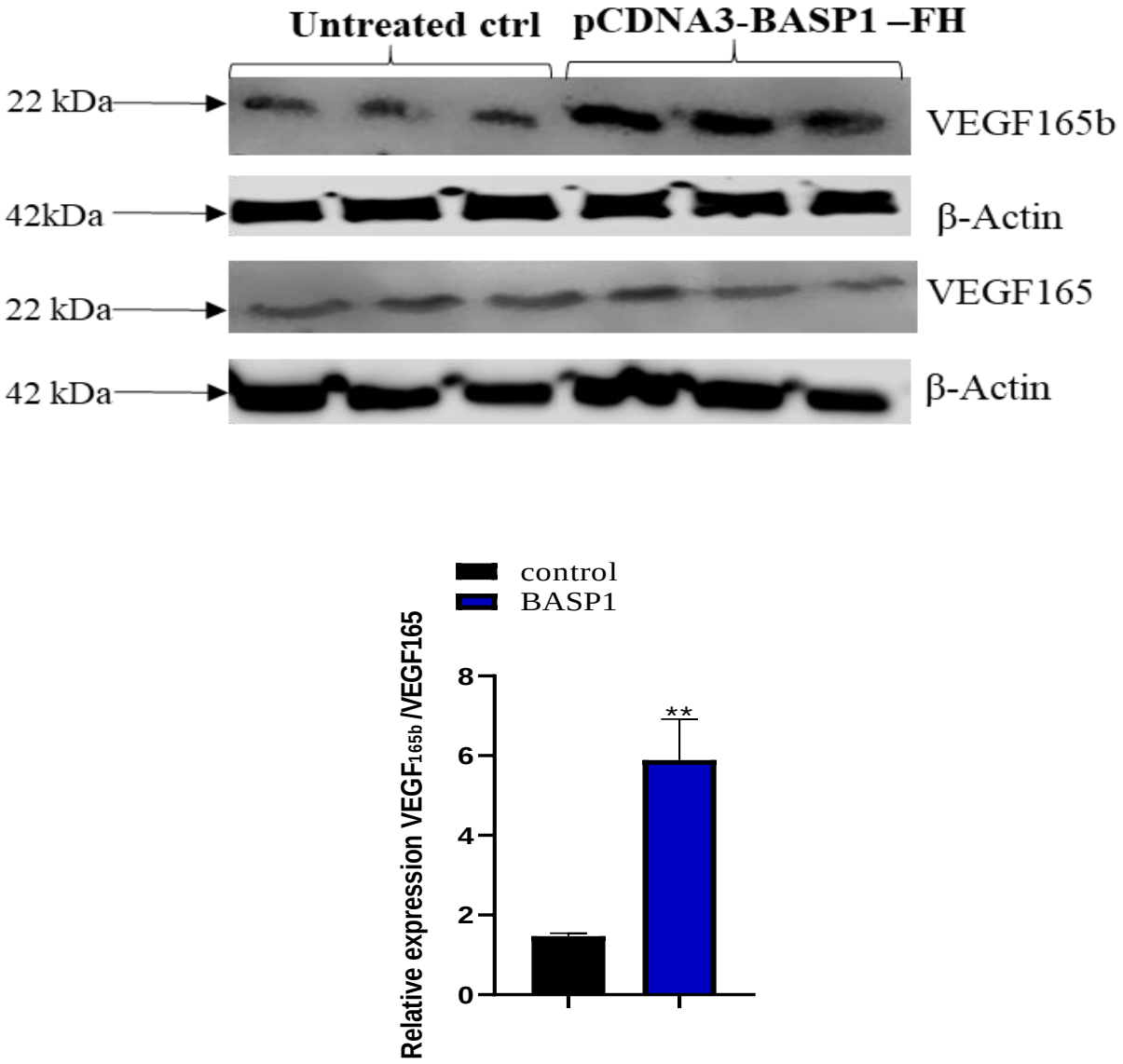

Figure 5. 5 Overexpression of WT1 co-suppressor BASP1 Affects VEGF alternative Splicing in PC3 cells.

Western blot analysis of VEGF 165 and VEGF 165b isoforms in PC3 cells after BASP1-expressing plasmid transfection (pCDNA-BASP1-FH). The blot was re-probed with actin which was used as a loading control. The graph represents relative expression determined by densitometric measurement of the bands and is expressed relative to VEGF 165. Bar-graph shown is the average of three independent experiments. (**P= 0.0090) a significant change of VEGF alternative splicing compared to the untreated group using unpaired t-test.

5.3.5 Effect of BASP1 overexpression on cell proliferation and viability

Guo *et al.*, 2016 demonstrated that BASP1 overexpression in vitro in KMH-2 cells and BHT101 resulted in limiting cellular proliferation and reducing cell viability. In vivo, BASP1 overexpression showed inhibitory activities against proliferation and tumorigenicity. In multiple tumours, WT1 plays a major role in tumour cell proliferation and inhibiting apoptosis (Sugiyama, 2010).

The described co-suppressive activity of BASP1 could play a role in limiting cellular proliferation and viability through suppressing WT1 target genes. Therefore the effects of BASP1 overexpression on the proliferation and viability of K562 and PC3 cells was investigated in this study.

BASP1 expressing plasmid was transfected into both cell lines followed by the MTT assay. Significant reductions in proliferation and viability occurred 48 h after transfection compared with the control group. Additionally, the statistical analysis in figure 5.6 indicates that BASP1 overexpression reduced K562 proliferation and cell viability (*P=0.0360 and *0.0015, respectively). A significant reduction in PC3 (figure 5.6 C&D) cellular proliferation and cell viability (**P 0.019 and ***=0.0002, respectively) was also observed. These findings suggested that BASP1 overexpression inhibits the proliferation and cell viability in K562 and PC3 cells.

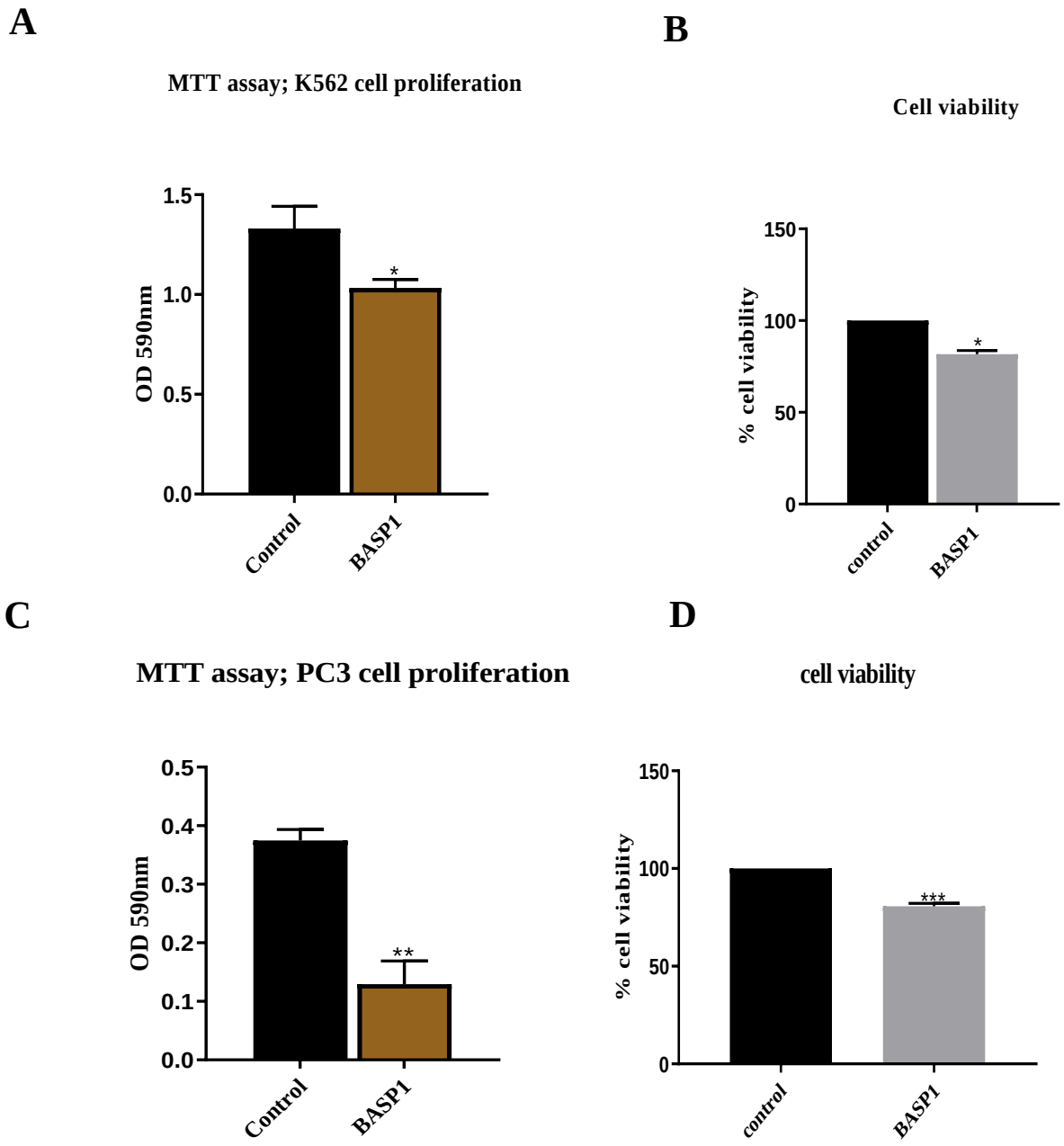

Figure 5. 6 Cellular proliferation and viability in K562 and PC3 cells after overexpression of BASP1.

MTT assays were used to analyse the effect of BASP1 expressing plasmid transfections for 48hrs on the cellular viability and proliferation in K562 (A&B) and PC3 (C&D) cells. The absorbance of each well was measured at 590 nm using a plate reader. Results represent the mean ± SEM of three experiments and are presented as a bar graph after normalizing to the respective controls. Cell viability = control- absorbance

of treatment wells/absorbance of control well ×100%. (*P=0.0360,*0.0015, **P 0.019, ***=0.0002 using unpaired t-test).

5.3.6 Effect of BASP1 overexpression on *SRPK1* promoter activity in WT1 negative MG63 cells

As previously described, BASP1 has been identified as a WT1 transcriptional co-suppressor as the WT1/BASP1 transcriptional complex binds and represses transcription of its target genes. The collective evidence in this part of the study suggests that BASP1 influences SRPK1 transcription through a co-suppressive mechanism that involves WT1. To provide further evidence for this mechanism, and as a further control, BASP1 was expressed in a WT1 negative cancer cell line, MG63 (osteosarcoma). MG63 cells were transiently co-transfected with full-length BASP1 expressing construct and the WT *SRPK1* promoter: luciferase reporter. BASP1 overexpression alone has no significant impact on SRPK1 transcription (Figure 5.7).

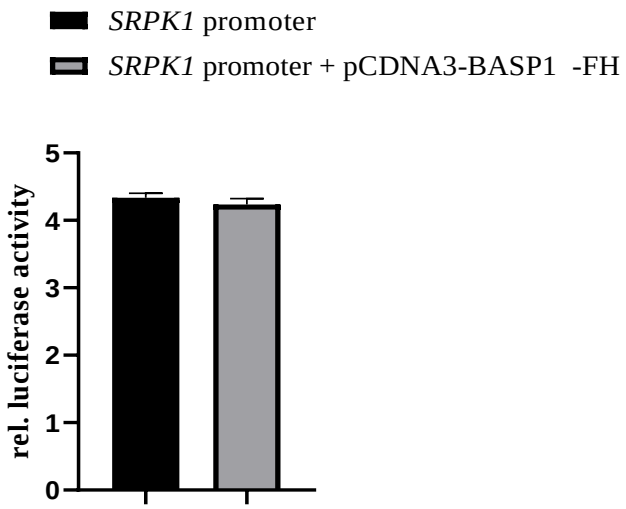

Figure 5. 7: Overexpression of BASP1 doesn't repress SRPK1 transcription in MG63.

Plasmid encodes wild-type BASP1 was co-transfected with the WT *SRPK1* promoters into MG63 cells. RLU = relative luciferase units. No significant change was observed using unpaired t-test. Three independent repeats are shown in each case.

5.4 Summary

Data in preceding chapters have shown that WT1 binds to *SRPK1* promoter and activates it. This was the opposite of what has been described before in podocytes wherein WT1 binds and represses SRPK1 expression. This could be attributed to the fact that WT1 interacts with other transcriptional cofactors that determine whether it works as a transcriptional activator or repressor of its target genes. Previous publications have identified that BASP1 is a WT1 co-suppressor that forms a transcriptional complex with WT1 and induces transcriptional repression of its target genes.

Given that WT1 binds to the *SRPK1* promoter and regulates its transcription, it is possible that BASP1 might be present at the *SRPK1* promoter and modulate its transcription in genetically engineered BASP1 expressing K562 cells. Via ChIP analysis of cross-linked chromatin harvested from B-K562 cells, the experiments first confirmed that BASP1 is associated with the *SRPK1* promoter (fig.5.1)

Furthermore, overexpression of BASP1 in PC3 and K562 cells using a plasmid construct increased the levels of BASP1 in the cells (fig.5.2) and reduced the transcriptional activity of SRPK1 (fig.5.3). This raises the possibility that BASP1 might be present at the *SRPK1* promoter by itself or in the form of a complex with WT1.

Western blot for endogenous BASP1, WT1 and SRPK1 in K562, B-K562, DU145 and PC3 cells suggests that when BASP1 is overexpressed, both WT1 and SRPK1 are downregulated. The downregulation of SRPK1 is consistent with BASP1 turning WT1 into a transcriptional repressor; the change in WT1 levels could be a result of BASP1 affecting an autoregulatory loop since WT1 is known to be able to regulate its own transcription (fig.5.4).

We also examined the effect of SRPK1 repression through BASP1 on the alternative splicing of VEGF. In podocytes, in which WT1 represses SRPK1 in the presence of BASP1, anti-angiogenic VEGF165b is expressed. BASP1 overexpression in PC3 resulted in a similar increase in levels of the anti-angiogenic isoform VEGF165b (fig.5.5). Furthermore, the overexpression of BASP1 also resulted in a reduction in cellular proliferation and viability of K562 and PC3 cells (fig.5.6). The modest changes are consistent with the fact that in transient transfections only a proportion of cells will have taken up the BASP1-expressing plasmid. Finally, in MG63 cells, which is not a WT1 expressing cell line, BASP1 overexpression did not affect *SRPK1* promoter activity (fig.5.7).

Taken together, the results presented in this chapter indicate that BASP1 is able to modulate the activity of WT1 on the transcriptional regulation of SRPK1. Results also confirm that BASP1 has the characteristics of a tumour suppressor. The latter could in part be mediated by the interaction of BASP1 with WT1, making it repress oncogenic splice factor kinases such as SRPK1.

6 Chapter Six: Effect of the ERG transcription factor on *SRPK1* transcription.

6.1 Background

SR proteins are essential for the regulation of alternative splicing of pre-mRNA. They play critical roles in the initiation of spliceosome assembly on pre-mRNA substrates. Each SR protein is characterised by substrate specificity towards specific pre-mRNAs. Hypo and hyperphosphorylation of SR proteins inhibit splicing; therefore, the phosphorylation of SR protein must be strictly regulated at the cellular level. The mechanisms through which SR protein phosphorylation is regulated are not yet fully explored. However, SRPK1 has been shown to phosphorylate these SR proteins utilizing their serine-arginine-rich domains as a substrate. SRPK1 and its best-studied substrate, SRSF1 are part of an essential pathway responsible for the regulation of the alternative splicing of vascular endothelial growth factor (VEGF) pro/antiangiogenic isoforms in renal epithelial cells (podocytes) and in colon carcinoma cells (Amin *et al.,* 2011 and Oltean *et al.,* 2012).

WT1 regulates the expression of SRPK1 in different contexts, repressing it in podocytes (Amin *et al.,* 2011) yet activating it in vascular endothelial cells (Wagner *et al.,* 2019). Results described in previous chapters show that WT1 activates SRPK1 transcription in K562 and PC3 cells; this activation is however prevented by the co-repressor BASP1. This finding has clear significance given the involvement of WT1 in many cancers. However, it is likely that other transcription factors contribute to SRPK1 regulation.

The ETS-related gene (ERG) has been described by several studies to regulate several cancer-associated target genes. ERG also plays a key role in regulating the anti-inflammatory response (Yuan *et al.*, 2009). They have shown that, through direct binding, ERG suppress the activity of *IL-8* promoter. Birdsey *et al.*, 2012 demonstrated that ERG also downregulates the expression of HDAC6 by interacting directly with its promoter in the HUVEC cell line. ERG is involved in the development of the vascular system, and in bone and blood development (Adamo and Ladomery, 2015). Therefore it was of interest to investigate whether or not ERG regulates SRPK1 transcription.

6.2 Aims and objectives

1. To investigate the transcriptional regulation of the splice factor kinase gene *SRPK1* by ERG.
2. To evaluate the impact of ERG knockdown or overexpression on the following:
    - Transcription and protein levels of SRPK1 in K562, PC3 and MG63 cell lines.
    - The alternative splicing of apoptotic factors *BCL2L1* and *caspase* 9
    - On cellular migration, invasion, viability, and proliferation.

6.3 Results

6.3.1 ERG binds the *SRPK1* promoter

The *ERG* oncogene encodes an ETS family transcription factor. ERG can bind a specific ETS site, with a core GGAA target sequence. Yuan *et al*., 2009 described how ERG associates with the *IL-8* promoter and downregulates its transcription in the HUVEC cell line. Furthermore, ERG transcriptionally represses the tumour suppressor *PTEN* (Adamo *et al.*, 2017). Chromatin Immunoprecipitation (ChIP) was performed on sheared cross-linked chromatin collected from the ERG-positive MG63 osteosarcoma cell line (figure 6.1). Primers specific to the *SRPK1* promoter used in previous chapters were used and PCR was performed to detect the genomic regions being pulled down by the antibodies. Figure 6.2. Suggests that ERG is binding to the *SRPK1* promoter. A rabbit monoclonal antibody against ERG was used; together with an anti- RNA polymerase II antibody as a positive control. Normal Mouse IgG served as a negative control. Input DNA was used as an additional positive control for subsequent PCRs. For additional confirmation, the amplicon was extracted from the gel and sent for sequencing (see Appendix).

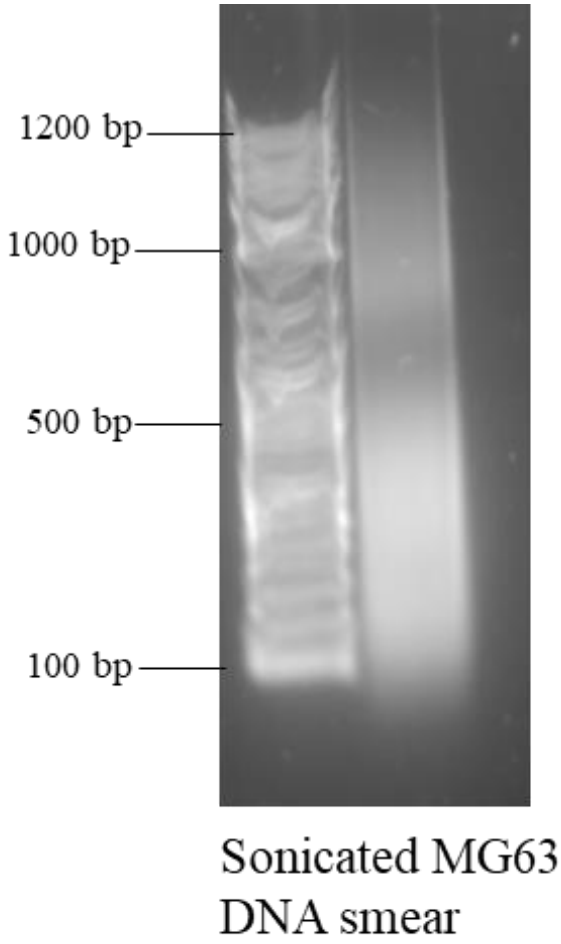

Figure 6. 1: Sonicated DNA smear for MG63 cells in preparation for Chromatin Immunoprecipitation (ChIP) assay.

Chromatin fragments resolved by agarose gel following sonication with varying sonication times, the cells were lysed and DNA sheared to about 1000bp using a sonicator**.** 6X of 50% power output for 15seconds followed by incubation on ice for 60seconds. The sizes of the generated DNA smears are between 200-1000bp which is optimal for the ChIP assay**.**

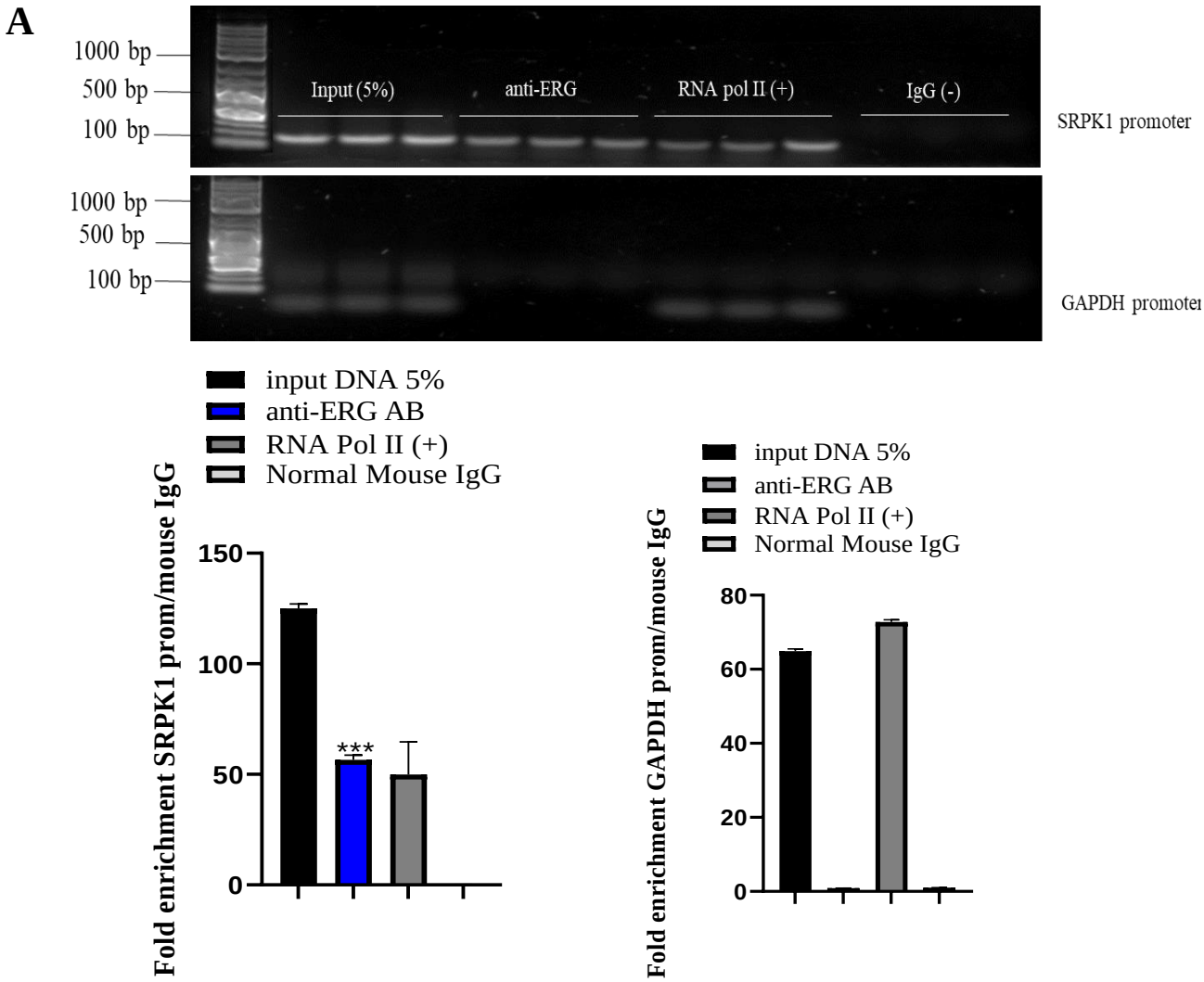

Figure 6. 2: ERG binds the SRPK1 promoter

Chromatin immunoprecipitation (ChIP, n = 3) was performed using a rabbit monoclonal antibody against ERG or anti- polymerase II antibody as a positive control. Normal Mouse IgG served as a negative control. Input 5% is the diluted sonicated chromatin which was used as an additional positive control for subsequent PCRs on the *SRPK1* promoter and the respective sequence. **A**. PCR assay for ChIP product for MG63 cells using primers to detect the region around the *SRPK1* transcriptional start site (TSS) and *GAPDH* promoters. Representative Agarose gel photographs of semi-quantitative ChIP PCR experiments for the *SRPK1* and *GAPDH* promoters. Data are expressed as means ± S.E.M. *** indicates $p < 0.0005$ which is statically significance using one way ANOVA test.

6.3.2 ERG suppresses SRPK1 transcription

The previous experiment suggests that ERG binds to the *SRPK1* promoter. The next question is to determine whether or not ERG might contribute to *SRPK1* transcriptional regulation in cancer cell lines. As a model system, the leukemic cell line K562 prostate cancer cell lines PC3 and osteosarcoma cell line MG63 were used for this purpose. Those K562 and PC3 cells are known to express SRPK1 but not ERG. MG63, on the other hand, is known to express both ERG and SRPK1. Cells were transfected with the wild-type *SRPK1*: Luciferase construct alone or cotransfected with a plasmid that expresses full length ERG. The results show that the *SRPK1* wild type promoter remained active when transfected alone but when ERG is overexpressed, the ratio of Luciferase to Renilla was significantly reduced in K562 (**p<0.0049), PC3 (***p<0.0005) and MG63 (**p<0.0021) cells (Figures 6.3). There was a trend in all of the three transfection repeats in all of the cell lines in which ERG overexpression appears to repress *SRPK1* promoter activity. RLU luminescence values are ± SE of experiments performed in triplicate. Therefore, findings support the hypothesis that ERG is binding to the *SRPK1* promoter and contributes to regulating its transcription specifically repressing it.

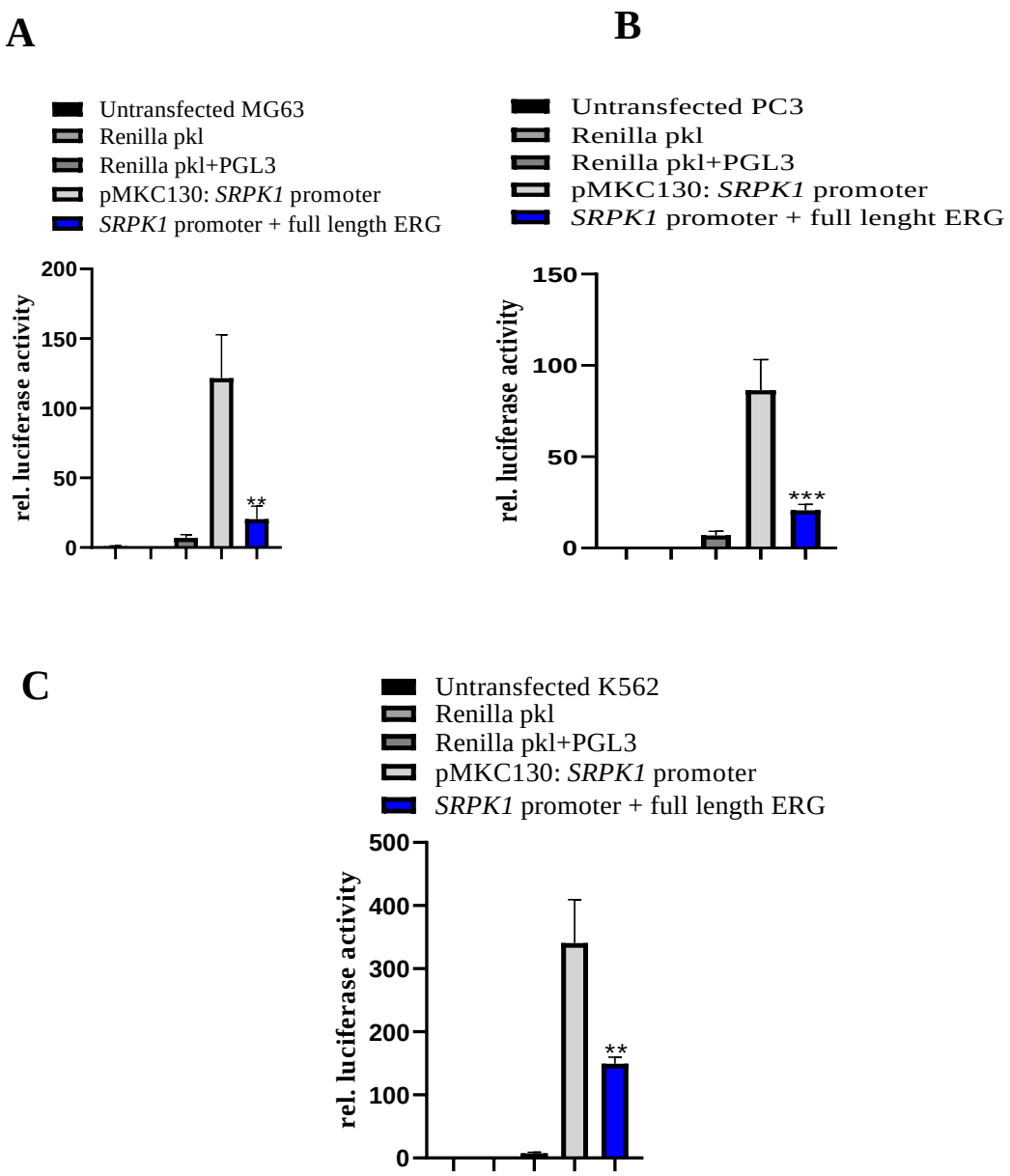

Figure 6. 3: DLR assay of SRPK1 promoter activity in MG63 (A), PC3 (B) and K562 (C) cells.

Measurement of *SRPK1* promoter activity using a dual luciferase reporter (DLR) assay. An *SRPK1*: Luciferase construct was transfected alone or cotransfected with a plasmid that expresses full length ERG. Plasmids were transfected into the cell lines with a Renilla expressing vector or empty vector as transfection control. Data are expressed as relative luciferase units (RLU). Data presented as mean ± S.E. for n=3. $^{**}p<0.0021$ or $^{***}p<0.0005$ or $^{**}p<0.0049$ for MG63, PC3 and K562 respectively which is statistically significant using one way ANOVA test. Figures show a reduction of promoter's activity in cells when cotransfected with full length ERG and high activity when only transfected with wild type promoter.

ERG, like other oncogenes and major transcriptional regulators, express several splice isoforms. In the current study, the focus was on studying the effect of (-/+7b) isoforms and the full length ERG on the regulation of SRPK1. These two ERG variants differ by the presence or the absence of a short cassette exon 7b that adds, in the frame, 24 amino-acids to the transcriptional activation domain. Exon 7b has been shown to be included at a higher rate in advanced prostate cancer (Hagen *et al*, 2014).

At first, to test which isoform suppresses *SRPK1* activity the most, different ERG isoforms were cotransfected with the *SRPK1* wild type promoter into the cells and DLR was carried out. The results suggest that all ERG isoforms equally suppressed *SRPK1* promoter activity. The statistical analysis in figure (6.4 A&B) shows. (+7b **p*<0.0254 in K562 cells or ***= 0.0005 in PC3 cells) (-7b **p*<0.0230 in K562 cells or ***= 0.0004 in PC3 cells) (Full length ERG **p*<0.0403 in K562 cells ****<0.0001 in PC3 cells)

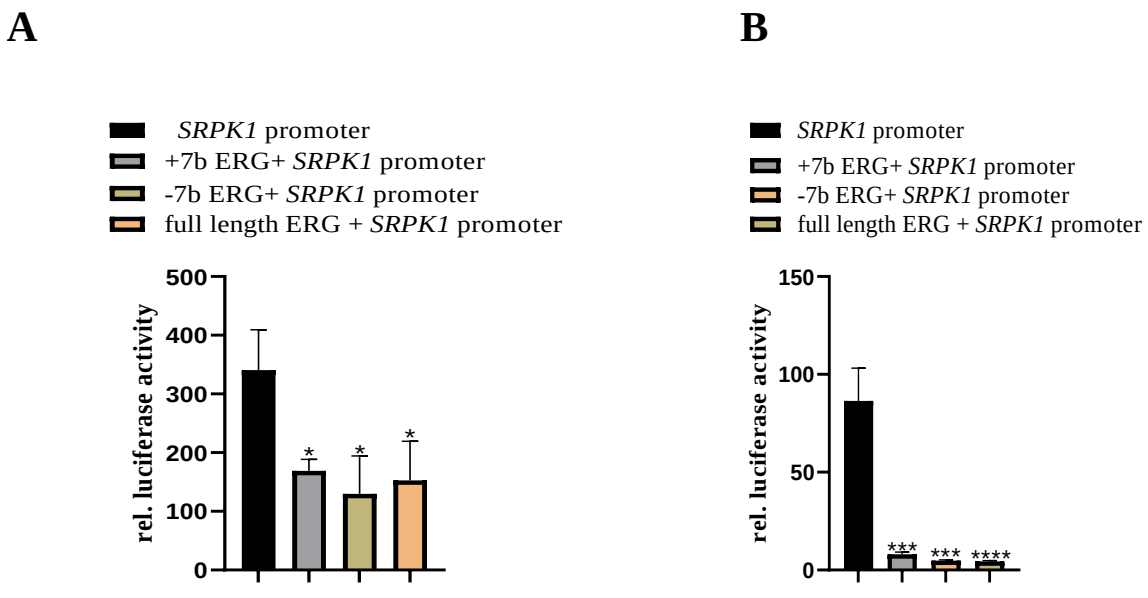

Figure 6.4 A&B: Transcriptional repression of SRPK1 promoter by different ERG isoforms in K562 and PC3 cells.

Measurement of *SRPK1* promoter activity using a dual luciferase reporter (DLR) assay. WT *SRPK1* promoter transfected alone or with +/- 7b and full length ERG isoforms expressing plasmids into K562

cells for 48 hours **(A).** Data are expressed as (RLU) and presented as mean ± S.E. for n=3. **(B)** Shows the same transfections into PC3 cells. Data are expressed as (RLU) and presented as mean ± S.E. for n=3. P values were obtained using one way ANOVA test.

The next step was to test the effect of the overexpression of full length ERG isoform, also +exon 7b, expressed from a different plasmid vector, on SRPK1 transcription. For that purpose, full length ERG isoform was transiently co-transfected with WT *SRPK1* promoter at increasing concentrations into MG63 cells line. (Figure 6.4.C) Shows that the full length ERG isoform significantly reduced *SRPK1* promoter in a dose-dependent manner.

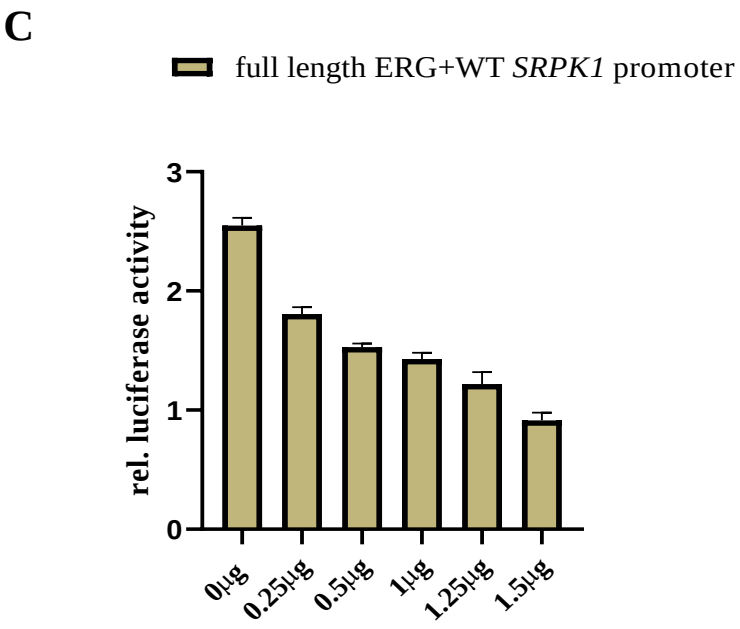

Figure 6.4 C: Transcriptional repression of SRPK1 promoter by full length ERG (+exon 7b) in MG63 cells.

Wild-type *SRPK1* promoter transfected alone or with an increasing concentration (0-1.5 µg) of a plasmid that expresses full length ERG (+exon 7b) in MG63**.** Data are expressed as relative luciferase units (RLU). Data presented as mean ± S.E. for n=3. The figure shows a reduction of the promoter's activity in cells when cotransfected with full length ERG and high activity when only transfected with wild type.

6.3.3 Effect of ERG overexpression on SRPK1 protein levels

Data obtained suggest that ERG interacts with the *SRPK1* promoter and represses its transcription. Adamo *et al.*, 2017 described how ERG represses the transcription of PTEN in DU145 cells; so it is capable of working as a transcriptional repressor. The effect of the transcriptional repression of *SRPK1* by ERG on SRPK1 protein levels was investigated. For this objective, at first, K562 cells (SRPK1 positive and ERG negative) were transiently transfected with -7b and +7b full-length ERG expressing plasmids separately. A western blot was performed on protein lysates prepared from the cell lines following the overexpression. (Figure.6.5.A &B) shows a significant decrease in SRPK1 bands following ERG isoform overexpression in K562 cells (**p=0.0057 for full length and ***p=0.0003 -7b).

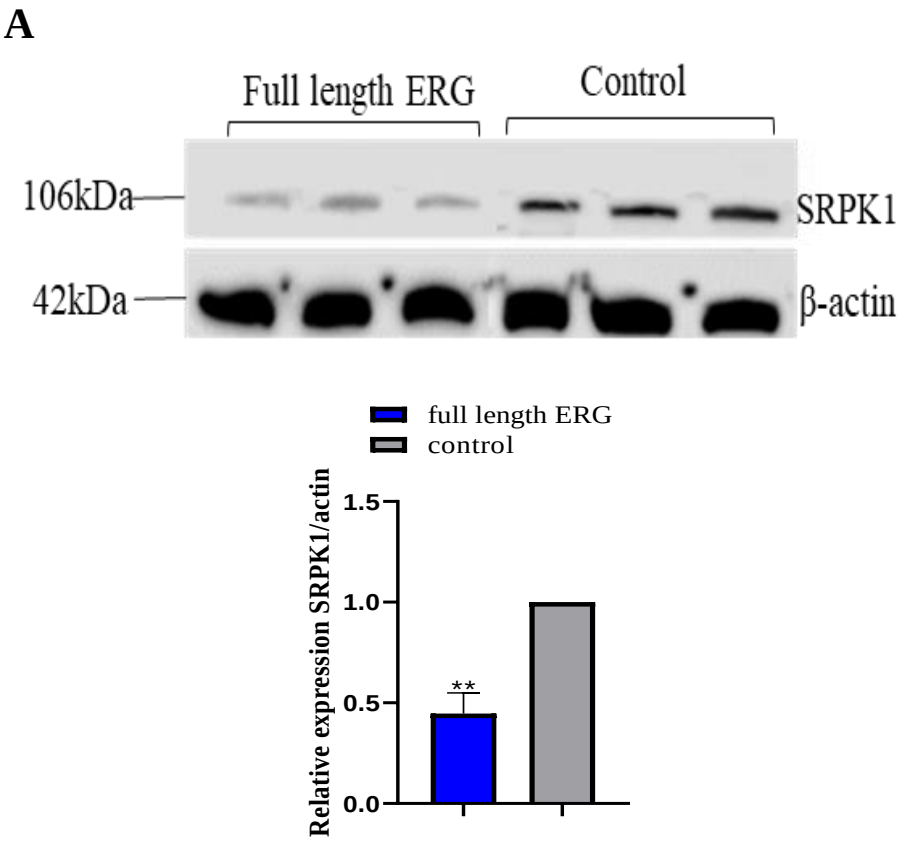

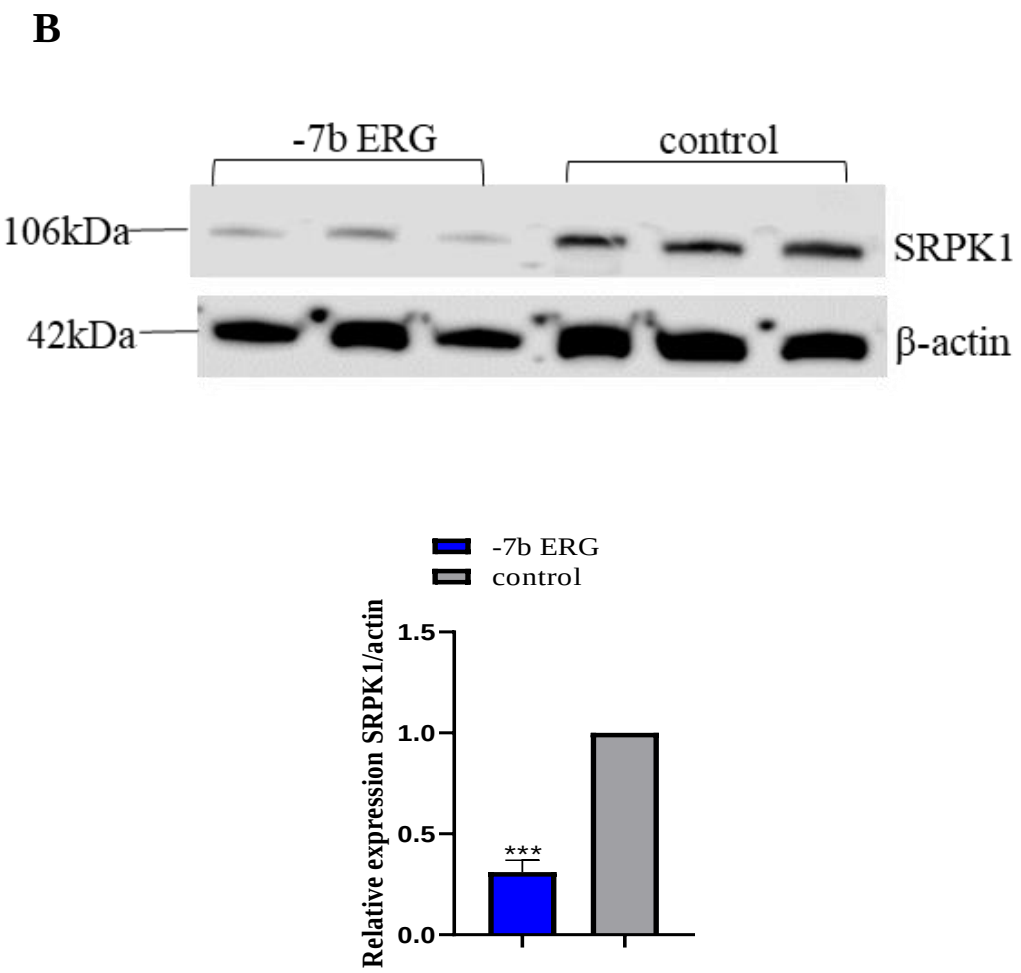

Figure 6.5 A&B: Repression of SRPK1 protein levels by -7b and full-length ERG isoforms in K562 cells.

Western blot of protein lysates from K562 cells. Cells were transiently transfected with - 7b or full length ERG (+7b) isoforms expressing plasmids for 48 hours. Membranes were blotted with anti-SRPK1 or anti-beta actin antibodies as a loading control. Graphs represent relative expression determined by densitometric measurement of the bands and are expressed relative to actin. The bar-graph shown is the average of three independent experiments. A significant reduction in SRPK1 levels as a result of overexpressing ERG. P values were obtained using unpaired t-test.

The next step was to transfect PC3 cells (SRPK1 positive and ERG negative) with -7b and +7b full-length ERG. A western blot was performed on protein lysates prepared from the cell line following the overexpression. (Figure.6.5.C&D) shows a significant decrease

in SRPK1 protein levels with ERG isoform overexpression in transfected PC3 cells (*p=0.0440 for +7b full-length) and (***p=0.006 for -7b).

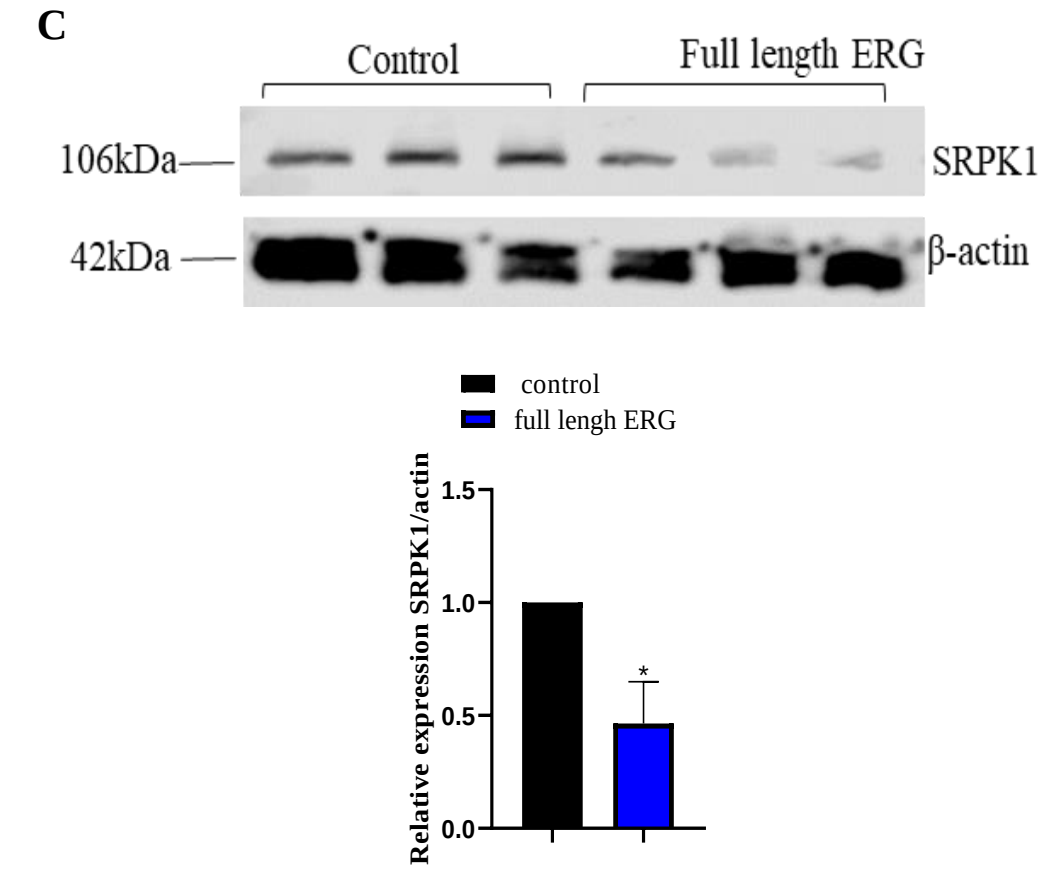

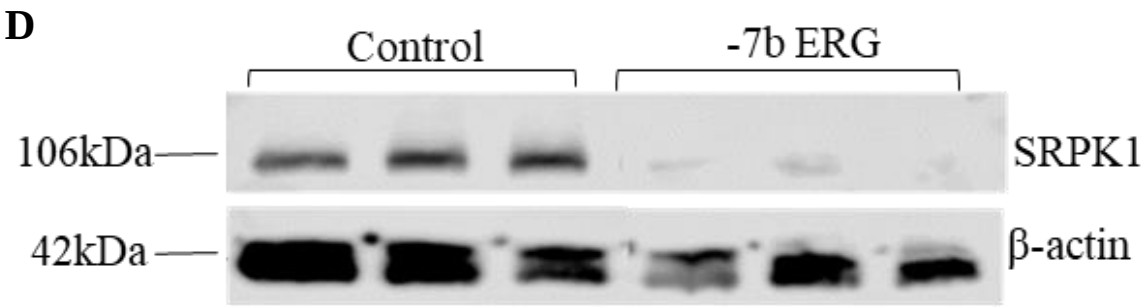

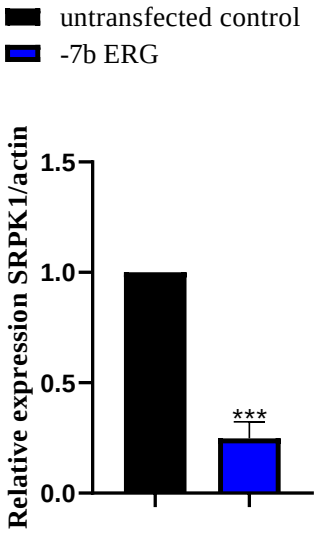

Figure 6.5 C& D: Repression of SRPK1 protein levels by +/- 7b ERG isoforms in PC3 cells.

Western blot of protein lysates from PC3 cells. Cells were transiently transfected with - 7b or full length ERG isoforms expressing plasmids for 48 hours. Membranes were blotted with anti-SRPK1 or anti-beta actin antibodies as a loading control. Graphs represent relative expression determined by densitometric measurement of the bands and are expressed relative to actin. Bar-graph shown is the average of three independent experiments. A significant reduction in SRPK1 levels was observed as a result of overexpressing ERG. P values were obtained using unpaired t-test.

6.3.4 Effect of ERG -siRNA knockdown on SRPK1 transcription and protein levels

The data obtained so far indicate that ERG binds to *SRPK1* promoter and repressed its expression. To further investigate SRPK1 regulation by ERG, siRNA-mediated knock-down of ERG was performed in the MG63 cell line. The same ERG and GL2 control siRNA sequences (table 2.1) previously described in (Urbinati *et al.*, 2016) were used in this study. To verify the transfection efficacy, ERG siRNA was tagged with CY5 fluorescent labels (Figure.6.6.A). At first, to verify that the knockdown has occurred, siRNA were transfected alone into the cells and western blot was performed on protein lysate was prepared from the MG63 cells following the siRNA knockdown (Figure.6.6.B

&C). Significant reduction in ERG protein was observed at higher concentration of the siRNA (100nM) which suggested that ERG knockdown was achieved.

A

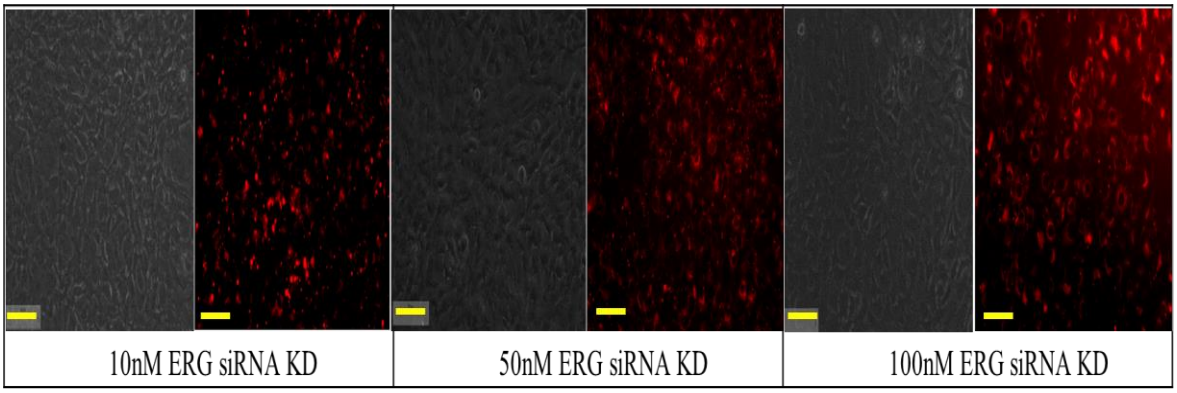

B

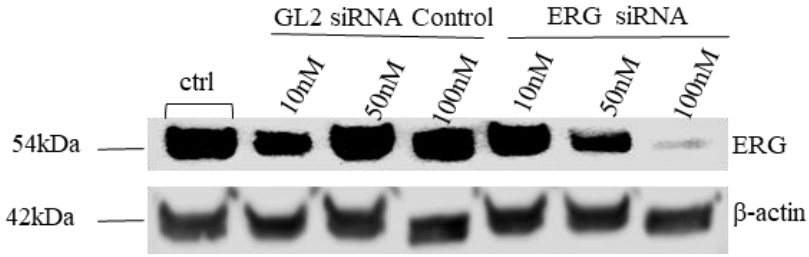

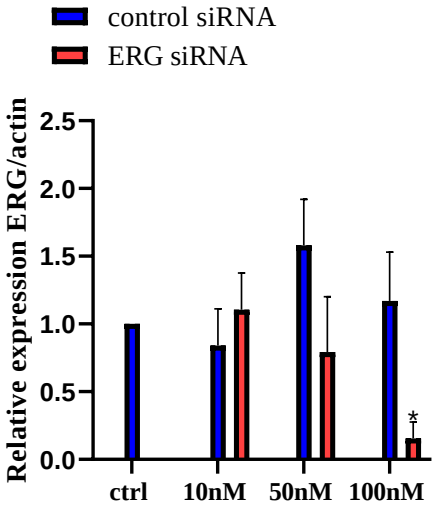

C

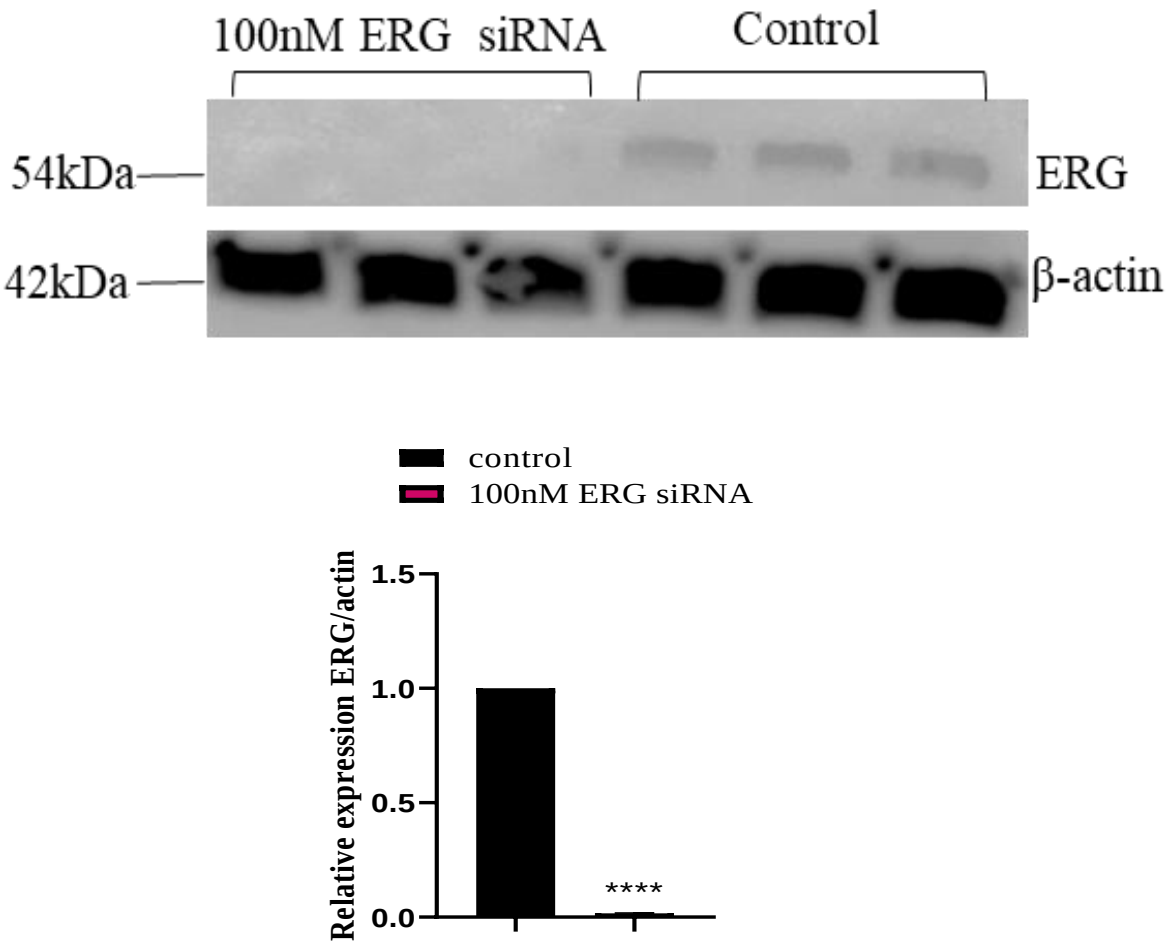

Figure 6.6: ERG knockdown in MG63 cells.

(A) Representative fluorescence microscopy images of CY5 tagged-ERG targeting siRNA transfected into MG63 cells (bright and fluorescent fields). MG63 cells were transfected with increasing concentration of ERG siRNA (10nM, 50nM and 100nM) (B) or 100nM siRNA alone (C) or control GL2 siRNA for 48 hours. B&C. Western blot of MG63 protein lysate after ERG siRNA knockdown. Membranes were blotted with anti-ERG or anti-beta actin antibodies as a loading control. Graphs represent relative expression determined by densitometric measurement of the bands and are expressed relative to actin. Bar-graph shown is the average of three independent experiments. **= $p<0.0129$ and ****= $p<0.0001$ significant change compared to control using 1 way ANOVA test and unpaired t test respectively.

The next step was to evaluate the effect of ERG knockdown on *SRPK1* transcription via co-transfecting the highest concentration of siRNA ERG with the WT *SRPK1* promoter reporter. (Figure.6.7.) shows that the activity of the wild type promoter significantly increased in MG63 cells (**** p<0.0001).

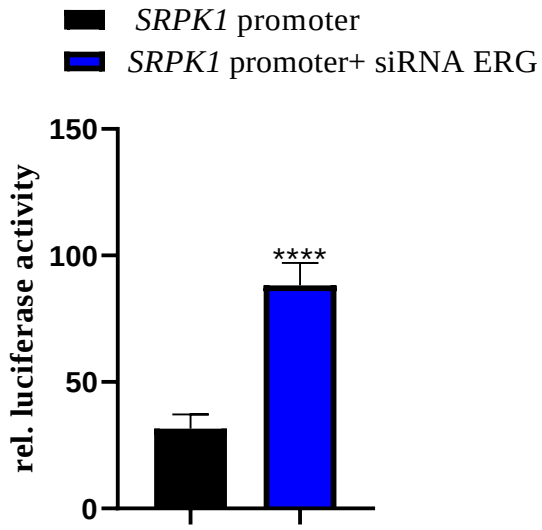

Figure 6.7: DLR assay of SRPK1 promoter activity following siRNA mediated ERG knockdown in MG63 cells.

Measurement of *SRPK1* promoter activity using a dual luciferase reporter (DLR) assay. WT *SRPK1* promoter was co-transfected with 100nM ERG siRNA into the cells. Data are expressed as relative luciferase units (RLU). Data presented as mean ± S.E. for n=3. **** p<0.0001, which is statistically significant using unpaired t test. The figure shows a reduction of the promoter's activity in cells where ERG was knocked down.

6.3.5 The effect of ERG Exon 4 skipping through splice switching oligonucleotides on SRPK1 transcription and protein levels

Splice-switching oligonucleotides (SSOs) are a new emerging molecular tool that has been recently used to change the way that exon segments of pre-mRNA are spliced (joined) together. They can be used to influence the rate of inclusion of a given exon.

So far, the experimental outcomes in this study suggest that ERG is an SRPK1 transcriptional repressor that binds to the *SRPK1* promoter and downregulates its expression. Increased ERG expression reduces SRPK1 levels, and conversely ERG knockdown increases SRPK1 levels.

To verify this conclusion using a different approach, two different splice-switching oligonucleotides that manipulate *ERG* pre-mRNA was used. The vivo-morpholino -7b-3'SS induces skipping of cassette exon 7b within the *ERG* pre-mRNA (Jumbe *et al.,* 2019) while vivo-morpholino 4-3'SS results in skipping of exon 4 which leads to diminishing ERG protein levels due to a premature stop codon resulting. Vivo-morpholinos are morpholinos with an oligodendromer that facilitates transfection. Sequences and concentrations are shown in table 2.2.

Initially, the E4 3′ –morpholinos were added to MG63 cells followed by an RNA extraction to perform a PCR to verify the efficiency of the SSOs. E4 3′ SSOs induced *ERG* exon 4 skipping at the 3′ splice sites (Figure 6.8.A). A PCR was performed using the primers listed in (table 2.6). The rate of *ERG* exon 4 inclusion was measured by quantifying the PCR bands and calculating the splicing ratio (percentage spliced in, PSI-Ψ) (Figure 6.8.B&C). A control SSO (scrambled exon 7b SSO sequence) was included in addition to untreated cells as controls. The most efficient exon skipping was observed with the E4 3′ SSO at 3μM (0.31 PSI-Ψ), where Ψ is the proportion of exon inclusion, compared to the control SSO that did not cause any significant changes to *ERG* exon 4 skipping 0.84 Ψ and 0.81 Ψ for untreated cells.

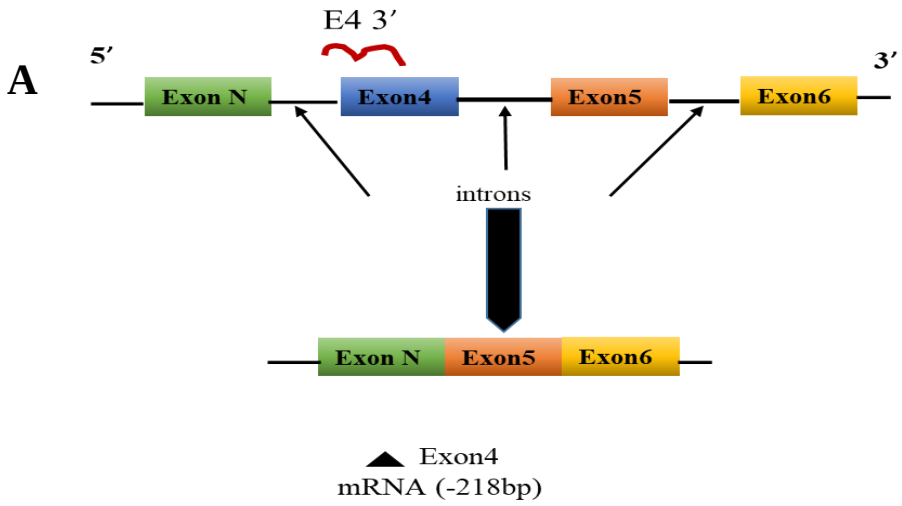
A
E4 3′
5′
3′
Exon N
Exon4
Exon5
Exon6
introns
Exon N
Exon5
Exon6
Exon4
mRNA (-218bp)

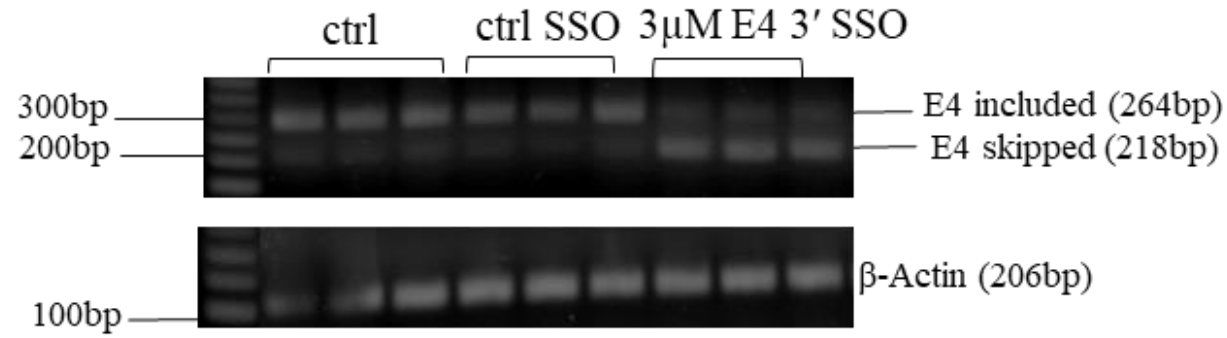
B
ctrl
ctrl SSO
3μM E4 3′ SSO
300bp
200bp
E4 included (264bp)
E4 skipped (218bp)
100bp
β-Actin (206bp)

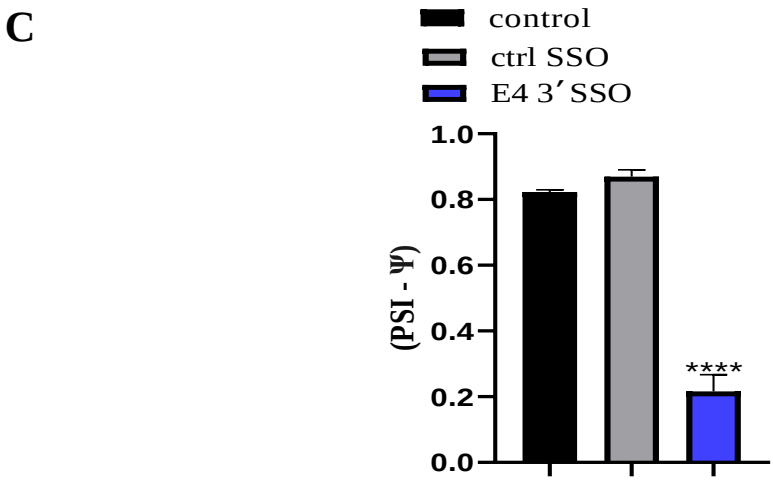
C
control
ctrl SSO
E4 3′SSO
1.0
0.8
0.6
0.4
0.2
0.0
(PSI - Ψ)
****

Figure 6.8: ERG mRNA levels in E4 3′ SSO transfected MG63 cells.

MG63 cells treated with 3μM of E4 3′ SSO for 48hrs followed by RNA extraction and cDNA synthesis. PCR was performed using *ERG* specific primers. (A) Design of SSOs targeting exon 4 of *ERG* (B) PCR gel at 48hrs showing band intensity and size and corresponding loading control, *β-actin*. (C) graph of densitometry reading showing the percent spliced in (PSI, ψ) ratio at 48hrs data presented as mean ± S.E. for n=3. **** $p<0.0001$ using 1 way ANOVA test. The result shows E4 3′ SSO resulted in near complete exon 4 skipping in MG63 cells. Three independent repeats are shown in each case.

Next, the effect of *ERG* exon 4 skipping on *SRPK1* transcription was tested. For this objective, The WT *SRPK1* promoter was co-transfected with the 3μM E4 3′ SSO concentration which induced significant skipping in the previous experiment at for 48 and 72 hrs. Following that, a DLR assay was carried out (Figure 6.9). A significant increase in *SRPK1* promoter's activity was observed after 72 hrs of 3μM E4 3′ SSO transfection (**** $p<0.0001$) and 48 hrs. (** $p<0.0022$). This indicates that the transcriptional activity of *SRPK1* increased following *ERG* exon 4 skipping.

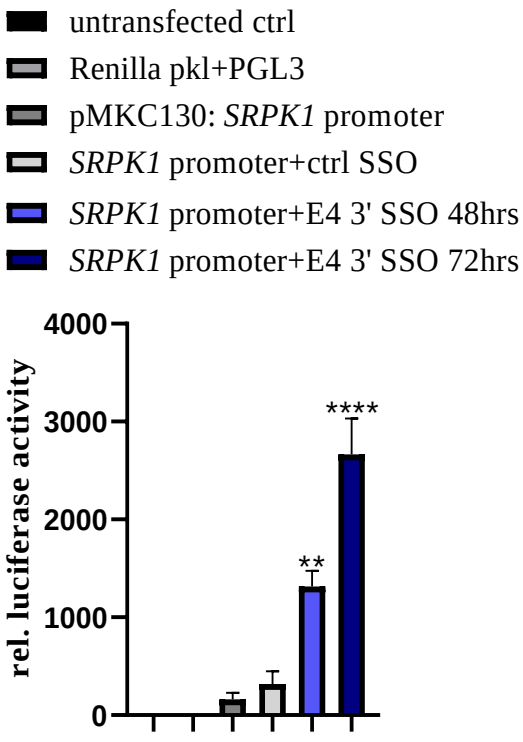

Figure 6.9: DLR assay of SRPK1 promoter activity in E4 3′ SSO transfected MG63 cells.

Measurement of *SRPK1* promoter activity using a dual luciferase reporter (DLR) assay. WT *SRPK1* promoter, was co-transfected with 3μM of E4 3′ SSO for 48hrs and 72hrs into the cells. Data is expressed as relative luciferase units (RLU). Data presented as mean ± S.E. for n=3. ** $p<0.0022$ and **** $p<0.0001$, which is statistically significant using 1 way ANOVA test. Figure shows significant increase of the promoter's activity in cells with *ERG*-Exon4 skipping.

Given the fact that ERG regulates SRPK1 and represses its transcription, the next part of this experiment was to determine if the reduction of ERG by E4 SSOs changes the transcriptional downregulation of SRPK1 and restores its expression at a protein level. For that aim, MG63 cells were transfected with 3μM of E4 3′ SSO for 48hrs and 72hrs. Western blot was performed on protein lysates prepared from the cells following the E4 SSOs transfection (Figure.6.10). A significant reduction in ERG expression (* = $p<0.0201$ for 48hrs and *=0.0220 for 72 hrs) correlated with a significant increase in SRPK1 expression (* = $p<0.0214$ for 48hrs and **** = $p<0.0001$ for 72 hrs) which suggest that diminishing ERG with E4 3′ SSO resulted in an increase in the SRPK1 expression in MG63 cell line.

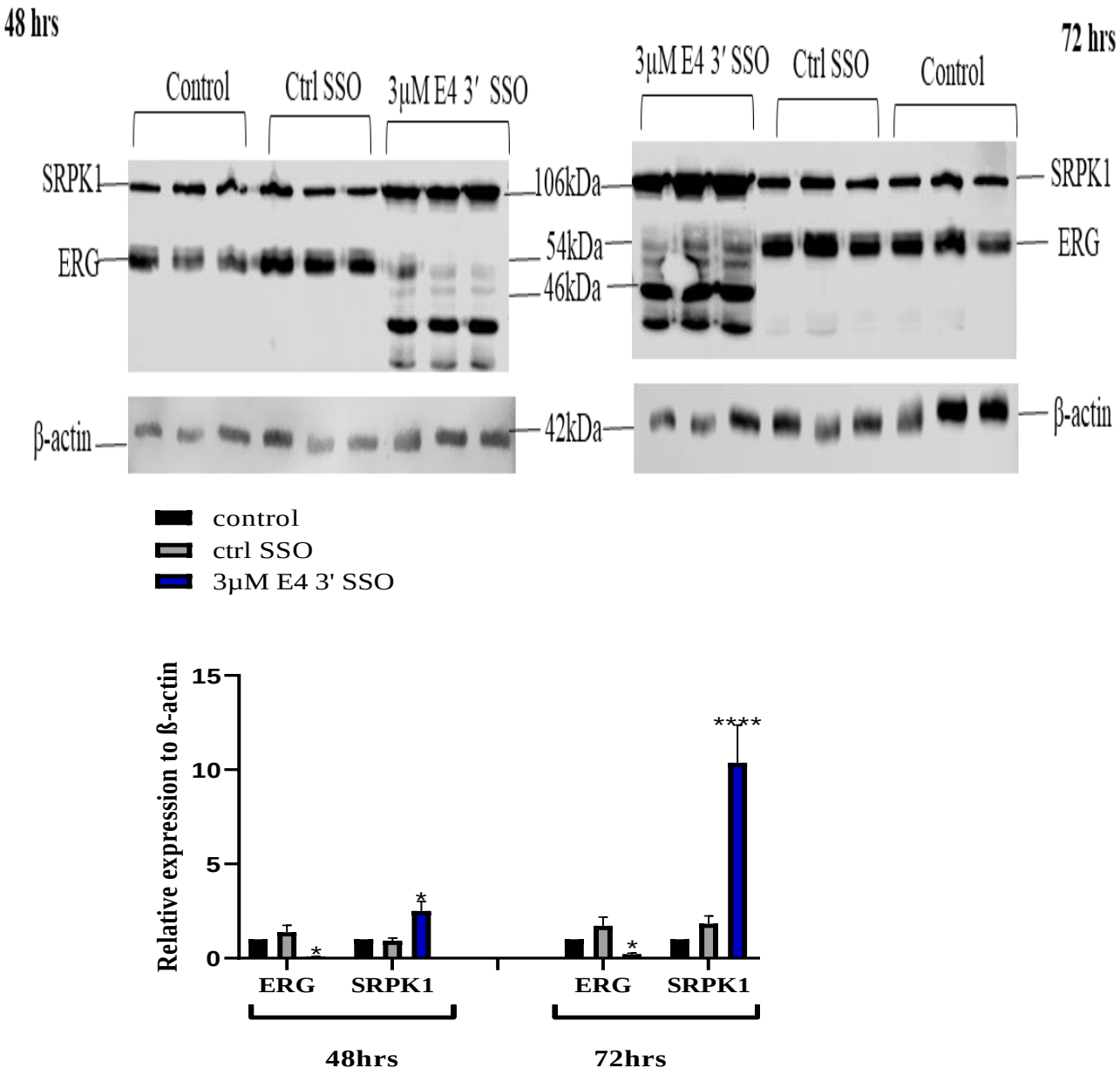

Figure 6.10: Effect of exon 4 skipping on ERG and SRPK1 protein levels.

MG63 cells were transfected with 3µM of E4 3′ SSO or control SSO for 48hrs and 72hrs. Cells were lysed and a Western blot was performed. Membranes were blotted with anti-ERG and anti SRPK1 or anti-beta actin antibodies as a loading control. The graph represents relative expression determined by densitometric measurement of the bands and is expressed relative to actin. Bar-graph shown is the average of three independent experiments. * = $p<0.0201$ and **** = $p<0.0001$ represent significant reduction in both ERG and SRPK1 levels compared to the untreated control using 2-way ANOVA test. Three independent repeats are shown in each case.

6.3.6 The effect of ERG Exon 7b skipping through splice switching oligonucleotides on SRPK1 transcription and protein levels

Subsequent to the previous findings, the effect of cassette exon 7b Skipping on *SRPK1* transcription and expression was tested in this study. The self-transfecting E7b 3′ – morpholinos were added to MG63 cells then followed by an RNA extraction to perform a PCR to verify the efficiency of the SSOs. E7b 3′ SSOs induced *ERG* exon 7b skipping b steric inhibition of the 3′ splice site (Figure 6.11.A). A PCR was performed using the proper primers listed in table 2.6 (ERG; Exon 7b skipping primers). The rate of ERG exon 7b inclusion was measured by quantifying the PCR bands and calculating the splicing ratio (PSI-Ψ) (Figure 6.11.B&C). A control SSO was included in addition to untreated cells as controls. The most efficient exon skipping was observed with the E7b 3′ SSO at 3μM (0.63 PSI-Ψ), where Ψ is the proportion of exon inclusion, compared to the control SSO that did not cause any significant changes to *ERG* exon E7b 3′ skipping 0.95 Ψ and 0.96 Ψ for untreated cells.

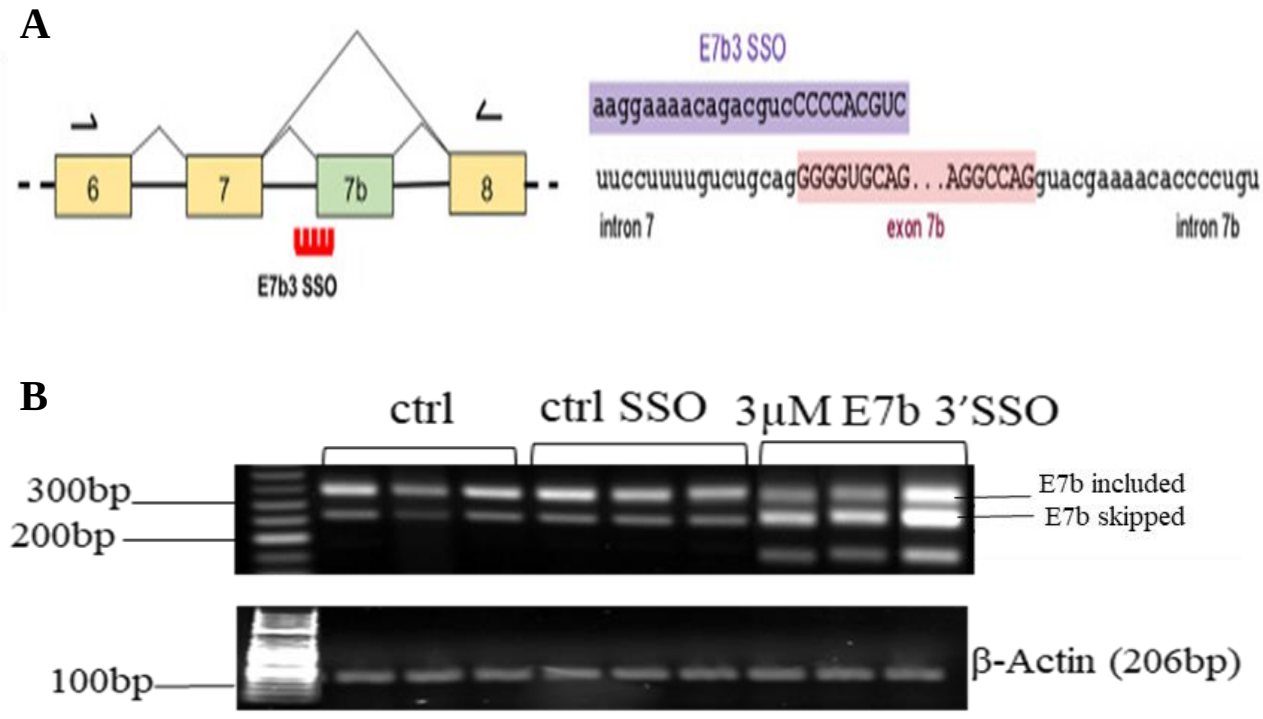

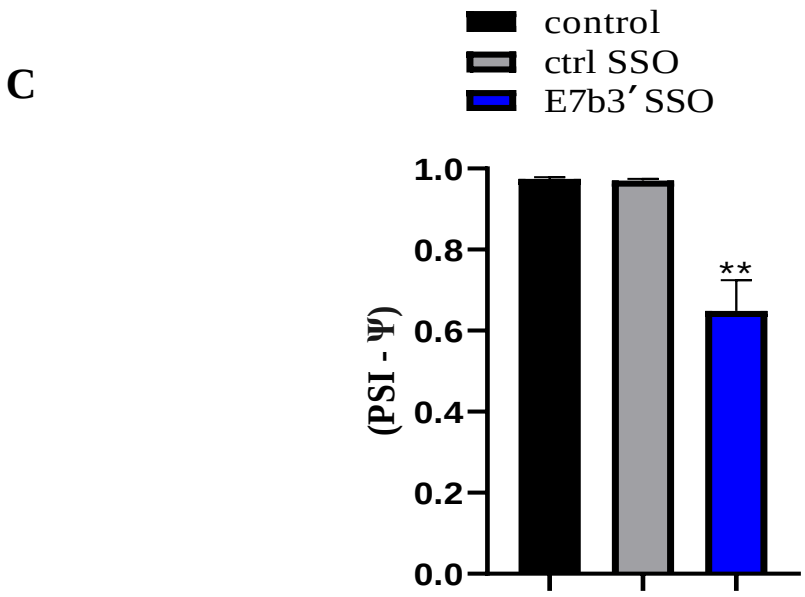

Figure 6.11: ERG mRNA levels in E7b 3′ SSO transfected MG63 cells.

MG63 cells treated with 3μM of E7b 3′ SSO for 48hrs followed by RNA extraction and cDNA synthesis. PCR was performed using ERG specific primers. (A) Design of SSOs targeting Exon7b of *ERG* (B) PCR gel at 48hrs showing band intensity and size and corresponding loading control, *β-actin*. (C) graph of densitometry reading showing the percent spliced in (PSI, ψ) ratio at 48hrs data presented as mean ± S.E. for n=3. ** p=0.0016 using 1 way ANOVA test. Three independent repeats are shown in each case.

Next, the effect of *ERG* exon 7b skipping on SRPK1 transcription was tested. For this objective, the WT *SRPK1* promoter was co-transfected with the 3μM E7b 3′ SSO concentration which induced significant skipping in the previous experiment at for 72 hrs. Following that, a DLR assay was carried out (Figure 6.12). No significant change in *SRPK1* promoter activity was observed after 72 hrs of 3μM E7b 3′ SSO. This indicates that the transcriptional activity of *SRPK1* wasn't significantly affected by *ERG* exon 7b Skipping.

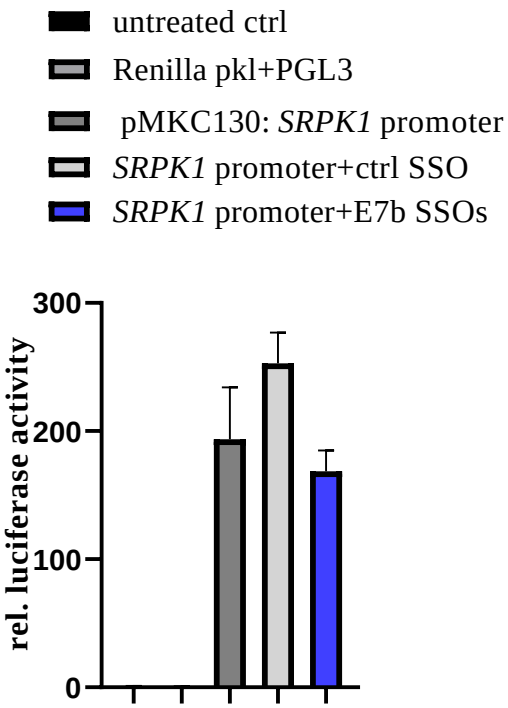

Figure 6.12: DLR assay of SRPK1 promoter activity in E7b 3′ SSO transfected MG63 cells.

Measurement of *SRPK1* promoter activity using a dual luciferase reporter (DLR) assay. WT *SRPK1* promoter was co-transfected with 3μM of E7b 3′ SSO for 72hrs into the cells. Data are expressed as relative luciferase units (RLU). Data presented as mean ± S.E. for n=3. No significant change was observed on the promoter activity with Exon7b skipping using 1 way ANOVA test. Three independent repeats are shown in each case.

The next part of this experiment was to determine whether exon 7b skipping changes SRPK1 protein levels. For that purpose, MG63 cells were transfected with 3μM of E7b 3′ SSO for 72hrs. A western blot was performed on protein lysates prepared from the cells following the E7b 3′ transfection (Figure.6.13) Consistent with the DLR data, no significant change was observed in ERG and SRPK1 expression, which suggests that exon 7b skipping in ERG did not change SRPK1 expression in the MG63 cell line. However there was, perhaps, a suggestion of an upward trend in SRPK1 expression.

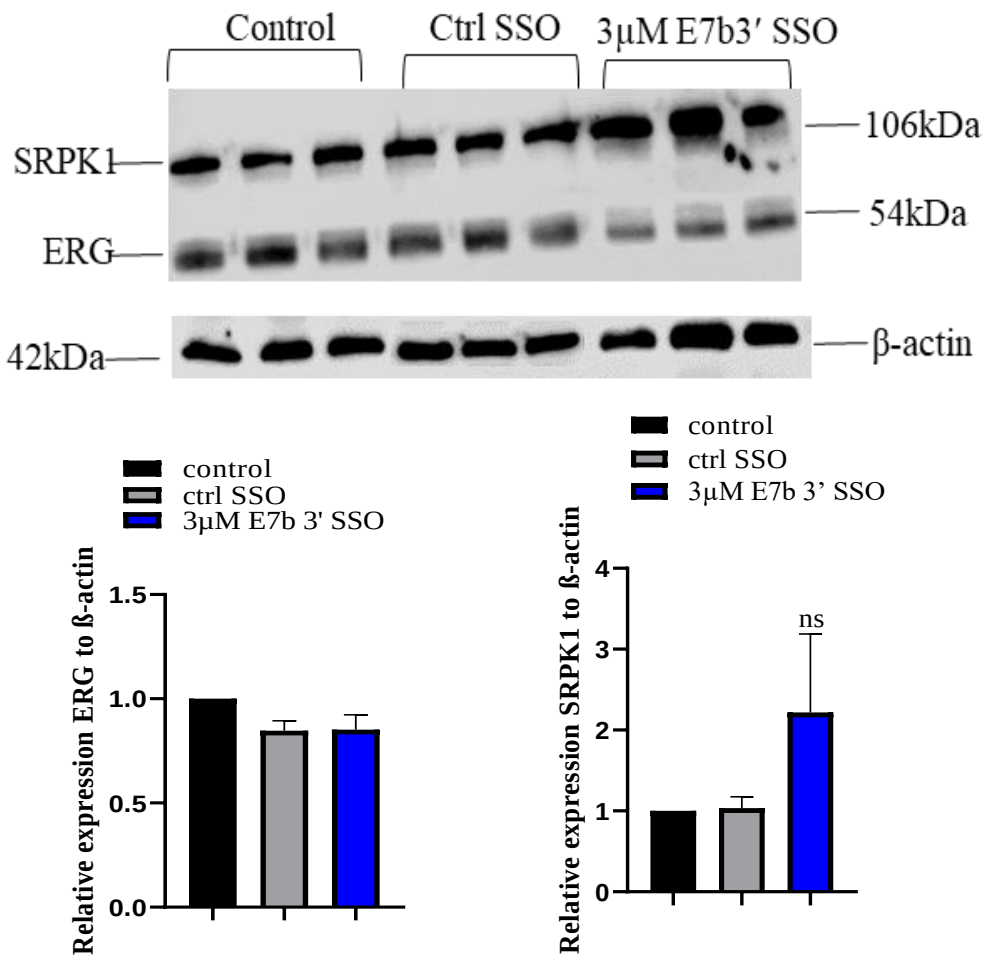

Figure 6.13: Effect of exon7b skipping on ERG and SRPK1 protein levels.

MG63 cells were transfected with 3μM of E7b 3′ SSO or control SSO for 72hrs. Cells were lysed and Western blot was performed. Membranes were blotted with anti-ERG and anti SRPK1 or beta-actin antibodies as a loading control. The graph represents relative expression determined by densitometric measurement of the bands and is expressed relative to actin. Bar-graph shown is the average of 3 independent experiments. No significant change was observed in ERG and SRPK1 levels using 1 way ANOVA test. Three independent repeats are shown in each case.

6.3.7 Effect of ERG overexpression on the alternative splicing of apoptotic factors *BCL2L1* and *caspase 9*

Several studies have described how downregulating endogenous ERG in cell lines that express it induces apoptosis. Birdsey *et al.*, 2008 for instance, has described that ERG inhibition by siRNA in HUVEC cells (ERG positive) resulted in the increased activation

of caspase 3 and 7. In a previous chapter of this study, SRPK1 inhibition leads to a significant increase in apoptosis. The data in the current part of the study suggest that ERG transcriptionally represses *SRPK1*. Thus, it was of interest to evaluate the effect of ERG overexpression in (ERG negative cells) on apoptotic markers e.g. *caspase* and *BCL2L1*. For that purpose, Caspases 3 and 7 staining was used to determine if overexpressing -7b and full-length ERG +7b is going to result in a change in the apoptotic activity in K562 and PC3 cell lines. (Figure 6.14) Shows that the activity of Caspase 3/7 detected by green detection reagent was significantly higher (****P<0.0001) in both cell lines where ERG has been overexpressed compared to the untransfected cells. This indicates that ERG overexpression induces apoptosis in K562 and PC3 cell lines (figure 6.14.A.B&C).

A

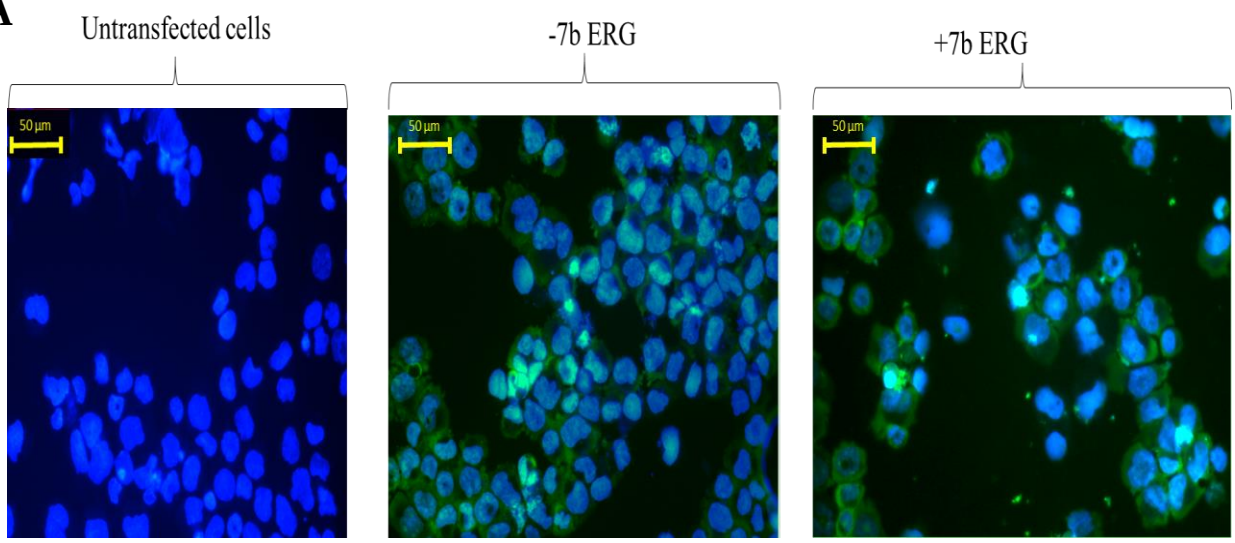

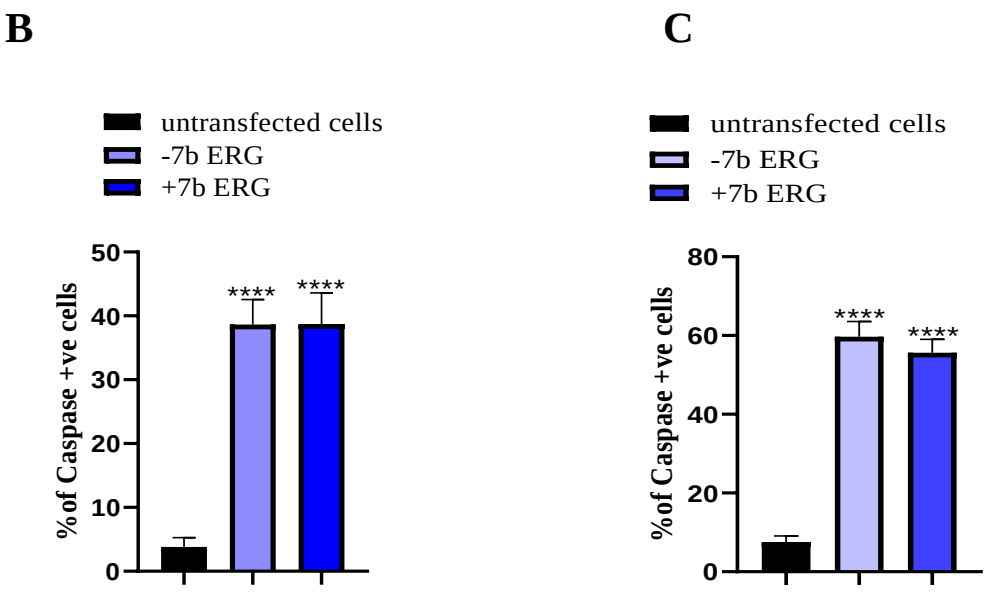

Figure 6.14: Caspase 3 and 7 staining in K562 and PC3 cells subjected to ERG overexpression.

K562 and PC3 cells were transfected with -7b and +7b full-length ERG isoforms expressing plasmids for 48 hours followed by Detection of active caspases 3 and 7 was performed using Caspase 3/7 Green Detection Reagent. **(A)** Representative images of stained K562 taken under a fluorescent microscope. The graph represents the number of active capase3/7 positive cells in K562 (B) and PC3 **(C)** cell lines which shows significance in the ratio of caspase activity in the cells after ERG overexpression, ****P<0.0001 using 1 way ANOVA test. n=9.

To further investigate the possibility of -7b and full-length ERG overexpression would result in any change in the splicing of other *caspase* family members such as *caspase-9* and another apoptotic factor such as *BCL2L1*, mRNA was extracted from the K562 and PC3 cells following -7b and +7b full-length ERG overexpression. Then a PCR was performed using the proper primers listed in table 2.6. (Caspase-9 NM_001229 and BCL2 like 1 (BCL2L1)xl NM_138578). PCR bands show that the splicing ratio (PSI-Ψ) of *caspase-9a/caspase-9b* mRNA was significantly higher in the ERG overexpression group compared to the control group while no significant change was observed in the

splicing ratio *Bcl-xl/Bcl-xs* in both cell lines (figure 6.15 & 6.17). In K562, (figure 6.15), the expression ratio (PSI-Ψ) *of caspase-9a/9b* isoform in the control was (0.57 PSI-Ψ), -7b isoform (0.82 PSI-Ψ) and +7b full-length ERG isoform (0.87 PSI-Ψ) (**P= 0.015 and ***= 0.0003 one way ANOVA). The expression ratio *caspase-9a/9b* isoform in the control was (0.44 PSI-Ψ) while in -7b isoform (0.80 PSI-Ψ) and full-length ERG isoform (0.83 PSI-Ψ) (**P= 0.0050 and **= 0.0032 one way ANOVA unpaired t-test) in PC3 cells (figure 6.16).

A

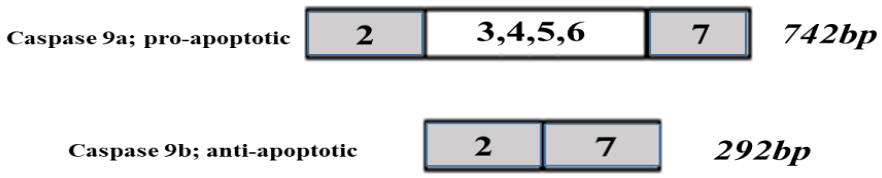

B

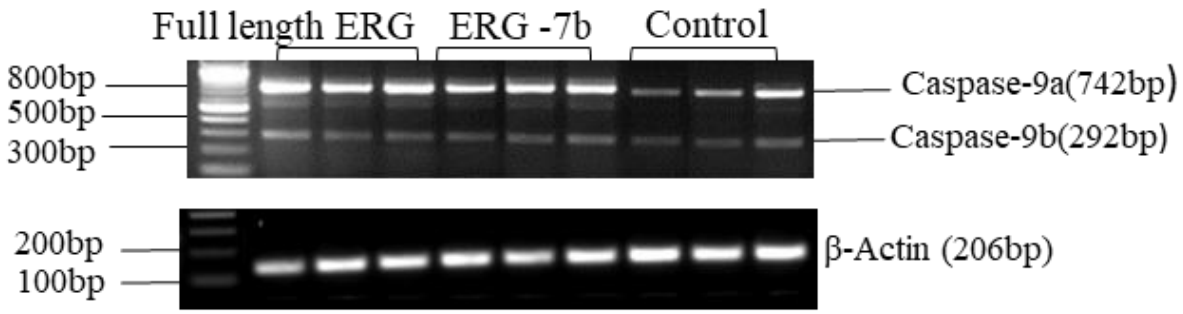

C

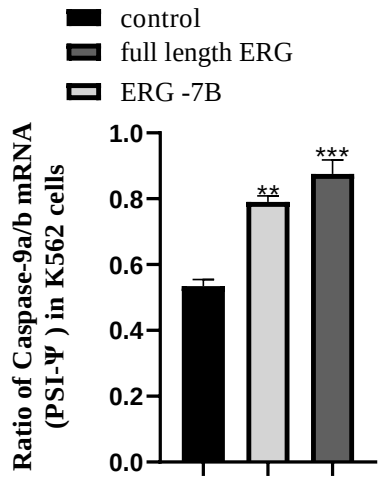

Figure 6.15: Caspase-9 mRNA levels in K562 cells where different ERG isoforms have been overexpressed.

K562 cells transfected with plasmids that express full-length ERG or ERG-7b isoforms for 48 hrs followed by RNA extraction and cDNA synthesis. PCR was performed using *Caspase-9* specific primers. (A) Representation of *Caspase-9* PCR amplicon sizes (B) and (C) showing band intensity and size and corresponding loading control, *β-actin*. Densitometry showing *caspase-9a/9b* PSI-Ψ values for 48hrs. The data suggests a significant change in splice ratio (PSI-Ψ) of *caspase-9* following ERG overexpression. P values were obtained using one way ANOVA test. *n*=3.

A

B

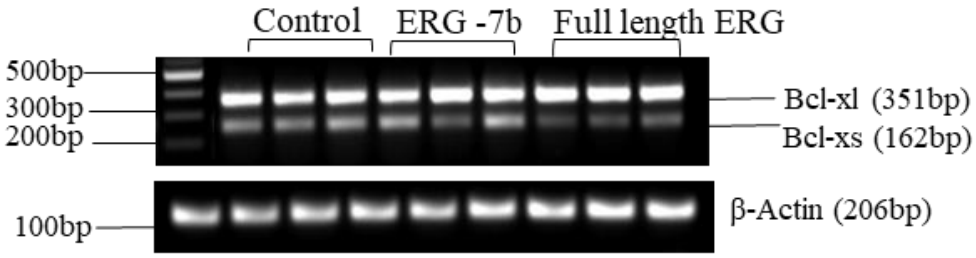

C

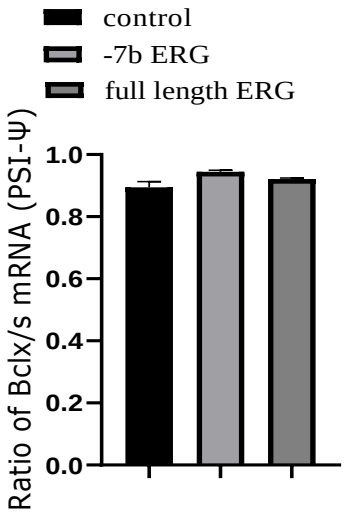

Figure 6.16: BCL2L1 mRNA levels in K562 cells where different ERG isoforms have been overexpressed.

K562 cells transfected with plasmids that express full-length ERG or ERG -7b isoforms for 48 hrs followed by RNA extraction and cDNA synthesis. PCR was performed using *Bcl* specific primers. **A**. Representation

of *Bcl* PCR amplicon sizes. (**B**) PCR gel at 48hrs showing band intensity and size and corresponding loading control, *β-actin*. **C**. Densitometry showing *Bcl-xl/s* PSI-Ψ values for 48hrs. The result shows no significant change in the splice ratio of *Bcl*. P values were obtained using one way ANOVA test. *n*=3.

A

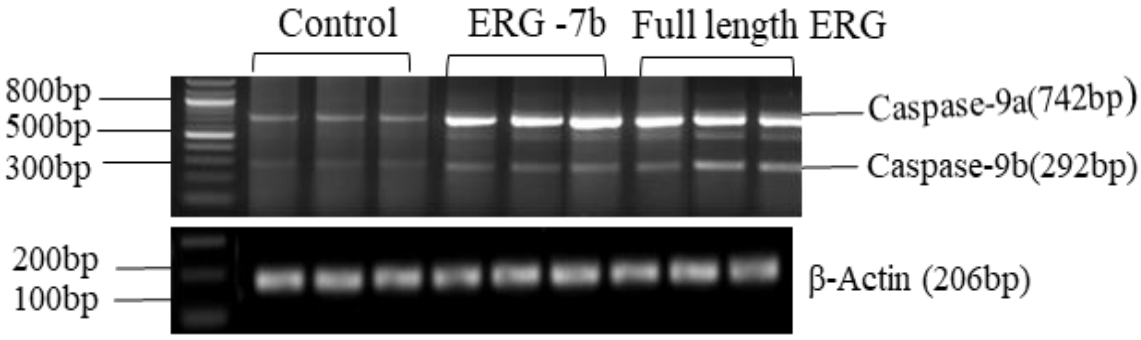

B

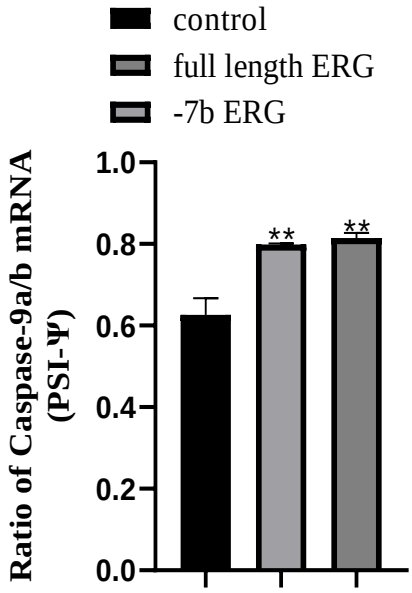

Figure 6.17: Caspase-9 mRNA levels in PC3 cells where different ERG isoforms have been overexpressed.

PC3 cells transfected with plasmids that express full-length ERG or ERG-7b isoforms for 48 hrs followed by RNA extraction and cDNA synthesis. PCR was performed using *Caspase-9* specific primers. **A**. and **B** showing band intensity and size and corresponding loading control, *β-actin*. Densitometry showing *caspase-9a/9b* PSI-Ψ values for 48hrs. The Result shows significance in splice ratio (PSI-Ψ) of *caspase-9* following ERG overexpression. P values were obtained using one way ANOVA test. *n*=3.

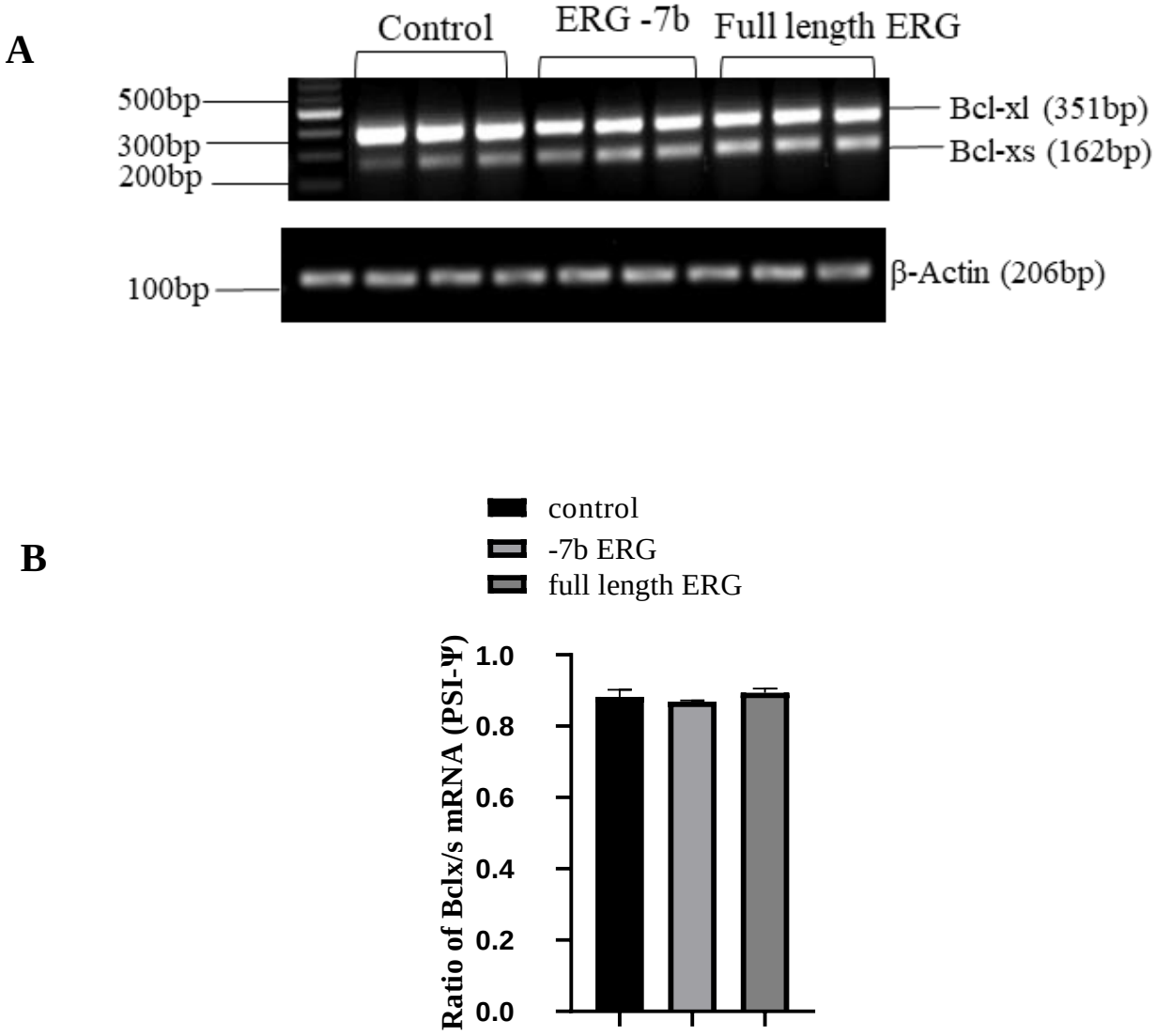

Figure 6.18: BCL2L1 mRNA levels in PC3 cells where different ERG isoforms have been overexpressed.

PC3 cells transfected with plasmids that express full-length ERG or ERG -7b isoforms for 48 hrs followed by RNA extraction and cDNA synthesis. PCR was performed using *BclX*-specific primers. (A) PCR gel at 48hrs showing band intensity and size and corresponding loading control, *β-actin*. (B) Densitometry showing *Bcl-xl/s* PSI-Ψ values for 48hrs. The result shows no significance (PSI-Ψ) in splice ratio of *Bcl*. *n*=3. No significant change was observed using one way ANOVA test.

6.3.8 The effect of *ERG* exon 4 skipping through splice switching oligonucleotides on the alternative splicing of apoptotic factors *BCL2L1* and *caspase* 9

Skipping of exon 7b of *ERG* mRNA is shown in Jumbe *et al.*, 2019 to induce apoptosis through increasing the activity of Caspase 3/7 activity in ERG positive VCaP prostate cancer cells. ERG inhibition by other means induced a similar effect in HUVEC cells (Birdsey *et al.*, 2008). In the previous section, exon 4 skipping in *ERG* mRNA resulted in the reduction of ERG protein and therefore, upregulation of SRPK1. Here we examine the effect of skipping of exon 4 on apoptotic markers e.g. *caspase* and *BCL2L1* in MG63 cells (ERG positive cells). For that purpose, caspases 3 and 7 staining was used to determine if exon 4 skipping is going to result in a change in the apoptotic activity in MG63 cell line. (Figure 6.19) Shows that the activity of Caspase 3/7 was significantly higher (****P<0.0001) in MG63 cell line where ERG expression has been diminished by exon 4 skipping compared to the untransfected cells. This indicates that ERG inhibition induces apoptosis in MG63 cell line.

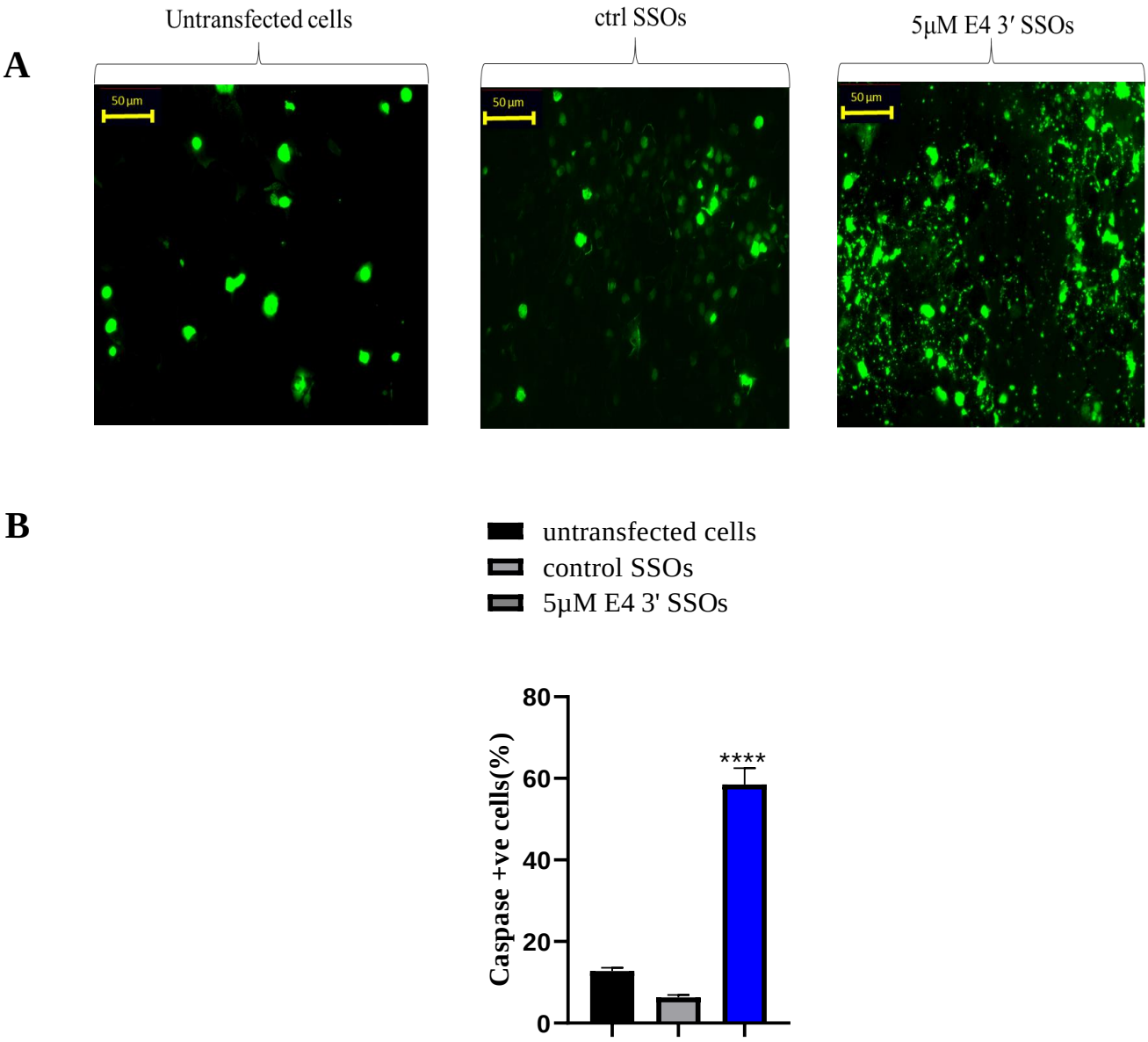

Figure 6.19: Caspase 3 and 7 staining in MG63 cells where ERG has been knocked down by E4 3′ SSOs.

Cells were transfected with 5µM E4 3′ SSOs for 72hrs followed by detection of active caspases 3 and 7 was performed using the caspase 3/7 Green Detection Reagent. (A) Representative Images of the stained MG63 cells taken under a fluorescent microscope. (B) The graph represents the percentage of caspase 3/7 positive cells in MG63 which show significance in the ratio of caspase activity in the cells after exon 4 skipping in *ERG*, ****P<0.0001 using one way ANOVA test. n=9

To further investigate the possibility of exon 4 skipping would result in any change in the splicing of other caspase family members such as *caspase-9* and another apoptotic factor such as *BCL2L* , mRNA was extracted from the MG63 cells following exon 4 skipping SSOs transfection at 1 or 5μM E4 3′ SSOs. Then a PCR was performed using the primers listed in table 2.6. PCR bands show that the splicing ratio (PSI-Ψ) of *caspase-9a/caspase-9b* mRNA was significantly higher in the exon 4 skipping group at 5μM compared to the control group and 1μM while no significant change was observed in the splicing ratio *Bcl-xl/Bcl-xs* in MG63 cells (figure 6.20). (Figure 6.20) shows the expression ratio (PSI-Ψ) of *caspase-9a/9b* isoform in the control was (0.55 PSI-Ψ), control SSOs (0.57 PSI-Ψ), 1μM E4 3′ SSOs (0.60 PSI-Ψ) and 5μM E4 3′ SSOs (0.74 PSI-Ψ) (*P= 0.0014 one way ANOVA).

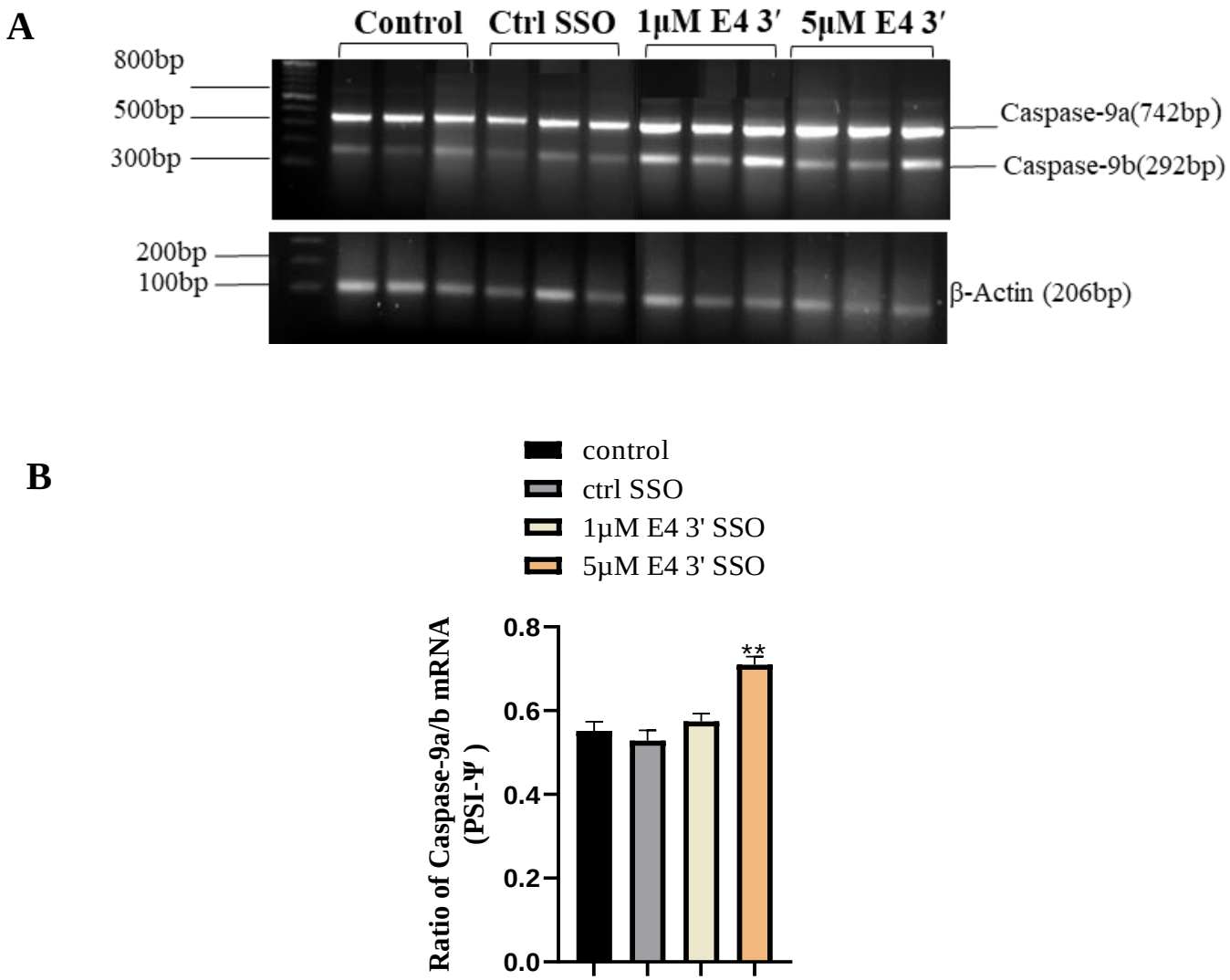

Figure 6.20: Caspase-9 mRNA levels in SSOs transfected MG63 cells.

MG63 cells transfected with (1 and 5µM) of E4 3′ SSOs or ctrl SSOs for 48hrs. Untransfected cells were used as control. RNA extraction and cDNA synthesis were performed following transfections. PCR was performed using *caspase-9* specific primers. **(A)** Showing band intensity and size and corresponding to the loading control, *β-actin*. **(B)**. Densitometry showing *caspase-9a/9b* PSI-Ψ values for 48hrs. The result shows significance in splice ratio of *caspase-9* when transfected with 5µM of E4 3′ SSOs. *P= 0.0014 one way ANOVA. *n*=3.

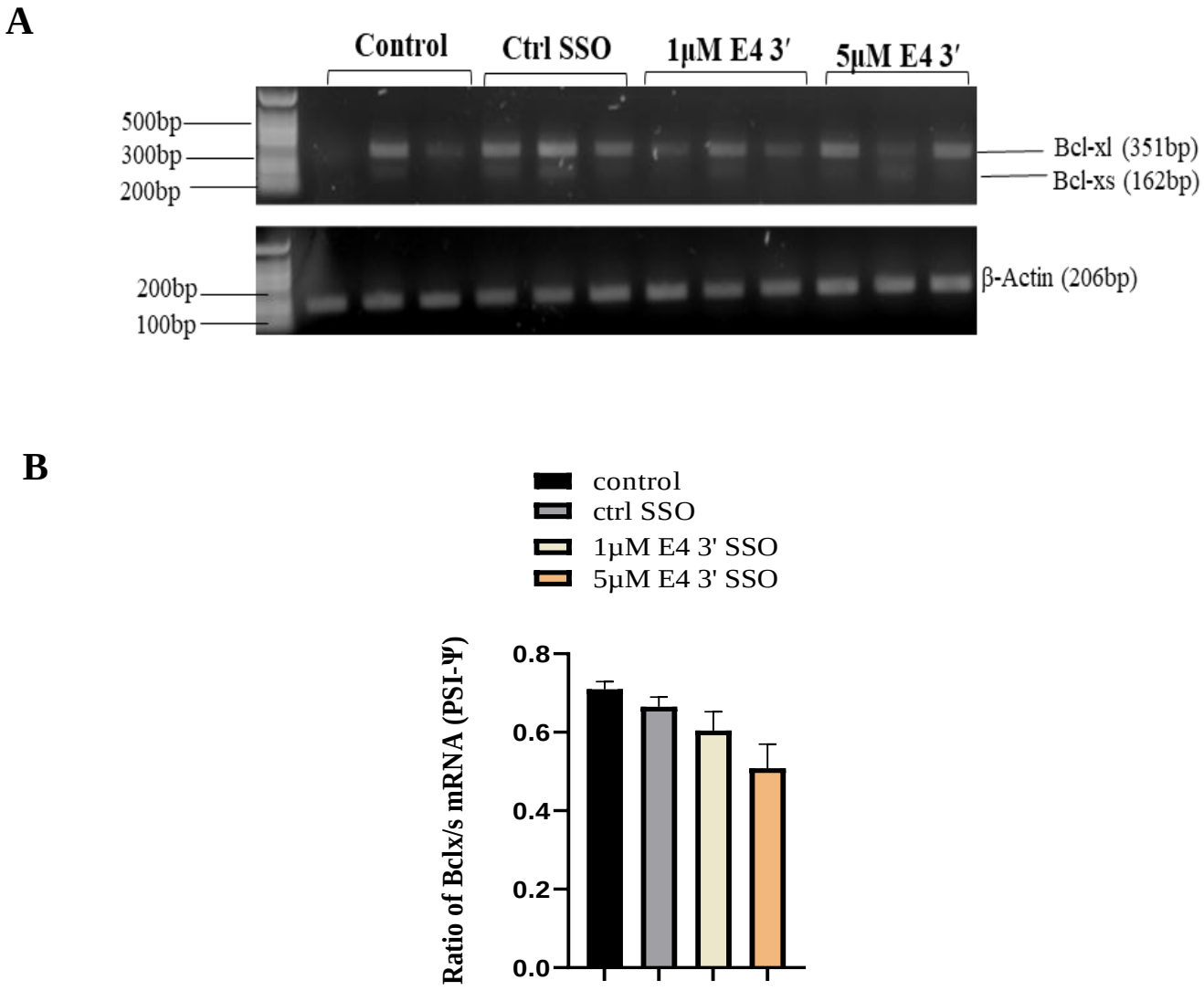

Figure 6.21: BCL2L1 mRNA levels in SSOs transfected MG63 cells.

MG63 cells transfected with (1 and 5μM) of E4 3′ SSOs or ctrl SSOs for 48hrs. Untransfected cells were used as control. RNA extraction and cDNA synthesis were performed following transfections. PCR was performed using *Bcl* specific primers. (**A**) PCR gel at 48hrs showing band intensity and size and corresponding loading control, *β-actin*. **B**. Densitometry showing *Bcl-xl/s* PSI-Ψ values for 48hrs. The result shows no statistically significant change in the splice ratio of *Bcl*.*P= 0.0014 one way ANOVA. *n*=3.

6.3.9 Effect of ERG overexpression on cell proliferation and viability

The data described in this chapter suggests that ERG is repressing the transcription of SRPK1. ERG has been described as driving cellular proliferation In PCa cell line VCaP (ERG positive), cellular proliferation and viability were decreased following an ERG knockdown (Liu *et al.*, 2016). In this part of the study, the effect of ERG overexpression on cellular proliferation and viability of K562 and PC3 cells was investigated. For this purpose, -7b and +7b full-length ERG isoforms expressing plasmids were used to overexpress ERG followed by MTT assay. A significant reduction in cellular proliferation and viability occurred 48 h after ERG overexpression in both cell lines. (Figure 6.22.A) shows the significant effect of -7b (*P= 0.0118) and full length +7b ERG (**P=0.0057) overexpression on cellular proliferation and viability of K562 cells (Figure 6.22.C, ****P<0.0001 and ***P= 0.0366 for -7b and full length ERG respectively). For PC3 cells, (Figure 6.22.B), a significant reduction in cellular proliferation (**P=0.0025 and = 0.0048 for -7b and+7b full length ERG respectively) and viability (Figure 6.22.D) (*P=0.0219 and *P= 0.061 for -7b and full length ERG respectively) was observed. Taken together, the results indicate that ERG overexpression in K562 and PC3 cell lines (ERG negative) resulted in a reduction in cellular proliferation and viability.

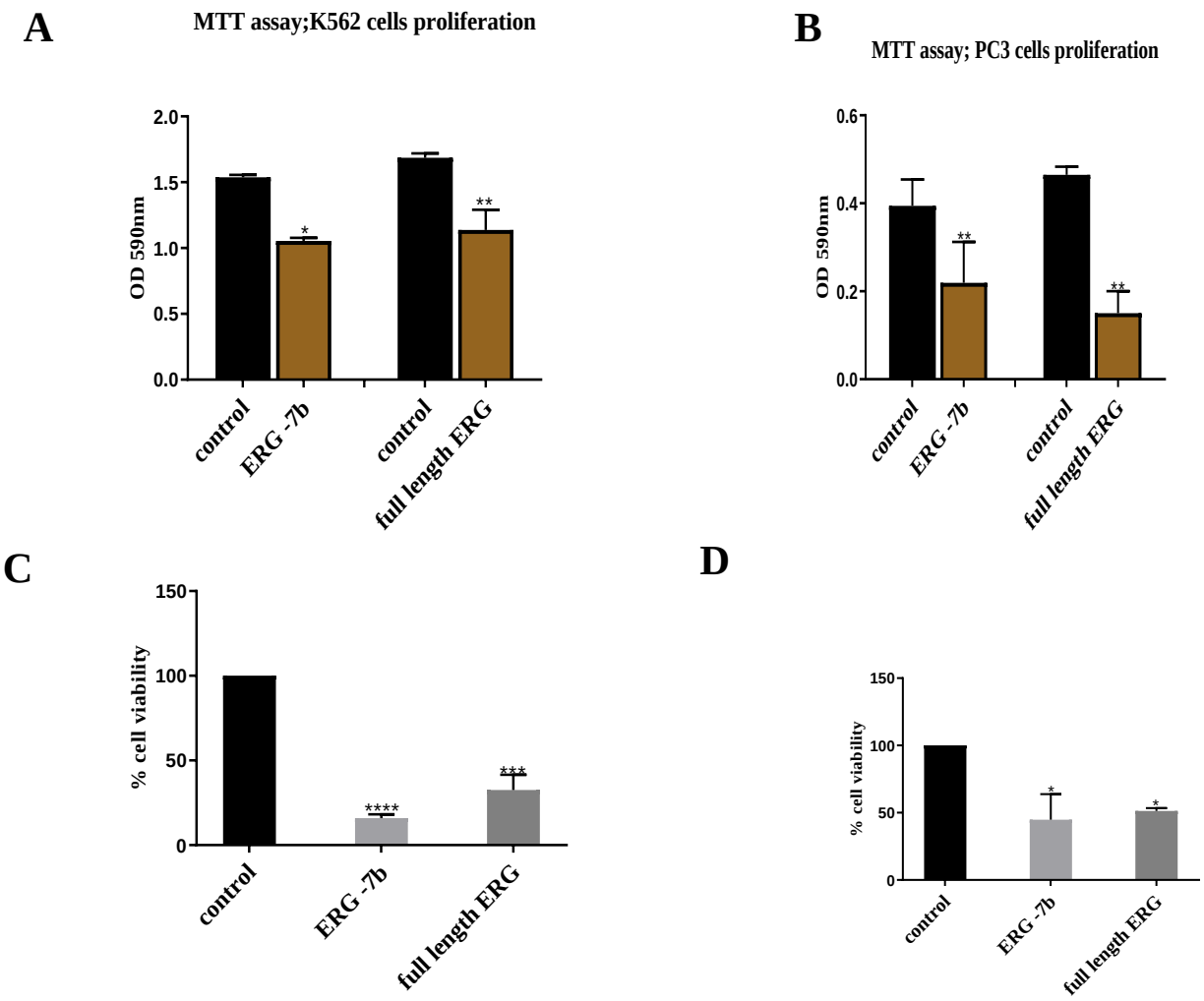

Figure 6.22: Cellular proliferation and viability in K562 and PC3 cells after overexpression of ERG isoforms.

MTT assays were used to analyse the effect of -7b and full length +7b ERG overexpression for 48hrs on the cellular viability **(C&D)** and proliferation **(A&B)** in K562 and PC3 cells. The absorbance (optical density; OD) of each well was measured at 590 nm using a plate reader. Results represent the mean ± SEM of three experiments and are presented as a bar graph after normalizing to the respective controls. Cell viability = control- absorbance of treatment wells/absorbance of control well ×100%. P values were obtained using one way ANOVA test.

6.3.10 Effect of splice switching oligonucleotides and ERG knockdown on MG63 cells proliferation and viability

Skipping of exon 7b reduces cell proliferation (Jumbe *et al.*, 2019) while other studies have described how downregulation of ERG resulted in the similar effect on ERG expressing cell lines (Liu *et al*., 2016 and Klezovitch *et al.*,2008). Therefore, the effect of ERG downregulation and exon 7b skipping on cellular proliferation and viability was investigated in the MG63 cell line. An MTT assay was performed following transfection with ERG siRNA, control SSOs, E4 SSOs and E7b SSOs. Figure 6.23 shows how ERG downregulation using siRNA and E4 SSOs as well as skipping of exon 7b resulted in a reduction in cellular proliferation and viability of the MG63 cells compared to the control SSOs and the untreated groups. Figure 6.23. A Shows a significant reduction in MG63 proliferation (*p= 0.0153, ***p=0.0005 and **p=0.0056) for siRNA ERG, 7b and E4 SSOs respectively. Figure 6.23. B shows a significant reduction in MG63 viability (*p=0.0153,*p= 0.0420 and **p= 0.0086) for siRNA ERG, 7b and E4 SSOs respectively. These findings suggested that overall ERG downregulation, as well as the skipping of exon 7b, affected proliferation and cell viability in MG63 cells.

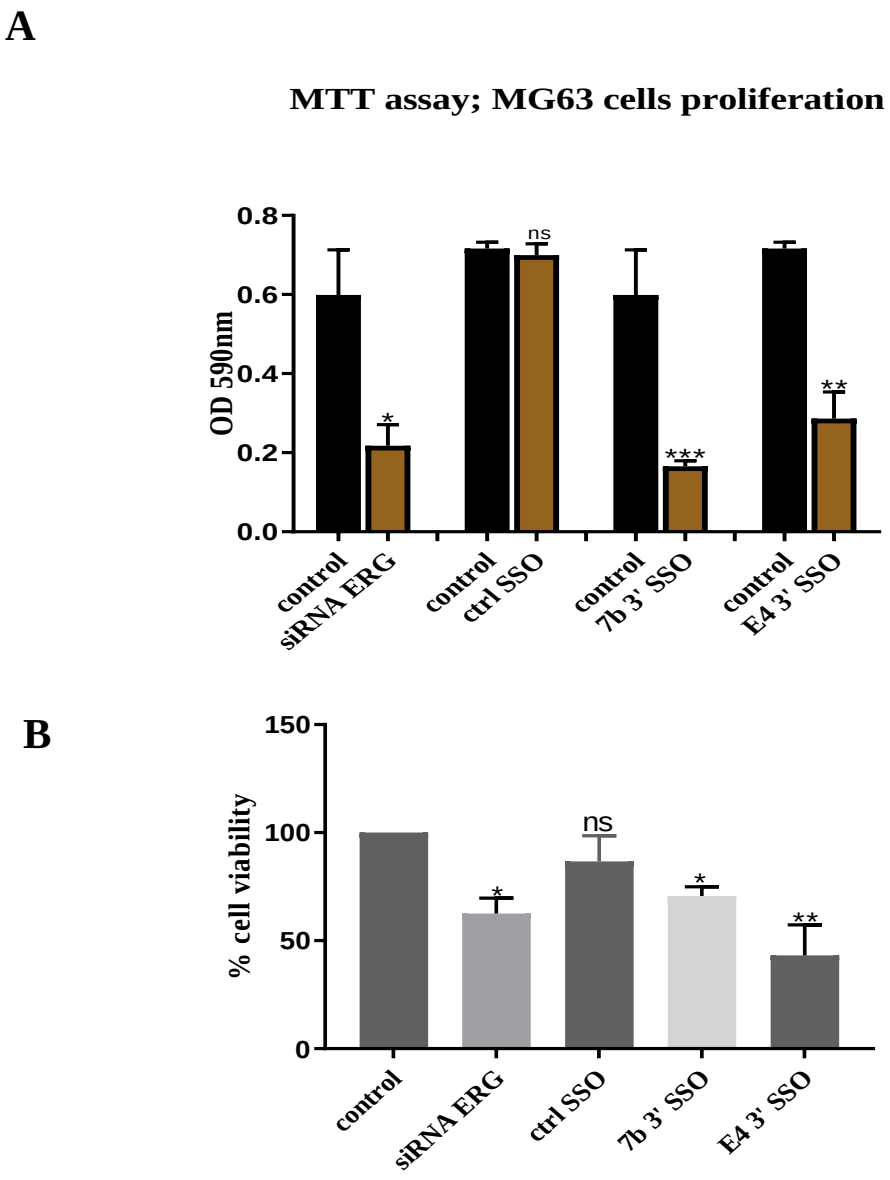

Figure 6.23: Cellular proliferation and viability in MG63 cells transfected with siRNA ERG and splice switching oligonucleotides.

MTT assays were used to analyse the effect of 7b 3′ or E4 3′ or control SSOs or 100nM ERG siRNA transfections for 48hrs on the cellular proliferation (A) and viability (B) in MG63 cells. The absorbance of each well was measured at 590 nm using a plate reader. Results represent the mean ± SEM of three experiments and are presented as a bar graph after normalizing to the respective controls. Cell viability = control- absorbance of treatment wells/absorbance of control well ×100%. P values were obtained using one way ANOVA test.

6.3.11 Effect of ERG inhibition on cell migration and invasion

ERG, which is a major oncogene, plays an important role in cellular migration and invasion. The migration and invasion of VCaP cell lines were remarkably reduced following siRNA knockdown of ERG (Liu *et al.,* 2016). In this study, the effect of ERG inhibition on MG63 cellular migration and invasion was measured. For that purpose, transwell migration and invasion assay were carried out following transfection with siRNA against ERG or E4 SSOs. (Figure 6.24) shows a significant difference in the number of migrating and invasive (Figure 6.25) MG63 cells following the downregulation of ERG compared to un-transfected cells groups (**** $p < 0.0001$). The outcome of this experiment demonstrates how ERG knockdown causes a significant decrease in MG63 migration and invasive capacity.

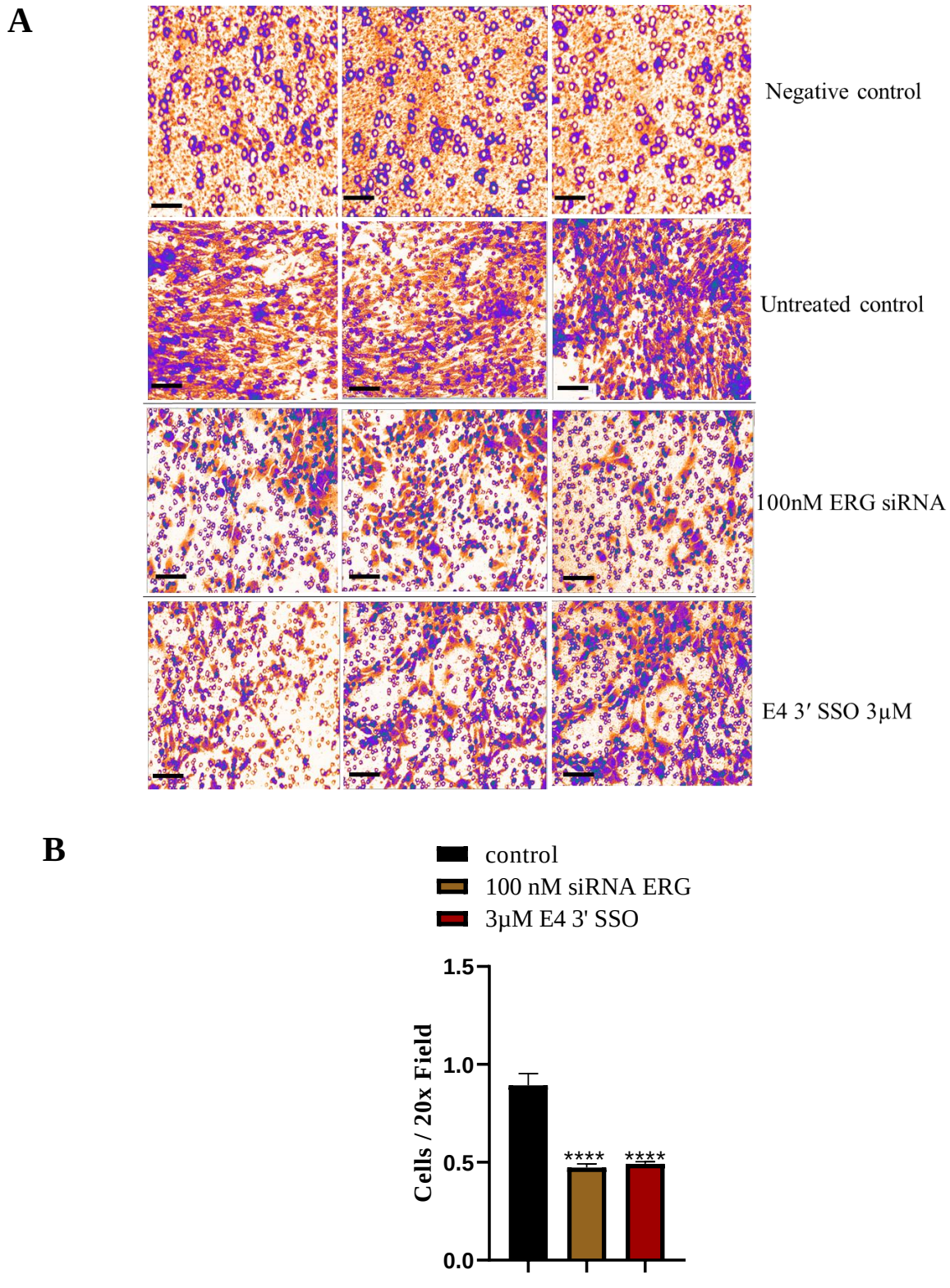

Figure 6.24: Transwell migration assay of MG63 cells.

MG63 cells transfected with 3µM E4 3′ SSO or with 100nM ERG siRNA for 48hrs. A. Representative images of MG63 cell transwell migration. After cell migration and staining with crystal violet, pictures of

the migrated cells (orange stained) were taken using a microscope with a 10x objective. (B) Quantification of cells migrating toward the FBS sublimated medium (Average of 5 picture fields at 100x total magnification). ****P=0.0001 using one way ANOVA test. Three independent repeats are shown in each case.

A

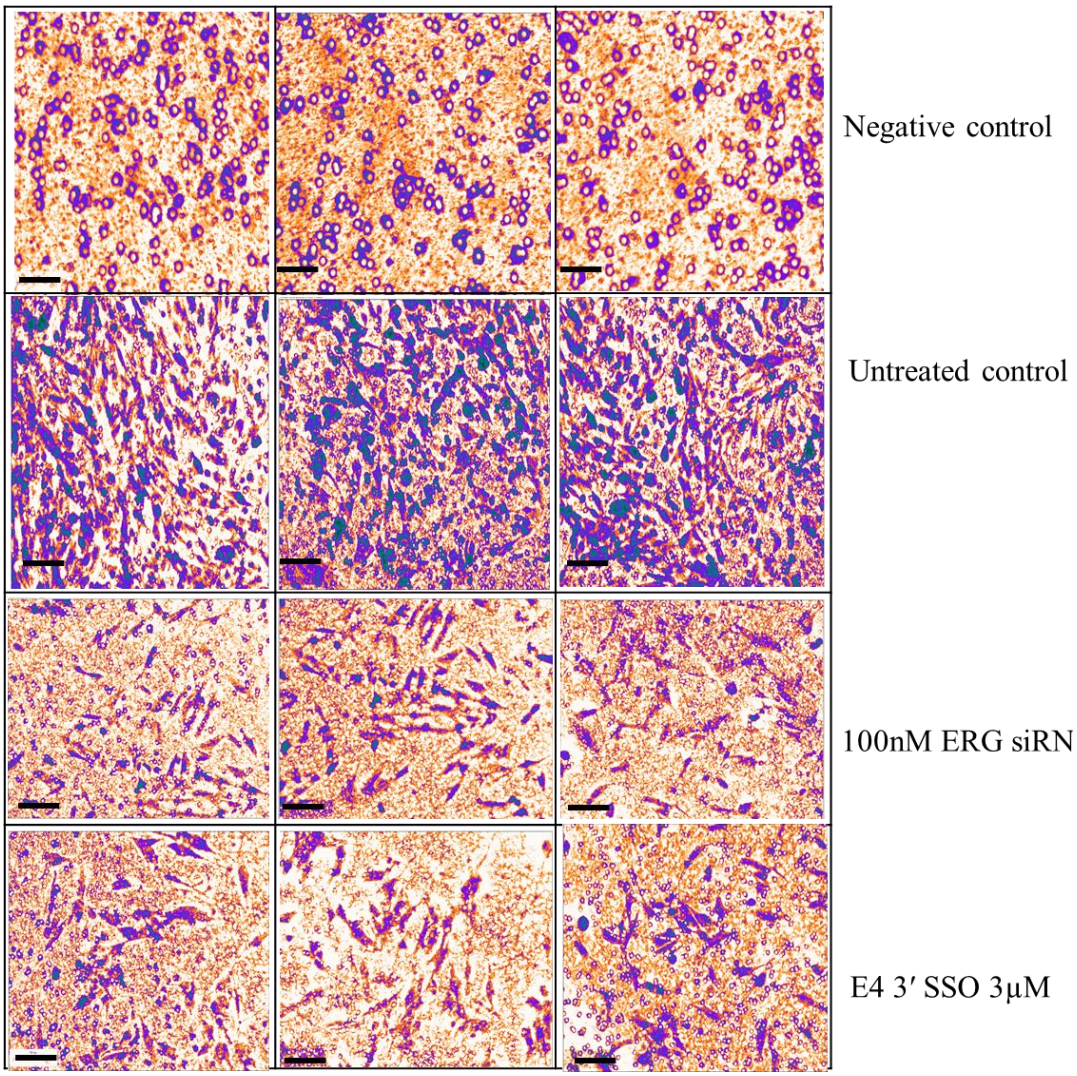

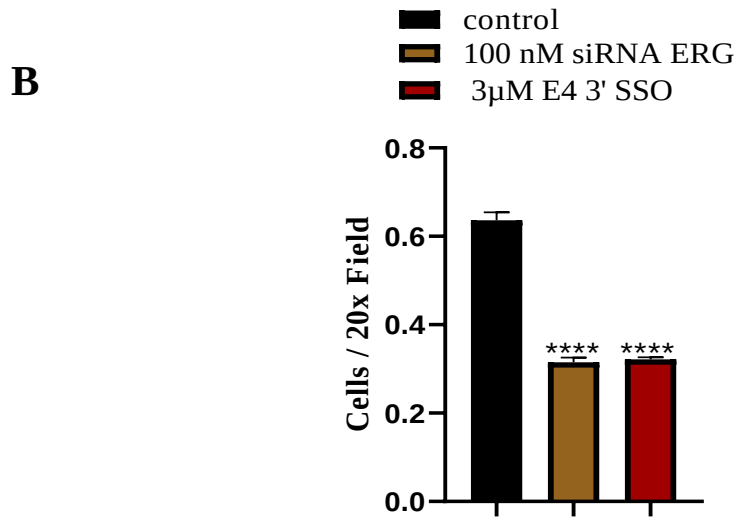

Figure 6.25: Transwell cell invasion assay of MG63 cells.

MG63 cells transfected with 3µM E4 3′ SSO or with 100nM ERG siRNA for 48hrs. **A**. Representative Pictures of MG63 cell transwell invasion. The transwell membrane was coated with Matrigel and then the cell- Serum-free medium was added on top of the Matrigel. After cell invasion and staining with crystal violet, pictures of the migrated cells (orange stained) were taken using a microscope with a 10x objective. (**B**) Quantification of invasive cells moving toward the FBS sublimated medium (Average of 5 picture fields at 100x total magnification). ****P=0.0001 using one way ANOVA test. Three independent repeats are shown in each case.

6.3.12 Cancer Cell Line Encyclopaedia comparison

All the findings in this study suggest that WT1, BASP1 and ERG are involved to some degree in regulating SRPK1. WT1 activates SRPK1 in the absence of BASP1. ERG, on the other hand, was shown to repress SRPK1. That raised the question about the levels of gene expression of *SRPK1* related to the expression of *WT1*, *BASP1* and *ERG*. Through RNA sequencing database available in in the expression atlas website (https://www.ebi.ac.uk/gxa/experiments/E-MTAB-2770/Results) (Expression, 2009), a simple comparison was made to show the expression levels of these genes in K562, PC3 and MG63 cell lines. Transcripts per million (TPM) is an RNA-seq metric unit that should be read as "for every 1,000,000 RNA molecules in the RNA-seq sample, x came from this gene/transcript." which reflect the levels of RNA molecules (Arrayserver.com, 2016). Results show that in K562, *BASP1* is totally absent whereas *WT1* is higher than it is levels in PC3 cells where *BASP1* is partially expressed. *SRPK1* is the highest in K562 compared to MG63 and PC3 cell lines and this could be due to the absence of *ERG*. In PC3 cells, a low level of *BASP1* is detected while *WT1* is very low and *SRPK1* present at low levels. *ERG* is expressed in the MG63 cell line where the expression of *BASP1* is the highest compared to K562 and PC3 cells, *WT1* was not detectable in MG63 cells while *SRPK1* is moderately expressed. Figure (6.26).

A **TPM values of RNA-seq of SRPK1, WT1, BASP1 and ERG in K562, PC3 and MG63.**

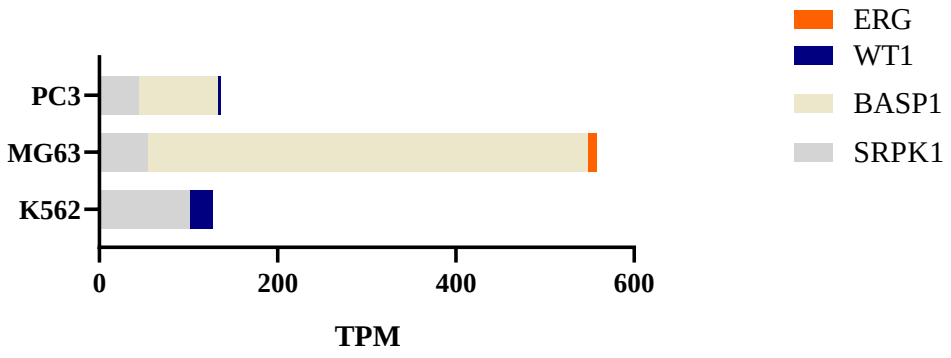

B

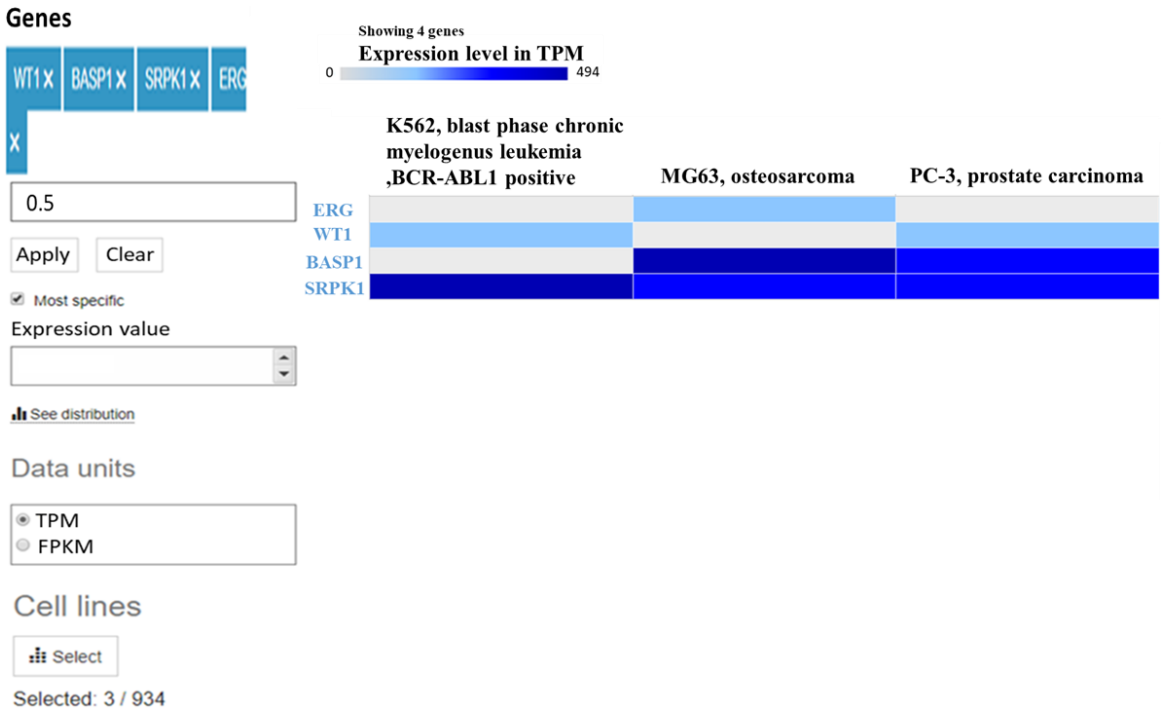

Figure 6.26: Comparison of RNA-seq

(A). graph of the Transcripts per million (TPM) values of RNA-seq of *SRPK1*, *WT1*, *BASP1* obtained from encyclopaedia report. (B) Cancer Cell Line Encyclopaedia report. Comparison between *SRPK1*, *WT1*, *BASP1* and *ERG* expression in K562, PC3 and MG63.

6.4 Summary

ERG expression is not prominent in K562 and PC3 cells; therefore, MG63 cells were the cell line of choice since they express ERG. ERG is a well-established transcription factor, and here we show that it binds to the *SRPK1* promoter and regulates *SRPK1* transcription. ChIP analysis confirmed that ERG associates with the *SRPK1* promoter (fig.6.2). Through overexpressing the full-length ERG using a plasmid construct, ERG was found to repress the transcription of SRPK1in K562, PC3 and MG63 cell lines (fig.6.3).

Moreover, full-length ERG, including both isoforms (+/- exon 7b), were shown to reduce the transcription of *SRPK1* as measured by the luciferase reporter, and also its expression at a protein level. A remarkable reduction in the activity of *SRPK1* promoter following the overexpression of (+/- 7b) ERG isoforms was observed in K562 and PC3 (fig.6.4) cells. Furthermore, western blots showed a significant reduction in SRPK1 following ERG overexpression in both cell lines (fig.6.5).

To further investigate *SRPK1* regulation by ERG, siRNA-mediated ERG knockdown combined with DLR assay was performed. The siRNA knockdown of ERG resulted not only in a reduction of ERG expression at a protein level (fig.6.6) and restored *SRPK1* promoter activity (fig.6.7).

For the purpose of learning more about the effect of ERG on SRPK1 expression, SSOs that alter the splicing of *ERG* mRNA were tested. SSOs that induce exon 4 skipping in the *ERG* mRNA were shown to switch the splicing of *ERG* at the mRNA level (fig.6.8). This particular splice switch diminishes the ERG protein expression by inducing a premature stop codon, and therefore the E4 3′ SSO combined with a DLR showed a significant increase in *SRPK1* promoter activity (fig.6.9). Moreover, following exon 4

skipping, western blot showed a reduction in ERG levels combined with a significant increase in SRPK1 expression (fig.6.10). Another SSO that induces cassette exon 7b skipping was tested. E7b 3′ SSO caused successful skipping of exon 7b in *ERG* mRNA (fig.6.11) but had no significant effect on SRPK1 expression (other than perhaps a marginal increase at the protein level) (fig.6.12 &13).

ERG is also implicated in the regulation of genes that are important for several biological functions of the cells. Genes that are involved in apoptosis are affected by ERG expression. For example, Caspase 3 and 7 activity was shown to increase following the overexpression of ERG isoforms in K562 and PC3 cells (fig.6.14). This was combined with a modest splicing switch favouring the pro-apoptotic *caspase-9a* isoform in both cell lines (fig.6.14, 15&17). Skipping of exon 4 in MG63 cells induced a similar effect on the activity of caspases 3 and 7(fig.6.19) and the alternative splicing of *caspase-9* (fig.6.20).

The overexpression, inhibition and E7b skipping of *ERG* seemed to impact cellular proliferation and viability. A significant reduction in proliferation and viability of K562 and PC3 cells was observed following ERG overexpression (fig.6.22). A similar effect was also observed in MG63 cells following exon 7b skipping and the inhibition of ERG with siRNA and E4 SSOs (fig.6.23).

MG63 cell migration and invasion seemed also to be influenced by exon 7b skipping and the inhibition of ERG with siRNA and E4 SSOs. A significant reduction in the migration and invasion of the MG63 cells was observed following ERG inhibition and exon 7b skipping (fig.4.24&25).

This thesis is focused on gaining a better understanding of the regulation of SRPK1. The main finding is that WT1 is activating SRPK1; it is then surely not coincidental that SRPK1 levels are the highest where WT1 is well expressed in K562 cells. The same is

noticeable in PC3 cells where there is a detectable amount of BASP1, which is a WT1 co-suppressor, and perhaps that ties in with lower SRPK1 levels compared to K562. However, in most genes multiple transcription factors, and also epigenetic effects combine to determine the extent to which a gene is switched on, and so the picture is complicated. To complicate the picture, evidence presented here suggests that the oncogene ERG surprisingly represses SRPK1. Consistent with this observation, *SRPK1* levels are lower in MG63 where *WT1* is absent and *ERG* is expressed (fig.6.26). If ERG is an oncogene, why does it repress SRPK1? The answer is likely linked to the fact that the oncogenic properties of any gene are relative to the context in which they operate. Perhaps in these cell lines, the set of co-factors that, presumably, cooperate with ERG, make it repress SRPK1. It is conceivable, that as is the case with WT1, in other contexts ERG might activate SRPK1 transcription. Further research will address these questions; what seems clear, is that both WT1 and ERG can contribute significantly to the transcriptional regulation of SRPK1.

The findings in this study suggest that both the transcription factor WT1 and the co-repressor BASP1 are present on the *SRPK1* promoter region. WT1 activates SRPK1 transcription however, this activation is prevented by the co-repressor BASP1 (fig.6.27 A&B). The transcription factor ERG was also shown to bind to the *SRPK1* promoter and represses its transcription. Yang *et al*., 2003 described that ERG represses the transcription of its target genes through interacting with HDAC. ERG may repress SRPK1 transcription through a similar mechanism (fig.6.27 C).

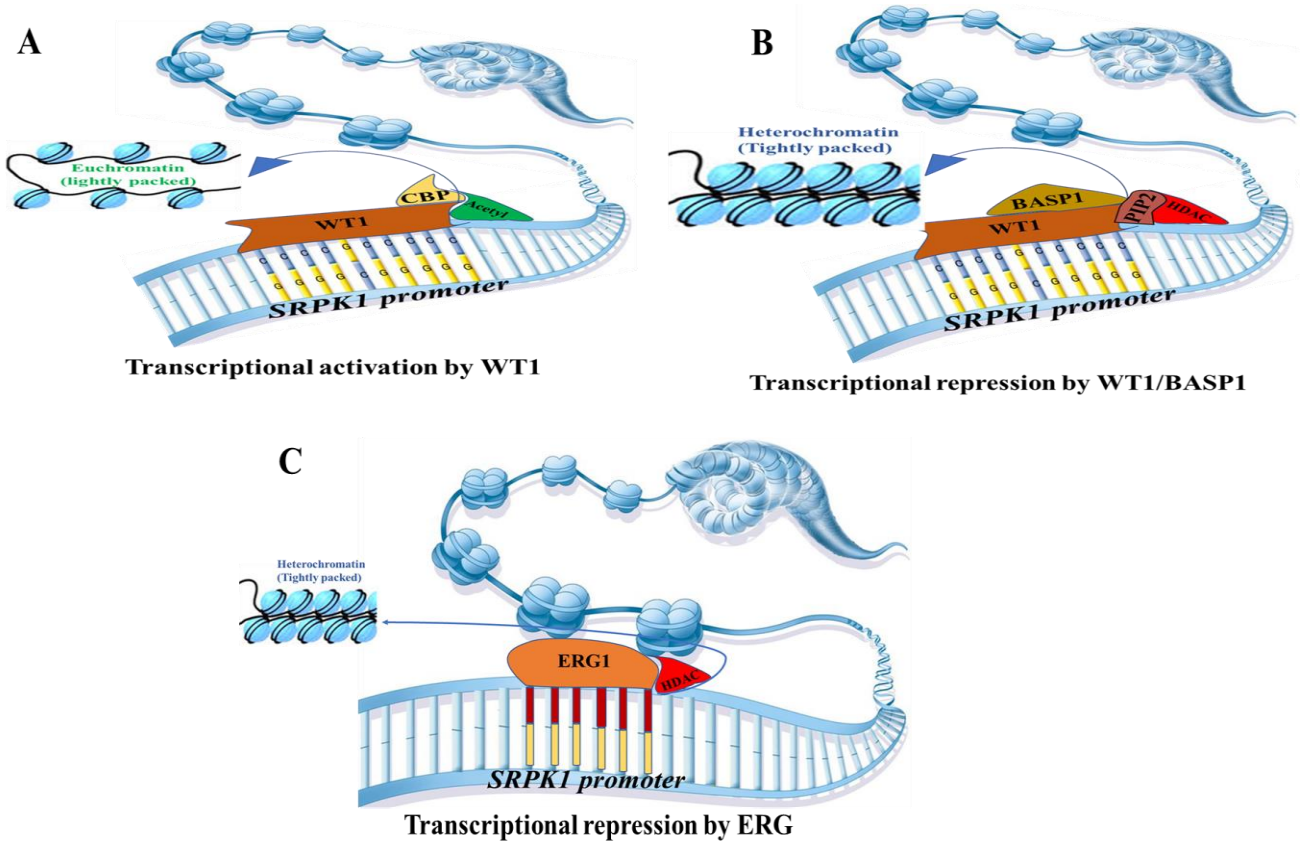

Figure 6.27: Transcriptional regulation of SRPK1.

A schematic of the model of the human SRPK1 transcriptional regulation by WT1, BASP1 and ERG. (A) WT1 binds to its putative binding site (GGGGCGGGGG) on the SRPK1 promoter and activate SRPK1 transcription. WT1 stimulates the transcription of its target genes via the recruitment of CBP (CREB binding protein), resulting in histone acetylation which relaxes the chromatin (Euchromatin) and activates transcription. (B) BASP1 forms a complex with WT1 and initiate the dissociation of CBP and the recruitment of HDAC1 (Histone Deacetylase) resulting in deacetylation of histones which condenses the chromatin (Heterochromatin) and subsequently represses SRPK1 transcription. PIP2 (phosphatidylinositol 4, 5 bisphosphate) facilitates the recruitment of HDAC. (C) ERG interacts with the SRPK1 promoter and represses SRPK1 transcription by interacting with HDAC and the formation of heterochromatin.

7 Chapter seven: General Discussion and future work

7.1 Discussion

7.1.1 Detection of the SRPK1a splice isoform and a potential autoregulatory loop

Despite its increasing profile and a growing body of literature on SRPK1, very little is known about how its expression is regulated. We began by looking at a potential splice isoform of SRPK1. The *SRPK1a* splice isoform has previously been described and detected in K562 leukaemia cells. Research by Sanidas *et al.*, 2010, suggests that SRPK1a associates with ribosomes in K562-SRPK1a cells, thereby suggesting that the kinase may have an active role in ribosome function and/or structure. The patterns of expression of SRPK1a in normal tissues has not been examined; its physiological significance remains unclear. Here, an attempt was made to detect the *SRPK1a* splice isoform in a range of cell lines. However, it could not be detected. It is conceivable that *SRPK1a* is expressed at very low levels, or perhaps the *SRPK1a* transcript adopts a loop structure at the RNA level, with extended double-stranded domains (E.Nikolakaki, unpublished observations) resulting in poor detection by Northern and RT-PCRs. It is also possible that in addition to SRPK1a, SRPK1 expresses additional splice isoforms; but none have been reported so far in the literature (Sanidas *et al.*, 2010). It is possible that SRPK1a might play several additional roles that yet to be identified once it extensively investigated but as we failed to detect it, we focused on canonical, full-length SRPK1.

The aim of this study was to gain a better understanding of how SRPK1 is regulated at the transcriptional level and this will be addressed later in the discussion. Here it is worth mentioning that evidence was found that SRPK1 might regulate its own expression via a

feedback loop, much like the splice factor kinase CLK1 does (Uzor *et al*., 2018). SPHINX-mediated inhibition of SRPK1 appeared to repress the transcription and the protein level of SRPK1, whereas the knock-down of SRPK1 using siRNA seemed to reduce only protein levels rather than transcription Thus SPHINX is inhibiting the enzyme and somehow this results in a feedback loop changing the expression of SRPK1. SRPK1 is not a transcriptional regulator; it is an enzyme that phosphorylates splicing factors but of course could be having an indirect effect because it is changing the alternative splicing of other potential SRPK1 regulators. Despite the amount of research on SRPK1 in a variety of contexts, there has not been a previous report of this effect. The extent to which SRPK1, like CLK1, might influence its own regulation, will be further investigated in future research.

7.1.2 Effect of SRPK1 inhibition with SPHINX on alternative splicing of VEGF-A, *BCL2L1 x and caspase-9*

SRPK1 plays an important role in the phosphorylation of SR proteins which are involved in the regulation of alternative splicing in development and disease. The ability of SRPK1 to influence the activity of splice factors is critical in multiple cellular pathways, including the regulation of angiogenesis. Angiogenesis is a vital process through which tumours form blood vessels and attain essential nutrients. Nevertheless, tumours can be very heterogeneous in their metabolism hence their dependency on nutrients and oxygen as some of the most aggressive tumours survive and proliferate with minimal energy supplies (Hanahan D *et al.*, 2011). In the context of angiogenesis, SRPK1 has been shown to phosphorylate the splice factor SRSF1 which then promotes the expression of the pro-angiogenic splice isoform of *VEGF-A*.

The alternative splicing of VEGF-A was shown to be affected by inhibition of SRPK1 in numerous studies. For instance, Mavrou *et al.,* 2014 has shown that by making a stable SRPK1 knockdown with shRNA, an increase in anti-angiogenic VEGF165b at the protein level was observed in PC3 cells. Through SRSF1, SRPK1 has been described in (Amin *et al.,* 2011) to be the most important regulator of VEGF165/VEGF165b splicing ratio in glomerular podocytes. On the contrary, up-regulation of SRPK1 was associated with higher pro-angiogenic VEGF isoform in several tumours such as hepatocellular carcinoma and breast cancer. This solidifies the link between SRPK1 and VEGF165/VEGF165b splicing. Here with SPHINX inhibition to SRPK1 resulted in an increase in the VEGF165b isoform which suggests that SPHINX treatment could inhibit tumour growth by inhibiting angiogenesis. This encourages novel studies into the potential use of small molecule inhibitors of SRPK1 in PCa as anti-angiogenic treatment. Several studies have evaluated the effects of SRPK1 inhibition on genes associated with apoptosis. For instance, Wang, *et al.,* 2017 described how knocking down SRPK1 affects the splicing of caspase-3 and therefore apoptosis. To expand on these findings and investigate the effects of SRPK1 inhibition we used the inhibitor SPHINX and examined the effect of SPHINX on the alternative splicing of *caspase 9* and *BCL2L1*. In the K562 cell line SRPK1 inhibition resulted in a splice shift in *caspase 9 and BCL2L1* toward the more apoptotic isoforms *caspase 9 a* and *Bcl-xs* while this inhibition has led to a weaker but significant change in PC3 cell line in caspase 9 splicing with no detectable change in *BCL2L1* splicing. It was interesting to note that SPHINX did not result in the exact same effect in different cell lines. It is possible that the influence of SRPK1 on alternative splicing is cell or tissue dependent.

7.1.3 Effect of SRPK1 inhibition on cell proliferation

Wang *et al.*, 2017 described that knocking down SRPK1 results in a reduction in cell viability in K562 cells. In this study, the inhibition of SRPK1 by a chemical inhibitor (SPHINX) and siRNA knockdown both resulted in reduced cell viability and proliferation in K562 and PC3 cell lines. Sanidas *et al.*, 2010 described the possible role that the SRPK1a isoform may play in the assembly process of the ribosomes associated with K562 differentiation; in contrast, SRPK1 favoured proliferation. Ren *et al.*, 2010 show that by regulating AKT and JNK pathways, SRPK1 mediates TGF-β2−induced proliferation and apoptosis. However, the opposite effect on cellular proliferation has also been reported namely that CRC cell proliferation was promoted by SRPK1 overexpression (Nan Yi *et al.*, 2018); therefore the influence of SRPK1 on cell proliferation may be cell line dependent.

Several recent studies have described how silencing SRPK1 using siRNA strongly reduces the migration and invasion of different cells. For instance, Chang Y *et al.*, 2015 determined that siRNA SRPK1 knockdown strongly reduced glioma cell migration and invasion by regulating the expression of MMP2 and MMP9. Wu *et al.*, 2017 reported that the upregulation of SRPK1 protein in NSCLC cells and tumour tissues was associated with potential migration and invasion, while lower expression of SRPK1 repressed migration and invasion of the NSCLC cells. Limited cellular migration and invasion in Caco2 and HT-29 cells following SRPK1 silencing using siRNA was recently described (Nan Yi *et al.*, 2018). Similarly, in this study, SRPK1 inhibition with SPHINX and siRNA SRPK1, consistent with the literature, reduced cell migration and invasion of PC3 cells measured via the transwell assay.

7.1.4 Transcriptional regulation of SRPK1 by WT1

WT1 is involved in the development of several organs, including the urogenital system and the gonads (Kreidberg *et al*., 1993). As a major transcription factor, WT1 plays significant roles in major biological functions. For instance, WT1 regulates early gonad development through the activation of an important regulator of gonadogenesis known as steroidogenic factor 1 (SF1). Both WT1 and LHX9 (which is another transcription factor), bind to and activate the SF1 promoter, leading to the expression of this key regulator of gonadogenesis, (Wilhelm *et al.,* 2002). In the glomerular podocytes, VEGF165b expression is important to keep normal glomerular filtration rates and permeability by regulating fenestral formation. Amin *et al.,* 2011 showed that WT1 binds to the *SRPK1* promoter in Denys Drash Syndrome (DDS) podocytes and alter VEGF splicing through transcriptional repression of SRPK1 by binding to a classic GC-rich sequence close to the transcription start site. This thesis investigated whether or not this binding also takes place in leukaemia and prostate cell lines. Through chromatin immunoprecipitation, this binding was confirmed to take place in K562 and PC3 cell lines. The physical binding of WT1 to the promoter is critical for the regulation of SRPK1 transcription. Hayes *et al.,* 2007 show that SRPK1 upregulation has been associated with pancreatic, breast and colorectal cancer. However, the regulation of SRPK1, including how it is upregulated in cancer is not well understood. Salesse *et al.,* 2011 show that the overexpression of the oncogenic tyrosine kinase Bcr-Abl in human hematopoietic progenitor cells results in increased SRPK1 mRNA and protein levels, which then correlates with alterations in pre-mRNA processing.

Given that WT1 is a well-established transcription factor that binds its target genes, Amin *et al.,* 2011 established that WT1 binds to the *SRPK1* promoter and represses its

transcription in glomerular podocytes. However, it should be noted that in some tissues SRPK1 expression is ubiquitous, whereas the expression of WT1 is not. However, WT1 is likely only one of several transcription factors that regulate SRPK1. Furthermore, WT1 can both activate and repress the same target genes depending on the coexpression of transcriptional cofactors (Toska & Roberts, 2014). For instance, WT1 transcriptionally regulates VEGF-A in LnCAP cells (Graham *et al.*, 2007); however, in cells where WT1 is not expressed, other transcription factors such as SP1, which is ubiquitously expressed, can instead regulate VEGF expression (Pore *et al.,* 2005). Therefore other factors are likely to regulate the expression of SRPK1.

Since WT1's developmental roles are now much more complex than first imagined; there is much scope for involvement of WT1 in SRPK1 regulation beyond glomerular podocytes. However, it cannot be assumed that WT1 repress SRPK1 expression in any cell line or tissue that express WT1, as a cofactor that is expressed in podocytes cell line might be absent in another cell type. It is conceivable that WT1 upregulates SRPK1 in some contexts, as WT1 can interact with both transcriptional activator and repressors (Roberts 2005). As SRPK1 levels are upregulated in pancreatic, breast and colorectal cancer, it is important to know what else could regulate SRPK1 expression.

This study suggests convincingly that WT1 is involved in the regulation of SRPK1 expression in leukaemia and prostate cancer cell lines. The *SRPK1* promoter activity is drastically reduced in prostate cancer cells transfected with a luciferase reporter construct with the WT1 binding site mutated in the *SRPK1* promoter. To investigate that further, co-transfection of siRNA that knocked down WT1 with the wild type *SRPK1* promoter resulted in a significant reduction in the promoter's activity. Knocking down WT1 in both cell lines resulted in an observable reduction in SRPK1 protein levels. Thus, the

implication is that WT1 activates SRPK1 transcription in leukaemia and prostate cancer cells. Whether or not that applies to other cancer types remains to be determined. Wagner *et al.,* 2019, to which this study contributed, shows that WT1 activates SRPK1 in tumour endothelium. When an inducible conditional vessel-specific knockout of WT1 was initiated, a reduction in WT1 and SRPK1 transcription was observed. It, therefore, seems clear that WT1 can activate SRPK1 transcription in the context of cancer.

Splice-switching oligonucleotides (SSOs) are an emerging new technology that can manipulate the splicing of a given transcript, we aimed to obtain a morpholino that causes exon skipping. However, a manufacturer error was made by the provider GeneTools where instead of targeting the *WT1* exonic splice junction, it was designed to target a sequence within the exon. Due to time constraints, it was not possible to re-design a WT1 SSO; however, this was not critical as the WT1 siRNAs worked. However, SSOs were used in this project to target the transcription factor ERG, as discussed later.

The –KTS isoform of WT1 is best at binding DNA since it forms a more stable complex with DNA compared to the +KTS isoform. The insertion of the KTS amino acids is in the linker region between zinc figure 3 and 4 of WT1. This insertion disrupts interactions of the linker region with the adjacent zinc fingers and thus lowers the stability of the WT1 (+KTS)-DNA complex (Laity *et al.,* 2000). +KTS isoform is known to have a role in posttranscriptional RNA processing and pre-mRNA splicing rather than transcriptional regulation.

The repressive activity of WT1 in DDS might be attributed to the inability of WT1 to regulate the transcription of a gene or genes involved in the regulation of VEGF alternative splicing as a point mutation in WT1 impairs its ability to bind DNA (Davies., *et al.,* 1998 and Larsson., 1995). In this study, *SRPK1* promoter's activity was stimulated

more significantly when –KTS isoform of WT1 was overexpressed into the cells while +KTS isoform didn't induce the same significance which suggests that –KTS is more involved in the activation process of SRPK1 transcription which agrees with the previous reasons. However, the expression of WT1 (+KTS) was not very prominent, perhaps due to a technical problem with the expressing construct. Therefore additional experiments are needed to compare the effect of +/-KTS WT1 isoforms on SRPK1 transcription in cancer cells.

7.1.5 *CASPASE-9* alternative splicing following WT1 siRNA knockdown

Several studies have highlighted that the WT1 promotes, in different ways, tumorigenesis in several types of cancer. Suppression of apoptosis is one of the proposed mechanisms through which WT1 exerts an oncogenic role. Through a transcriptional mechanism, WT1 was found to upregulate the anti-apoptotic Bcl-2 protein making rhabdoid (G401) cell lines more resistant to apoptosis (Mayo *et al.*, 1999). Knocking down WT1 in several leukemic cell lines enhanced apoptosis. K Ito, *et al.*, 2017 described that WT1-specific siRNA knockdown activated caspase-3 and -9 in the intrinsic apoptosis pathway.

The specific loss of WT1 expression through siRNA knockdown and its implication on apoptosis was examined in this study. *Caspase 9* splicing, which plays an important role in apoptosis seemed to be significantly affected by WT1 knockdown. Through increased caspase 3/7staining and detecting changes in *caspase-9* mRNA splicing, knocking down WT1 appeared to make K562 and PC3 cells more apoptotic. However, there was no detectable change in *BCL2L1* alternative splicing.

7.1.6 Effect of siRNA mediated WT1 knockdown on cell growth

WT1's influence on cellular proliferation and viability is complex in a way similar to its ability to suppress and activate the same target gene in different tissue contexts. For example, Parenti *et al.*, 2014 demonstrated that silencing WT1 with siRNA resulted in limiting cellular proliferation in neurofibromatosis type 1(sNF96.2) cell line which could be attributed to the fact that WT1 plays a major role cycle progression. Another study on G401 presented different findings. Hong *et al.*, 2017 show that reducing WT1 protein expression by WT1 siRNA markedly increased G401 cellular proliferation. In this cell line, this effect could be attributed to the over-arching effect of a microRNA. MiR-590 reduces WT1 expression in G401 cell line whereas miR-590 also promotes proliferation; in other words, proliferation is not WT1-dependent in this cell line

In the current study, the effect of WT1 knockdown and overexpression on cellular proliferation and viability of K562 and PC3 was investigated. siRNA was used to downregulate WT1 which resulted in a reduction in the WT1 protein levels and associated with marked reduction in cellular proliferation and cell viability which agrees with the antiproliferative effect in described (Parenti *et al.*, 2014) unlike the pro-proliferative effect of WT1 siRNA described in (Hong *et al.*, 2017).

(-/+ KTS) WT1 isoforms expressing plasmids were used to investigate the impact of WT1 upregulation on proliferation and viability in K562 and PC3 cells in the current study. –KTS WT1 isoform, which forms a more stable complex with DNA, significantly reduced cellular proliferation and viability while + KTS WT1 didn't have that effect. However, as previously discussed, it was not clear whether or not the +KTS expressing plasmid was working efficiently; additional experiments will address this question.

Overexpression of WT1 is a common feature in lung cancer. In non-small-cell lung cancer cells, miR-361 is downregulated while WT1 is overexpressed where it plays an oncogenic effect through promoting cell migration and invasion of NSCLC cells. Exogenous overexpression of miR-361 resulted in suppressing the migration and invasion of NSCLC cells. However, a similar effect was observed with WT1 knockdown. WT1 was identified as a direct target gene of miR-361 which revealed the molecular mechanism underlying the rapid growth and metastasis of NSCLC and identified the association between miR-361 and WT1 (Yang, *et al.*, 2016).

In the present study, a similar effect on migration and invasion was determined in PC3 cells following WT1 knockdown by siRNA. These findings indicated that it may be beneficial to investigate novel therapy that targets WT1 in prostate cancer which could inhibit rapid growth and metastasis.

7.1.7 BASP1 as a tumour suppressor

Increasing evidence implicates BASP1 in transcriptional control and tumourigenicity in a variety of cell and tissue types throughout the human body (Tang *et al*., 2017). BASP1 has been shown to exert tumour suppressor activity and to be a target of repression in a diverse range of cancer cell types including breast cancer cells, acute myelogenous leukaemia cells, hepatocellular carcinoma cells and thyroid cancer cells (Zhou *et al.*, 2018, Guo *et al.*, 2016 and Marsh *et al.*, 2017). Within these cancer cell types, BASP1 has been shown to exert a number of different effects including reducing proliferation, migration and colony formation, as well as increasing apoptosis. New evidence demonstrates the complexity of the functions of BASP1 as it has, by contrast, been found to possess tumour promoting activity in cervical cancer cells (Tang *et al.*, 2017). Again, it was found that BASP1 has multiple effects in the cancer type including increasing

proliferation, colony formation and tumourigenicity, as well as being associated with stage progression and poor prognosis.

The transcriptional regulatory properties of WT1 is highly tissue-specific as it can act as a transcriptional activator or repressor sometimes for the same target genes depending on the tissue and the surrounding molecular environment as WT1 usually interact with several interaction partners as described in (Roberts, 2005). It has been described that the overexpression of WT1 often combined by lower expression of BASP1 and vice versa. During kidney development, for instance, BASP1 expression overlaps with WT1. In the embryonic stages of kidney development, WT1 levels are higher since it plays a critical role the in condensation of the metanephric mesenchyme onto the ureteric bud proliferation and then differentiation into the epithelia of the nephron. Later on, BASP1 becomes more prominent in the adult kidneys, specifically in non-proliferative glomerular podocytes.

BASP1 has been identified as a transcriptional co-suppressor that interacts with WT1. Through a transcriptional complex (WT1/BASP1), BASP1 converts WT1 from a transcriptional activator to a repressor of its target genes (Carpenter *et al.*, 2004).

The exact mechanisms through which BASP1 exerts tumour suppressor activity in breast cancer cells, acute myelogenous leukaemia cells, hepatocellular carcinoma cells and thyroid cancer is not yet entirely clear, but multiple studies have found that BASP1 possesses transcriptional coregulatory activities. BASP1 has been shown to interact with several major transcription factors including WT1, MYC and ERα in a variety of cell types (Carpenter *et al.*, 2004 and Marsh *et al.*, 2017). In the BASP1-WT1 interaction, BASP1 binds to WT1 and converts it from a transcriptional activator to a transcriptional repressor of WT1 target genes. BASP1 does this by inducing the dissociation of CBP and

the recruitment of HDAC1 to the WT1 transcriptional complex (Toska *et al.*, 2014). In the case of the BASP1-MYC interaction, BASP1 has been shown to block MYC-induced changes in fibroblasts, but it is not known by what mechanism this occurs. More recently, the BASP1-ERα interaction has been investigated, and BASP1 has been shown, in breast cancer cells, to interact with ERα and localise directly at the promoters of ERα target genes. This interaction was found to have significant effects on the transcriptional activity of ERα in response to treatment with the ERα ligand tamoxifen (Marsh *et al.*, 2017). In some cases, it is possible that BASP1 binds independently to the promoter region of a target gene; however, this binding is not mandatory to achieve this repression. For instance, Hartl *et al.*, 2009 has described how MYC and BASP1 transcriptional repression happens despite the lack of specific typical MYC binding site on the 5′ control region of BASP1. Transcriptional repression may occur independently through protein-protein interactions. On the other hand, several studies confirmed that BASP1 binds to the promoter of target genes to achieve the co-repression. Green *et al.*, 2009 has revealed via a chip assay that WT1 and BASP1 bind the promoter of the *podocalyxin*, *Bak* and c-*Myc* genes in podocytes. Co-immunoprecipitation was used to pull down WT1/BASP1 complex using anti-BASP1 polyclonal antibodies confirming the interaction (Carpenter *et al.*, 2004).

Overexpression of BASP1 reduces proliferation, apoptosis and migration in thyroid cancer cells (Guo *et al.*, 2016). Here, the effect of BASP1 overexpression on cellular viability and proliferation was evaluated, the results suggest that BASP1 exerted antitumor activities by reducing viability and proliferation of K562 and PC3 cells. This could be attributed to the induction of the G1 phase arrest in cell division cycle. This results from the overexpression of BASP1 since it is capable of suppressing the

expression cyclin D1, which then elevates the expression of p21 and p27, and induce G1 phase arrest. This suggests that BASP1 may serve as an effective target for limiting the cellular proliferation of K562 and PC3 cells.

7.1.8 The WT1/BASP1 repressive complex and the transcription of SRPK1

In the present study, the data confirms that BASP1 turns WT1 into a repressor of SRPK1. WT1 represses SRPK1 in podocytes, and it is surely not a coincidence that BASP1 is also expressed in posocytes. A chIP for BASP1 was performed in B-K562 cells where SRPK1 was repressed in contrast to regular K562 cells. In regular K562 cells, WT1 activates SRPK1 in normal K562 cells in which BASP1 is not expressed. It seems likely that as elsewhere, in K562 cells, WT1 and BASP1 are physically interacting with each other. Through a chIP assay, BASP1 appeared to be associating with *SRPK1* promoter and regulate its transcription. The interaction of WT1 with BASP1 in B-K562 cells has already been confirmed by immunoprecipitation (Goodfellow *et al*., 2011).

In summary, the evidence presented in this study is and in Wagner *et al*., 2019 is that WT1 activates SRPK1 expression, while represses it in podocytes (Amin *et al.*, 2011). As discussed before, multiple factors could participate in this dual activity of WT1. Since BASP1 was described to be one of the multiple proteins that interact with WT1 and help to define its transcriptional influence on other genes. During the differentiation of podocyte precursor cell line, the overexpression of podocalyxin linked to the upregulation of WT1. However, when BASP1 is present on the podocalyxin promoter, the transcriptional activity of podocalyxin is reduced. The WT1/BASP1 repressive complex maintains the downregulated *c-Myc* and *Bak* promoters in a podocyte precursor cell line. Through incorporating a luciferase reporter with a wild-type *podocalyxin* promoter or a construct that lacks the ability to respond to WT1, Green *et al.*, 2008 show that the

transcriptional activity of wild-type *podocalyxin* is higher in the wild type compared to that where WT1 cannot function. This indicates that WT1 activates the *podocalyxin* promoter. However, this WT1 mediated activation turns into repression when BASP1 is overexpressed as the activity of the wild type promoter goes down.

A similar effect was noticed in this study with *SRPK1* promoter. WT1-mediated transcriptional activation of the *SRPK1* promoter turned into downregulation when BASP1 was overexpressed in PC3 cells. In BASP1 expressing K562 cells, SRPK1 transcriptional activity was down-regulated compared to regular K562 cells where BASP1 is not expressed at detectable levels. Altogether, this suggests that there is a dynamic interaction between WT1 and BASP1, and the absence of BASP1 facilitates the transcriptional activation of SRPK1 in K562 and PC3 cell lines and by inference in cancer more generally.

As described in Carpenter *et al.,* 2004, BASP1 and WT1 are co-expressed in podocytes. In the early stages of kidney development, WT1 is expressed as it is essential for development. As the podocytes become more differentiated in adult kidney, BASP1 expression is established, presumably consistent with the need to stop proliferation.

BASP1 expression in K562 cells is undetectable, therefore Goodfellow *et al.,* 2011 generated K562 cells with steady BASP1 expression (B-K562) to study the WT/BASP1 interaction and to provide a better understanding on the transcriptional reprogramming and morphological changes mediated by BASP1 in K562 cells. As discussed they used co-immunoprecipitation and immunoblotting to demonstrate how BASP1 and WT1 interact.

Therefore, it was of interest to evaluate the endogenous protein levels of WT1, BASP1 and SRPK1 in K562 and B-K562 cells and compare them to other cancer cell lines.

Immunoblotting showed that WT1 and SRPK1 levels are similar in PC3, DU145, and K562 cells. BASP1, on the other hand, was barely detectable in PC3, DU145 and absent in K562 cells. In B-K562 cells where BASP1 was forcibly expressed, WT1, and SRPK1 levels were reduced compared to PC3, DU145, and K562. This is consistent with the downregulation of SRPK1 by WT1/BASP1 also consistent with the previous DLR findings, however. Another incidental observation is that levels of WT1 itself are reduced in B-K562 cells. This observation could be explained by the fact that WT1 can autoregulate its transcription (Malik *et al*., 1994).

7.1.9 Effect of BASP1 on VEGF-A splicing

VEGF-A (often referred to as VEGF) is a key growth factor that plays important roles in regulating angiogenesis and other vital cellular pathways. VEGF is highly expressed in the podocytes of the kidney glomerulus where it facilitates the development of the ureteric bud. Certain VEGF isoforms, VEGF165 specifically, have been described to promote angiogenesis (Hanahan D *et al.*, 2011); whereas the VEFG165b isoform is antiangiogenic and expressed in podocytes in a context where de novo angiogenesis is not required. Numerous studies have linked the downregulation or the inhibition of SRPK1 to the altered VEGF165 splicing as previously discussed.

Stable SRPK1 knockdown resulted in an increase in VEGF165b at the protein level was observed in PC3 cells (Mavrou *et al.*, 2014). In this study PC3 cells were chosen to investigate the effect of SRPK1 downregulation by WT1/BASP1 complex on the VEGF165/VEGF165b splicing. Downregulation of SRPK1 by BASP1 overexpression resulted in an increase in the VEGF165b isoform which suggests that a possible inhibition of angiogenesis may occur and therefore, BASP1 could be considered as an angiogenesis suppressor.

7.1.10 ERG as a transcriptional regulator

As previously discussed it is likely that SRPK1 transcriptional regulation is influenced by several transcription factors, not just WT1. Due to ongoing research in the laboratory on ERG and the presence of potential binding sites in the SRPK1 promoter, this study investigates ETS-related gene transcription factor ERG as a potential regulator of SRPK1. ERG, like WT1, is a complex transcription factor with several developmental roles, and a clear involvement in cancer, particularly prostate cancer (Adamo and Ladomery, 2016). Adamo *et al.,* 2017 demonstrated that ERG suppresses PTEN which is an important tumour suppressor in prostate and other cancers. Like WT1, ERG binds to the promoter of its target genes and helps regulate transcription. This study investigated wither or ERG binds to the SRPK1 promoter in an ERG expressing cell line, the osteosarcoma cell line MG63 (PC3, DU145 and K562 cells do not express ERG). Through chIP, binding was confirmed to take place in MG63 cell line.

Similar binding of ERG to the *PTEN* promoter contributes to the repression of PTEN expression in prostate cancer cells (Adamo *et al.,* 2017). This binding was identified by chIP then a dual-luciferase: renilla (DLR) transcription assay was performed where *PTEN* promoter co-transfected with increasing amounts of the ERG expressing plasmid into DU145 dells (ERG negative). This showed that the reduction in *PTEN* promoter activity with increasing amounts of co-transfected ERG. To expand on these findings, the *PTEN*: luciferase construct was transfected into VCaP cells (prostate cancer, ERG positive) where an ERG knockdown was performed using siRNA against ERG. This downregulation of ERG restored the activity of *PTEN* promoter (Adamo *et al.,* 2017).

ERG is also involved in EMT. For example, (Nagai *et al.,* 2018) have shown that ERG and FLI1 are critical transcriptional activators for endothelial cells specific genes. They

activate EC-specific genes and prevent the endothelial-to-mesenchymal transition through repressing mesenchymal-like genes. Moreover, a combined knockdown of ERG and FLI1 triggered the endothelial-to-mesenchymal transition.

After obtaining evidence that ERG interacts with the *SRPK1* promoter, K562 and PC3 cells (ERG negative) were transfected with ERG expressing plasmids (-/+ exon 7b, an in-frame cassette exon of ERG thought to increase its oncogenic properties when included (Hagen *et al*, 2014). Following that, a significant reduction in SRPK1 expression both at the transcriptional and the protein levels was observed. Cotransfection of increasing amounts of full-length ERG-expressing plasmids with the *SRPK1* promoter: luciferase construct has demonstrated an increasing reduction in *SRPK1* promoter activity.

To expand on this, morpholinos (SSO) that induce ERG exon 4 (a constitutive exon) and 7b (cassette exon) skipping and siRNA against ERG was used to determine whether or not knocking down ERG and skipping exon 4 and 7b would result in the upregulation of SRPK1. siRNA reduces total ERG protein levels while exon 4 skipping by the SSOs resulted in making a premature stop codon which leads to nonsense-mediated decay which also reduces ERG protein. Reduction of ERG protein by exon 4 SSOs and siRNA against ERG resulted in a significant increase in SRPK1 protein and promoter activity. However, the other SSO against the cassette exon (E7b) resulted in exon 7b skipping without a clear increase in SRPK1 levels.

In summary, it appears that at least in K562 and PC3 cells, ERG is a repressor, not an activator of SRPK1. This was perhaps surprising as ERG is a presumed oncogene, and SRPK1 upregulation is generally thought to be associated with a cancer phenotype, but that would be a simplistic interpretation. However, several transcription factors are likely

to influence overall SRPK1 expression in MG63 cells, and SRPK1 may be less important in any given cancer, especially as there are several other splice factor kinases, such as the CLKs, that could play a more prominent role, in any given cancer. Furthermore, as is the case with WT1, it is possible that ERG activates SRPK1 instead of repressing it, depending on the presence of other cofactors. These are open questions; the key finding here is that SRPK1 is a new transcriptional target of ERG.

7.1.11 ERG and apoptosis

Several studies have emphasised that ERG plays several key roles in regulating critical processes such as apoptosis. For instance, a change in caspase 3 and 7 activity was observed when ERG was subjected to siRNA knockdown (Birdsey *et al.*, 2008). Caspase splicing, which plays an important role in apoptosis seemed to be significantly affected by ERG overexpression. Through active Caspases 3 and 7 staining and detecting the change in *Caspase-9* proapoptotic (a) and antiapoptotic (b) isoform levels, ERG expression appeared to make K562 and PC3 cells more apoptotic. However, there was no detectable change in *BCL2L1* splicing.

To further expand on these findings, the effect of ERG downregulation in MG63 (ERG positive cells) on apoptosis was examined. Caspase 3 and 7 activity was shown to increase following ERG downregulation. Reduction of ERG resulted in a significant splicing change in *Caspase 9* favouring the pro-apoptotic isoform *caspase-9a*.

As a major transcriptional regulator, ERG influences cellular proliferation and viability through regulating genes in major cellular pathways. (Liu *et al.*, 2016 and Klezovitch *et al.*, 2008) described how downregulation of ERG in VCaP cells showed a decrease in cellular viability and proliferation. This agrees with the findings in this study where ERG expression was targeted with ERG siRNA and exon 4 skipping SSOs resulted in a similar

biological effect. Overexpression or downregulation of ERG results in altered expression of its downstream target genes which now include SRPK1. This splice kinase plays major roles in maintaining cellular viability. Earlier in this project, we showed how knocking down SRPK1 resulted in a significant reduction in K562 and PC3 proliferation and viability. ERG overexpression in ERG-negative cell lines such as K562 and PC3 apparently repressed SRPK1 and correlated with a reduction in cellular proliferation and viability. However, this cannot necessarily be fully attributed to SRPK1 as ERG regulates many other key genes.

The evolutionarily conserved cassette exon 7b was described by (Jumbe *et al.,* 2019) to play an important role in the proliferation of MG63 and VCaP cells. They show by Ki-67 activity that the skipping of exon 7b induced by SSOs resulted in a reduction of cellular proliferation. The same effect was confirmed here by MTT assay following E7b SSOs transfection into MG63 cells. However, the contribution of exon 7b to the ability of ERG to regulate SRPK1 is not entirely clear and will require further investigation.

The regulatory function of ERG extends to regulate multiple biologically important pathways such as inflammation, angiogenesis, haematopoiesis, migration and invasion. For example, HDAC6, which is involved in EC motility and migration, is an ERG target. ERG was shown to bind its promoter and regulate its expression. Following inhibition of ERG in HUVECs cells, HDAC6 expression decreased combined with a decrease in HUVEC cells migration (Birdsey *et al.,* 2011). In another study, following siRNA knockdown of ERG in VCaP cell line, the migration and invasion were remarkably decreased (Liu *et al.,* 2016).

Here in this study, a recently described, innovative approach that switches the splicing of a given gene beside siRNA was used to inhibit ERG expression and then evaluate cellular

migration and invasion. Both exon 4 skipping and siRNA ERG knockdown in MG63 cells resulted in a significant reduction in cellular migration and invasion. These findings indicated that ERG could be a useful target for a novel therapy that inhibits the rapid growth and metastasis in different cancers. SRPK1 was also identified as a novel ERG target; future research will determine the physiological importance of its regulation by ERG.

7.2 Significance of the research

The serine/arginine-rich proteins (SR proteins) are a large superfamily of nuclear RNA binding proteins (Zhou and Fu, 2013). The activity of SR proteins is highly regulated by the reversible phosphorylation of serine residues in the RS domain. Several protein kinases have been identified that phosphorylate SR proteins; the serine/arginine protein kinase family (SRPKs), cyclin-dependent like kinases (Cdc-like-kinase) or Clk/Sty (also known as Clk1), DNA topoisomerase I and phosphatidylinositol 3-kinase (AKT). The SRPKs phosphorylate SR proteins with high efficiency and specificity. However, the Clk/Sty family are dual specific kinases that phosphorylate serine/threonine and tyrosine residues. Thus, SRPKs phosphorylate SR proteins with greater efficiency and specificity than Clk/Sty. Despite this, Clk/Sty phosphorylates more residues than SRPKs in the RS domain of SRSF1. Numerous studies have revealed that members of SRPK are responsible for the nuclear import of phosphorylated SRSF1, while Clk/Sty members play key roles in interrupting phosphorylated SRSF1 (Ghosh and Adams, 2011). We have not considered here whether or not WT1 and ERG might also regulate the CLK splice factor kinases; it might be of interest to consider this possibility in future research.

SRPK1 has been shown to be upregulated in colon, breast and pancreatic cancers. However, the mechanism that causes its upregulation in these cancers is also unknown. To date it is known that overexpression of the oncogenic tyrosine kinase Bcr-Ab1 in human hematopoietic progenitor cells results in increased SRPK1 mRNA and protein levels, which correlate with alteration in pre-mRNA processing (Saless *et al.,* 2004) in this study, SRPK1 has shown to be activated by WT1 alone and suppressed by WT1/BASP1 complex or ERG.

Inhibiting SRPK1 levels could be a potential therapeutic target. In the present study, both the knockdown of SRPK1 mRNA levels by siRNA and the inhibition of its activity using a small molecular inhibitor SPHINX promoted the anti-angiogenic VEGF in the prostate cancer cell line. The cellular survival rate, as well as their invasive and migration abilities, were compromised as a result of SRPK1 inhibition. Manipulating the potential SRPK1 transcriptional regulators has shown to shift the tumorigenicity of the cells through altering key cellular pathways such as apoptosis.

However, pharmacological inhibition of SRPK1 could result in multiple side effects given its general role in the regulation of splice factor activity. It can be expected that SRPK1 will be able to regulate the alternative splicing of other genes. In addition, SRPK1 has been shown to be a cisplatin-sensitive protein (Schenk *et al.,* 2001). Cisplatin is a commonly used anti-cancer drug, and down-regulation of SRPK1 results in human ovarian cancer cells being less sensitive to the drug. Thus it is important to be cautious as more work has to be done to determine whether or not SRPK1 could be a potential therapeutic target.

Clearly then there are complexities to be considered by future research. However, some important findings have resulted here. We have established that WT1 can upregulate

SRPK1 in cancer; that BASP1 is involved; and that another transcription factor and oncogene, ERG, contributes to SRPK1 regulation. The fact that both WT1 and ERG can contribute to SRPK1 regulation raises a number of important questions. Perhaps these oncogenes orchestrate significant changes in alternative splicing patterns in cancer, through the regulation of SRPK1, and potentially other splice factor kinases. A better understanding of these pathways could lead to novel therapeutic opportunities; for example, targeting WT1, could results in higher expression of antioangiogenic VEGF165b through reduced SRPK1.

7.3 Future directions

7.3.1 Global RNA Sequencing and gene promoter scan

One of the goals of future work investigating SRPK1 in leukaemia and prostate cancer cells is to perform RNA sequencing analyses in several cell lines. RNA sequencing would allow the effects of SRPK1 inhibition and transcriptional manipulation through inhibition of WT1 and ERG to be compared to those of other cells. The crossover and differences between the cell types could then be analysed to investigate the differences in SRPK1 mechanisms in different cell types. This data could reveal currently unknown roles of SRPK1 orchestrated by WT1, BASP1 and ERG in cancer cells.

Gene promoter scan is a powerful tool that could identify other transcription factors that contribute to the regulation of SRPK1 transcription. In this study, WT1, BASP1 and ERG were shown through chIP to bind to the *SRPK1* promoter. How these, and other transcription factors interact to regulate SRPK1 transcription in cancer remains to be investigated in more details.

7.3.2 SRPK1 kinase activity

It was observed that SRPK1 is upregulated in both leukaemia and prostate cell lines which suggests that the elevated expression of SRPK1 level leads to increased splice factor kinase activity. This presumably results in the hyperphosphorylation of SRSF1, an oncogenic splice factor; but this was not measured directly here. An experiment that measures the kinase activity in both cell lines would be useful to prove that there is indeed an increase in the protein kinase activity of SRPK1 as a result of its upregulation. An increase in SRPK1 kinase activity resulting in activation of SRSF1 and other SR protein splice factors would result in significant changes in the alternative splicing of several key cancer-associated genes. This could also be investigated in more detail.

7.3.3 Investigating other SRPK1 isoforms

As very little is known about the different splice isoforms of SRPK1 in development and disease. The importance of SRPK1a remains unclear. We were unable to detect it, but this does not necessarily disprove its existence in *vivo*. A mouse model could be made to study their possible different roles in prostate and leukemic cancers. The possibility of whether or not the WT1/SRPK1/SRSF1 pathway affects the alternative splicing of SRPK1 itself should also be investigated. But in addition to SRPK1a, there may be additional SRPK1 splice isoforms; none have been described in the literature so far, but it is conceivable that others exist.

7.3.4 SRPK1 intracellular localization

SRPK1 localisation in the cell could also be an important parameter and it is known that SRPK1 autophosphorylates affecting its localisation and activity (Zhou *et al.*, 2012). Akt inhibitors (MK2206 and wortmannin) to determine whether or not, through the

autophosphorylation of SRPK1, they change SRPK1's intracellular localization. It will also be of interest to examine the effect of growth factors (EGF, IGF-1) on SRPK1 autophosphorylation and intracellular localization, as well as the effect of cellular stress including hypoxia on the same parameters. The autophosphorylation and localization of SRPK1 will be correlated with the alternative splicing of cancer-associated genes known to be downstream of SRPK1, e.g. *VEGF-A*.

To gain further insights into the regulation of SRPK1, the intrinsic stability of SPRK1 mRNA could be assessed. PC3 cells could be treated with actinomycin D, a transcription inhibitor, and the levels of SRPK1 mRNA measured in a 72h time course. Then the effect of Akt inhibitors and various growth factors known to activate SRPK1 on the stability of its mRNA could be determined.

7.3.5 Inducible expression of ERG/WT1 and SRPK1 regulation

The findings here suggest that SRPK1 expression is activated by WT1 and the knockdown of WT1 resulted in a reduction in the *SRPK1* transcription and expression. This study also suggests that ERG repress SRPK1 and knocking down ERG by SSOs and siRNA restored SRPK1 activity and increased its expression. However, this effect is temporary as it ends once the siRNA/SSOs concentration is reduced as the cell division continues. Therefore, it would be interesting in the future to generate a cell line with inducible expression of ERG and WT1. This could be achieved by using the cells with plasmids where the promoter could be switched on and off using a steroid or tetracycline-induced promoter.

7.3.6 SRPK1 expression and EMT Markers

EMT markers are an important aspect of tumour biology as they perform an important tool in evaluating the metastatic ability of deferent tumours. EMT could be significantly affected by SRPK1. Looking at the effect of manipulating the ERG, WT1, BASP1-SRPK1 axis on the expression of EMT markers may provide an insight into the influence of SRPK1 on the metastatic ability of prostate, and other cancer cells.

8 References

Adamo, P. and Ladomery, M.R. (2015) The oncogene ERG: a key factor in prostate cancer. Oncogene. 35 pp.403.

Adamo, P., Porazinski, S., Rajatileka, S., Jumbe, S., Hagen, R., Cheung, M., Wilson, I. and Ladomery, M. (2017) The oncogenic transcription factor ERG represses the transcription of the tumour suppressor gene PTEN in prostate cancer cells. 14 pp.5605-5610

Ambrosino, C., Tarallo, R., Bamundo, A., Cuomo, D., Franci, G., Nassa, G., Paris, O., Ravo, M., Giovane, A., Zambrano, N., Lepikhova, T., Jänne, O.A., Baumann, M., Nyman, T.A., Cicatiello, L. and Weisz, A. (2010). Identification of a hormone-regulated dynamic nuclear actin network associated with estrogen receptor α in Human Breast Cancer Cell Nuclei. Molecular & Cellular Proteomics, 9(6), pp.1352–1367.

Amin, E.M., Oltean, S., Hua, J., Gammons, M.V.R., Hamdollah-Zadeh, M., Welsh, G.I., Cheung, M., Ni, L., Kase, S., Rennel, E.S., Symonds, K.E., Nowak, D.G., Pokora-Royer, B., Saleem, M.A., Hagiwara, M., Schumacher, V.A., Harper, S.J., Hinton, D.R., Bates, D.O. and Ladomery, M.R. (2011) WT1 mutants reveal SRPK1 to be a downstream angiogenesis target by altering VEGF splicing. Cancer Cell. 20 (6), pp.768-780.

Anderson, M.K., Hernandez-Hoyos, G., Diamond, R.A. and Rothenberg, E.V. (1999) Precise developmental regulation of Ets family transcription factors during specification and commitment to the T cell lineage. Development. 126 (14), pp.3131.

Artibani, M., Sims, A.H., Slight, J., Aitken, S., Thornburn, A., Muir, M., Brunton, V.G., Del-Pozo, J., Morrison, L.R., Katz, E., Hastie, N.D. and Hohenstein, P. (2017). WT1 expression in breast cancer disrupts the epithelial/mesenchymal balance of tumour cells and correlates with the metabolic response to docetaxel. Scientific Reports, 7(1) pp.45-55.

Aubol, B.E., Jamros, M., McGlone, M.L. and Adams, J.A. (2013) Splicing kinase SRPK1 conforms to the landscape of its SR protein substrate. Biochemistry. 52 (43), pp.10.1021/bi4010864.

Bacher, U., Weissmann, S., Kohlmann, A., Schindela, S., Alpermann, T., Schnittger, S., Kern, W., Haferlach, T. and Haferlach, C. (2012) TET2 deletions are a recurrent but rare phenomenon in myeloid malignancies and are frequently accompanied by TET2 mutations on the remaining allele. British Journal of Haematology. 156 (1), pp.67-75.

Baldus, C.D., Burmeister, T., Martus, P., Schwartz, S., Gökbuget, N., Bloomfield, C.D., Hoelzer, D., Thiel, E. and Hofmann, W.K. (2006) High expression of the ETS transcription factor ERG predicts adverse outcome in acute T-lymphoblastic leukemia in adults. Jco. 24 (29), pp.4714-4720.

Baralle, D. and Baralle, M. (2005) Splicing in action: assessing disease causing sequence changes. J Med Genet. 42 (10), pp.737-748.

Barbaux, S., Niaudet, P., Gubler, M.-C., Grünfeld, J.-P., Jaubert, F., Kuttenn, F., Fékété, C.N., Souleyreau-Therville, N., Thibaud, E., Fellous, M. and McElreavey, K. (1997). Donor splice-site mutations in WT1 are responsible for Frasier syndrome. Nature Genetics, 17(4), pp.467–470

Batson, J., Toop, H.D., Redondo, C., Babaei-Jadidi, R., Chaikuad, A., Wearmouth, S.F., Gibbons, B., Allen, C., Tallant, C., Zhang, J., Du, C., Hancox, J.C., Hawtrey, T., Da Rocha, J., Griffith, R., Knapp, S., Bates, D.O. and Morris, J.C. (2017) Development of potent, selective SRPK1 inhibitors as potential topical therapeutics for neovascular eye disease. ACS Chem.Biol. 12 (3), pp.825-832.

Birdsey, G.M., Dryden, N.H., Amsellem, V., Gebhardt, F., Sahnan, K., Haskard, D.O., Dejana, E., Mason, J.C. and Randi, A.M. (2008) Transcription factor Erg regulates angiogenesis and endothelial apoptosis through VE-cadherin. Blood. 111 (7), pp.3498-3506.

Birdsey, G.M., Shah, A.V., Dufton, N., Reynolds, L.E., Osuna Almagro, L., Yang, Y., Aspalter, I.M., Khan, S.T., Mason, J.C., Dejana, E., Göttgens, B., Hodivala-Dilke, K., Gerhardt, H., Adams, R.H. and Randi, A.M. (2015) The endothelial transcription factor ERG promotes vascular stability and growth through Wnt/ β -catenin signaling. Developmental Cell. 32 (1), pp.82-96.

Birdsey, G., Dryden, N., Shah, A., Hannah, R., D Hall, ,Matthew, Haskard, D., Parsons, M., Mason, J., Zvelebil, M., Gottgens, B., J Ridley, ,Anne and Randi, A. (2011) The transcription factor Erg regulates expression of histone deacetylase 6 and multiple pathways involved in endothelial cell migration and angiogenesis.

Bullock, N. and Oltean, S. (2017) the many faces of SRPK1. The Journal of Pathology. 241 (4), pp.437-440.

Bush, S., Chen, L., Tovar-Corona, J. and Urrutia, A. (2017) Alternative splicing and the evolution of phenotypic novelty. Philosophical Transactions of the Royal Society B: Biological Sciences. 372, pp.517-525.

C Long, Jennifer and F Caceres, Javier (2009) The SR protein family of splicing factors: master regulators of gene expression. The Biochemical journal. 417, pp.15-27.

Cappai, R. and Barnham, K.J. (2008) Delineating the mechanism of alzheimer's disease a beta peptide neurotoxicity. Neurochemical Research. 33 (3), pp.526-532.

Carpenter, B., Hill, K.J., Charalambous, M., Wagner, K.J., Lahiri, D., James, D.I., Andersen, J.S., Schumacher, V., Royer-Pokora, B., Mann, M., Ward, A. and Roberts, S.G.E. (2004) BASP1 is a transcriptional cosuppressor for the Wilms' tumor suppressor protein WT1. Molecular and Cellular Biology. 24 (2), pp.537-549.

Cartegni, L., Chew, S.L. and Krainer, A.R. (2002) Listening to silence and understanding nonsense: exonic mutations that affect splicing. Nature Reviews Genetics. 3 (4), pp.285-298.

Chang, Y., Wu, Q., Tian, T., Li, L., Guo, X., Feng, Z., Zhou, J., Zhang, L., Zhou, S., Feng, G., Han, F., Yang, J. and Huang, F. (2015) The influence of SRPK1 on glioma apoptosis, metastasis, and angiogenesis through the PI3K/Akt signaling pathway under normoxia. Tumour Biology: The Journal of the International Society for Oncodevelopmental Biology and Medicine. 36 (8), pp.6083-6093.

Cho, H. P., Liu, Y., Gomez, M., Dunlap, J., Tyers, M. and Wang, The dual-specificity phosphatase CDC14B bundles and stabilizes microtubules. Molecular and Cellular Biology. 25, pp. 4541-4551.

Chow, S LT, Gelinas RE, Broker TR, Roberts R. (1977) an amazing sequence arrangement at the 50 ends of adenovirus 2 messenger RNA. Cell. 12(1), pp. 1-8

de Brot, S., Ntekim, A., Cardenas, R., James, V., Allegrucci, C., Heery, D., Bates, D., Odum, N., Persson, J. and Mongan, N. (2015) Regulation of vascular endothelial

growth factor (VEGF) in prostate Cancer. Endocrine-related cancer. 22, pp. 107-123.

Davies, R.C., Calvio, C., Bratt, E., Larsson, S.H., Lamond, A.I. and Hastie, N.D. (1998). WT1 interacts with the splicing factor U2AF65 in an isoform-dependent manner and can be incorporated into spliceosomes. Genes & Development, 12(20), pp.3217–3225.

Deramaudt, T. B., Remy, P. and Stiegler, P. (2001) Identification of interaction partners for two closely-related members of the ETS protein family, FLI and ERG. Gene. 274(1), pp. 169-177.

DiFeo, A., Narla, G., Camacho-Vanegas, O., Nishio, H., Rose, S.L., Buller, R.E., Friedman, S.L., Walsh, M.J. and Martignetti, J.A. (2006) E-cadherin is a novel transcriptional target of the KLF6 tumor suppressor. Oncogene. 25 pp.6026.

Duncan, P.I., Stojdl, D.F., Marius, R.M. and Bell, J.C. (1997). In vivo regulation of alternative pre-mRNA splicing by the Clk1 protein kinase. Molecular and cellular biology, 17(10), pp.5996–6001.

Early, P., Huang, H., Davis, M., Calame, K. and Hood, L. (1980) An immunoglobulin heavy chain variable region gene is generated from three segments of DNA: VH, D and JH. Cell. 19(4), pp. 981-992.

Epand, R. M., Epand, R. F. and Maekawa, S. (2003) The arrangement of cholesterol in membranes and binding of NAP-22. Chemistry and Physics of Lipids. 122(1), pp. 33-39.

Feng, H.-Z., Chen, X., Hossain, M.M. and Jin, J.-P. (2012). Toad heart utilizes exclusively slow skeletal muscle troponin T. Journal of Biological Chemistry, 287(35), pp.53–64.

Fiszbein, A. and Kornblihtt, A.R. (2016) Histone methylation, alternative splicing and neuronal differentiation. Neurogenesis (Austin, Tex.). 3 (1), pp.e1204844

Gammons, M.V., Lucas, R., Dean, R., Coupland, S.E., Oltean, S. and Bates, D.O. (2014) Targeting SRPK1 to control VEGF-mediated tumour angiogenesis in metastatic melanoma. British Journal of Cancer. 111 (3), pp.477-485.

Gessler, M., König, A. and Bruns, G. A. P. (1992) The genomic organization and expression of the WT1 gene. Genomics. 12(4), pp. 807-813.

Ghosh, G. and Adams, J.A. (2011). Phosphorylation mechanism and structure of serine-arginine protein kinases. The FEBS journal, 278(4), pp.587–97

Gonçalves, V., Henriques, A., Pereira, J., Neves Costa, A., Moyer, M.P., Moita, L.F., Gama-Carvalho, M., Matos, P. and Jordan, P. (2014) Phosphorylation of SRSF1 by SRPK1 regulates alternative splicing of tumor-related Rac1b in colorectal cells. Rna (New York, N.Y.). 20 (4), pp.474-482.

Goodfellow, S.J., Rebello, M.R., Toska, E., Zeef, L.A.H., Rudd, S.G., Medler, K.F. and Roberts, S.G.E. (2011) WT1 and its transcriptional cofactor BASP1 redirect the differentiation pathway of an established blood cell line. The Biochemical Journal. 435 (1), pp.113-125.

Gout, S., Brambilla, E., Boudria, A., Drissi, R., Lantuejoul, S., Gazzeri, S. and Eymin, B. (2012) Abnormal expression of the pre-mRNA splicing regulators SRSF1, SRSF2, SRPK1 and SRPK2 in non-small cell Lung carcinoma. Plos One. 7 (10), pp.e46539.

Graham, K., Li, W., Williams, B.R.G. and Fraizer, G. (2006). Vascular endothelial growth factor (VEGF) is suppressed in WT1-transfected LNCaP cells. Gene expression, 13(1), pp.1–14.

Green, L.M., Wagner, K.J., Campbell, H.A., Addison, K. and Roberts, S.G.E. (2009) Dynamic interaction between WT1 and BASP1 in transcriptional regulation during differentiation. Nucleic Acids Research. 37 (2), pp.431-440.

Guo, R., Yu, Y., Chen, J., Chen, Y., Shen, N. and Qiu, M. (2016) Restoration of brain acid soluble protein 1 inhibits proliferation and migration of thyroid cancer cells. Chinese Medical Journal. 129 (12), pp.1439-1446.

Gustafsson Sheppard, N., Jarl, L., Mahadessian, D., Strittmatter, L., Schmidt, A., Madhusudan, N., Tegnér, J., Lundberg, E.K., Asplund, A., Jain, M. and Nilsson, R. (2015) The folate-coupled enzyme MTHFD2 is a nuclear protein and promotes cell proliferation. Scientific Reports. 5 pp.15029-15040.

Haber, D.A., Sohn, R.L., Buckler, A.J., Pelletier, J., Call, K.M. and Housman, D.E. (1991) Alternative splicing and genomic structure of the Wilms tumor gene WT1. Proceedings of the National Academy of Sciences. 88 (21), pp.9618-9622.

Hagen, R.M., Adamo, P., Karamat, S., Oxley, J., Aning, J.J., Gillatt, D., Persad, R., Ladomery, M.R. and Rhodes, A. (2014) Quantitative analysis of ERG expression and Its splice isoforms in formalin-fixed, paraffin-embedded prostate cancer samples: association with seminal vesicle invasion and biochemical Recurrence. American Journal of Clinical Pathology.T. 142 (4), pp.533-540.

Hanahan, D. and Weinberg, R. (2011) Hallmarks of cancer: The next generation. Cell. 144(5), pp. 646-674.

Hartl, M., Nist, A., Khan, M.I., Valovka, T. and Bister, K. (2009) Inhibition of Myc-induced cell transformation by brain acid-soluble protein 1 (BASP1). Proceedings of the National Academy of Sciences of the United States of America. 106 (14), pp.5604-5609.

Hayes, G.M., Carrigan, P.E., Beck, A.M. and Miller, L.J. (2006). Targeting the RNA Splicing Machinery as a Novel Treatment Strategy for Pancreatic Carcinoma. Cancer Research, 66(7), pp.3819–3827.

Hollink, I. H., van den Heuvel-Eibrink, M. M., Zimmermann, M., Balgobind, B. V., Arentsen-Peters, S. T., Alders, M., Willasch, A., Kaspers, G. J., Trka, J., Baruchel, A., de Graaf, S. S., Creutzig, U., Pieters, R., Reinhardt, D., & Zwaan, C. M. (2009). Clinical relevance of Wilms tumor 1 gene mutations in childhood acute myeloid leukemia. Blood, 113(23), 5951-5960.

Hong, L., Zhao, X., Shao, X. and Zhu, H. (2017) MiR-590 Regulates WT1 during proliferation of G401 cells. Molecular Medicine Reports. 16 pp. 247-253

IMosevitskiĭ, M., P Caponi,J., Iu Skladchikova, G., A Novitskaia, ,V. and Plekhanov, A. (1996) Specific properties and primary structure of BASP1 protein, initially detected in neuronal axonal terminals. Biokhimiia (Moscow,). 61 pp. 1209-20

Inoue, K., Ogawa, H., Sonoda, Y., Kimura, T., Sakabe, H., Oka, Y., Miyake, S., Tamaki, H., Oji, Y., Yamagami, T., Tatekawa, T., Soma, T., Kishimoto, T., & Sugiyama, H. (1997). Aberrant overexpression of the Wilms tumor gene (WT1) in Human Leukemia. Blood, 89(4), 1405-1412.

Ito, K., Oji, Y., Tatsumi, N., Shimizu, S., Kanai, Y., Nakazawa, T., Asada, M., Jomgeow, T., Aoyagi, S., Nakano, Y., Tamaki, H., Sakaguchi, N., Shirakata, T., Nishida, S., Kawakami, M., Tsuboi, A., Oka, Y., Tsujimoto, Y. and Sugiyama, H. (2006) Antiapoptotic function of 17AA(+) WT1 (Wilms' tumor gene) isoforms on the intrinsic apoptosis pathway. Oncogene. 25 pp.4217-4229.

Jumbe, S. L., Porazinski, S. R., Oltean, S., Mansell, J. P., Vahabi, B., Wilson, I. D. and Ladomery, M. R. (2019) The evolutionarily conserved cassette exon 7b drives ERG's oncogenic properties. Translational Oncology. 12(1), pp. 134-142.

Keren, H., Lev-Maor, G. and Ast, G. (Nature Reviews Genetics volume 11, pages 345–355 (2010) Alternative splicing and evolution: diversification, exon definition and function. Nature Reviews Genetics. 11 (5), pp.345-355.

Khan, T.K., Yang, B., Thompson, N.L., Maekawa, S., Epand, R.M. and Jacobson, K. (2003) binding of NAP-22, a calmodulin-binding neuronal protein, to raft-like domains in model membranes. Biochemistry. 42 (17), pp.4780-4786.

Kimmelman, A.C., Qiao, R.F., Narla, G., Banno, A., Lau, N., Bos, P.D., Nuñez Rodriguez, N., Liang, B.C., Guha, A., Martignetti, J.A., Friedman, S.L. and Chan, A.M. (2004). Suppression of glioblastoma tumorigenicity by the Kruppel-like transcription factor KLF6. Oncogene, 23(29), pp.5077–83

Klamt, B., Koziell, A., Poulat, F., Wieacker, P., Scambler, P., Berta, P. and Gessler, M. (1998) Frasier syndrome is caused by defective alternative splicing of WT1 leading to an altered ratio of WT1 +/−KTS splice isoforms. Human Molecular Genetics. 7 (4), pp.709-714.

Klezovitch, O., Risk, M., Coleman, I., Lucas, J.M., Null, M., True, L.D., Nelson, P.S. and Vasioukhin, V. (2008) A causal role for ERG in neoplastic transformation of prostate epithelium. Proceedings of the National Academy of Sciences of the United States of America. 105 (6), pp.2105-2110.

Komeno, Y., Yan, M., Matsuura, S., Lam, K., Lo, M., Huang, Y., Tenen, D.G., Downing, J.R. and Zhang, D. (2014) Runx1 exon 6-related alternative splicing isoforms differentially regulate hematopoiesis in mice. Blood. 123 (24), pp.3760-3769.

Korshunova, I., Caroni, P., Kolkova, K., Berezin, V., Bock, E. and Walmod, P.S. (2008) Characterization of BASP1-mediated neurite outgrowth. Journal of Neuroscience Research. 86 (10), pp.2201-2213.

Kreidberg, J. A., Sariola, H., Loring, J. M., Maeda, M., Pelletier, J., Housman, D. and Jaenisch, R. (1993) WT-1 is required for early kidney development. Cell. 74(4), pp. 679-691.

Laity, J.H., Dyson, H.J. and Wright, P.E. (2000). Molecular basis for modulation of biological function by alternate splicing of the Wilms' tumor suppressor protein. Proceedings of the National Academy of Sciences, 97(22), pp.11932–11935.

Larsson, S. H., Charlieu, J., Miyagawa, K., Engelkamp, D., Rassoulzadegan, M., Ross, A., Cuzin, F., Heyningen, V. v. and Hastie, N. D. (1995) Subnuclear localization of WT1 in splicing or transcription factor domains is regulated by alternative splicing. Cell. 81(3), pp. 391-401.

Lee, K.Y., Jeon, Y.J., Kim, H.G., Ryu, J., Lim, D.Y., Jung, S.K., Yu, D.H., Chen, H., Bode, A.M. and Dong, Z. (2017) The CUG-translated WT1, not AUG-WT1, is an oncogene. Carcinogenesis. 38 (12), pp.1228-1240.

Li, X., Song, J., Liu, J., Wu, S., Wang, L., Gong, L. and Lin, X. (2014) Serine arginine protein kinase 1 is associated with breast cancer progression and poor patient survival. Medical Oncology. 31 (8), pp.83.

Liu, B., Gu, X., Huang, T., Luan, Y. and Ding, X. (2016) Identification of TMPRSS2-ERG mechanisms in prostate cancer invasiveness: involvement of MMP-9 and Plexin B1. 37 (1), pp.201-208.

Liu, H., Hu, X., Zhu, Y., Jiang, G. and Chen, S. (2016) Up-regulation of SRPK1 in non-small cell lung cancer promotes the growth and migration of cancer cells. Tumor Biology. 37 (6), pp.7287-7293.

Maekawa, S., Murofushi, H. and Nakamura, S. (1994) Inhibitory effect of calmodulin on phosphorylation of NAP-22 with Protein Kinase C. 269 (30), pp.19462-5.

Malik, K.T.A., Poirier, V., Ivins, S.M. and Brown, K.W. (1994) Autoregulation of the human WT1 gene promoter. *FEBS Letters*. 349 (1), pp.75-78.

Mani, R., Iyer, M.K., Cao, Q., Brenner, J.C., Wang, L., Ghosh, A., Cao, X., Lonigro, R.J., Tomlins, S.A., Varambally, S. and Chinnaiyan, A.M. (2011) TMPRSS2-ERG-mediated feed-forward regulation of wild-type ERG in human prostate cancers. Cancer Research. 71 (16), pp.5387-5392.

Mani, R., Tomlins, S.A., Callahan, K., Ghosh, A., Nyati, M.K., Varambally, S., Palanisamy, N. and Chinnaiyan, A.M. (2009) Induced chromosomal proximity and gene fusions in prostate cancer. Science (New York, N.Y.). 326 (5957), pp.1230-1230.

Marsh, L.A., Carrera, S., Shandilya, J., Heesom, K.J., Davidson, A.D., Medler, K.F. and Roberts, S.G. (2017) BASP1 interacts with oestrogen receptor α and modifies the tamoxifen response. Cell Death & Disease. 8 (5), pp.e2771-e2771.

Martin, B.L. and Kimelman, D. (2012) Canonical Wnt signaling dynamically controls multiple stem cell fate decisions during vertebrate body formation. Developmental Cell. 22 (1), pp.223-232.

Mason, M. R. J., Lieberman, A. R., Grenningloh, G. and Anderson, P. N. (2002) Transcriptional upregulation of SCG10 and CAP-23 is correlated with regeneration

of the axons of peripheral and central neurons in vivo. Molecular and Cellular Neuroscience. 20(4), pp. 595-615.

Mavrou, A., Brakspear, K., Hamdollah-Zadeh, M., Damodaran, G., Babaei-Jadidi, R., Oxley, J., Gillatt, D.A., Ladomery, M.R., Harper, S.J., Bates, D.O. and Oltean, S. (2015) Serine-arginine protein kinase 1 (SRPK1) inhibition as a potential novel targeted therapeutic strategy in prostate cancer. Oncogene. 34 (33), pp.4311-4319.

Mayo, M.W., Wang, C.-Y., Drouin, S.S., Madrid, L.V., Marshall, A.F., Reed, J.C., Weissman, B.E. and Baldwin, A.S. (1999). WT1 modulates apoptosis by transcriptionally upregulating the bcl-2 proto-oncogene. The EMBO Journal, 18(14), pp.3990–4003.

Metzeler, K.H., Dufour, A., Benthaus, T., Hummel, M., Sauerland, M., Heinecke, A., Berdel, W.E., Büchner, T., Wörmann, B., Mansmann, U., Braess, J., Spiekermann, K., Hiddemann, W., Buske, C. and Bohlander, S.K. (2009) ERG expression is an independent prognostic factor and allows refined risk Stratification in cytogenetically normal acute myeloid leukemia: a comprehensive analysis of ERG, MN1, and BAALC transcript levels using oligonucleotide microarrays. 27 (30), pp.5031-5038.

Montano, G., Cesaro, E., Fattore, L., Vidovic, K., Palladino, C., Crescitelli, R., Izzo, P., Turco, M.C. and Costanzo, P. (2013) Role of WT1-ZNF224 interaction in the expression of apoptosis-regulating genes. Human Molecular Genetics. 22 (9), pp.1771-1782.

Moorthy, A.V., Chesney, R.W. and Lubinsky, M. (1987). Chronic renal failure and XY gonadal dysgenesis: “Frasier” syndrome--a commentary on reported cases. American journal of medical genetics. Supplement, 3, pp.297–302.

Moribe, T., Iizuka, N., Miura, T., Stark, M., Tamatsukuri, S., Ishitsuka, H., Hamamoto, Y., Sakamoto, K., Tamesa, T. and Oka, M. (2008). Identification of novel aberrant methylation of BASP1 and SRD5A2 for early diagnosis of hepatocellular carcinoma by genome-wide search. International journal of oncology, 33(5), pp.949–58.

Mosevitsky, M. I., Capony, J. P., Skladchikova, G. Y., Novitskaya, V. A., Plekhanov, A. Y. and Zakharov, V. V. (1997) The BASP1 family of myristoylated proteins abundant in axonal termini. Primary structure analysis and physico-chemical properties. Biochimie. 79(6), pp. 373-384. Mosevitsky, M. I., Novitskaya, V. A., Plekhanov, A. Y. and Skladchikova, G. Y. (1994) Neuronal protein GAP-43 is a member of novel group of brain acid-soluble proteins (BASPs). Neuroscience Research. 19(2), pp. 223-228.

Murthy, N., Subramanian, U., Anant, S. and Subramanian, N. (1999) The replication inhibition activity of the WT1 tumor suppressor protein resides in its N-terminal 298 amino acid region, and does not require specific binding of the protein to the replication origin sequence. 13 (6), pp.1275-80.

Nagai, N., Ohguchi, H., Nakaki, R., Matsumura, Y., Kanki, Y., Sakai, J., Aburatani, H. and Minami, T. (2018) Downregulation of ERG and FLI1 expression in endothelial cells triggers endothelial-to-mesenchymal transition. 14 (11), e1007826.

Nalini, V., Segu, R., Deepa, P.R., Khetan, V., Vasudevan, M. and Krishnakumar, S. (2013) Molecular insights on post-chemotherapy retinoblastoma by microarray gene expression analysis. Bioinformatics and Biology Insights. 7 pp.289-306.

Nam, R., Sugar, L., Yang, L., Encioiu, E., Stanimirovic, A., Yang, W. and Seth, A. (2007) Expression of TMPRSS2: ERG gene fusion in prostate cancer cells is an important prognostic factor for cancer progression. Cancer Res. 67 (9), pp.5673.

Narla, G., DiFeo, A., Yao, S., Banno, A., Hod, E., Reeves, H.L., Qiao, R.F., Camacho-Vanegas, O., Levine, A., Kirschenbaum, A., Chan, A.M., Friedman, S.L. and Martignetti, J.A. (2005) Targeted inhibition of the KLF6 splice variant, KLF6 SV1, suppresses prostate cancer cell growth and spread. Cancer Res. 65 (13), pp.5761.

Naro, C., Barbagallo, F., Chieffi, P., Bourgeois, C.F., Paronetto, M.P. and Sette, C. (2014) The centrosomal kinase NEK2 is a novel splicing factor kinase involved in cell survival. Nucleic Acids Research. 42 (5), pp.3218-3227.

Ngo, J. C. K., Gullingsrud, J., Giang, K., Yeh, M. J., Fu, X., Adams, J. A., McCammon, J. A. and Ghosh, G. (2007) SR Protein Kinase 1 Is Resilient to Inactivation. Structure. 15(1), pp. 123-133.

Nikolakaki, E., Kohen, R., M Hartmann, A., Stamm, S., Georgatsou, E. and Giannakouros, T. (2001) Cloning and characterization of an alternatively spliced form of SR protein kinase 1 that interacts specifically with scaffold attachment Factor-B. 276 (43), pp.40175-40182.

Ogryzko, V. V., Schiltz, R. L., Russanova, V., Howard, B. H. and Nakatani, Y. (1996) The transcriptional coactivators p300 and CBP Are histone acetyltransferases. *Cell*. 87(5), pp. 953-959.

Oltean, S., Gammons, M., Hulse, R., Hamdollah-Zadeh, M., Mavrou, A., Donaldson, L., Salmon, A., Harper, S., Ladomery, M. and Bates, D. (2012) SRPK1 inhibition in vivo: modulation of VEGF splicing and potential treatment for multiple diseases. Biochemical Society Transactions. 40 (4), pp.831-835.

Parenti, R., Cardile, V., Graziano, A.C.E., Parenti, C., Venuti, A., Bertuccio, M.P., Furno, D.L. and Magro, G. (2014) Wilms' tumor gene 1 (WT1) silencing inhibits proliferation of malignant peripheral nerve sheath tumor sNF96.2 cell line. PloS On. 9 (12), pp.e114333.

Paschka, P., Marcucci, G., Ruppert, A.S., Whitman, S.P., Mrózek, K., Maharry, K., Langer, C., Baldus, C.D., Zhao, W., Powell, B.L., Baer, M.R., Carroll, A.J., Caligiuri, M.A., Kolitz, J.E., Larson, R.A. and Bloomfield, C.D. (2008) Wilms' Tumor 1 Gene Mutations Independently Predict Poor Outcome in Adults With Cytogenetically Normal Acute Myeloid Leukemia: A Cancer and Leukemia Group B Study. Jco. 26 (28), pp.4595-4602.

Plocinik, R.M., Li, S., Liu, T., Hailey, K.L., Whitesides, J., Ma, C.-T., Fu, X.-D., Gosh, G., Woods, V.L., Jennings, P.A. and Adams, J.A. (2011). Regulating SR protein phosphorylation through regions outside the kinase domain of SRPK1. Journal of molecular biology, 410(1), pp.131–45

Pore, N., Jiang, Z., McGarry, M. and Maity, A. (2005) Iressa (gefitinib) decreases vascular endothelial growth factor (VEGF) expression by hypoxia inducible factor-1 (HIF-1) independent and dependent mechanisms. Cancer Research. 65 (9), pp.476-476.

Pratt, W.B. and Toft, D.O. (2003). Regulation of signaling protein function and trafficking by the hsp90/hsp70-based chaperone machinery. Experimental biology and medicine, 228(2), pp.111–33

Rauscher, F., Morris, J., Tournay, O., Cook, D. and Curran, T. (1990) Binding of the Wilms' tumor locus zinc finger protein to the EGR-1 consensus sequence. Science. 250 (4985), pp.1259-1262.

Reddy, E.S., Rao, V.N. and Papas, T.S. (1987) The ERG gene: a human gene related to the ETS oncogene. Proceedings of the National Academy of Sciences of the United States of America. 84 (17), pp.6131-6135.

Reeves, H. L., Narla, G., Ogunbiyi, O., Haq, A. I., Katz, A., Benzeno, S., Hod, E., Harpaz, N., Goldberg, S., Tal-Kremer, S., Eng, F. J., Arthur, M. J. P., Martignetti, J. A. and Friedman, S. L. (2004) Kruppel-like factor 6 (KLF6) is a tumor-suppressor gene frequently inactivated in colorectal cancer. Gastroenterology. 126(4), pp. 1090-1103.

Ren, G., Sheng, L., Liu, H., Sun, Y., An, Y. and Li, Y. (2015) The Crucial Role of SRPK1 in TGF-β-induced proliferation and apoptosis in the esophageal squamous Cell carcinomas. Medical Oncology. 32(7), pp. 209-219.

Rennel, E.S., Harper, S.J. and Bates, D.O. (2009) Therapeutic potential of manipulating VEGF splice isoforms in oncology. Future Oncology. 5 (5), pp.703-712.

Rose, E. A., Glaser, T., Jones, C., Smith, C. L., Lewis, W. H., Call, K. M., Minden, M., Champagne, E., Bonetta, L., Yeger, H. and Housman, D. E. (1990) Complete physical map of the WAGR region of 11p13 localizes a candidate Wilms' tumor gene. Cell. 60(3), pp. 495-508.

Salesse, S., Dylla, S.J. and Verfaillie, C.M. (2004). P210BCR/ABL-induced alteration of pre-mRNA splicing in primary human CD34+ hematopoietic progenitor cells. Leukemia, 18(4), pp.727–33

Sanidas, I., Kotoula, V., Ritou, E., Daans, J., Lenz, C., Mairhofer, M., Daniilidou, M., Kolbus, A., Kruft, V., Ponsaerts, P. and Nikolakaki, E. (2010) The ratio of SRPK1/SRPK1a regulates erythroid differentiation in K562 leukaemic cells.

Biochimica Et Biophysica Acta (BBA) - Molecular Cell Research. 1803 (12), pp.1319-1331.

Sanidas, I., Kotoula, V., Ritou, E., Daans, J., Lenz, C., Mairhofer, M., Daniilidou, M., Kolbus, A., Kruft, V., Ponsaerts, P. and Nikolakaki, E. (2010) The ratio of SRPK1/SRPK1a regulates erythroid differentiation in K562 leukaemic cells. Biochimica Et Biophysica Acta (BBA) - Molecular Cell Research. 1803(12), pp. 1319-1331.

Schenk, P.W., Boersma, A.W., Brandsma, J.A., den Dulk, H., Burger, H., Stoter, G., Brouwer, J. and Nooter, K. (2001). SKY1 is involved in cisplatin-induced cell kill in Saccharomyces cerevisiae, and inactivation of its human homologue, SRPK1, induces cisplatin resistance in a human ovarian carcinoma cell line. Cancer research, 61(19), pp.6982–6.

Scholz, H. and Kirschner, K.M. (2005). A role for the Wilms' tumor protein WT1 in organ development. Physiology (Bethesda, Md.), 20, pp.54–9.

Schwartzman, J., Mongoue-Tchokote, S., Gibbs, A., Gao, L., Corless, C.L., Jin, J., Zarour, L., Higano, C., True, L.D., Vessella, R.L., Wilmot, B., Bottomly, D., McWeeney, S.K., Bova, G.S., Partin, A.W., Mori, M. and Alumkal, J. (2011) A DNA methylation microarray-based study identifies ERG as a gene commonly methylated in prostate cancer. Epigenetics. 6 (10), pp.1248-1256.

Shafe, A., Davies, J.A., Spraggon, L., Michael, L., Ladomery, M., Hastie, N. and Hohenstein, P. (2003) Development of an siRNA-based method for repressing specific genes in renal organ culture and its use to show that the WT1 tumour suppressor is required for nephron differentiation. Human Molecular Genetics. 13 (2), pp.235-246.

Shafe, A., Davies, J.A., Spraggon, L., Michael, L., Ladomery, M., Hastie, N. and Hohenstein, P. (2003) Development of an siRNA-based method for repressing specific genes in renal organ culture and its use to show that the WT1 tumour suppressor is required for nephron differentiation. Human Molecular Genetics. 13 (2), pp.235-246.

Shepard, P.J. and Hertel, K.J. (2009) The SR protein family. Genome Biology. 10 (10), pp.242-242.

Shon, W., L Folpe, Andrew and J Fritchie,Karen (2014) ERG expression in chondrogenic bone and soft tissue tumors. Journal of clinical pathology. 68, pp.125-9.

Siqueira, R.P., Barbosa, Ã., Polêto, M.D., Righetto, G.L., Seraphim, T.V., Salgado, R.L., Ferreira, J.G., Barros, M.V.d.A., de Oliveira, L.L., Laranjeira, A.B.A., Almeida, M., Júnior, A.S., Fietto, J.L.R., Kobarg, J., de Oliveira, E.B., Teixeira, R.R., Borges, J., Yunes, J.A. and Bressan, G.C. (2015) Potential antileukemia effect and structural analyses of SRPK inhibition by N-(2-(Piperidin-1-yl)-5-(Trifluoromethyl)Phenyl)Isonicotinamide (SRPIN340). Plos One. 10 (8), pp.e0134882.

Skotheim, R. I. and Nees, M. (2007) Alternative splicing in cancer: Noise, functional, or systematic? The International Journal of Biochemistry & Cell Biology. 39(7), pp. 1432-1449.

Spector, D.L. and Lamond, A.I. (2011) Nuclear speckles. Cold Spring Harbor Perspectives in Biology. 3 (2), pp.a000646.

Sugiyama, H. (2010) WT1 (Wilms' Tumor Gene 1): Biology and cancer immunotherapy. Japanese Journal of Clinical Oncology. 40 (5), pp.377-387.

Tang, H., Wang, Y., Zhang, B., Xiong, S., Liu, L., Chen, W., Tan, G. and Li, H. (2017) High brain acid soluble protein 1(BASP1) is a poor prognostic factor for cervical cancer and promotes tumor growth. Cancer Cell International. 17 pp.97; 97-97.

Tazi, J., Bakkour, N. and Stamm, S. (2009) Alternative splicing and disease. Biochimica Et Biophysica Acta (BBA) - Molecular Basis of Disease. 1792(1), pp. 14-26.

Thoms, J., Birger, Y., Foster, S., Knezevic, K., Kirschenbaum, Y., Chandrakanthan, V., Von Jonquieres, G., Spensberger, D., W Wong, ,Jason, Helen Oram, S., J Kinston, ,Sarah, Groner, Y., Lock, R., Mackenzie, K., Göttgens, B., Izraeli, S. and Pimanda, J. (2011) ERG promotes T-Acute lymphoblastic leukemia and is transcriptionally regulated in leukemic cells by a stem cell Enhancer. 117 (26), pp.7079-89.

Tomlins, S.A., Laxman, B., Varambally, S., Cao, X., Yu, J., Helgeson, B.E., Cao, Q., Prensner, J.R., Rubin, M.A., Shah, R.B., Mehra, R. and Chinnaiyan, A.M. (2008) Role of the TMPRSS2-ERG gene fusion in prostate cancer. Neoplasia (New York, N.Y.). 10 (2), pp.177-188.

Tomlins, S.A., Rhodes, D.R., Perner, S., Dhanasekaran, S.M., Mehra, R., Sun, X., Varambally, S., Cao, X., Tchinda, J., Kuefer, R., Lee, C., Montie, J.E., Shah, R.B., Pienta, K.J., Rubin, M.A. and Chinnaiyan, A.M. (2005) Recurrent fusion of TMPRSS2 and ETS transcription factor genes in prostate cancer. Science. 310 (5748), pp.644-8.

Toska, E., Shandilya, J., Goodfellow, S.J., Medler, K.F. and Roberts, S.G.E. (2014) Prohibitin is required for transcriptional repression by the WT1-BASP1 complex. Oncogene. 33 (43), pp.5100-5108.

Toska, E., Campbell, H.A., Shandilya, J., Goodfellow, S.J., Shore, P., Medler, K.F. and Roberts, S.G.E. (2012) Repression of transcription by WT1-BASP1 requires the

myristoylation of BASP1 and the PIP2-dependent recruitment of histone deacetylase. Cell Reports. 2 (3), pp.462-469.

Toska, E., Campbell, H.A., Shandilya, J., Goodfellow, S.J., Shore, P., Medler, K.F. and Roberts, S.G.E. (2012) Repression of transcription by WT1-BASP1 requires the myristoylation of BASP1 and the PIP2-dependent recruitment of histone deacetylase. Cell Reports. 2 (3), pp.462-469.

Uzor, S., Zorzou, P., Bowler, E., Porazinski, S., Wilson, I. and Ladomery, M. (2018) Autoregulation of the human splice factor kinase CLK1 through exon skipping and intron retention. *Gene*. 670pp. 46-54.

Vanaja, D.K., Cheville, J.C., Iturria, S.J. and Young, C.Y.F. (2003) Transcriptional silencing of zinc finger protein 185 identified by expression profiling is associated with prostate cancer progression. Cancer Res. 63 (14), pp.3877-82.

Venables, J.P. (2006) Unbalanced alternative splicing and its significance in cancer. Bioessays. 28 (4), pp.378-386.

Wagner, K., El Maï, M., Ladomery, M., Belali, T., Leccia, N., Michiels, J. and Wagner, N. (2019) Altered VEGF splicing isoform balance in tumor endothelium involves activation of splicing factors Srpk1 and Srsf1 by the Wilms' Tumor Suppressor WT1. Cells. 8 (1), pp.41-59.

Wang, H., Ge, W., Jiang, W., Li, D. and Ju, X. (2017) SRPK1 siRNA suppresses K562 cell growth and induces apoptosis via the PARP caspase3 pathway. Molecular medicine reports. 17 (1), pp.2070-76.

Wang, P., Zhou, Z., Hu, A., de Albuquerque, C.P., Zhou, Y., Hong, L., Sierecki, E., Ajiro, M., Kruhlak, M., Harris, C., Guan, K., Zheng, Z., Newton, A.C., Sun, P., Zhou, H. and Fu, X. (2014) Both decreased and increased SRPK1 levels promote cancer by

interfering with PHLPP-mediated dephosphorylation of Akt. Molecular Cell. 54 (3), pp.378-391.

Weatheritt, R. J., Sterne-Weiler, T., & Blencowe, B. J. (2016). The ribosome-engaged landscape of alternative splicing. Nature structural & molecular biology, 23(12), 17–23.

Wilhelm, D. and Englert, C. (2002) The wilms tumor suppressor WT1 regulates early gonad development by activation of Sf1. Genes & development. 16 (13), pp. 1839-51.

Wu, F., Li, J., Du, X., Weisan, Z., Lei, P. and Zhang, Q. (2017) Chimeric antibody targeting SRPK-1 in the treatment of non-small cell lung cancer by inhibiting growth, migration and invasion. 16 (2), pp.2121-27.

YANG, L., MEI, Q., ZIELINSKA-KWIATKOWSKA, A., MATSUI, Y., BLACKBURN, M.L., BENEDETTI, D., KRUMM, A.A., TABORSKY, G.J. and CHANSKY, H.A. (2003) An ERG (ets-related gene)-associated histone methyltransferase interacts with histone deacetylases 1/2 and transcription co-repressors mSin3A/B. Biochemical Journal. 369 (3), pp.651-657

Yang, S., Zhang, Y., Zhao, X., Wang, J. and Shang, J. (2016). Micro RNA-361 targets Wilms' tumor 1 to inhibit the growth, migration and invasion of non-small-cell lung cancer cells. Molecular Medicine Reports, 14(6), pp.5415–5421

Yi, N., Xiao, M., Jiang, F., Liu, Z., Ni, W., Lu, C., Ni, R. and Chen, W. (2018) SRPK1 is a poor prognostic indicator and a novel potential therapeutic target for human colorectal cancer. OncoTargets and Therapy. 11 pp.5359-5370.

Yin, Z., Ren, J. and Guo, W. (2015) Sarcomeric protein isoform transitions in cardiac muscle: A journey to heart failure. Biochimica Et Biophysica Acta (BBA) - Molecular Basis of Disease. 1852 (1), pp.47-52.

Yuan, L., Nikolova-Krstevski, V., Zhan, Y., Kondo, M., Bhasin, M., Varghese, L., Yano, K., Carman, C.V., Aird, W.C. and Oettgen, P. (2009) Anti-inflammatory effects of the ETS factor ERG in endothelial cells are mediated through transcriptional repression of the interleukin-8 gene. Circulation Research. 104 (9), pp.1049-1057.

Zhao, N. and Zhang, J. (2018) Role of alternative splicing of VEGF-A in the development of atherosclerosis. Aging. 10 (10), pp.2695-2708.

Zhong, Xiang-Yang et al. (2009) Regulation of SR protein phosphorylation and alternative splicing by modulating kinetic interactions of SRPK1 with molecular chaperones. Genes & development vol. 23 (4), pp. 482-95.

Zhou, L., Fu, L., Lv, N., Liu, J., Li, Y., Chen, X., Xu, Q., Chen, G., Pang, B., Wang, L., Li, Y., Zhang, X. and Yu, L. (2018) Methylation-associated silencing of BASP1 contributes to leukemogenesis in t (8; 21) acute myeloid leukemia. Experimental & Molecular Medicine. 50 (4), pp.44; 44-44.

Zhou, Z. and Fu, X. (2013) Regulation of splicing by SR proteins and SR protein-specific kinases. Chromosoma. 122 (3), pp.191-207.

Zhou, Z., Qiu, J., Wen, L., Zhou, Y., Plocinik, R.M., Li, H., Hu, Q., Ghosh, G., Adams, J.A., Rosenfeld, M.G. and Fu, X. (2012) The Akt-SRPK-SR Axis constitutes a major pathway in transducing EGF signaling to regulate alternative splicing in the nucleus. Molecular cell. 47 (3), pp.422-33.

9 Appendices

9.1 Plasmid preps

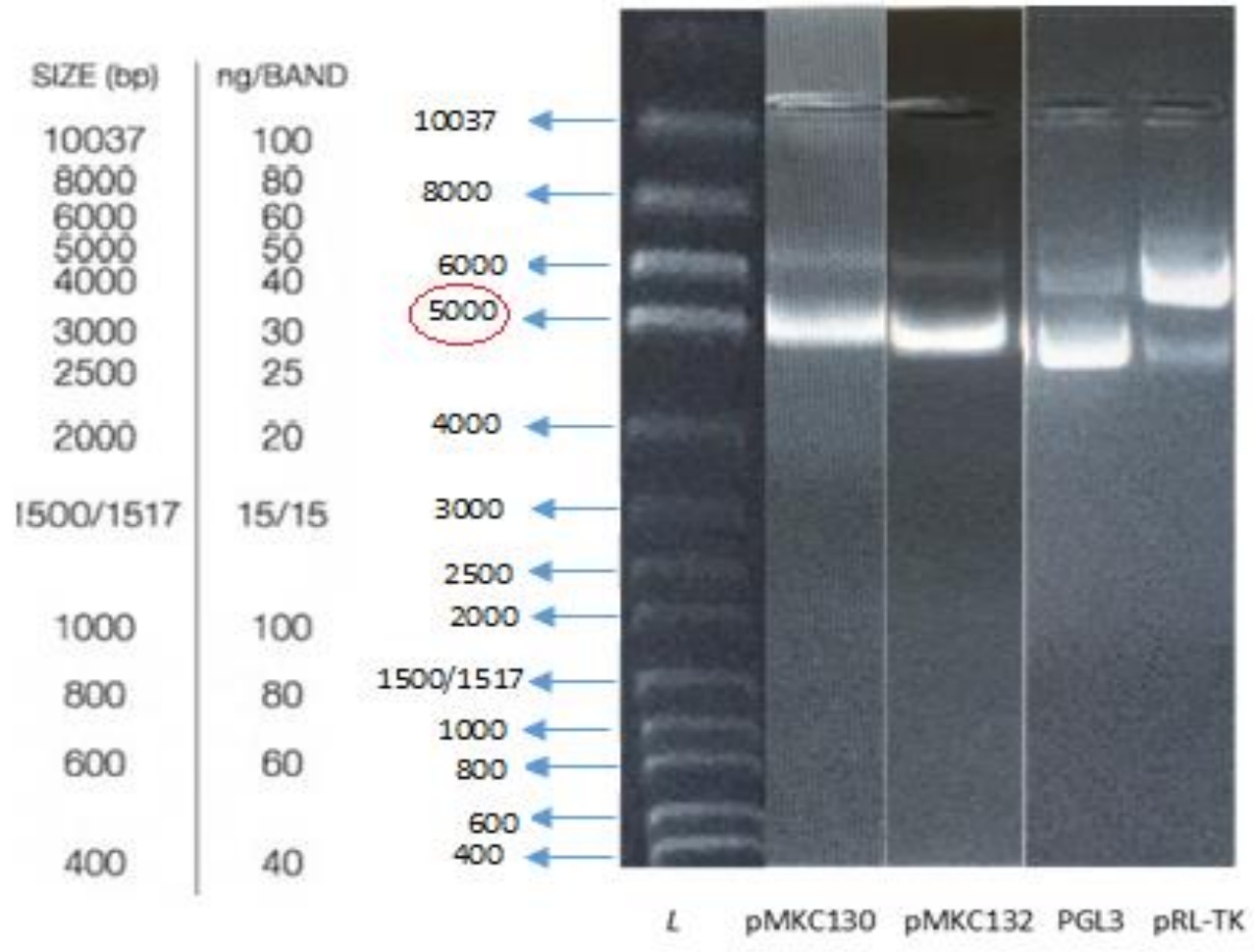

Figure 9. 1 Plasmid preparation.

Miniprepped plasmids separated by 1% agarose gel electrophoresis for 45 minutes at 100 V against. Both plasmids at the approximate size of 5000bp

Plasmid Midipreps

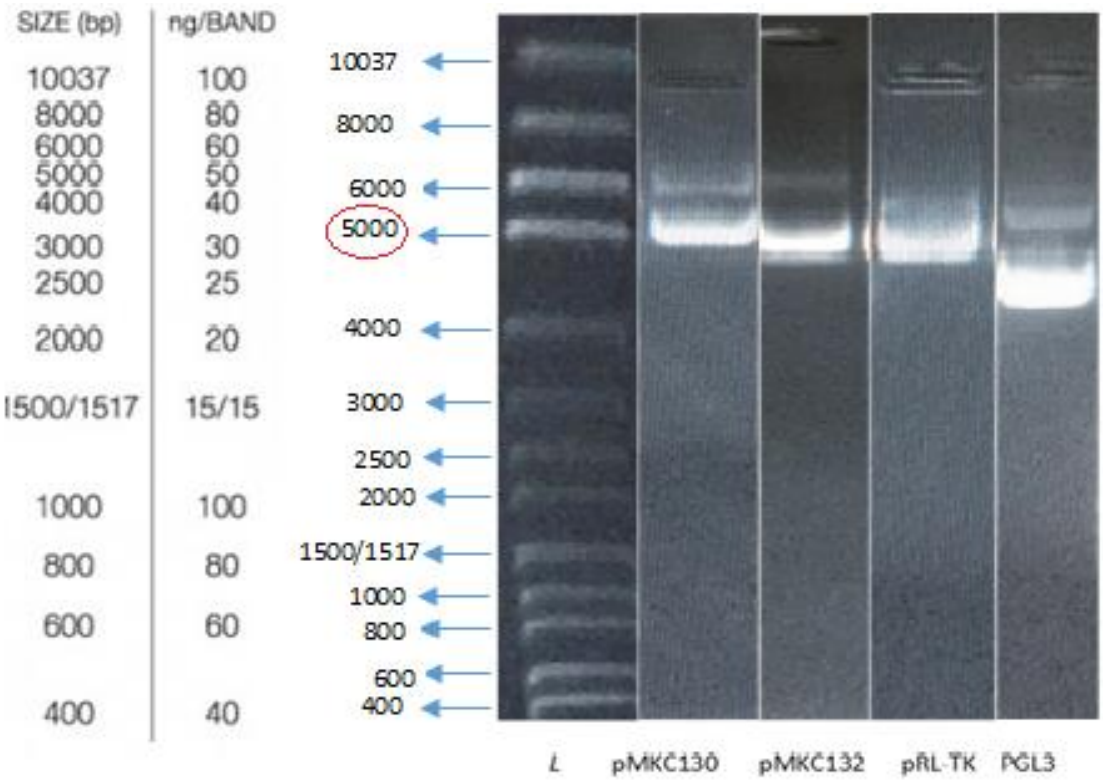

Figure 9. 2 Plasmid Midiprep

Midiprep plasmid running in 1% agarose gel for 45 minutes. The yield of both plasmids at the approximate size of 5000bp.

9.2 Restriction digests and plasmids validations

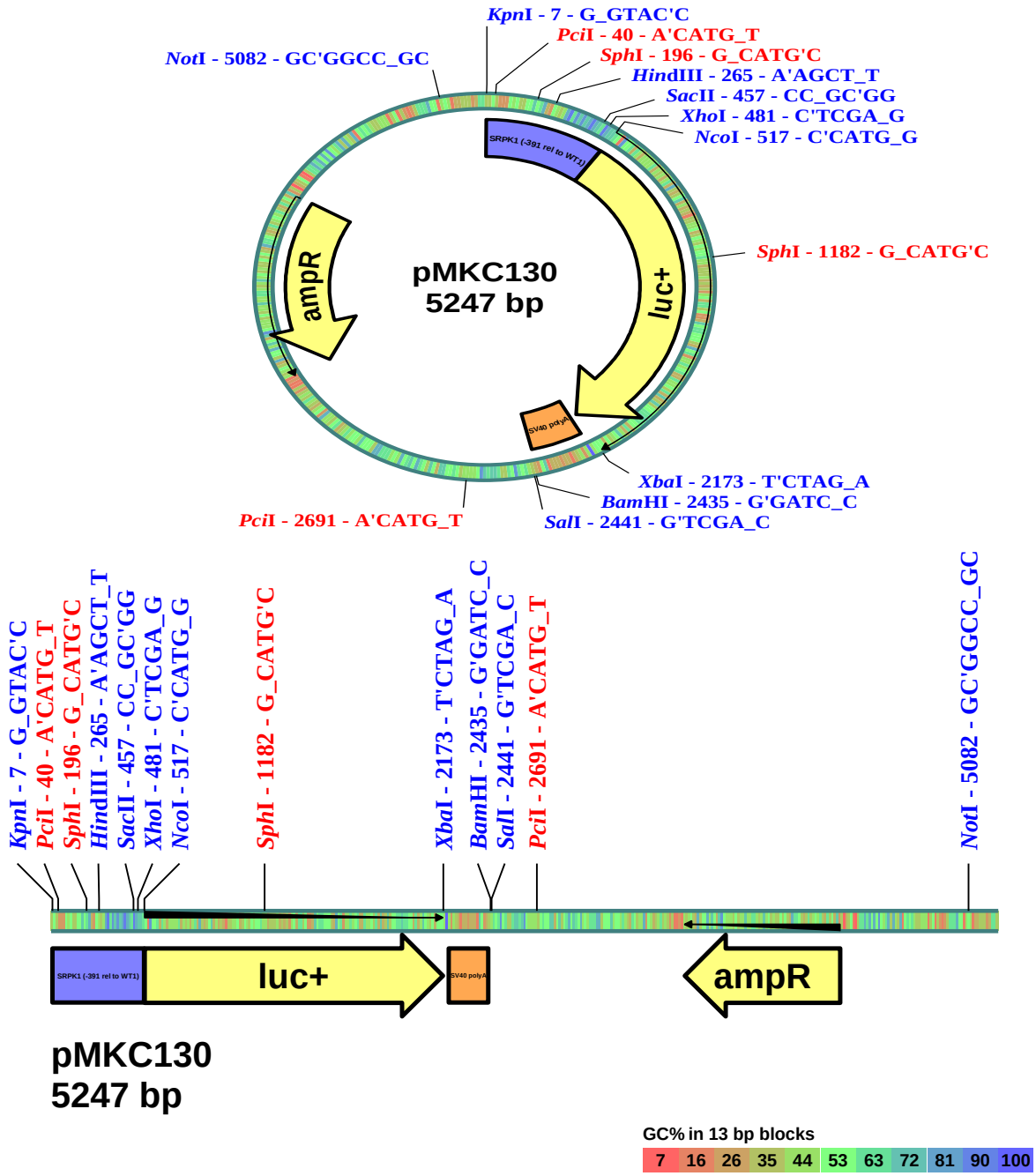

Figure 9. 3 Wild type SRPK1 promoter.

pMKC130; PGL3 basic vector with 511 bp (-391 relative to WT1) human SRPK1 promoter)

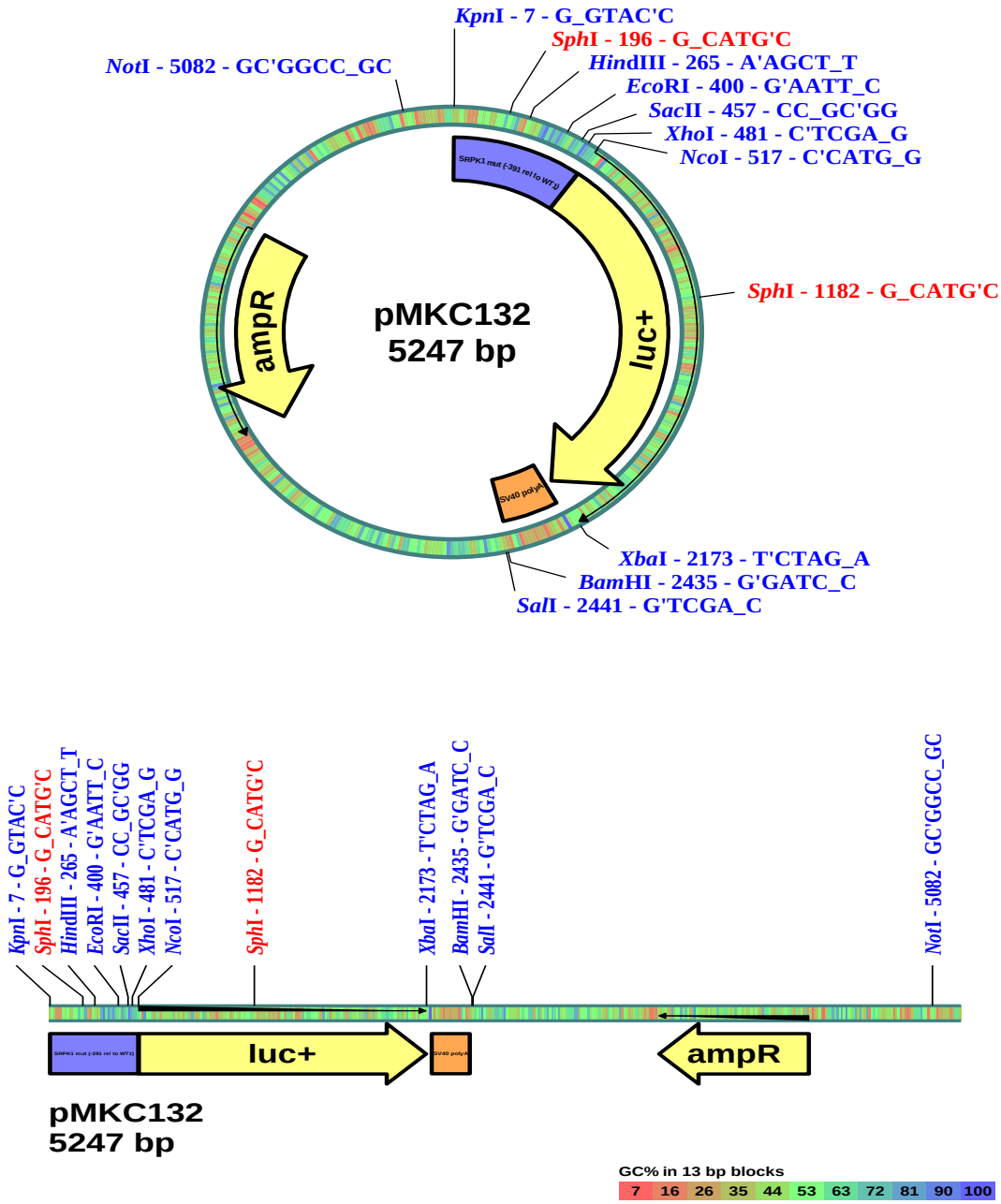

Figure 9. 4 Mutant SRPK1 promoter

pMKC132; PGL3 basic vector with mutant 511 bp (-391 relative to WT1) human SRPK1 promoter with (GGGGCGGGGG replaced by GAATTCAAAA =EcoRI). To help distinguish pMKC130 from pMKC132, an additional EcoRI restriction enzyme site has been created within the mutagenized WT1 binding site in plasmid pMKC132.

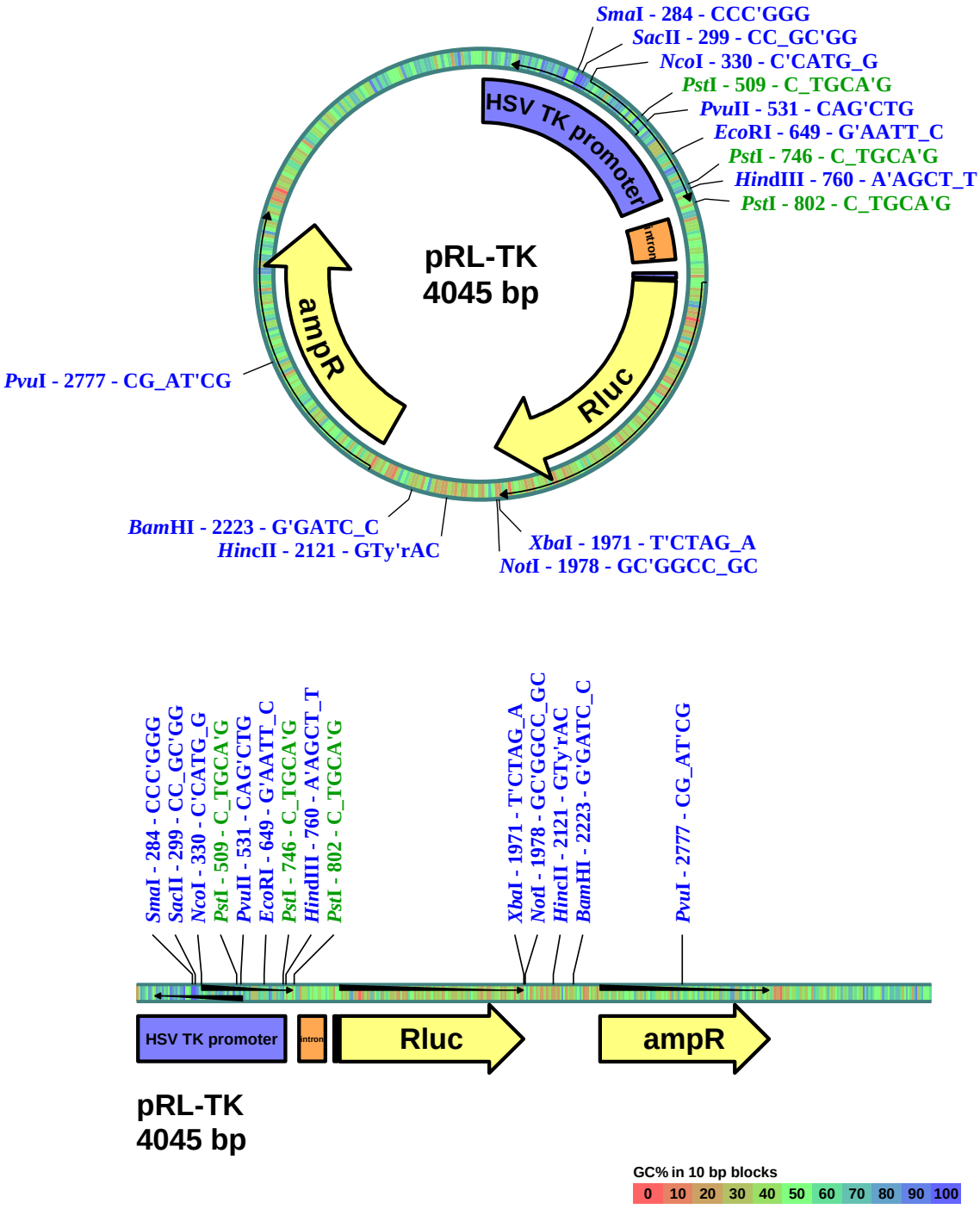

Figure 9. 5: Firefly and Renilla Luciferase Reporter Vectors.

Plasmid pRL-TK (ampicillin resistant plasmid containing Renilla luciferase gene).

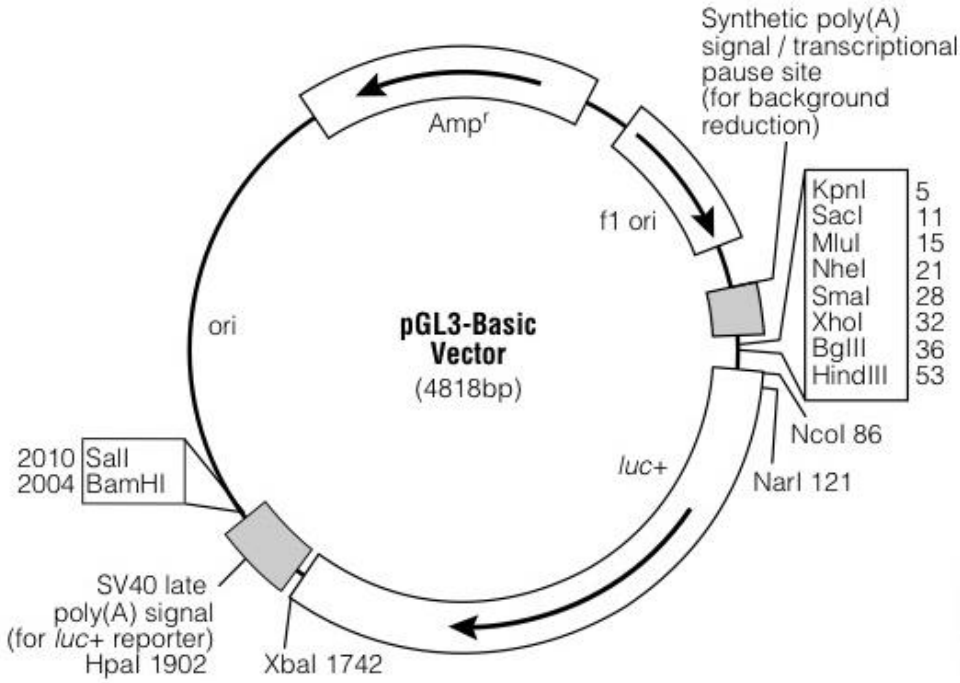

Figure 9. 6 PGL3 plasmid map

PGL3 basic vector contains a modified firefly luciferase gene (luc+) and a gene conferring ampicillin resistance in *E. coli*.

Restriction digests of pGL3 plasmids

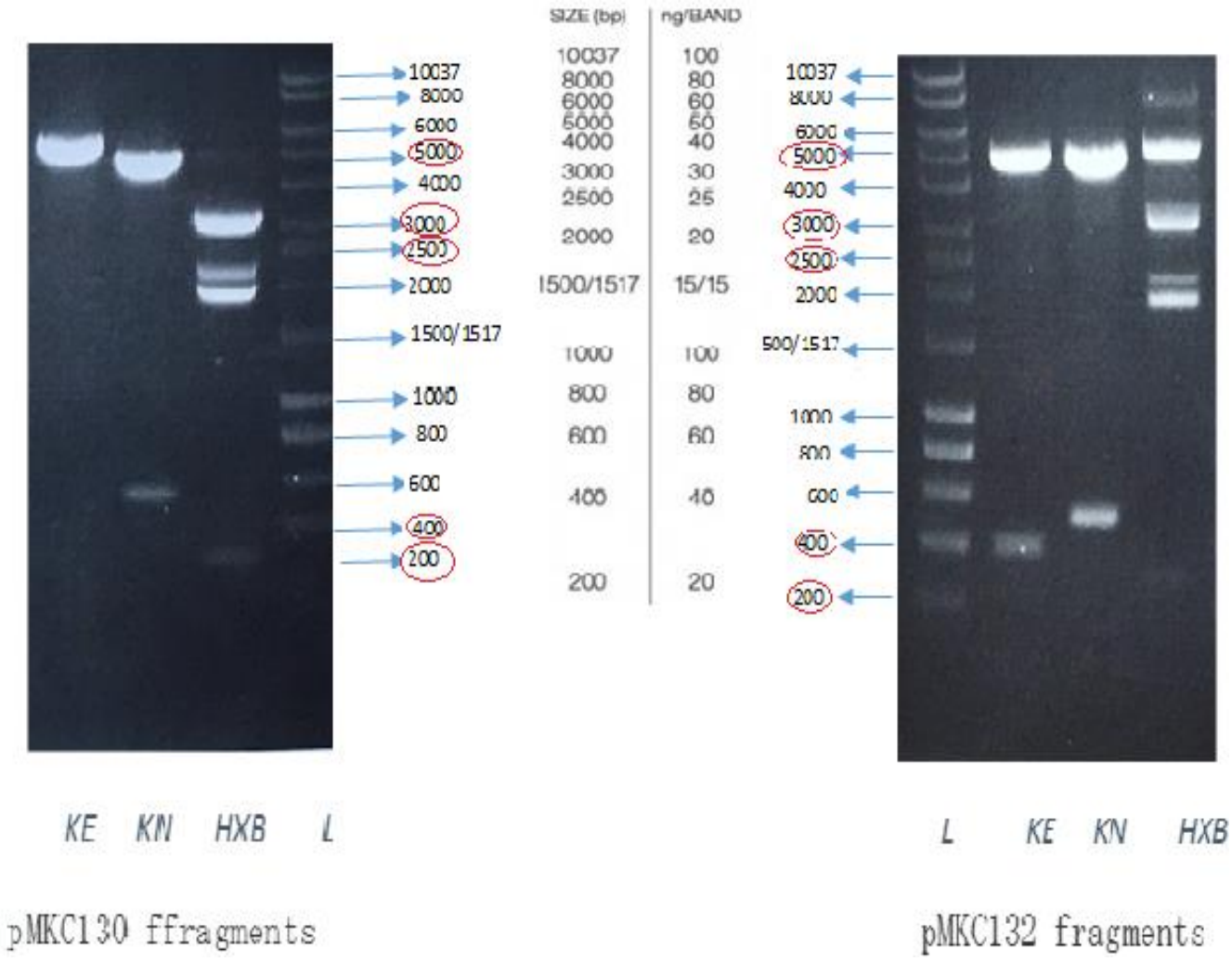

Figure 9. 7 Enzymes digests.

Restriction enzymes digests KE (KpnI &EcoRI), KN (KpnI & Nco I) and HXB(XbaI, HindIII & BamHI) and using HyperLadder™ 1kb DNA marker. Then separated in 1% agarose gel for 45 minutes.

Plasmid	Restriction enzyme	Resulted segments
pMKC130	(KpnI and EcoRI)	single fragment of 5000 bp (no EcoRI enzyme site)
	(KpnI and Nco I)	2 fragments of 5000bp (contains ampicillin resistance and luciferase sequences) and 400bp (contains sequence of interest; in SRPK1 -391 relative to WT1)
	(HindIII , XbaI and,BAMIII)	3 fragment of 3000bp (ampicillin resistance sequence) 2500bp (luciferase sequence) and 200bp (part of the promoter sequence)
pMKC132	(KpnI and EcoRI)	2 fragments of 400bp (contains sequence of interest; SRPK1 mut -391 relative to WT1) and 5000bp (contains ampicillin resistance and luciferase sequences)
	(KpnI and Nco I)	2 fragments of 5000bp (ampR and Luc+) and 510bp (sequence of interest)
	(HindIII , XbaI and,BAMIII)	3 fragments;3000bp (ampicillin resistance sequence) 2500bp (luciferase sequence) and 200bp (part of the promoter sequence)

***Table 9. 1: Results for restriction digests for the wiled type SRPK1 promoter (*pMKC130) & *mutant SRPK1 promoter* (pMKC132).**

Restriction digests of pCDNA-BASP1 plasmids

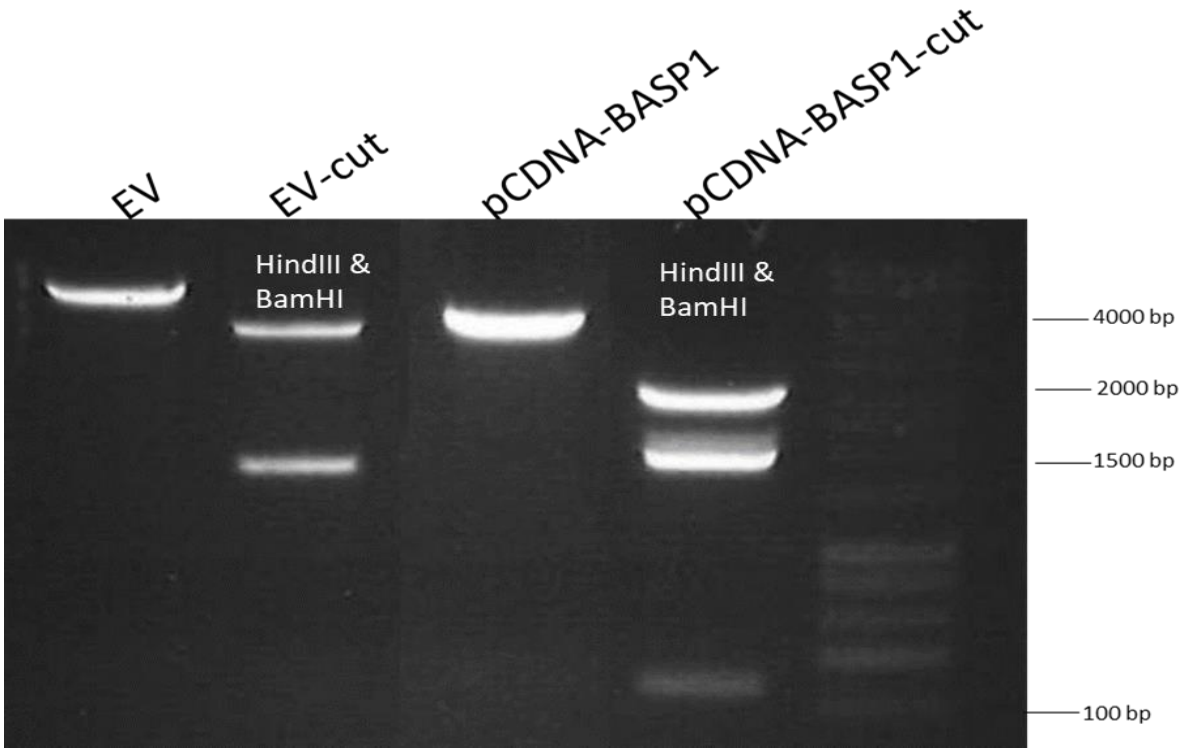

Figure 9. 8 Restriction digests of BASP1 plasmids

Restriction enzymes digests using HindIII & BamHI and using HyperLadder™ 1kb DNA marker. Then separated in 1% agarose gel for 45 minutes.

Linearization of ERG plasmids

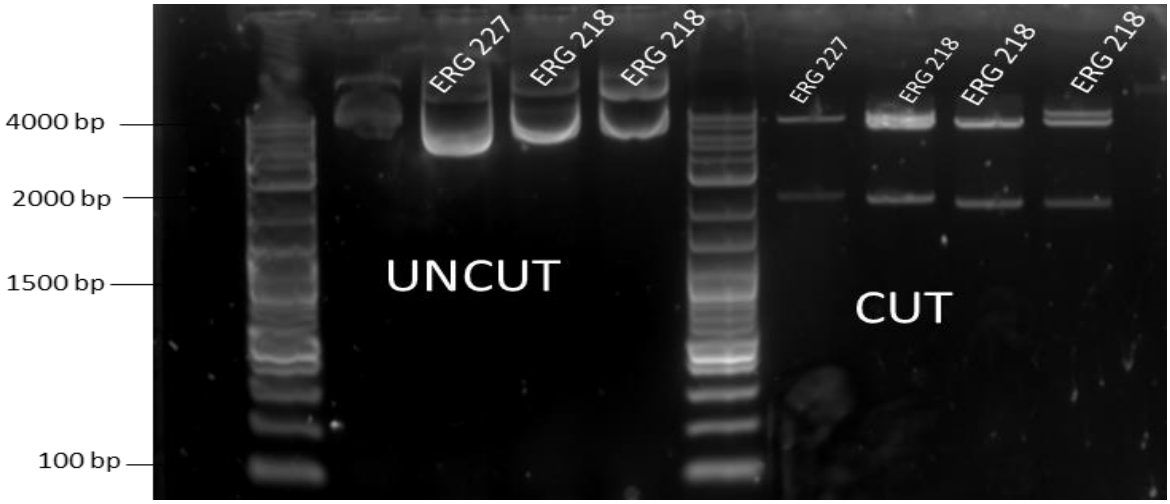

Figure 9. 9 Restriction digests of ERG plasmids

Restriction enzymes Double digest using XhoI and SalI and using HyperLadder™ 1kb DNA marker. Then separated in 1% agarose gel for 45 minutes.

ERG (-/+7b) plasmids validation; DDK tag western blots

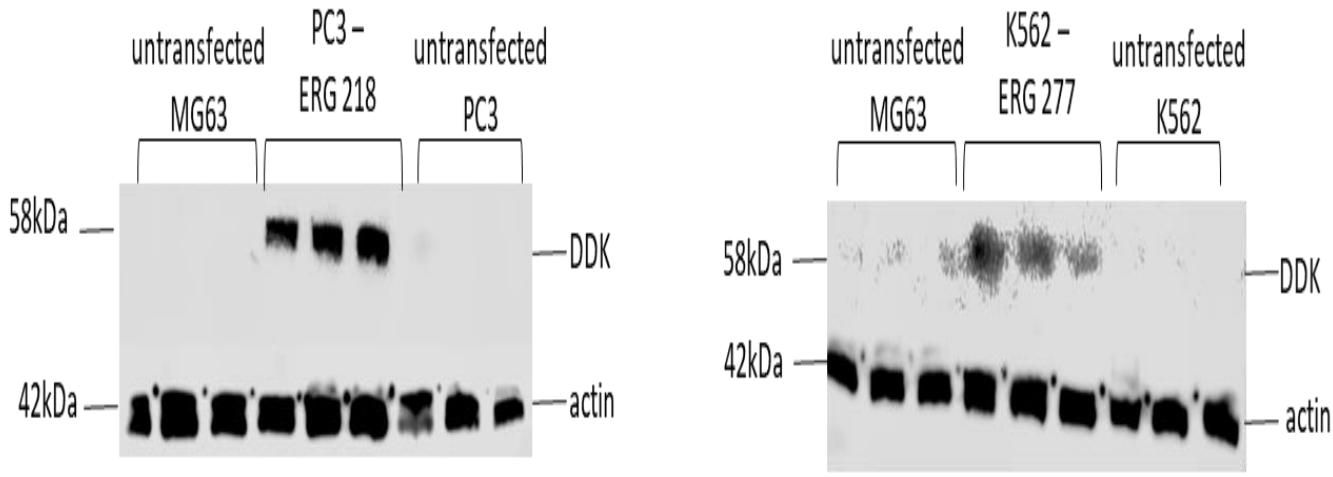

Figure 9. 10: DDK tag western blots

PC3 and K562 Cells were transfected with ERG 218/227 plasmids where the protein has DDK as epitope tag. The cell lysates were collected after 48 hours. Lysates from MG63, PC3 and K562 cells were used as negative controls. Then western blot was performed using Monoclonal ANTI-FLAG® M2 antibody against DDK. Actin was used as a loading control. Three independent transfections are shown.

9.3 Sequencing and NCBI Nucleotide Blast of Chip pull downs

Figure 9. 11: WT1-SRPK1 pull down sequencing

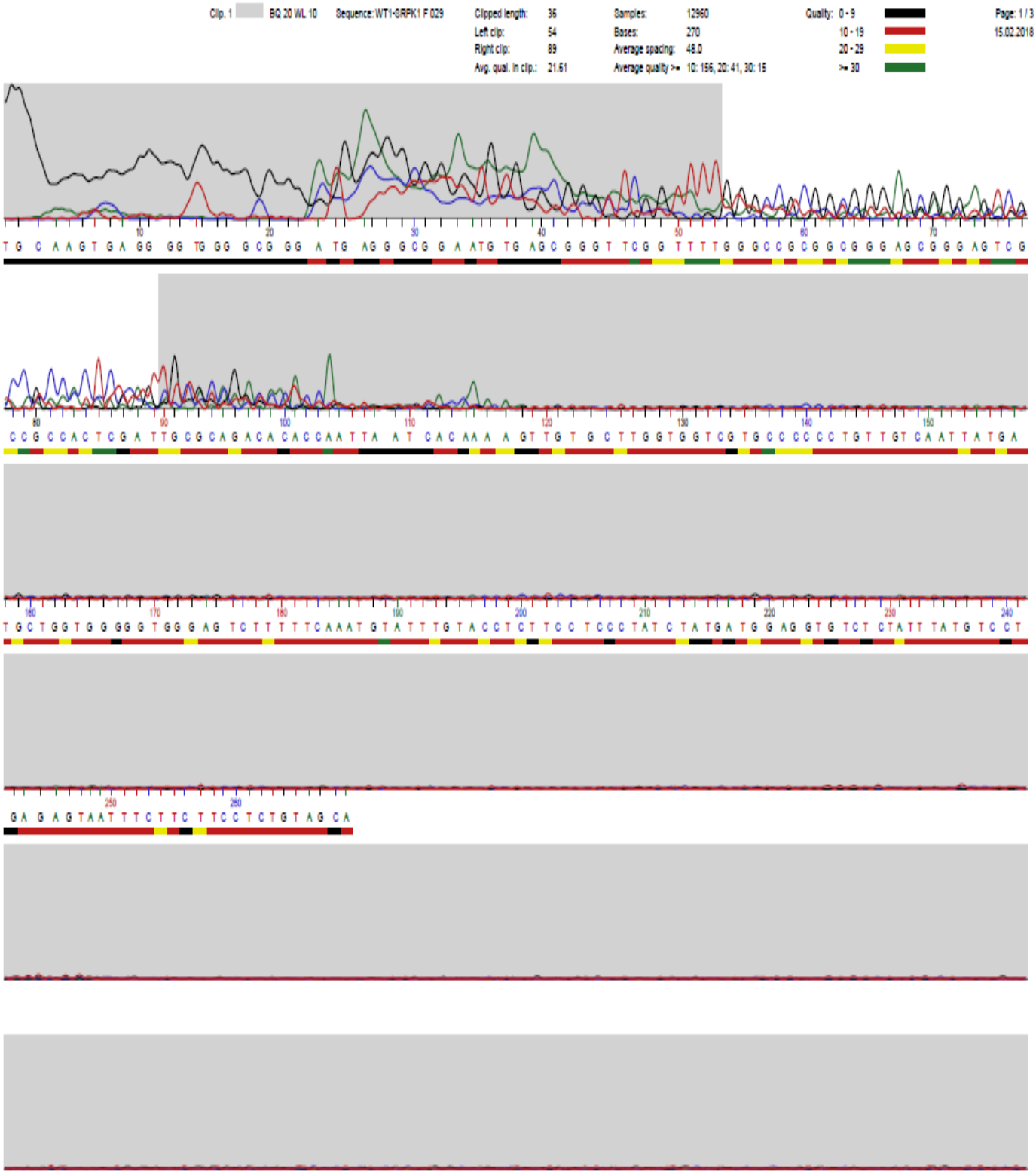


Clip. 1
BQ 20 WL 10
Sequence: WT1-GRPK1 F 029
Clipped length: 36
Left clip: 54
Right clip: 89
Avg. qual. in clip.: 21.61
Samples: 12960
Bases: 270
Average spacing: 48.0
Average quality >= 10: 156, 20: 41, 30: 15
Quality: 0 - 9
10 - 19
20 - 29
>= 30
Page: 2 / 3
15.02.2018

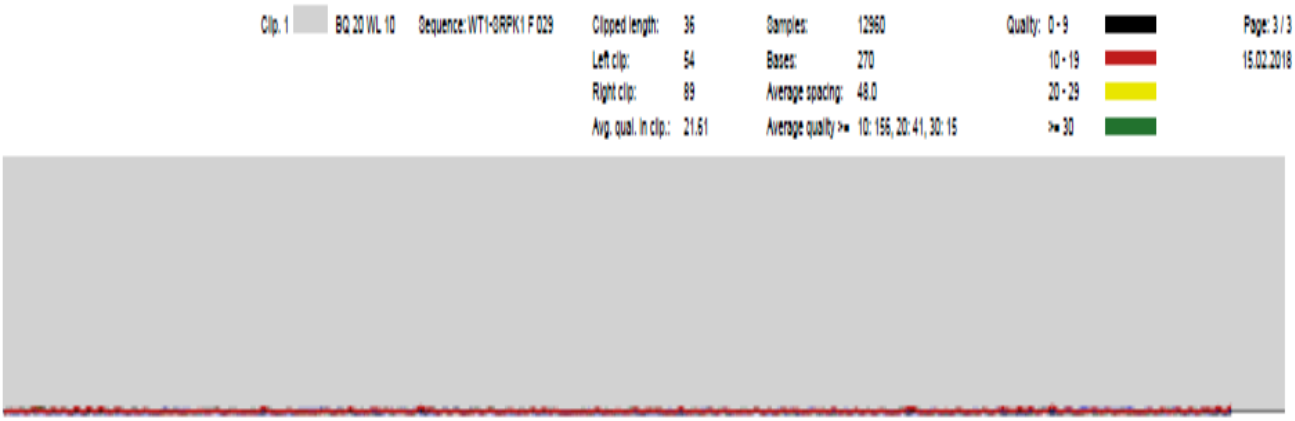

Figure 9. 12: WT1-SRPK1 sequencing result; NCBI Nucleotide Blast

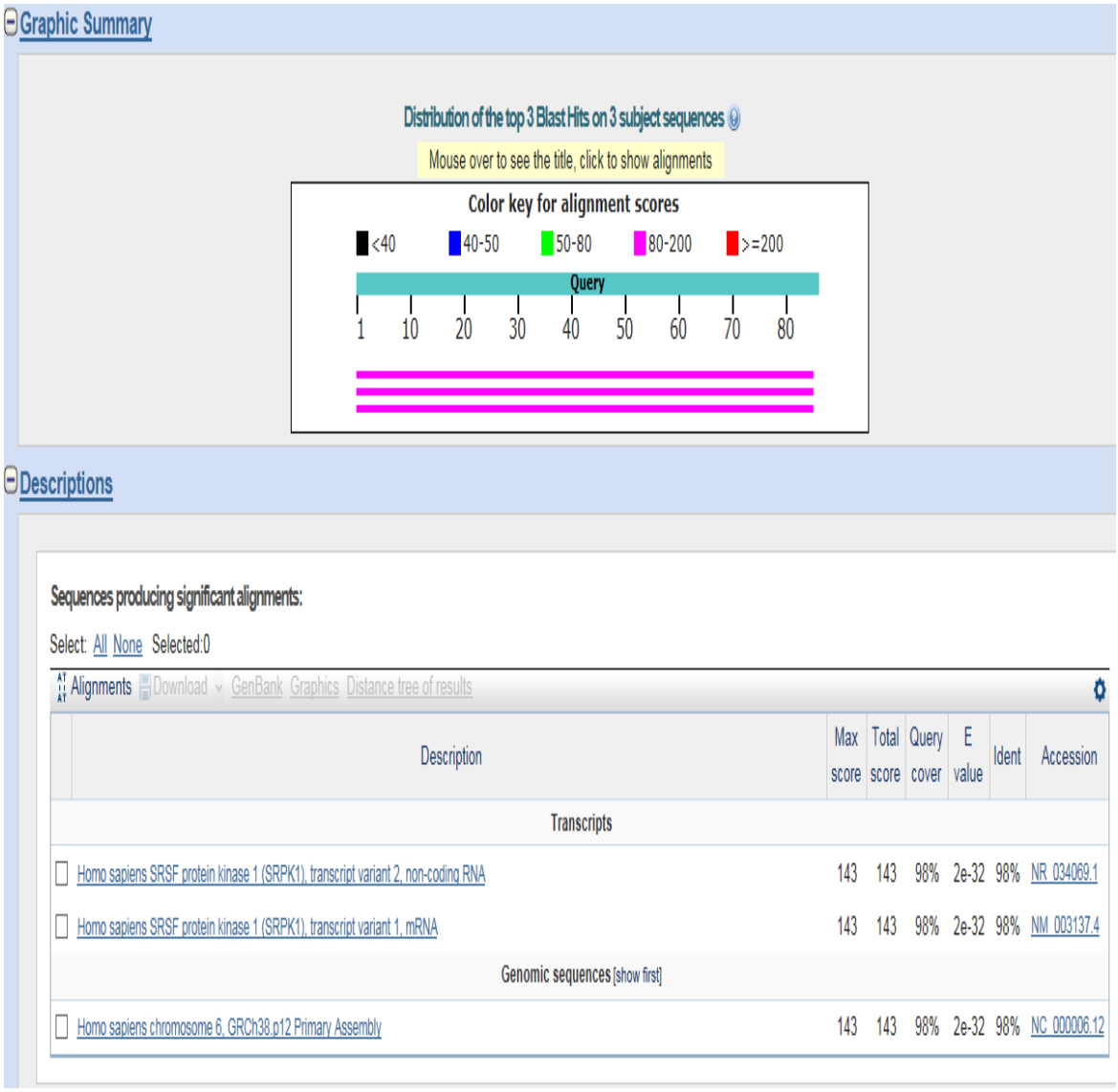

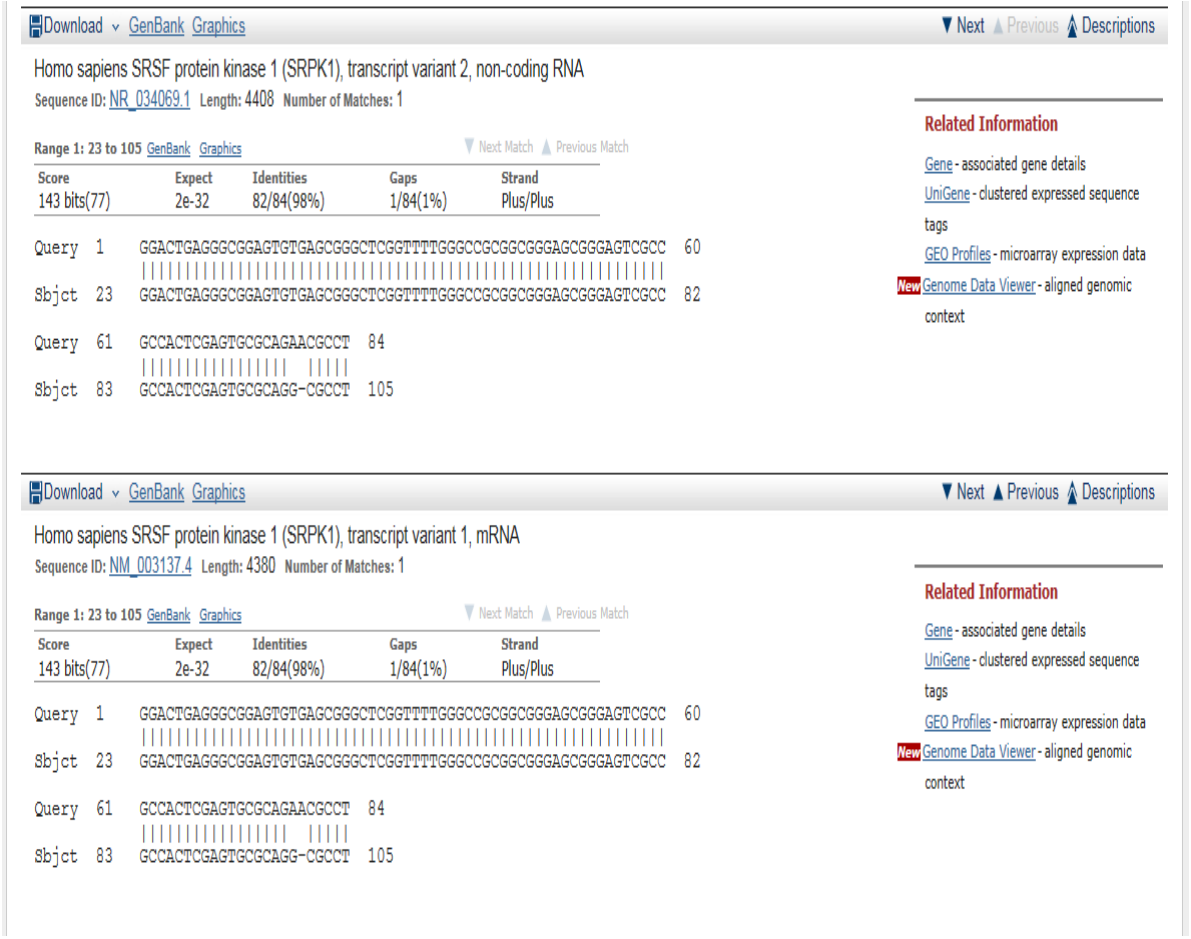

Download ▾ GenBank Graphics ▼ Next ▲ Previous ▲ Descriptions

Homo sapiens SRSF protein kinase 1 (SRPK1), transcript variant 2, non-coding RNA

Sequence ID: NR_034069.1 Length: 4408 Number of Matches: 1

Range 1: 23 to 105 GenBank Graphics ▼ Next Match ▲ Previous Match

Score	Expect	Identities	Gaps	Strand
143 bits(77)	2e-32	82/84(98%)	1/84(1%)	Plus/Plus

```
Query  1    GGACTGAGGGCGGAGTGTGAGCGGGCTCGGTTTTGGGCCGCGGCGGGAGCGGGAGTCGCC  60
            ||||||||||||||||||||||||||||||||||||||||||||||||||||||||||||
Sbjct  23   GGACTGAGGGCGGAGTGTGAGCGGGCTCGGTTTTGGGCCGCGGCGGGAGCGGGAGTCGCC  82

Query  61   GCCACTCGAGTGCGCAGAACGCCT  84
            |||||||||||||||| |||||
Sbjct  83   GCCACTCGAGTGCGCAGG-CGCCT  105
```

Related Information

Gene - associated gene details

UniGene - clustered expressed sequence tags

GEO Profiles - microarray expression data

New Genome Data Viewer - aligned genomic context

Download ▾ GenBank Graphics ▼ Next ▲ Previous ▲ Descriptions

Homo sapiens SRSF protein kinase 1 (SRPK1), transcript variant 1, mRNA

Sequence ID: NM_003137.4 Length: 4380 Number of Matches: 1

Range 1: 23 to 105 GenBank Graphics ▼ Next Match ▲ Previous Match

Score	Expect	Identities	Gaps	Strand
143 bits(77)	2e-32	82/84(98%)	1/84(1%)	Plus/Plus

```
Query  1    GGACTGAGGGCGGAGTGTGAGCGGGCTCGGTTTTGGGCCGCGGCGGGAGCGGGAGTCGCC  60
            ||||||||||||||||||||||||||||||||||||||||||||||||||||||||||||
Sbjct  23   GGACTGAGGGCGGAGTGTGAGCGGGCTCGGTTTTGGGCCGCGGCGGGAGCGGGAGTCGCC  82

Query  61   GCCACTCGAGTGCGCAGAACGCCT  84
            |||||||||||||||| |||||
Sbjct  83   GCCACTCGAGTGCGCAGG-CGCCT  105
```

Related Information

Gene - associated gene details

UniGene - clustered expressed sequence tags

GEO Profiles - microarray expression data

New Genome Data Viewer - aligned genomic context

Figure 9. 13: BASP1-SRPK1 pull down sequencing

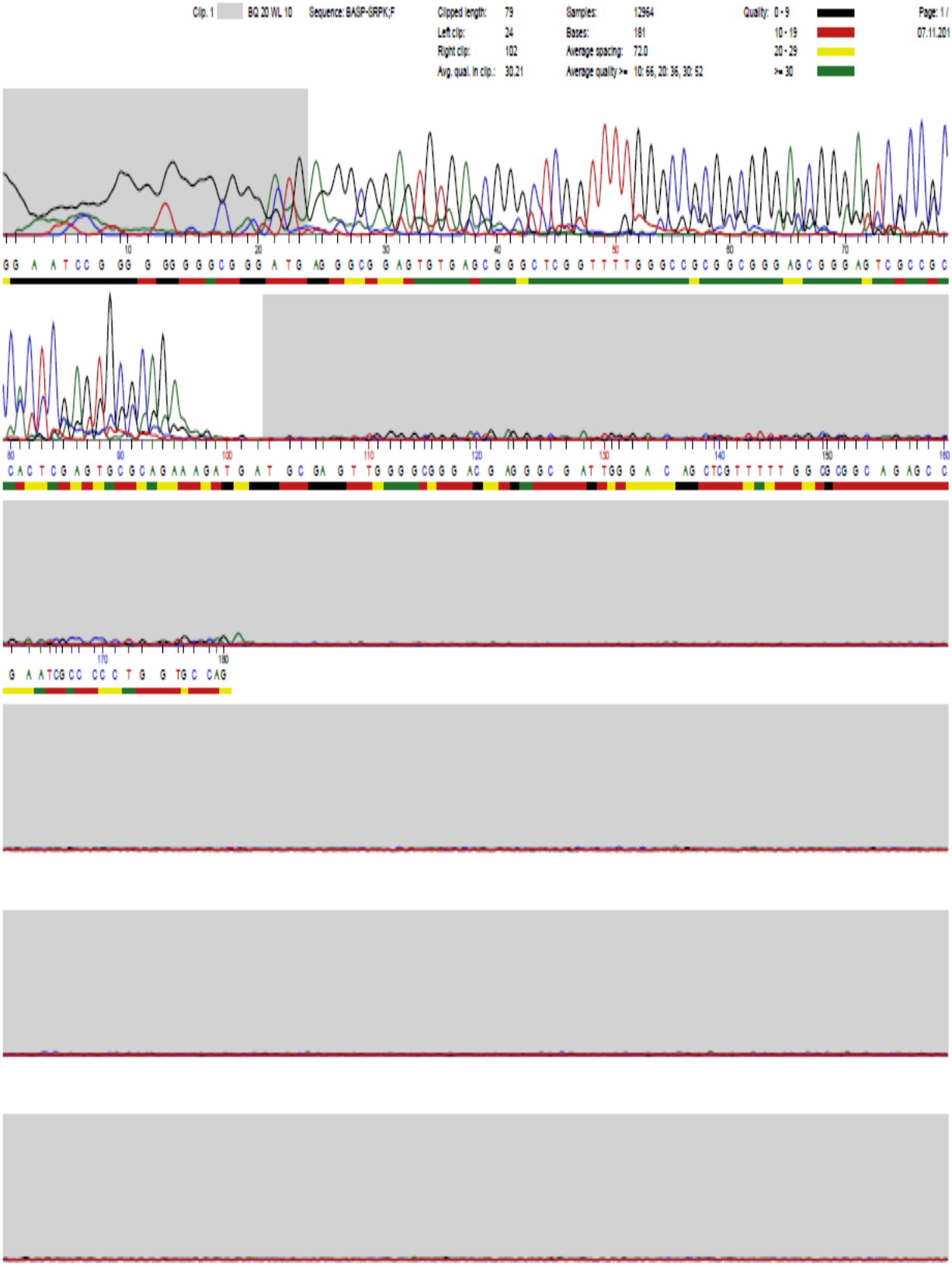

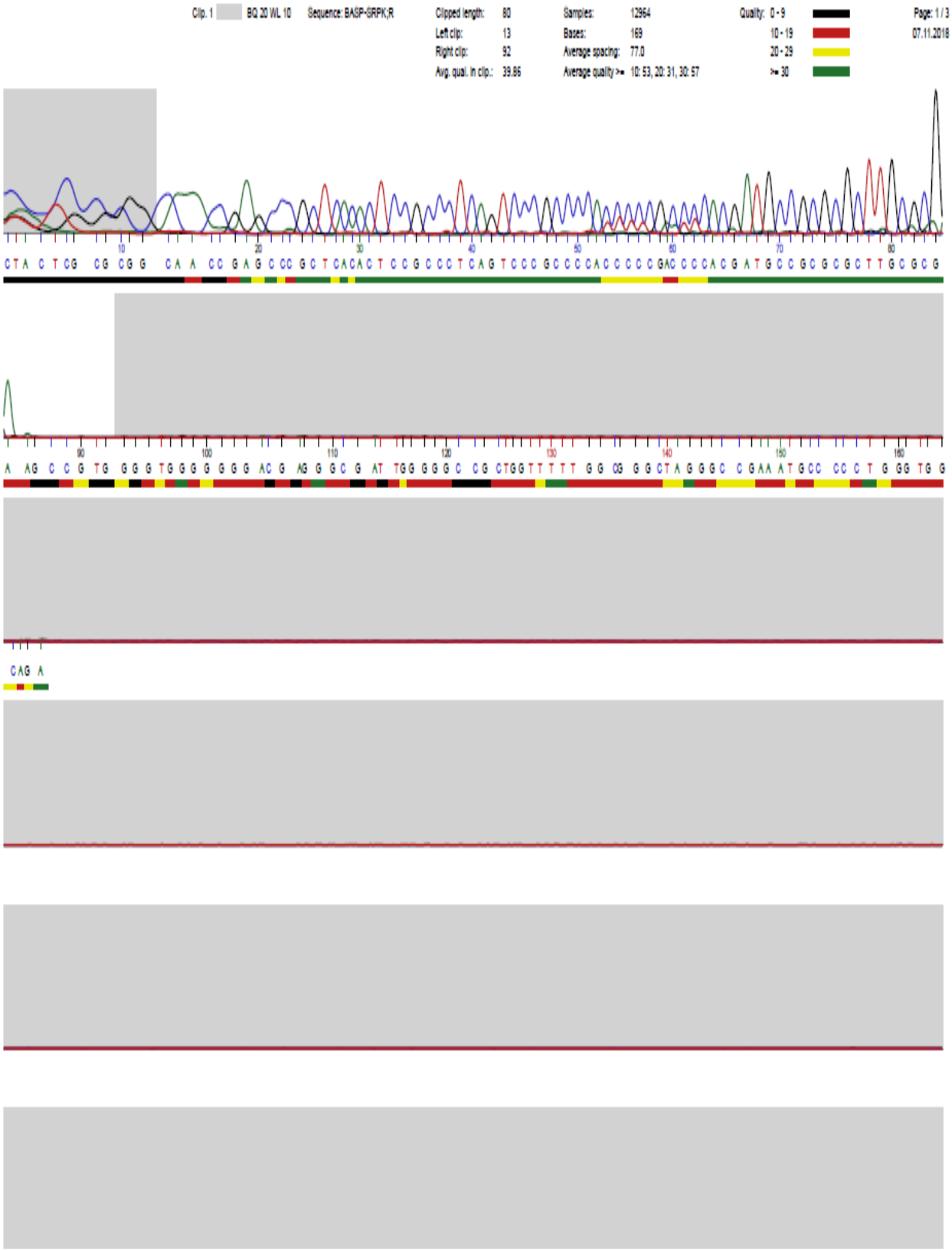
Clip. 1 BQ 20 WL 10 Sequence: BASP-SRPK;R
Clipped length: 80
Left clip: 13
Right clip: 92
Avg. qual. in clip.: 39.86
Samples: 12964
Bases: 169
Average spacing: 77.0
Average quality >= 10: 53, 20: 31, 30: 57
Quality: 0 - 9
10 - 19
20 - 29
>= 30
Page: 1 / 3
07.11.2018

Figure 9. 14: BASP1-SRPK1 sequencing result; NCBI Nucleotide Blast

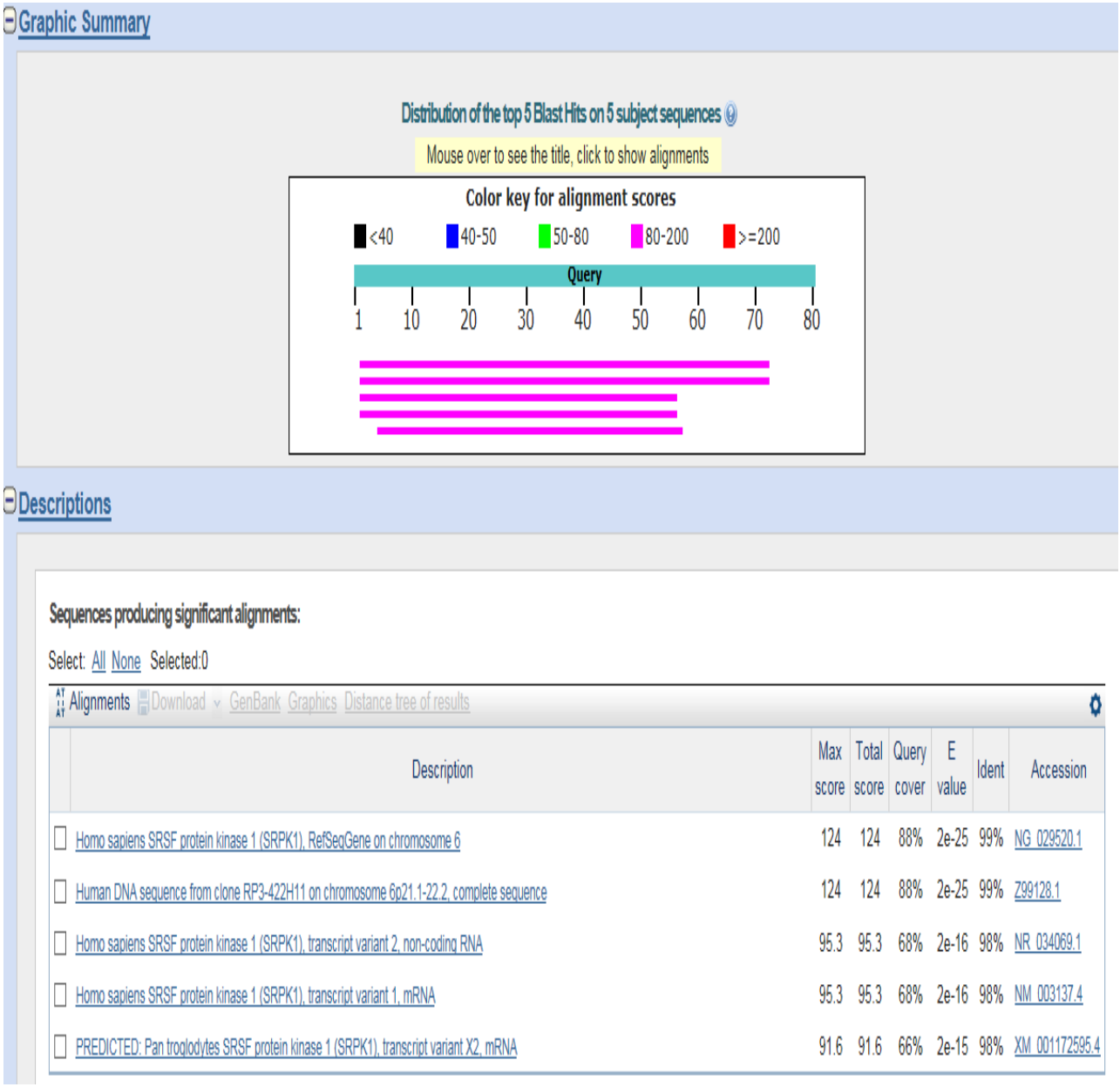

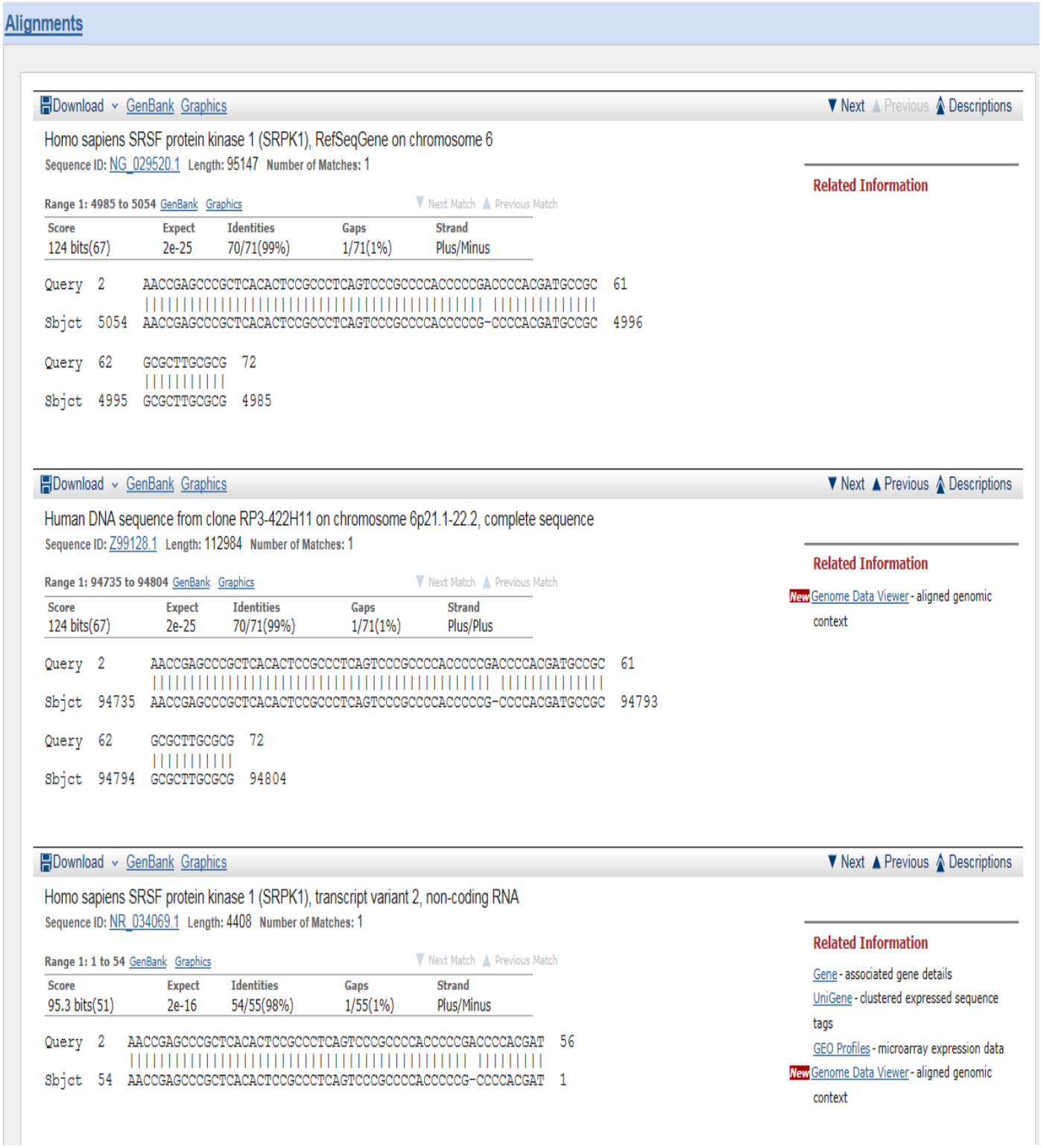

Alignments

Download GenBank Graphics ▼ Next ▲ Previous Descriptions

Homo sapiens SRSF protein kinase 1 (SRPK1), RefSeqGene on chromosome 6

Sequence ID: NG_029520.1 Length: 95147 Number of Matches: 1

Range 1: 4985 to 5054 GenBank Graphics ▼ Next Match ▲ Previous Match

Score	Expect	Identities	Gaps	Strand
124 bits(67)	2e-25	70/71(99%)	1/71(1%)	Plus/Minus

```
Query  2     AACCGAGCCCGCTCACACTCCGCCCTCAGTCCCGCCCCACCCCCGACCCCACGATGCCGC  61
             ||||||||||||||||||||||||||||||||||||||||||||||||| ||||||||||||||
Sbjct  5054  AACCGAGCCCGCTCACACTCCGCCCTCAGTCCCGCCCCACCCCCG-CCCCACGATGCCGC  4996

Query  62    GCGCTTGCGCG  72
             ||||||||||||
Sbjct  4995  GCGCTTGCGCG  4985
```

Related Information

Download GenBank Graphics ▼ Next ▲ Previous Descriptions

Human DNA sequence from clone RP3-422H11 on chromosome 6p21.1-22.2, complete sequence

Sequence ID: Z99128.1 Length: 112984 Number of Matches: 1

Range 1: 94735 to 94804 GenBank Graphics ▼ Next Match ▲ Previous Match

Score	Expect	Identities	Gaps	Strand
124 bits(67)	2e-25	70/71(99%)	1/71(1%)	Plus/Plus

```
Query  2      AACCGAGCCCGCTCACACTCCGCCCTCAGTCCCGCCCCACCCCCGACCCCACGATGCCGC  61
              ||||||||||||||||||||||||||||||||||||||||||||||||| ||||||||||||||
Sbjct  94735  AACCGAGCCCGCTCACACTCCGCCCTCAGTCCCGCCCCACCCCCG-CCCCACGATGCCGC  94793

Query  62     GCGCTTGCGCG  72
              ||||||||||||
Sbjct  94794  GCGCTTGCGCG  94804
```

Related Information

New Genome Data Viewer - aligned genomic context

Download GenBank Graphics ▼ Next ▲ Previous Descriptions

Homo sapiens SRSF protein kinase 1 (SRPK1), transcript variant 2, non-coding RNA

Sequence ID: NR_034069.1 Length: 4408 Number of Matches: 1

Range 1: 1 to 54 GenBank Graphics ▼ Next Match ▲ Previous Match

Score	Expect	Identities	Gaps	Strand
95.3 bits(51)	2e-16	54/55(98%)	1/55(1%)	Plus/Minus

```
Query  2   AACCGAGCCCGCTCACACTCCGCCCTCAGTCCCGCCCCACCCCCGACCCCACGAT  56
           ||||||||||||||||||||||||||||||||||||||||||||||||| |||||||||
Sbjct  54  AACCGAGCCCGCTCACACTCCGCCCTCAGTCCCGCCCCACCCCCG-CCCCACGAT  1
```

Related Information

Gene - associated gene details

UniGene - clustered expressed sequence tags

GEO Profiles - microarray expression data

New Genome Data Viewer - aligned genomic context

Figure 9. 15: ERG pull down-PCR sequencing; forward primers

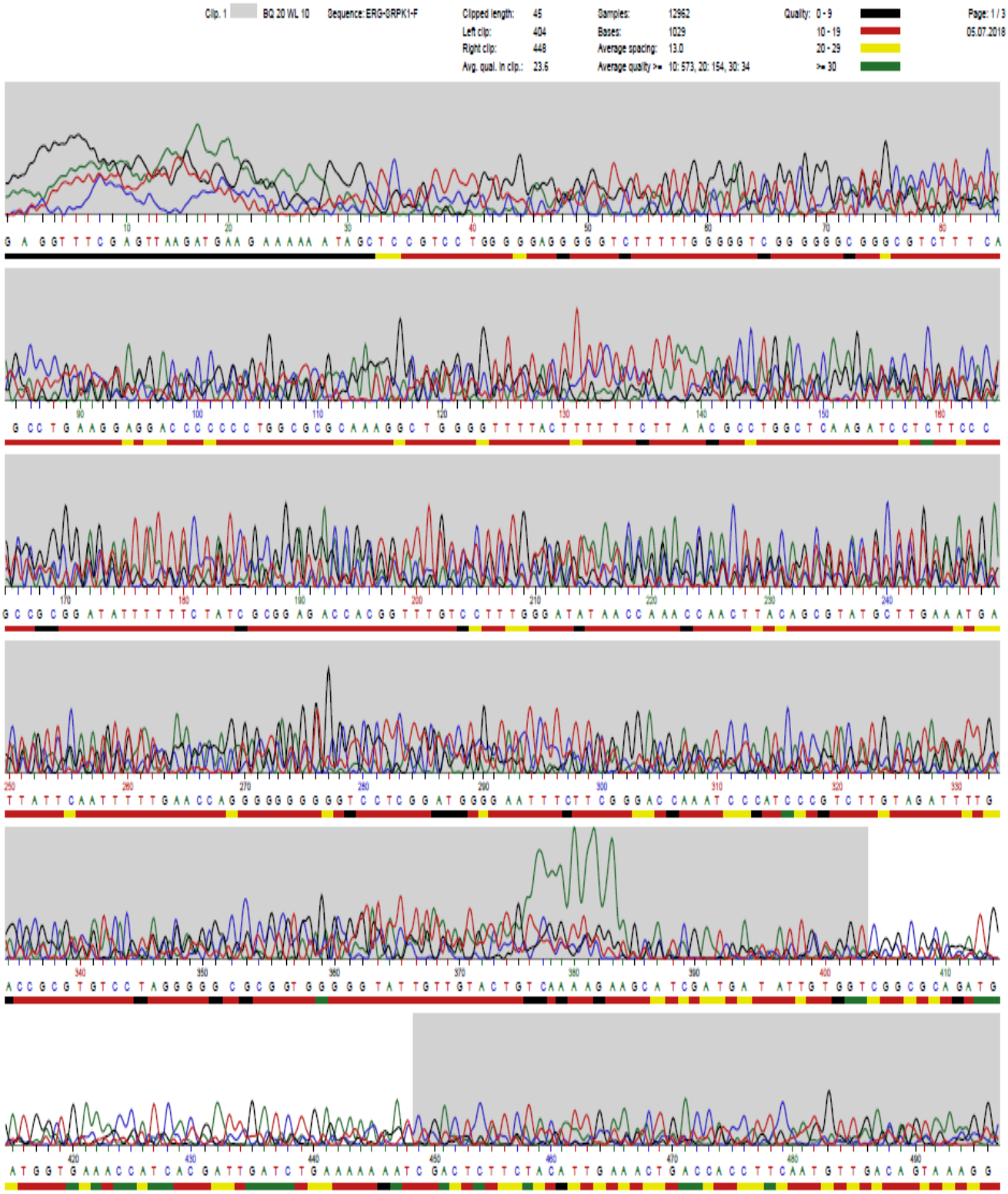

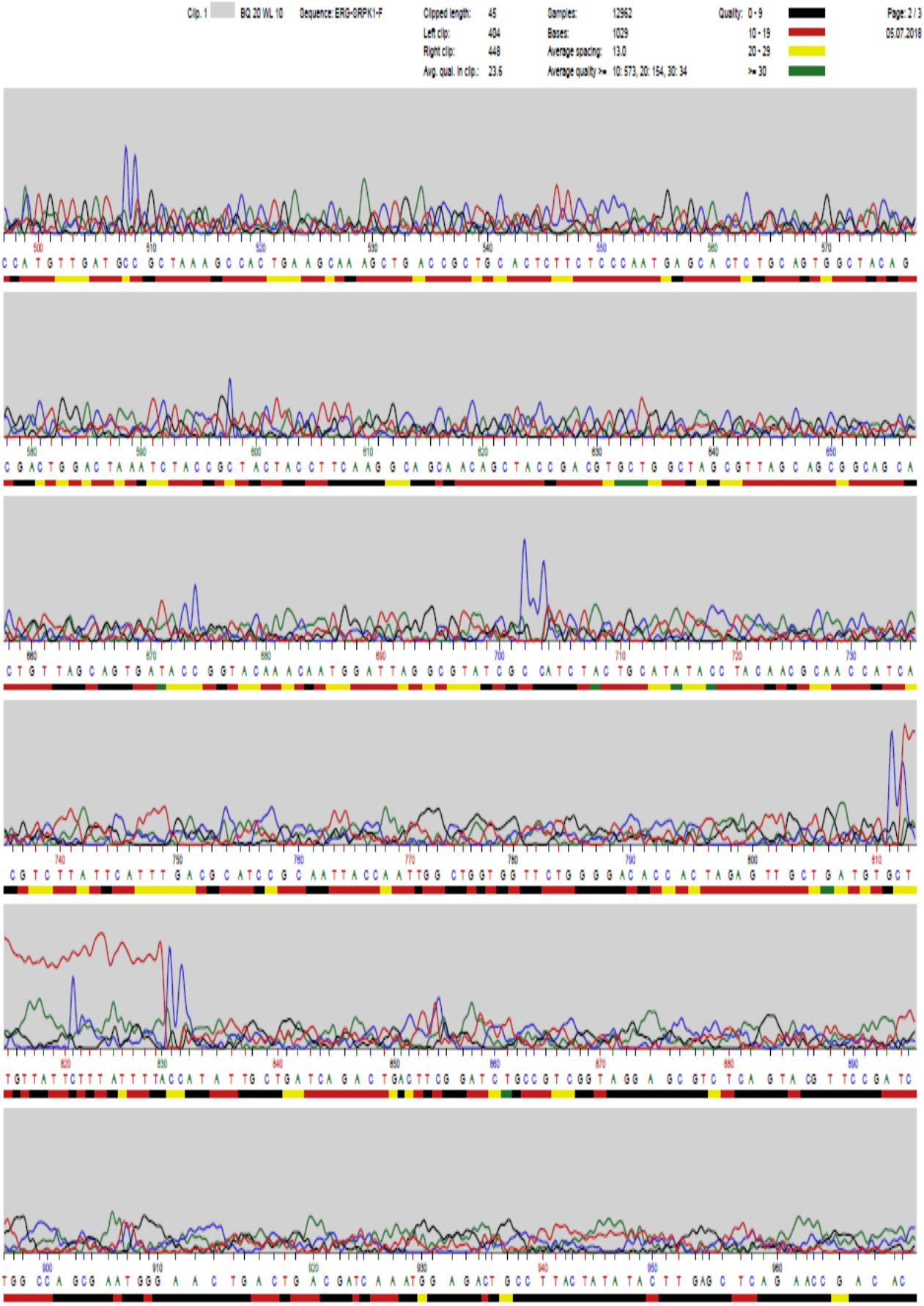
Clip. 1
BQ 20 WL 10
Sequence: ERG-GRPK1-F
Clipped length: 45
Left clip: 404
Right clip: 448
Avg. qual. in clip.: 23.6
Samples: 12962
Bases: 1029
Average spacing: 13.0
Average quality >=: 10: 573, 20: 154, 30: 34
Quality: 0 - 9
10 - 19
20 - 29
>= 30
Page: 2 / 3
05.07.2018

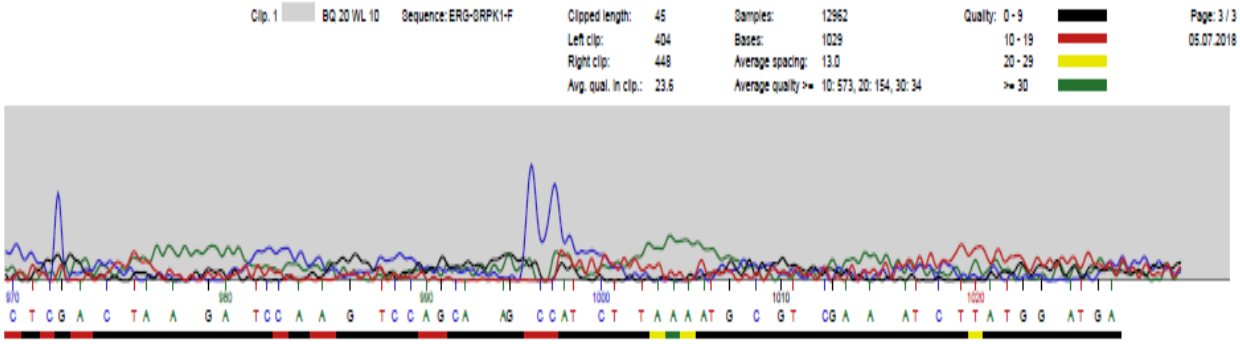

Figure 9. 16: ERG-SRPK1 sequencing result; NCBI Nucleotide Blast

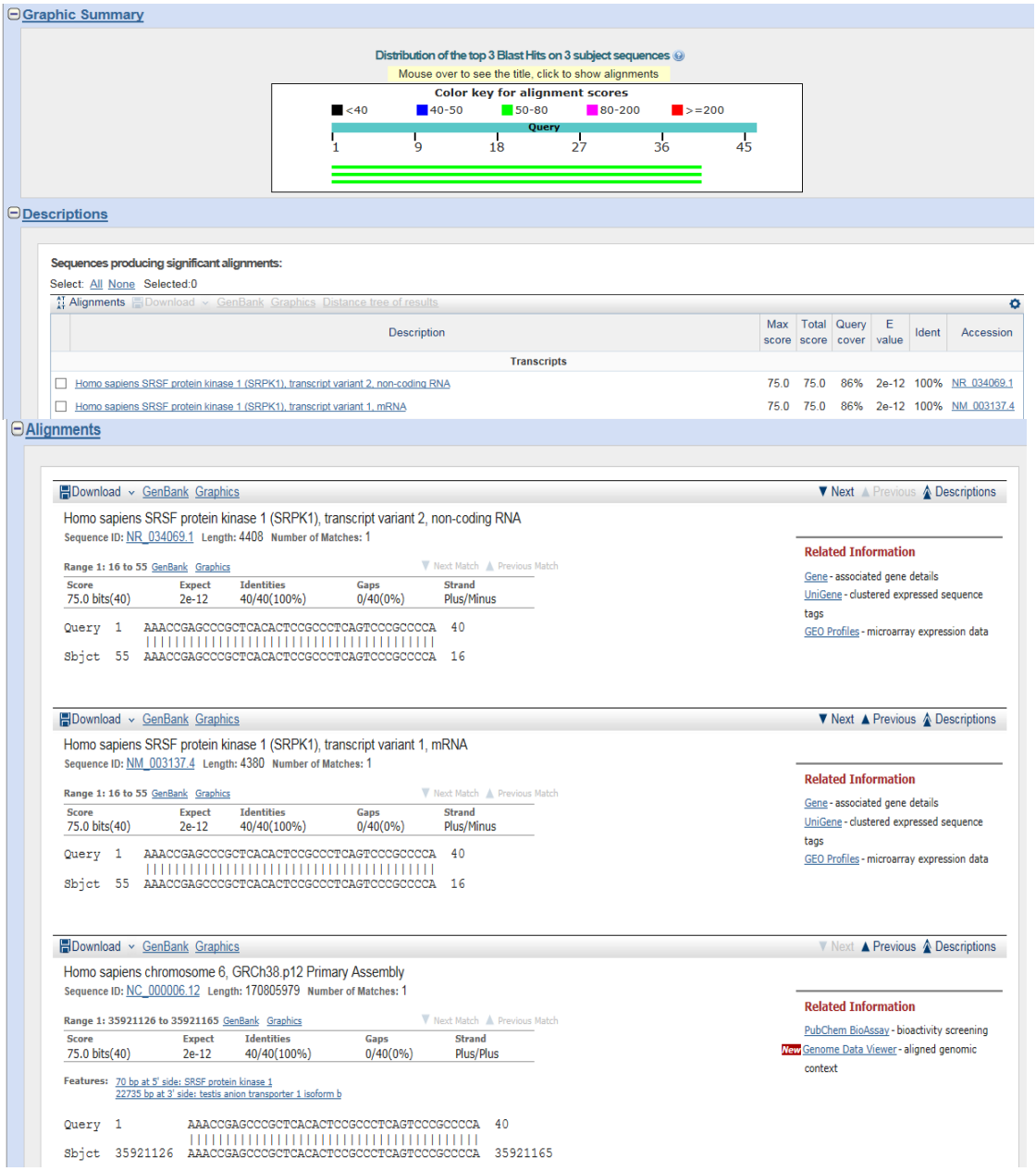

9.4 TPM values of RNA-sequences

Gene (TPM) / Cell line	WT1	BASP1	ERG	SRPK1
K562	26	Undetectable	Undetectable	101
PC3	3	89	Undetectable	44
MG63	Undetectable	494	10	54

Table 9. 2: TPM values of RNA-seq of SRPK1, WT1, BASP1 and ERG in K562, PC3 and MG63.